UNIVERSIDADE DE LISBOA
FACULDADE DE MEDICINA VETERINÁRIA

IN VIVO EVALUATION OF THE ROLE OF DELTA-LIKE 4/NOTCH SIGNALING IN THE DEVELOPMENT OF INTESTINAL TUMORS

MARINA MARTINS BADENES

Orientadores: Professor Doutor António José de Freitas Duarte
Professor Doutor Luís Filipe Lopes da Costa

Tese especialmente elaborada para obtenção do grau de Doutor em Ciências Veterinárias na Especialidade de Ciências Biológicas e Biomédicas

2016

UNIVERSIDADE DE LISBOA
FACULDADE DE MEDICINA VETERINÁRIA

IN VIVO EVALUATION OF THE ROLE OF DELTA-LIKE 4/NOTCH SIGNALING IN THE DEVELOPMENT OF INTESTINAL TUMORS

MARINA MARTINS BADENES

Orientadores: Professor Doutor António José de Freitas Duarte
Professor Doutor Luís Filipe Lopes da Costa

Tese especialmente elaborada para obtenção do grau de Doutor em Ciências Veterinárias na Especialidade de Ciências Biológicas e Biomédicas

Júri:
Presidente: Doutor Rui Manuel de Vasconcelos e Horta Caldeira
Vogais:

- Doutor Luís Filipe Lopes da Costa
- Doutor António José de Freitas Duarte
- Doutor Rui Pedro Brás Martins Faísca
- Doutor Fernando António da Costa Ferreira
- Doutora Raquel Maria da Silva Graça Almeida
- Doutora Tânia Gilot Mendes de Carvalho

2016

To Nuno, Pedro, Zé, Sara, Carmen and Sofía

Acknowledgements

First of all, I owe sincere and deep gratitude to my thesis advisor Doctor António Duarte for this great opportunity. His guidance, enthusiasm, comprehension, critical and constructive spirit and share of knowledge were extremely important for the development of this work.

I also have to thank my co-supervisor Doctor Luís Lopes da Costa for his encouragement, help and commitment.

I am very grateful for all the help that Doctor Alexandre Trindade gave me. He shared with me his great scientific knowledge, guided me and helped me overcome the difficulties and to establish a structured path in my work.

I had a great advantage to work and learn with an extremely competent pathologist, Dr. Hugo Pissarra. I must also thank the rest of the Anatomic Pathology team of the Faculty of Veterinary Medicine, especially Sandra Carvalho, for her technical support.

Being part of a great team, I am thankful to the companionship and help from my colleagues Dr. Ana Fernandes, Doctor Dusan Djokovic, Doctor Daniel Murta, Dr. Catarina Carvalho, Dr. Rita Pedrosa, Dr. Joana Gigante, Dr. Liliana Silva, and Doctor Ana Tavares.

I also would like to thank the Bioimaging unit of the Molecular Medicine Institute for their technical support.

I appreciate the fruit-bearing collaboration with Dr. Parkash S. Gill from the University of Southern California - Keck School of Medicine, Los Angeles (USA).

Importantly, I would like to express my gratitude to the Faculty of Veterinary Medicine (Lisbon University), and to the Centre for Interdisciplinary Research in Animal Health for being such a stimulating scientific center.

Finally, I would like to thank the unconditional support and care of my family. They are my truly inspiration.

Funding

I thank the Portuguese Foundation for Science and Technology for the financial support in both the Project PTDC/CVT/115703/2009 and my grant SFRH / BD / 61125 / 2009.

UNIÃO EUROPEIA

Fundo Social Europeu

Title – *In vivo* evaluation of the role of Delta-like 4/Notch signaling in the development of intestinal tumors

Abstract

Colorectal cancer (CRC) is the third most common malignancy and the second leading cause of cancer-related death in the Western world. Dll4/Notch signaling has been shown to regulate tumor angiogenesis and cancer stem cell maintenance in CRC, but how it affects the intestinal precancerous lesions that lead to CRC initiation is not known. Therefore we evaluated the role of Dll4/Notch pathway during intestinal tumorigenesis. For that we used two well-established mouse models of CRC, the *Apc*$^{Min/+}$ autochthonous transgenic model and the azoxymethane plus dextran sodium sulphate chemically induced model of chronic colitis associated-cancer (CAC). First we analyzed the protein expression pattern of Dll4 and other Notch pathway members in these settings relatively to that in the normal gut. Then we evaluated the effect of endothelial-specific or ubiquitous Dll4 deregulation and performed a therapeutic trial with the Dll4 inhibitor Dll4-Fc. This protein was administered alone, and in combination with the epidermal growth factor receptor (EGFR)-specific tyrosine kinase inhibitor erlotinib to assess if the anti-Dll4 therapy mediated vascular defects impaired the delivery of other anti-cancer drugs to the tumors. We observed that the Notch pathway is activated in the two studied models of CRC. The normal protein expression pattern of Notch pathway members in the gut is altered in chronic colitis and in *Apc*$^{Min/+}$ and colitis-driven intestinal tumors. Dll4 is the most upregulated ligand in the intestinal adenomas in both models of CRC and is present in both tumor epithelium and stroma. Both Dll4 blockade (endothelial-specific and ubiquitously) and activation (endothelial-specific) have an inhibitory effect on intestinal tumor initiation and growth by promoting a noncompetent vasculature or decreasing the vessel density, respectively. Besides its angiogenic related effects, Dll4/Notch pathway promotes excessive inflammation in CAC, sustains the tumor stem cell pool and tumor proliferation synergistically with Wnt signaling, and inhibits differentiation mainly of the secretory cells. In addition, the effectiveness of erlotinib is not affected by Dll4-Fc, where these therapies additively inhibit intestinal tumorigenesis.

Keywords: Dll4/Notch, CRC, *Apc*$^{Min/+}$, CAC, EGFR

Título – Avaliação *in vivo* da função da sinalização intercelular Dll4/Notch no desenvolvimento de tumores intestinais

Resumo

O cancro colo-rectal (CCR) é o terceiro tipo de cancro mais comum e é uma das principais causas de morte no Mundo Ocidental. O CCR geralmente desenvolve-se esporadicamente, mas também pode ser hereditário como na síndrome polipose adenomatosa familiar (PAF). A PAF está associada à ativação da via de sinalização Wnt através de mutações no gene supressor tumoral *Adenomatous Polyposis Coli (APC)*, que também ocorre frequentemente nos CCR esporádicos. O desenvolvimento do CCR também pode estar associado a inflamação crónica, nomeadamente à doença de Crohn (CD) e à colite ulcerativa (UC).

Infelizmente o desenvolvimento de novas estratégias terapêuticas ou preventivas que tenham como alvo vias de sinalização críticas no desenvolvimento do CCR continua a ser extremamente necessário. Uma dessas estratégias tem como alvo a angiogénese tumoral. O primeiro agente anti-angiogénico a ser aprovado foi o Bevacizumab, que é usado em combinação com outros fármacos no tratamento do CCR metastático. No entanto, a utilização deste fármaco leva ao aparecimento de efeitos secundários e resistência tumoral e em tumores não metastáticos não se tem mostrado eficaz. Assim, continua a ser necessário desenvolver melhores estratégias terapêuticas anti-angiogénicas.

A via de sinalização Notch está envolvida em múltiplas decisões de destino celular e em eventos fisiológicos e patológicos nos mamíferos. Estudos em modelos de xenotransplantes e autóctones no ratinho indicaram que o bloqueio da via Dll4/Notch inibe o desenvolvimento tumoral ao promover a formação de vasos sanguíneos disfuncionais nos tumores. No entanto, a terapia com inibidores de Dll4/Notch pode provocar toxicidade, promover o desenvolvimento do cancro através do aumento dos níveis de hipoxia, limitar o acesso de outros fármacos ao tumor e tornar-se ineficaz pela capacidade dos tumores de "normalização" dos defeitos vasculares. Deste modo, a estratégia oposta, nomeadamente a ativação de Dll4/Notch, também tem sido estudada como terapia oncológica anti-angiogénica. No entanto, foi demonstrado que a sobre-expressão de Dll4 nas células tumorais pode promover ou inibir o crescimento tumoral em diferentes tipos de cancro através da redução ou do aumento dos níveis de hipoxia e de apoptose, respectivamente. Porém, esta estratégia ainda não foi estudada no CCR.

No CCR, para além do efeito angiogénico, a via Dll4/Notch poderá também regular positivamente o *pool* de células estaminais cancerígenas e deste modo promover a carcinogénese. No entanto, este efeito nunca foi estudado nas lesões intestinais pré-malignas que caracterizam a iniciação tumoral do CCR.

Deste modo, neste trabalho pretendeu-se avaliar a via Dll4/Notch na tumorigénese intestinal. Para este efeito, utilizaram-se dois modelos pré-estabelecidos de CCR em ratinho. Um dos

modelos consiste no ratinho transgénico *Apc*$^{Min/+}$, no qual uma mutação pontual no gene *Apc* causa o desenvolvimento espontâneo de múltiplos adenomas no intestino delgado e no grosso. O outro é um modelo induzido por químicos, no qual a administração do carcinogénio azoximetano associado a quatro ciclos do agente pró-inflamatório sulfato de dextrano sódico levam ao aparecimento de cancro colo-rectal associado a colite crónica (CAC). Procedeu-se então à avaliação do padrão de expressão proteica de Dll4 e de outros componentes da via Notch na colite crónica, nos tumores associados a esta e nos tumores *Apc*$^{Min/+}$ relativamente ao intestino normal. Em seguida, analisou-se o efeito da desregulação genética de *Dll4* no desenvolvimento tumoral nos dois modelos. Para avaliar se os efeitos do bloqueio da via Dll4/Notch eram apenas associados ao seu fenótipo vascular, compararam-se ratinhos *Apc*$^{Min/+}$ com perda-de-função endotelial-específica e ubíqua de *Dll4*. Também se analisaram ratinhos *Apc*$^{Min/+}$ com sobre-expressão endotelial de *Dll4* para avaliar se esta estratégia alternativa poderá ser considerada no tratamento do CCR. A ativação de *Dll4* foi feita especificamente no endotélio, porque estudos anteriores indicaram que a sobre-expressão de *Dll4* no epitélio tumoral poderá favorecer o desenvolvimento tumoral. No caso do modelo de CAC, fez-se uma análise de ratinhos heterozigóticos constitutivos ubíquos para *Dll4*. Seguidamente, realizou-se um ensaio terapêutico nos dois modelos de CCR com o inibidor de Dll4, a proteína de fusão Dll4-Fc, que se liga aos receptores Notch e age como dominante-negativo. Esta proteína foi também administrada em combinação com o inibidor da tirosina-quinase do receptor do factor de crescimento epidérmico (EGFR) erlotinib para avaliar se os defeitos vasculares resultantes da terapia anti-Dll4 impedem o acesso de outros fármacos aos tumores. A associação foi feita com o erlotinib pela importância da via de sinalização EGFR no desenvolvimento do CCR e de já ter sido demonstrado haver uma interação entre as vias EGFR e Notch noutros tipos de cancro.

Os resultados obtidos confirmaram que a via Notch está ativa nos dois modelos de CCR através dos efetores Hes1 e Hes5. Adicionalmente, o padrão de expressão proteica dos membros da via Notch no intestino normal sofre variações significativas na colite crónica e tanto nos tumores associados a inflamação como nos *Apc*$^{Min/+}$. Dll4 é o ligando mais sobre-expresso nos adenomas intestinais nos dois modelos de CCR e está presente no epitélio e no estroma tumorais. Este adquire expressão ectópica nas células absortivas nos dois modelos e a sua expressão aumenta sobretudo na *lamina propria* na colite crónica e no epitélio tumoral nos dois modelos.

Tanto o bloqueio genético (endotelial-específico e ubíquo) e farmacológico, como a ativação (endotelial-específica) de Dll4 levam a uma redução significativa do volume tumoral intestinal e sobretudo do número destes tumores por animal. Nos ratinhos *Apc*$^{Min/+}$, o efeito na multiplicidade tumoral é mais acentuado no intestino delgado e o efeito no volume tumoral mais no intestino grosso. No bloqueio de Dll4 o efeito anti-tumoral está associado à formação de uma vasculatura disfuncional nos adenomas, enquanto que na ativação de

Dll4, este efeito está associado à redução da densidade vascular intra-tumoral. Consequentemente, em ambos os casos, a privação dos tumores de vasos sanguíneos competentes leva ao aumento dos níveis de hipoxia, que por sua vez causa um aumento da apoptose intra-tumoral. Adicionalmente, reduz moderadamente os níveis de proliferação tumoral e da expressão do marcador de células estaminais *leucine-rich repeat-containing G-protein-coupled receptor 5* (*Lgr5*), mas não do *B cell–specific Moloney murine leukemia virus insertion site 1* (*Bmi1*). No entanto, o efeito positivo da via Dll4/Notch na manutenção das células estaminais tumorais e na proliferação tumoral parece não ser só provocado pelo fenótipo vascular. Estes efeitos poderão ser provocados pela regulação negativa da expressão dos inibidores de quinase dependentes de Ciclina *Cdkn1b e Cdkn1c* através da inibição da expressão de *Atoh1*. Para além disso, poderão também estar associados à regulação positiva de *c-myc*, Ciclina D1 e D2 possivelmente através da inibição da expressão de *Klf4* não dependente da ativação da via Wnt. Deste modo, Dll4/Notch parece regular a tumorigénese intestinal em sinergia com a via Wnt. Por outro lado, a via Dll4/Notch parece também promover por mecanismos não-angiogénicos o desenvolvimento neoplásico, provocando um aumento de displasia nos tumores e perda de diferenciação epitelial tumoral, sobretudo das células secretoras (caliciformes e de Paneth) através da redução da expressão de *Atoh1* e *Klf4*. No entanto, o efeito desta via na diferenciação destas células não é tão acentuado como o descrito relativamente à inibição de toda a via Notch.

No ensaio terapêutico constatou-se que a eficácia do erlotinib não é negativamente afetada pelo Dll4-Fc, em que o aumento de extravasação vascular nos tumores poderá levar à acumulação do erlotinib no local. A associação destes fármacos mostrou-se até ser benéfica. Estes inibem de forma aditiva a tumorigénese intestinal, através da regulação negativa de c-Myc e Ciclina D1 e D2 de forma maioritariamente independente da via Wnt. Como já previamente descrito, erlotinib mostrou ser ineficaz na redução do tamanho e desenvolvimento tumorais. Este fármaco também não afetou a apoptose intra-tumoral, possivelmente por haver uma redução da hipoxia consequente da "normalização" da vasculatura tumoral. Tal pode estar associado ao observado aumento da ativação de Notch1 nos tumores tratados com erlotinib. Por outra parte, Dll4-Fc parece afectar negativamente a ativação da via EGFR, sobretudo do seu alvo Akt. O efeito angiogénico de Dll4-Fc é mais potente que o do erlotinib, o que leva à inibição do crescimento e desenvolvimento tumorais quando associados. Adicionalmente, esta associação terapêutica também promove a diferenciação epitelial inespecífica, possivelmente pelo aumento menos pronunciado da expressão de *Atoh1* nestes tumores.

No modelo de CAC a ação anti-tumoral do bloqueio genético e farmacológico de Dll4 pode ser também devida à observada redução da inflamação excessiva e da expressão de importantes promotores de CAC, tais como a via anti-apoptótica e pró-proliferativa *Tnf-α*/*Nfkb2*/*Il-6*, e do aumento da expressão do inibidor de CAC *Tgf-β*.

Deste modo, neste trabalho constatou-se que a via Dll4/Notch promove a iniciação e desenvolvimento dos adenomas intestinais *Apc*$^{Min/+}$ e dos associados a colite, através da regulação dos seguintes processos: angiogénese, inflamação, proliferação, apoptose, diferenciação/transformação neoplásica e manutenção das células estaminais tumorais. Os resultados pré-clínicos obtidos indicam que tanto a inibição como a ativação desta via e, sobretudo, a associação de terapias anti-DLL4 e anti-EGFR, poderão ser benéficos no tratamento de CRC em estádios iniciais, assim como para prevenção em pacientes com predisposição para esta doença, nomeadamente com PAF ou IBD.

Palavras-chave: Dll4/Notch, CCR, *Apc*$^{Min/+}$, CAC, EGFR

TABLE OF CONTENTS

1 OBJECTIVES 1

2 INTRODUCTION 1

3 LITERATURE REVIEW 4

3.1 Intestinal morphology and homeostasis 4

3.2 Signaling pathways in intestinal development and CRC 7

3.2.1 Wnt signaling 7

3.2.2 Notch signaling 8

3.2.2.1 Notch in intestinal homeostasis 9

3.2.2.2 Notch in CRC 11

3.2.2.3 Notch during chronic inflammation 13

3.2.2.4 Delta-like 4 15

3.2.3 TGF-β pathway 17

3.2.4 EGFR signaling 17

3.2.5 VEGF/VEGFR signaling 18

3.3 Colorectal cancer 19

3.3.1 Etiology 19

3.3.2 CRC carcinogenesis 20

3.3.3 CAC carcinogenesis 23

3.4 Mouse models of colorectal cancer 26

3.4.1 The *Apc*$^{Min/+}$ model 26

3.4.2 The azoxymethane plus dextran sulfate sodium chemically induced model 26

4 EXPERIMENTAL WORK 28

4.1 Chapter I - Delta-like 4/Notch signaling promotes *Apc*$^{Min/+}$ tumor initiation through angiogenic and non-angiogenic related mechanisms 28

4.1.1 Abstract 28

4.1.2 Introduction 29

4.1.3 Methods 30

4.1.3.1 Experimental animals 30

4.1.3.2 Macroscopic analysis of the intestine 30

4.1.3.3 Histopathological analysis 31

4.1.3.4 Immunohistochemical analysis 31

4.1.3.5 Immunofluorescence analysis 31

4.1.3.6 Quantitative transcriptional analysis 32

4.1.3.7 Statistical analysis 32

4.1.4 Results 33

4.1.4.1 Notch pathway is upregulated in *Apc*$^{Min/+}$ small and large intestine tumors relatively to the normal intestine 33

4.1.4.2 Endothelial-specific but mainly ubiquitous inhibition of Dll4 function delays the development of intestinal tumors in *Apc*$^{Min/+}$ mouse 37
4.1.4.3 Endothelial-specific and ubiquitous Dll4 deletion have similar negative impact in the tumor vasculature, promoting hypoxia and apoptosis in the *Apc*$^{Min/+}$ tumors 40
4.1.4.4 Ubiquitous deletion of Dll4 has a significantly stronger effect than endothelial-specific Dll4 deletion in the inhibition of *Apc*$^{Min/+}$ tumor proliferation and neoplastic transformation 44
4.1.4.5 Ubiquitous deletion of *Dll4* has a stronger inhibitory effect than the endothelial-specific blockade on *Apc*$^{Min/+}$ tumor stem cell maintenance independently of β-catenin activation 45
4.1.4.6 Ubiquitous, but not endothelial-specific deletion of Dll4, promotes epithelial differentiation and secretory lineage commitment in the *Apc*$^{Min/+}$ tumors 50
4.1.5 Discussion 53
4.2 Chapter II – Delta-like 4 endothelial overexpression decreases the vascularity of intestinal adenomas in *Apc*$^{Min/+}$ mice reducing tumor multiplicity and growth 57
4.2.1 Abstract 57
4.2.2 Introduction 58
4.2.3 Methods 59
4.2.3.1 Experimental animals 59
4.2.3.2 Macroscopic analysis 59
4.2.3.3 Histopathological analysis 59
4.2.3.4 Immunofluorescence analysis 60
4.2.3.5 Quantitative transcriptional analysis 60
4.2.3.6 Statistical analysis 61
4.2.4 Results 61
4.2.4.1 Endothelial Dll4 overexpression inhibits the *Apc*$^{Min/+}$ tumor initiation and development 61
4.2.4.2 Endothelial overexpression of Dll4 promotes apoptosis by inhibiting angiogenesis in the *Apc*$^{Min/+}$ tumors 63
4.2.4.3 Endothelial overexpression of Dll4 decreases proliferation and Lgr5+ stem cell density, without affecting the neoplastic transformation and differentiation, in the *Apc*$^{Min/+}$ tumors 66
4.2.5 Discussion 69
4.3 Chapter III - Delta-like 4/Notch inhibition has a synergistic effect with anti-Egfr therapy on *Apc*$^{Min/+}$ tumorigenesis 72
4.3.1 Abstract 72
4.3.2 Introduction 73
4.3.3 Methods 74
4.3.3.1 Experimental animals 74
4.3.3.2 Macroscopic analysis of the intestine 74
4.3.3.3 Histopathological analysis 74

4.3.3.4 Immunofluorescence analysis 75
4.3.3.5 Quantitative transcriptional analysis 76
4.3.3.6 Statistical analysis 76
4.3.4 Results 76
4.3.4.1 Dll4-Fc potentiates the inhibitory effect of erlotinib in the small intestine tumor multiplicity of *Apc*$^{Min/+}$ mice 76
4.3.4.2 The inhibition of Egfr pathway activation in *Apc*$^{Min/+}$ intestinal tumors is one of the mechanisms responsible for the observed additive effect of Dll4-Fc and erlotinib therapy 78
4.3.4.3 Erlotinib treatment induces Notch1 activation in *Apc*$^{Min/+}$ intestinal tumors 78
4.3.4.4 Dll4-Fc promotes an intestinal tumor dysfunctional and immature pro-angiogenic phenotype with increased hypoxia and apoptosis, even when associated to erlotinib therapy 83
4.3.4.5 Association of Dll4-Fc to erlotinib has a synergistic effect inhibiting the tumor cell proliferation and tumor stem cell maintenance 88
4.3.4.6 Association of Dll4-Fc to erlotinib promotes unspecific intestinal lineage differentiation of proliferative tumor stem cells 93
4.3.5 Discussion 97
4.4 Chapter IV - Delta-like 4/Notch signaling blockade inhibits the development of chronic colitis-associated colorectal cancer in a mouse model 101
4.4.1 Abstract 101
4.4.2 Introduction 102
4.4.3 Methods 103
4.4.3.1 Chemical induction of CAC 103
4.4.3.2 Evaluation of anti-tumor efficacy of Dll4 blockade 103
4.4.3.3 Macroscopic analysis of the large intestine 103
4.4.3.4 Histopathological analysis 103
4.4.3.5 Immunohistochemical analysis 104
4.4.3.6 Immunofluorescence analysis 104
4.4.3.7 Quantitative transcriptional analysis 105
4.4.3.8 Statistical analysis 105
4.4.4 Results 106
4.4.4.1 Notch pathway members are strongly expressed in chronic colitis and CAC 106
4.4.4.2 Dll4 blockade reduces the formation and size of colitis-driven CR tumors 107
4.4.4.3 Dll4 blockade deregulates angiogenesis in CAC 110
4.4.4.4 Dll4 inhibition reduces chronic colitis and CR tumor inflammation 112
4.4.4.5 Dll4 blockade decreases the number of Lgr5 positive stem cells and increases secretory lineage differentiation in the large intestine inflammatory and tumoral lesions 117
4.4.5 Discussion 120
5 CONCLUSIONS 124
6 REFERENCES 129
7 ANNEX I – Dll4 transgenic mouse strains 150

8 ANNEX II – Primer pair sequences list 151

9 ANNEX III – Collaborations 155

LIST OF FIGURES

Figure 1 - Mouse small and large intestine histology. *In* (King, 2002) 5

Figure 2 - Model for the differentiation of the intestinal epithelial cell types. *In* (Gerbe et al., 2011) 6

Figure 3- The Notch pathway. *In* (Radtke, Fasnacht, & Macdonald, 2010) 9

Figure 4 - Notch signaling in intestinal homeostasis. *In* (Vooijs, Liu, & Kopan, 2011) 10

Figure 5 - Model of the sequence of events in CRC development. *In* (Fearon & Vogelstein, 1990) 21

Figure 6 - Notch pathway expression pattern in the small and large intestine and in $Apc^{Min/+}$ intestinal adenomas 36

Figure 8 - Dll4 is expressed in tumoral Paneth cells and endothelium, and near tumoral and normal Lgr5+ cells 38

Figure 11 - Endothelial-specific and ubiquitous Dll4 deregulation affects similarly the $Apc^{Min/+}$ tumor angiogenesis 41

Figure 12 - Endothelial-specific and ubiquitous Dll4 deregulation promotes equally hypoxia and apoptosis in $Apc^{Min/+}$ tumors 43

Figure 12 (continuation) - Endothelial-specific and ubiquitous Dll4 deregulation promotes equally hypoxia and apoptosis in $Apc^{Min/+}$ tumors 44

Figure 13 - Ubiquitous deletion of Dll4 has a greater inhibitory effect in the $Apc^{Min/+}$ tumorigenesis and neoplastic transformation than the endothelial-specific deletion 46

Figure 14 - Histopathological classification of the $Apc^{Min/+}$ small and large intestine lesions. 49

Figure 15 - Dll4 endothelial-specific and ubiquitous deregulation does not affect the intestinal $Apc^{Min/+}$ associated β-catenin activation 49

Figure 16 (continuation) - Ubiquitous, but not endothelial-specific, loss of Dll4 promotes intestinal differentiation towards the secretory lineages 52

Figure 17 - *Dll4* endothelial-specific overexpression delays the tumor initiation and development in $Apc^{Min/+}$ mouse 62

Figure 18 - Confirmation of Dll4/Notch mediated *Hey2* overexpression in $Apc^{Min/+}$ endoDll4OE tumors 63

Figure 19 - Dll4 endothelial-specific overexpression inhibits angiogenesis, despite increasing the vessels maturity and functionality in $Apc^{Min/+}$ tumors 64

Figure 20 - Dll4 endothelial-specific activation promotes hypoxia and apoptosis in $Apc^{Min/+}$ tumors 65

Figure 21 - Dll4 endothelial-specific overexpression does not affect the activation of β-catenin in *Apc*$^{Min/+}$ intestinal tumors 67
Figure 22 - Endothelial overexpression of Dll4 decreases proliferation and Lgr5+ stem cell density, not affecting the neoplastic progression and differentiation, in the *Apc*$^{Min/+}$ tumors . 67
Figure 23 - Endothelial Dll4 overexpression seems independent of Cyclin D1 protein expression in *Apc*$^{Min/+}$ intestinal tumors 69
Figure 24 - Dll4-Fc therapy promotes the anti-tumoral activity of erlotinib treatment by reducing the *Apc*$^{Min/+}$ tumor number and volume 77
Figure 25 - Both Dll4-Fc and erlotinib treatments affect the EGFR and Notch pathways in the *Apc*$^{Min/+}$ tumors 79
Figure 26 - Impact of erlotinib and Dll4-Fc treatments, alone and in combination, on the activation of Egfr pathway in *Apc*$^{Min/+}$ small intestine tumors 80
Figure 27 - Effect of erlotinib and Dll4-Fc therapies, alone and in combination, on Egfr pathway activation in *Apc*$^{Min/+}$ large intestine tumors 82
Figure 28 - Dll4-Fc promotes dysfunctional angiogenesis, even when associated with erlotinib treatment, in *Apc*$^{Min/+}$ small intestine tumors 84
Figure 29 - Dll4-Fc promotes dysfunctional angiogenesis, even with concomitant erlotinib therapy, in *Apc*$^{Min/+}$ large intestine tumors 85
Figure 30 - Dll4-Fc promotes *Vegf/Vegfr* gene expression in *Apc*$^{Min/+}$ tumors, even when associated with erlotinib treatment 87
Figure 31 - Dll4-Fc promotes hypoxia and apoptosis, even with concomitant erlotinib therapy, in *Apc*$^{Min/+}$ small and large intestine tumors 87
Figure 32 - Dll4-Fc plus erlotinib have a cumulative negative effect on tumor proliferation and tumor stem cell maintenance in the *Apc*$^{Min/+}$ small intestine 90
Figure 33 - Dll4-Fc plus erlotinib have a cumulative negative effect on tumor proliferation and tumor stem cell maintenance in the *Apc*$^{Min/+}$ large intestine 91
Figure 34 - Dll4-Fc and erlotinib therapies seem to be independent from associated β-catenin activation in the small and large intestine *Apc*$^{Min/+}$ tumors 93
Figure 35 - Dll4-Fc increases the epithelial differentiation, even when associated with erlotinib, and promotes the secretory cell fate in *Apc*$^{Min/+}$ small intestine tumors 95
Figure 36 - Dll4-Fc increases the epithelial differentiation, even when associated with erlotinib, and promotes the secretory cell fate in *Apc*$^{Min/+}$ large intestine tumors 96
Figure 37 - Notch pathway expression pattern in chronically inflamed CR and in CAC 108
Figure 38 - *Dll4*$^{+/-}$ and Dll4-Fc treated mice display a marked reduction in the number and size of colitis-driven CR tumors 109
Figure 39 - Confirmation of the efficacy of the Dll4/Notch pathway blockade 110
Figure 40 - Colitis-driven CR tumors of *Dll4*$^{+/-}$ and Dll4-Fc treated mice display increased vascular density and impaired vascular functionality 111

Figure 41 - *Dll4*$^{+/-}$ and Dll4-Fc treated mice display reduced colitis 113
Figure 42 - Dll4 blockade downregulates innate immunity, M1 macrophage polarization and inflammatory mediators in colitis-driven CR tumors 114
Figure 43 - Dll4 blockade reduces the number of cells positive to IL-4 and mainly to IL-17A and IFN-γ in colitis-driven CR tumors 115
Figure 44 - Dll4 blockade inhibits helper and cytotoxic T cell, but not B cell, accumulation and elevates the number of regulatory T cells in colitis-driven CR tumors 116
Figure 45 – Colitis-driven CR tumors with Dll4 inhibition show increased apoptosis, reduced proliferation, decreased number of Lgr5 positive stem cells, and induction of secretory differentiation 118
Figure 46 - In inflamed large intestine Dll4 inhibition does not affect the number of Lgr5 positive cells, but slightly increases secretory lineages differentiation 119

LIST OF TABLES

Table 1 - Summary of sites of Notch pathway protein expression in the normal small intestine 35
Table 2 - Summary of sites of Notch pathway protein expression in the normal large intestine 35

LIST OF ABBREVIATIONS

ACF – aberrant crypt focus

AES – amino terminal enhancer of split

ADAM – a disintegrin and metalloprotease

Akp3 – alkaline phosphatase 3

Apc – adenomatous polyposis coli

APC – antigen presenting cell

AOM – azoxymethane

Atoh1 – protein atonal homolog 1

ArgI – arginase I

BCAC – beta-catenin-accumulated crypts

bHLH – basic helix-loop-helix

Bmi1 – B lymphoma Mo-MLV insertion region 1 homolog

CAC – colitis-associated cancer

CapIri – capecitabine and irinotecan

CapOx – capecitabine and oxaliplatin

CBCs – columnar base cells

CD – Crohn's disease

CD4/8 – cluster of differentiation 4/8

Cdkn – cyclin-dependent kinase inhibitor

cDNA – complementary deoxyribonucleic acid

CIMP – CpG island methylator phenotype

CRC – colorectal cancer

CSC cancer stem cell

CT – control

DAB – 3,3'-diaminobenzidine

DALM – dysplasia-associated lesion or mass

DAPI – 4´,6-diamidino-2-phenylindole dihydrochloride hydrate

DC – dendritic cell

DCC – deleted in colorectal cancer

Dll – delta-like

DSS – dextran sulfate sodium

EAE – encephalomyelitis

EC – endothelial cell

EGF/R – epidermal growth factor/receptor

FAP – familial adenomatous polyposis

FOBT – fecal occult blood test

FOLFIRI – folinic acid, fluorouracil, and irinotecan

FOLFOX – folinic acid, fluorouracil, and oxaliplatin

FOXP3 – forkhead box P3

GSI – gamma-secretase inhibitor

GSK3β – glycogen synthase kinase-3beta

H-E – hematoxylin and eosin

Hes – hairy and enhancer of split

Hey – hairy/enhancer-of-split related with YRPW motif protein

HNPCC – hereditary non-polyposis colorectal cancer

IBD – inflammatory bowel disease

IL – interleukin

IFN – interferon

iNOS – inducible nitric oxide synthase

Jag – Jagged

KLF4 – Krüppel-like factor 4

KO – knockout

KRAS – Kirsten rat sarcoma viral oncogene homolog

LEF1 – lymphoid enhancer-binding factor 1

Lgr5 – leucine-rich repeat-containing G-protein coupled receptor 5

LOH – loss of heterozygosity

LPS – lipopolysaccharides

Lyz – lysozyme

LT – lymphotoxin

MAPK – mitogen-activated protein kinase

MCP-1 – monocyte chemoattractant protein-1

Min – multiple intestinal neoplasia

mRNA – messenger ribonucleic acid

MSI – microsatellite instability

Muc – mucin

N1/3 – Notch1/Notch3

NF-κB – factor nuclear kappa B

Ngn/Neurog – neurogenin

NICD – Notch intracellular domain

OS – overall survival

PAS – Periodic Acid-Schiff

PBS – phosphate buffered saline

PCNA – proliferating cell nuclear antigen

PECAM-1 – platelet endothelial cell adhesion molecule 1

PFS – progression-free survival

PI3K – Phosphoinositide 3-kinase

PIK3CA – phosphatidylinositol-4,5-bisphosphate 3-kinase, catalytic subunit alpha

PTEN – phosphatase and tensin homolog

RBP-jκ – recombination signal binding protein for immunoglobulin kappa J region

RNA – ribonucleic acid

qRT-PCR – quantitative reverse transcription polymerase chain reaction

RT-PCR – real time polymerase chain reaction

rtTA – reverse tetracycline-controlled transactivator

SEM – standard error of the mean

αSMA – alpha smooth muscle actin

STAT – signal transducer and activator of transcription

Tc – T cytotoxic

TCF – T-cell factor

TEC – thymic epithelial cell

TGF – transforming growth factor

Th – T helper

TKI – tyrosine kinase inhibitor

TLR – toll-like receptor

TNF – tumor necrosis factor

TUNEL – terminal deoxynucleotidytransferase-mediated dUTP nick end labeling

UC – ulcerative colitis

VEGF/R – vascular endothelial growth factor/receptor

1 OBJECTIVES

The main purpose of this work is to identify the role of Dll4/Notch during intestinal tumorigenesis using two mouse models. This thesis is divided in four chapters:

1) Characterization of the protein expression pattern of Notch pathway in *Apc*$^{Min/+}$ tumors compared with the normal WT small and large intestine. This was followed by an evaluation of ubiquitous and endothelial-specific blockade of *Dll4* in the *Apc*$^{Min/+}$ model
2) Analysis of endothelial-specific overexpression of *Dll4* in the *Apc*$^{Min/+}$ model
3) Evaluation of anti-Dll4 (Dll4-Fc) therapy and of its association with the EGFR inhibitor (erlotinib) in the *Apc*$^{Min/+}$ model
4) Characterization of the protein expression pattern of Notch pathway in chronic colitis and in colitis-associated cancer (CAC). This was followed by an evaluation of genetic and therapeutic (Dll4-Fc) Dll4 blockade effect on chronic colitis-associated intestinal tumorigenesis using a chemically induced model (by a carcinogen and a pro-inflammatory agent administration)

2 INTRODUCTION

Colorectal cancer (CRC) is one of the main causes of death in the Western world. It is the third most common cancer type and approximately half a million people die of this disease every year (Jemal et al., 2011). CRC is a very heterogeneous disease that is caused by the interaction of genetic and environmental factors. The majority of CRCs are sporadic (Bogaert & Prenen, 2014). Only a small proportion of cases are hereditary, as familial adenomatous polyposis (FAP) (Bogaert & Prenen, 2014). CRC can also be associated to chronic inflammation, as a long-term complication of Crohn's disease (CD) (Ekbom, Helmick, Zack, & Adami, 1990) and ulcerative colitis (UC) (Svartz & Ernberg, 1949). Mouse models of CRC allow us to understand the mechanisms that lead to initiation and progression of this disease (Corpet & Pierre, 2005). Despite increasing advances, prognosis for advanced CRC patients remains bleak due to recurrence and toxicity (Eng, 2009), reinforcing the need for novel therapeutic intervention, preventive strategies and chemopreventive agents. The Notch signaling pathway can provide opportunities to address this urgent need. This pathway is involved in multiple and relevant cell functions in the normal development and in physiological and pathological processes (Aster, 2014). Notch receptors, ligands, and target genes are expressed in the embryonic and adult intestine (Sander & Powell, 2004; Schroder

& Gossler, 2002). Functionally Notch and Wnt signaling cooperatively regulate cell proliferation and tumorigenesis in the intestine (Fre et al., 2009). Studies indicated that Dll4/Notch blockade inhibits tumor growth by promoting dysfunctional and immature tumor angiogenesis in a variety of xenograft and autochthonous models of different types of cancer, including CRC (Djokovic et al., 2010; Hoey et al., 2009; Noguera-Troise et al., 2006; Ridgway et al., 2006; Scehnet et al., 2007). However, there are concerns about the ability of nonfunctional blood vessels to normalize leading to tumor regrowth and that this noncompetent vasculature may impair the delivery of other anti-cancer drugs to the tumors. In addition, there are also concerns about potential toxicity of chronic Dll4 blockade (Djokovic et al., 2010; J. L. Li, Jubb, & Harris, 2010; Minhong Yan et al., 2010) and hypoxia-induced malignancy (Hayden, 2009). Therefore, activation of Dll4, which negatively regulates VEGF signaling (Williams, Li, Murga, Harris, & Tosato, 2006), is being considered as an anti-angiogenic strategy to treat cancer (J. L. Li et al., 2007; Segarra et al., 2008). However, reports showed contradictory results regarding the effect of Dll4 activation on tumor growth and further studies are necessary to unveil this question. In CRC this approach has never been studied, but as blocking Dll4 in the colorectal tumor has a direct anti-cancer effect (Hoey et al., 2009), the opposite approach may presumably promote cancer. Nevertheless, we can speculate that the activation of Dll4 specifically in the endothelium can possibly represent a beneficial strategy to suppress CRC growth.

Dll4-mediated signaling and therapeutic approaches have been extensively studied in cancer, mainly focusing on its angiogenic phenotype. In CRC Dll4/Notch signaling seems to have an additional role maintaining the cancer stem cell population (M. Fischer et al., 2010; Hoey et al., 2009). However, little is known about the impact of this pathway on benign or premalignant colorectal tumors and it may be useful to understand the role of this pathway on CRC initiation and to develop possible chemoprevention strategies and nonsurgical treatment for benign tumors without the need of chemotherapeutics, mainly in patients highly predisposed to develop CRC.

Therefore, our goal was to analyze the expression and dissect the functions of Dll4/Notch in two well-established mouse models that mimic the development of human CRC. One of the models used is the autochthonous transgenic mouse model *Apc*$^{Min/+}$ (Yasuhiro Yamada & Mori, 2007). The other is induced by the carcinogen azoxymethane followed by the pro-inflammatory agent dextran sulfate sodium salt administration to promote chronic colitis-associated cancer (CAC) (Clemens Neufert, Christoph Becker, & Markus F. Neurath, 2007). Additionally, we analyzed if the noncompetent vasculature associated to anti-Dll4 therapy impaired the delivery of other anti-cancer drugs to the tumor. One of the strategies used in the clinics to improve the efficacy of standard CRC treatment is blocking EGFR pathway (Rolfo et al., 2014). In addition, a relationship of Notch and EGFR pathways was found in lung, breast and skin cancers and in gliomas (Dong, Li, Wang, Weber, & Michel, 2010; H.

Yamaguchi, Chang, Hsu, & Hung, 2014). Therefore we combined the Dll4/Notch inhibitor Dll4-Fc, a fusion protein that binds to Notch receptors and acts as dominant-negative, with an EGFR tyrosine kinase inhibitor (TKI), erlotinib. This allowed us to understand if this association could be beneficial to treat patients with CRC. These studies were converted into the four chapters of this thesis:

1. Delta-like 4/Notch signaling promotes *Apc*$^{Min/+}$ tumor initiation through angiogenic and non-angiogenic related mechanisms

Badenes, M., Trindade, A., Pissarra, H., Costa, L., Duarte, A.

2. Delta-like 4 endothelial overexpression decreases the vascularity of intestinal adenomas in *Apc*$^{Min/+}$ mice reducing tumor multiplicity and growth

Badenes, M., Trindade, A., Pissarra, H., Costa, L., Duarte, A.

3. Delta-like 4/Notch inhibition has a synergistic effect with anti-Egfr therapy on *Apc*$^{Min/+}$ tumorigenesis

Badenes, M., Trindade, A., Pissarra, H., Liu, R., Krasperonov, V., Gill, S.P., Costa, L., Duarte, A.

4. Delta-like 4/Notch signaling blockade inhibits the development of chronic colitis-associated colorectal cancer in mouse model

Badenes, M., Trindade, A., Pissarra, H., Liu, R., Carinhas, J., Krasperonov, V., Gill, S.P., Costa, L., Duarte, A.

3 LITERATURE REVIEW

3.1 Intestinal morphology and homeostasis

In mammals the functions of the intestinal tract are digestion, absorption of nutrients, expelling waste and protection against luminal pathogens. The demands of these functions are compensated by its remarkable capacity for cell renewal, where the turnover rate for the entire epithelial population is approximately 60 hours (Cheng & Bjerknes, 1983).

The intestinal tract is divided in the small and large intestine. The small intestine comprises the duodenum, jejunum and ileum. The large intestine consists of the cecum, colon, rectum and the anal canal. The human colon is divided into different sections (i.e. ascending, transverse and descending colon) with the presence of taenia coli and compartmentalization in haustra, which are absent in the mouse colon.

The intestinal tract can be divided into four concentric layers. The mucosa in the innermost layer and is composed by the epithelium (columnar simple), the *lamina propria* (a layer of connective tissue) and the *muscularis mucosae* (a thin layer of smooth muscle). The *lamina propria* besides having numerous blood and lymphatic vessels and collagen has lymphocytes and plasma cells. These cells form part of the defense mechanisms against invading pathogens along with intra-epithelial lymphocytes and lymphoid aggregates that are found in the *lamina propria* and submucosa. The submucosa consists of a dense layer of connective tissue with blood and lymphatic vessels and the Meissner's nervous plexus. The *muscularis externa* has an inner circular layer and a longitudinal outer layer of smooth muscle. Between the two muscle layers we find the myenteric or Auerbach's plexus. The *adventitia* or serosa is the outermost layer and consists of several layers of connective tissue (Fig. 1). However, certain regions of the intestine have some exclusive characteristics. For example, the duodenum has Brünner glands in the submucosa and the ileum has lymphatic aggregates in the submucosa called Peyer's patches (Reed & Wickham, 2009).

Figure 1 - Mouse small and large intestine histology. *In* (King, 2002)

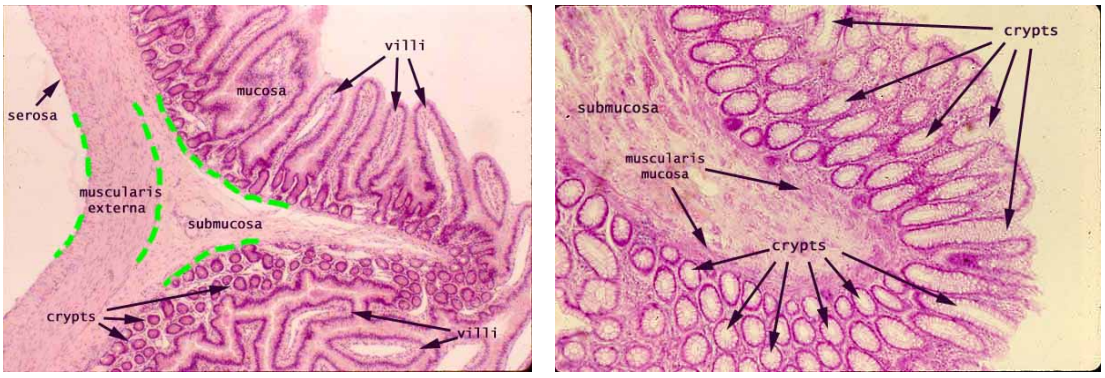

SMALL INTESTINE LARGE INTESTINE

To increase the absorptive surface area, the small intestine has finger-like projections into the intestinal lumen called *villi*. Furthermore each *villus* has many *microvilli*, which are enterocyte membrane protrusions that form the brush border. The *villi* contain terminally differentiated cells connected to the crypts of Lieberkühn. These are finger-like invaginations into the underlying connective tissue that harbor the proliferative compartment. The large intestine instead of *villi* has a flat surface epithelium. The crypt epithelium cycles asynchronously, and new crypts arise through bifurcation (crypt fission) during adult life as the intestinal tract continues to grow (Totafurno, Bjerknes, & Cheng, 1987). Stem cell numbers have been estimated to be 4-6 per crypt in the adult (Marshman, Booth, & Potten, 2002; Potten, 1998). However their precise location within the crypts is unclear. The consensus is that in the large intestine stem cells reside at the bottom of the crypts, while for the small intestine there is a unifying theory based on the +4 model and stem cell zone model (Bach, Renehan, & Potten, 2000; Bjerknes & Cheng, 1999; Booth & Potten, 2000) (Bach et al., 2000; Booth & Potten, 2000; Stappenbeck, Mills, & Gordon, 2003; W. M. Wong & Wright, 1999). This theory indicates that are two distinct stem cell pools. One is the columnar base cells (CBCs) (Cheng & Leblond, 1974) with a high turnover, expressing the leucine-rich repeat-containing G-protein coupled receptor 5 (Lgr5) (Barker et al., 2007). The other is a quiescent label retaining population located 4 cells above the Paneth cells, expressing B lymphoma Mo-MLV insertion region 1 homolog (Bmi1) (Potten, Owen, & Booth, 2002; Sangiorgi & Capecchi, 2008). These two distinct stem cell populations act cooperatively to support normal physiologic cell replenishment and tissue repair (L. Li & Clevers, 2010). However, +4 cells are also labeled with Lgr5 lineage markers (Snippert et al., 2010), suggesting that both lineages are derived from CBCs. Additionally, it seems that the immediate descendants of stem cells located up to position 7 could be recruited to become new stem cells after injury (Marshman et al., 2002; Potten, 1998) Crypt stem cells have symmetric and asymmetric division. Thus, they self-renew throughout life and generate a transient population of progenitor cells called the transit-amplifying cells. After several rounds

of division, these cells differentiate into absorptive cells or enterocytes/colonocytes and secretory cells. The absorptive cells are involved in nutrient uptake and secretion of hydrolases and constitute the majority of cells in the intestinal epithelium. Secretory cells consist of the mucus-producing goblet cells, the hormone-producing enteroendocrine cells, the opioids and cyclooxygenase enzymes-secreting tuft cells and the antimicrobial lysozyme and defensins-producing Paneth cells. The epithelium contains also other cell types with poorly defined functions named cup cells and Peyer's patch-associated M (or microfold) cells (Potten, 1998) (Fig. 2).

Figure 2 - Model for the differentiation of the intestinal epithelial cell types. *In* (Gerbe et al., 2011)

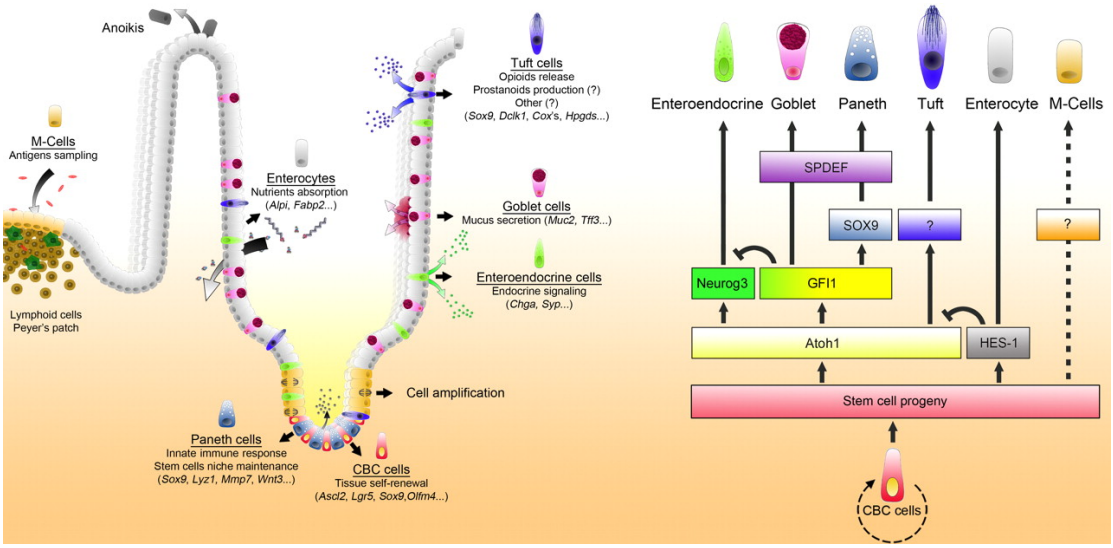

Excluding Paneth cells, the differentiated cells are located in the top of the intestinal epithelium and have an average life span of less than a week. Then they undergo apoptosis and are shed into the intestinal lumen, a process called exfoliation. Paneth cells migrate into the crypt bottom, where they reside for about 20 days before being phagocytized. These cells are only present in the small intestine (Porter, Bevins, Ghosh, & Ganz, 2002). Besides secreting bactericidal substances, Paneth cells also produce large amounts of factors, such as epidermal growth factor (EGF), transforming growth factor α (TGF-α) and Wnt3, and they express the Notch ligand Dll4 (Sato et al., 2011). *In vitro* studies indicated that these cells seem important for Lgr5+ stem cell renewal (Sato et al., 2011). Whether this occurs *in vivo* is currently under debate. As they are absent in the colon, CD24+ cells adjacent to Lgr5+ stem cells may function similarly to the Paneth cell niche in this region (Sato et al., 2011).

Epithelial homeostasis is ensured through three mechanisms. First, cells are being continuously shed at the tip of the epithelium to counterbalance the crypt cell production

(Potten, 1998). Second, the cells in the intestinal epithelium are continuously moving upwards with a transit time of approximately 5 days, excluding the Paneth and stem cells. And third, there are two distinct proliferative and differentiated compartments (Hermiston, Wong, & Gordon, 1996). Coordination between cell renewal, transit amplification, terminal differentiation, and apoptosis requires a precise interplay among several signaling pathways. In addition, the regulation to maintain this balance is highly flexible and dynamic, as proliferation of precursor cells is accelerated in response to injury (Buczacki et al., 2013; Tian et al., 2011).

3.2 Signaling pathways in intestinal development and CRC

Some developmental signaling pathways, such as Wnt, Notch, TGF-β/Bone morphogenic protein and Hedgehog, play a critical role tightly regulating and controlling the differentiation and homeostasis of the intestine. Moreover, the same pathways appear to be deregulated in several hereditary and sporadic CRCs (Radtke, Clevers, & Riccio, 2006). Other important pathways implicated in CRC development are EGFR (Krasinskas, 2011) and VEGF/VEGFR signalings (Mihalache & Rogoveanu, 2014).

3.2.1 Wnt signaling

There are about 20 different secreted Wnt proteins, which bind to about 10 different Frizzled receptors. In the absence of Wnt signals, β-catenin is retained in a multi-protein complex including APC, the scaffold protein axin, casein kinase-1 and glycogen synthase kinase-3β (GSK3β), where it is phosphorylated and subsequently degraded (Huelsken & Birchmeier, 2001). Transduction of canonical Wnt signals results in nuclear translocation of β-catenin, which interacts with the transcription factors Lymphoid enhancer-binding factor 1 (LEF1)/T-cell factor (TCF) resulting in activation of target genes (de Lau, Barker, & Clevers, 2007). Wnt signaling plays multiple roles during gut homeostasis. It is considered the gatekeeper for crypt progenitor cells by controlling the progenitor gene expression program. It is also necessary for differentiation of the secretory cell lineages and separation of proliferating undifferentiated and post-mitotic differentiated cells (Pinto, Gregorieff, Begthel, & Clevers, 2003). This gradient of β-catenin-TCF activity imposes restrictions on the migratory behavior of the intestinal epithelial cells by establishing the expression of EphB2/3 receptors and their Ephrin-B1/2 ligands inversely along the crypt/*villus* axis. Additionally, this is also responsible for the positioning of Paneth cells near the base of the crypts (Batlle et al., 2002). Additionally, Wnt signaling also regulates these cells maturation, as a substantial number of TCF4 target genes are typical Paneth cell markers such as defensins and peptidoglycan recognition proteins (van Es, Jay, et al., 2005). β-catenin has an additional role as a component of adherent junctions as it binds to the cytoplasmic tail of Cadherin proteins, thereby linking them to the cytoskeleton of

epithelial cells. The mechanisms controlling whether β-catenin joins the signaling pool or is part of adherens junctions is currently unknown (Nelson & Nusse, 2004).

Most sporadic CRCs show bi-allelic inactivation of the *APC* gene. A high percentage of remaining tumors show activating mutations in β-catenin or axin (Giles, van Es, & Clevers, 2003; Huelsken & Birchmeier, 2001; Polakis, 2000). These phenomena lead to increased nuclear translocation of β-catenin and constitutive signaling (Sansom, 2004) and this seems to occur early during CRC development (Bienz & Clevers, 2000). Gene expression profile analysis of CRC tumor cells revealed a set of about 100 β-catenin/TCF target genes (van de Wetering et al., 2002). These molecules are consistently expressed in dysplastic crypts and adenomas and also in normal intestinal progenitors cells at the bottom of the crypts (van de Wetering et al., 2002). Therefore it seems that adenoma cells represent the transformed counterpart of crypt cells (van de Wetering et al., 2002). Additionally, these target genes, such as c-myc (He et al., 1998), cyclin D1 (Tetsu & McCormick, 1999) and matrix metalloproteinase matrilysin (Brabletz, Jung, Dag, Hlubek, & Kirchner, 1999; Crawford et al., 1999), are responsible for tumor proliferation and malignant progression.

3.2.2 Notch signaling

The Notch signaling is a highly conserved evolutionary regulatory pathway. The denomination has its origin in the discovery of notches at the margin of wing blades of fruit flies (*Drosophila melanogaster*) with partial Notch gene loss of function (Moohr, 1919; Morgan, 1917). Notch signaling regulates numerous cell processes, such as proliferation, apoptosis, fate decisions and differentiation, during both fetal and postnatal development (Artavanis-Tsakonas, Rand, & Lake, 1999). Mammals possess four receptors (Notch1-4) (Gridley, 1997), and five ligands: Jagged1 and Jagged2 (homologues of Serrate) and Delta-like1, 3 and 4 (homologues of Delta) (Artavanis-Tsakonas et al., 1999). The Notch receptors and their ligands are single-pass transmembrane protein molecules with large extracellular domains that basically consist of epidermal growth factor (EGF)-like repeats (Bray, 2006). Notch signaling is initiated by ligand binding to the extracellular domain of Notch receptors, triggering proteolytic cleavages within the receptor. This is first mediated by ADAM-family metalloproteases and next by γ-secretase activity (Bray, 2006). The liberated Notch intracellular domain (NICD) then translocates to the nucleus and binds the transcription factor recombination signal binding protein for immunoglobulin kappa J region (RBP-jκ), converting it from a transcriptional repressor into a transcriptional activator by displacing corepressor complexes (Hsieh, Zhou, Chen, Young, & Hayward, 1999; Jeffries, Robbins, & Capobianco, 2002; Zhou et al., 2000) and recruiting coactivators (Jeffries et al., 2002; L. Wu et al., 2000) (Fig. 3). The most studied Notch target genes are the basic helix-loop-helix (bHLH) transcription factors of the hairy and enhancer of split (HES) family and HES-related repressor proteins (HERP, HESR, HRT or HEY) (A. Fischer & Gessler, 2007;

Iso et al., 2001; Ohtsuka et al., 1999). Canonically, these proteins inhibit the expression of target genes by forming complexes with co-repressors (A. Fischer & Gessler, 2007). Recent studies indicated that Notch exerts biological functions also non-canonically, by enhancing NF-κB activity (Shin et al., 2006) and post-translationally targeting Wnt/beta-catenin signaling (Andersen, Uosaki, Shenje, & Kwon, 2012). Additionally, Notch signaling without direct cell contact has also been reported (Lu et al., 2013; Sheldon et al., 2010).

Figure 3- The Notch pathway. *In* (Radtke, Fasnacht, & Macdonald, 2010)

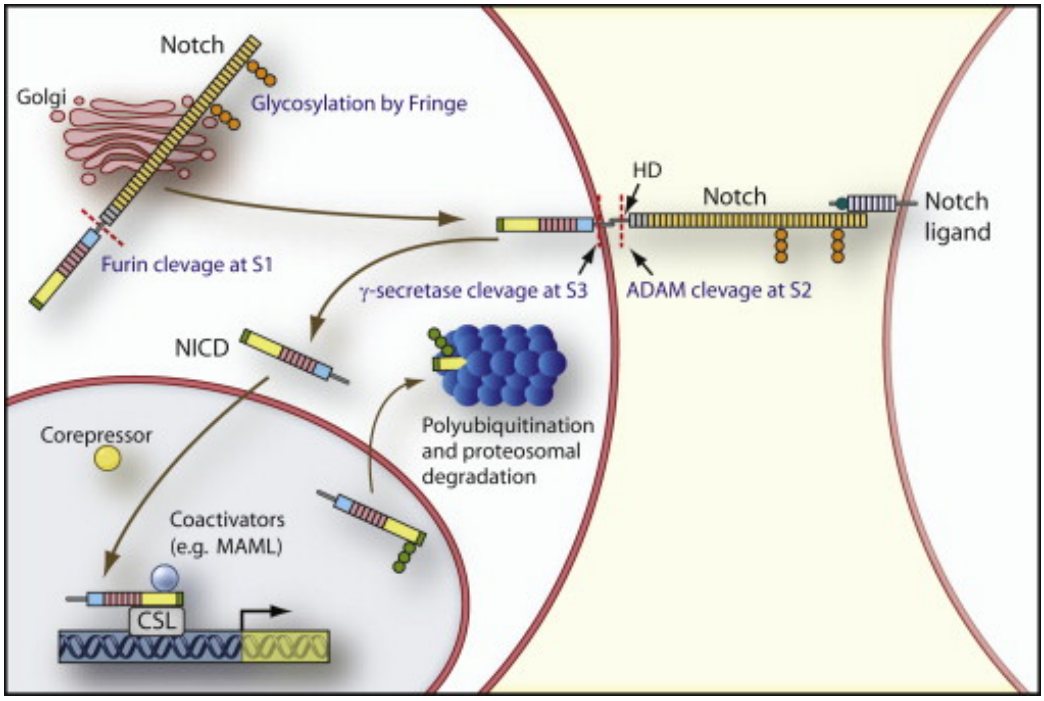

3.2.2.1 Notch in intestinal homeostasis

Notch receptors, ligands, and canonical target genes are expressed in the embryonic and adult intestine. Studies indicated that Notch1 is expressed in the crypt epithelium, in a few differentiated *villus* epithelial cells, and in the endothelium. Notch2 is only expressed in scattered cells within the crypt epithelium of the small intestine and in smooth muscle cells. Notch3 and Notch4 expression is restricted to the endothelium and the mesenchyme. Notch ligands Jagged1 and Jagged2 follow mostly the expression pattern of Notch1 in the epithelium and of Notch2 in the smooth muscle (Sander & Powell, 2004; Schroder & Gossler, 2002). Dll1 and Dll4 are both expressed in the crypt epithelium and in goblet cells and Dll4 is also in the endothelium (Benedito & Duarte, 2005; Schroder & Gossler, 2002) and in Paneth cells (Sato et al., 2011). N1ICD and Hes1, 5, 6, and 7 are detected in the crypt epithelium (Schroder & Gossler, 2002; Vooijs et al., 2007). Additionally, the expression of Hes1 is coincident with Ki-67 labeling of proliferating cells (Kayahara et al., 2003). Hes5 is also expressed in the *villus* epithelium (Schroder & Gossler, 2002). This wide expression pattern suggests that Notch signaling may play multiple roles in the

intestine. The first direct genetic evidence showing an essential role of Notch signaling for the gut homeostasis was derived from inducible tissue specific inactivation of RBP-jκ. Notch pathway appears to synergize with Wnt signaling as gatekeepers of self-renewal in the intestinal epithelium (Fre et al., 2009). Studies of Notch 1 and 2 loss- and gain-of-function and toxicology studies of γ-secretase inhibitors (GSIs) suggested that Notch 1 and 2 are redundant and essential for the maintenance of intestinal progenitor/stem cell compartment by repressing of the cyclin-dependent kinase inhibitors 1B and 1C. They also showed that Notch has an additional role suppressing secretory fate when transit-amplifying cells differentiate (Fre et al., 2005; Milano et al., 2004; Riccio et al., 2008; Stanger, Datar, Murtaugh, & Melton, 2005; van Es, van Gijn, et al., 2005; VanDussen et al., 2012; Vooijs et al., 2007; G. T. Wong et al., 2004) (Fig. 4).

Figure 4 - Notch signaling in intestinal homeostasis. *In* (Vooijs, Liu, & Kopan, 2011)

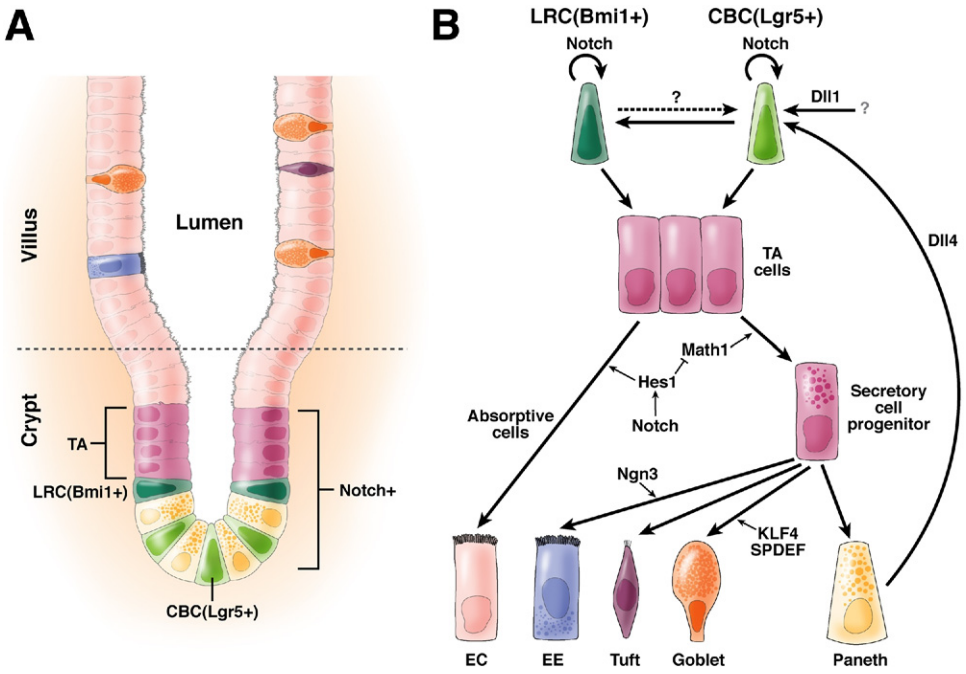

Interestingly, ectopic expression of N1ICD in intestinal crypts is characterized by Hes1 (but not Hes5) up-regulation and suppression of Atoh1 and Neurogenin3 (Ngn-3) in the cycling progenitors cells (Fre et al., 2005; Stanger et al., 2005). Atoh1 is required for the differentiation of secretory cell lineages and is transcriptionally repressed by Hes1 in the intestine (Yang, Bermingham, Finegold, & Zoghbi, 2001). In addition, Hes1 seems to repress the goblet cell fate driver Krüppel-like factor 4 (KLF4) upstream and downstream of Atoh1 (Ghaleb, Aggarwal, Bialkowska, Nandan, & Yang, 2008; Kim & Shivdasani, 2011). However, it seems that KLF4 acts downstream of Atoh1 and probably in a redundant manner (van Es, de Geest, van de Born, Clevers, & Hassan, 2010). Therefore Notch-mediated Hes1 expression regulates a binary cell fate decision of intestinal

progenitors that have to choose between absorptive or secretory cell fates. Additionally, it may also control the binary cell fate decision that occurs within secretory cell lineages that specifies enteroendocrine *versus* mucus secreting cells, which is regulated by Ngn-3 (Jenny et al., 2002). In post-mitotic *villus* epithelial cells N1ICD overexpression is accompanied by elevated expression of Hes5 (but not Hes1) and leads to increased goblet cell numbers with other secretory cell types unaffected (Zecchini, Domaschenz, Winton, & Jones, 2005). Thus, Notch may induce goblet cell fate through Hes5 in a Hes1-Atoh1–independent manner in post-mitotic precursors. Additionally, Notch may also affect Paneth cell localization directly by inducing the expression of Ephrin-B1 and indirectly by down-regulating EphB3 through β-catenin/TCF4 inactivation (Batlle et al., 2002; Koo et al., 2009)
There is significant crosstalk between Notch and Wnt signaling during intestinal homeostasis, as these two pathways interact through GSK3β (Espinosa, Ingles-Esteve, Aguilera, & Bigas, 2003; Koo et al., 2009). Furthermore, Notch ligands are transcriptionally regulated by Wnt-β-catenin through multiple TCF/LEF1 binding sites in their promoters (Galceran, Sustmann, Hsu, Folberth, & Grosschedl, 2004; Hofmann et al., 2004; Rodilla et al., 2009). As Wnt signaling is important for Paneth cells maintenance (van Es, Jay, et al., 2005), this pathway may drive Dll4 expression. Additional regulation of Notch pathway by Wnt may be through direct transcriptional regulation of the Wnt target gene *Musashi* expressed in CBCs (Kayahara et al., 2003). It seems that Wnt signaling is more important in controlling proliferation while Notch pathway has a more important role in suppressing cell fate during development (Fre et al., 2009).
Genetic loss of *Dll1*, but not of *Dll4* or *Jag1*, causes increased goblet cell numbers in the adult intestine, suggesting that Dll1 is the most important Notch ligand in the crypt. Nevertheless, simultaneous inactivation of Dll4, but not Jagged1, with Dll1 leads to enhanced goblet cell metaplasia and proliferative arrest (Pellegrinet et al., 2011). This suggests that Dll4 can compensate for Dll1 loss whereas Jagged1 is not signaling in the niche. It seems that differentiated Dll-expressing committed secretory cells signal back to Notch-expressing progenitors to control cell number and fate, analogous to the possible Paneth-CBC interaction in the crypt.

3.2.2.2 Notch in CRC

Sporadic CRC usually develops from certain precancerous conditions such as colorectal adenomatous polyps and inflammatory bowel disease (IBD). Increased Notch signaling may be linked to the increased susceptibility of CRC development in these precancerous conditions (Fre et al., 2009; Gersemann et al., 2009; Okamoto et al., 2009; Rodilla et al., 2009; van Es, van Gijn, et al., 2005).
Studies have shown that Notch receptors, ligands and some target genes are expressed in adenomas from $Apc^{Min/+}$ mice (van Es, van Gijn, et al., 2005), in colorectal cancer cell lines

and primary carcinomas (Fernandez-Majada et al., 2007; Guilmeau, Flandez, Mariadason, & Augenlicht, 2010; Jubb et al., 2009; Peignon et al., 2011; Rodilla et al., 2009). A report indicated that Notch1 and Hes1 showed progressively increased expression from normal colonic mucosa to primary and metastastic colon cancer (Meng et al., 2009). However, other studies reported that Hes1 expression is reduced in colon carcinomas and corresponding metastases compared with adenomas (Fre et al., 2009; Veenendaal et al., 2008). Interestingly, high Notch1 expression is associated with poor survival, whereas high Notch2 expression is associated with better survival (Chu et al., 2011; Zecchini et al., 2005). Other authors found no significant difference in survival between Hes1-expressing tumors and non-expressing tumors (Reedijk et al., 2008).

Lineage tracing in $Apc^{Min/+}$ mice has shown that the tumor-initiating cells in $Apc^{-/-}$ adenomas arise from Notch1 marked clones (Vooijs et al., 2007). Accordingly, *in vitro* experiments showed that Notch activation is important for expansion of tumor-initiating cells from CRC specimens (Sikandar et al., 2010). Notch pathway blockade through gamma secretase inhibitors (GSIs) and targeting Jagged1 significantly inhibited the formation of intestinal adenoma in $Apc^{Min/+}$ mice and suppressed growth in colon cancer cell lines (Dai et al., 2014; Ghaleb et al., 2008; Rodilla et al., 2009; Zheng et al., 2009). Additionally, Notch inhibition induced re-differentiation of colonic adenoma cells into secretory cells (van Es, van Gijn, et al., 2005). Thus, Notch activation may be an essential initial event triggering CRC and may function as an oncogene (Qiao & Wong, 2009).

During colorectal carcinogenesis Notch interacts with numerous pathways, including Wnt (Qiao & Wong, 2009). Activation of the Notch and the Wnt pathways occurs simultaneously in proliferating adenomas, as in intestinal crypts. However, GSI treatment of adenomas induces secretory cell differentiation and reduces proliferation, despite the fact that Wnt signaling remains active (van Es, van Gijn, et al., 2005). Nevertheless, a study revealed that the Notch ligand Jagged1 is a direct target of Wnt signaling (Rodilla et al., 2009). However, not all tumors with elevated Wnt signaling display elevated Jagged1 (Guilmeau et al., 2010).

In addition, the receptors Notch1 and 4 and the ligands Jagged1, Dll1, and Dll4 are expressed by vascular endothelial cells and are involved in sprouting angiogenesis promoting tumor growth (Kerbel, 2008).

Notch signaling may also affect the later stages of CRC. Indeed, Sonoshita *et al.* reported that the Notch inhibitor amino terminal enhancer of split (AES) gene is downregulated in human colon liver metastases and in the invasive front of primary tumors (Sonoshita et al., 2011). Furthermore, genetic depletion of this gene in *Apc* mutant mice caused marked tumor invasion and intravasation that were suppressed by Notch signaling inhibition (Sonoshita et al., 2011).

Additionally, activation of Notch signaling may also contribute to the development of CRC

treatment resistance (Akiyoshi et al., 2008; Meng et al., 2009).

Consequently, inactivation of Notch signaling may be used to treat CRC and may involve several mechanisms of action, such as inhibition of cell proliferation associated genes (c-Myc, cyclin-D1), Phosphoinositide 3-kinase (PI3K)/ protein kinase B (AKT), EGF/EGFR, NF-κB and TGF-β pathways, anti-apoptotic genes, angiogenesis and CSCs (Qiao & Wong, 2009). Although much is known, anti-cancer Notch-based effective therapies, such as Notch receptors and ligands specific antibodies, decoys, GSIs and blocking peptides, are still in development and being tested in preclinical and clinical trials. GSIs have been the most broadly developed, but they lack specificity and are associated to gastrointestinal side effects and low response rates (Previs, Coleman, Harris, & Sood, 2015). More selective and potent inhibitors and selected combinations with chemotherapy or other biologically targeted drugs are being pursued.

3.2.2.3 Notch during chronic inflammation

In more recent years, investigators found increasing evidence that Notch plays important roles during T cell-mediated immune responses, in particular for the regulation of CD4+ T helper (Th) cell differentiation. Th1 cells are activated by IL-12 secreted by the antigen-presenting cells (APCs) and produce the classical proinflammatory cytokines interferon (IFN)-γ and tumor necrosis factor (TNF)-α, and IL-2. Th1 response is responsible for killing intracellular parasites by macrophages (by superoxide and nitric oxid secretion), activating cytotoxic lymphocytes and in excess they perpetuate autoimmune diseases (Mayer, 2010). Th2 cells produce IL-4, IL-5, IL-6 and IL-13, which promote IgE and eosinophilic responses in atopy, and also the anti-inflammatory IL-10 cytokine (Roda, Marocchi, Sartini, & Roda, 2011). In excess, Th2 responses counteract the Th1 mediated microbicidal action. Therefore Th1 and Th2 subpopulations are mutually regulated to maintain a balanced immune response. Specifically, IFN-γ downregulates the Th2-mediated responses, while IL-4, IL-10, and IL-13 inhibit the Th1-mediated responses (Roda et al., 2011). There is a third Th subpopulation, the Th17 cells, which produce IL-17, IL-17F, IL-22, and IL-21. Th17 cells promote the elimination of pathogens during host defense reactions and induce tissue inflammation during autoimmune diseases (Korn, Bettelli, Oukka, & Kuchroo, 2009). TGF-β plus IL-6, IL-21, IL-23, STAT3 and RORγt, and α are involved in Th17 cells development. The Th17 lineage is in close relationship with CD4+CD25+FOXP3+ regulatory T cells (Tregs), as TGF-β also induces differentiation of naive T cells into Foxp3+ Tregs in the peripheral immune compartment (Korn et al., 2009). These cells have an important immunosuppressive role negatively regulating hyperactive T cell responses in peripheral tissues by the production of inhibitory cytokines such as IL-10 and TGF-β, suppression by cytolysis, suppression by metabolic disruption, and suppression by modulation of dendritic-cell (DC) maturation or function (Sakaguchi, Wing, Onishi, Prieto-Martin, & Yamaguchi,

2009; Vignali, Collison, & Workman, 2008).

Within the immune system, Notch receptors are expressed on T cells and interact with the ligands expressed mainly on APCs (Amsen et al., 2004; Maillard, Fang, & Pear, 2005; E. Yamaguchi et al., 2002). Studies indicated that APCs driving a Th1 cell response show upregulation of Dll4 and/or Dll1 (Amsen et al., 2004; Skokos & Nussenzweig, 2007; Sun, Krawczyk, & Pearce, 2008), while upregulation of Jagged ligands occur during Th2 cell responses (Amsen et al., 2004; Krawczyk, Sun, & Pearce, 2008; Rutz et al., 2008; Skokos & Nussenzweig, 2007; Sun et al., 2008). Indeed, ectopic expression of Dll ligands on DCs promoted Th1 cell response and inhibited Th2 cell differentiation by interfering with IL-4 receptor signaling, whereas Jagged ligands on APCs induced Th2 cell differentiation (Amsen et al., 2004; Krawczyk et al., 2008). Additionally, Dll4 expressing DCs induce IL-10 production by Th1 cells *in vitro* and *in vivo* upon Toll-like receptor (TLR) stimulation (Rutz et al., 2008). Moreover, blocking Dll4/Notch signaling enhanced Th2 differentiation and cytokine production in Th2-mediated diseases (Fukushima et al., 2008; Jang, Schaller, Berlin, & Lukacs, 2010). Studies indicated that Notch3, rather than Notch1, may be implicated in Dll-induced Th1 cell differentiation, through regulation of protein kinase C theta (Jurynczyk, Jurewicz, Raine, & Selmaj, 2008; Maekawa et al., 2003; Minter et al., 2005; Tacchini-Cottier, Allenbach, Otten, & Radtke, 2004). However, Notch1 signaling with Dll4 seems to be the main mediator of the Th1 cell response during graft-versus-host-disease (Tran et al., 2013) and to upregulate the Th1 IFN-γ cytokine in peripheral T cells through NF-kB activation (Shin et al., 2006). Additionally, Notch may also mediate Th1 differentiation through transcriptionally regulating the expression of the transcription factor T-bet (Minter et al., 2005). However, genetic loss-of-function experiments indicated that Notch signaling is dispensable for Th1 cell differentiation, but essential for the development of Th2 cell immune responses in physiological settings such as parasite infection (Amsen et al., 2007). Additionally, the Th2 promoters Il4 and Gata3 were identified as two direct Notch target genes (Amsen et al., 2007; Amsen et al., 2004; Fang et al., 2007; S. Tanaka et al., 2006). Moreover, GATA3 may help to render the Il4 enhancer accessible to Notch (Fang et al., 2007). Furthermore, Dll4-expressing DCs, when activated with TLR ligands or *Mycobacterium* antigens, can also promote the generation of Th17 cells through activation of the specific transcription factor RORγt (Ito et al., 2009; Mukherjee, Schaller, Neupane, Kunkel, & Lukacs, 2009). In autoimmune diseases GSI-mediated inhibition and anti-Dll4 therapy ameliorated the disease by suppressing Th1 and Th17 cell responses (Bassil et al., 2011; Jiao et al., 2014; Minter et al., 2005; Mukherjee et al., 2009; Takeichi et al., 2010). Additionally, inhibition of Dll4 alleviated experimental autoimmune encephalomyelitis (EAE) by promoting Treg development through downregulation of JAK3/STAT5 pathway (Bassil et al., 2011). Inhibition of Dll1 also attenuated EAE by decreasing the frequencies of Th1 and Th2

effector cells while inhibition of Jagged1 exacerbated this disease (Elyaman et al., 2007). However, inhibition of both ligands had no effect on frequencies of Th17 and Treg cells (Elyaman et al., 2007). Therefore this data suggests that Dll ligands on DCs seem to promote pathogenic Th1 and Th17 cells, whereas Jagged ligands might suppress autoimmunity. Additionally, Notch may suppress autoimmunity through its influence on Treg cells as Notch ligands (mostly Jagged) and overexpression of N3ICD positively enhance Treg cell differentiation and function (Anastasi et al., 2003; Campese et al., 2009; Kared et al., 2006; Vigouroux et al., 2003). Specifically, Notch may regulate Treg cells by cooperating with TGF-β signaling components (P-Smad3) to activate FOXP3 expression (Samon et al., 2008).

In addition, DLL4 and all Notch receptors are expressed and functional in macrophages and Dll4/Notch signaling inhibition seems to reduce atherosclerotic inflammation through decreased macrophage accumulation, diminished expression of monocyte chemoattractant protein-1 (MCP-1) and lower levels of NF-κB activation (Fukuda et al., 2012; Fung et al., 2007). A concept is emerging that macrophages can be polarized to favor inflammation (M1) or to suppress inflammation (M2). M1 macrophages are induced in response to lipopolysaccharides (LPS) and IFN-γ and produce inducible nitric oxide synthase (iNOS), TNF-α, IL-1, IL-6, and IL-12 (Y. C. Liu, Zou, Chai, & Yao, 2014). M2 macrophages express arginase-1 and mannose receptor and are induced in response to IL-4, IL-10 and IL-13. This type of macrophages also stimulates cell proliferation, collagen production, angiogenesis, tissue remodeling and tumor progression (El Kaffas et al., 2014). Dll4 seems to have a role skewing macrophages towards a pro-inflammatory phenotype (M1) (Fukuda et al., 2012).

3.2.2.4 Delta-like 4

Delta-*like* 4 is one of the Notch pathway ligands in mammals (Krebs et al., 2004). Binding studies and *in vitro* signal transduction studies indicate that DLL4 is readily able to signal through all Notch receptors, which is even complicated by the potential compensatory action of other Notch ligands. LacZ reporter studies in developing mouse embryos have revealed Dll4 expression in the vascular, nervous, gastrointestinal and urinary system and in the thymus (Benedito & Duarte, 2005).

Genetic studies indicated that Dll4 haploinsufficiency and overexpression result in embryonic lethality due to vascular defects (Duarte, 2004; Gale, 2004; Krebs et al., 2004; A. Trindade et al., 2008). Thus, Dll4 seems to be a crucial regulator of the angiogenic process. Further studies indicated that DLL4, through Notch1 and 4, appears to play key roles regulating ECs and bone marrow-derived EC progenitors during physiological and tumor angiogenesis (Dufraine, Funahashi, & Kitajewski, 2008; Real et al., 2011). DLL4-

Notch signaling takes part of a negative feedback loop in the angiogenic process (Lobov et al., 2007). VEGF induces the expression of DLL4 and Notch1 (Patel et al., 2005; Ridgway et al., 2006), while DLL4-Notch signaling inhibits the VEGF pathway by decreasing VEGFR2 and increasing VEGFR1 expression (Harrington et al., 2008; Patel et al., 2005; Ridgway et al., 2006; Williams et al., 2006). Normally, DLL4-Notch signaling restricts the numbers of tip cells in response to VEGF. Therefore, inhibition of DLL4 leads to increased tip cell formation and reduced numbers of stalk cells in angiogenic regions (Hellström et al., 2007). The effect of DLL4 on sprouting angiogenesis is also mediated through regulation of matrix metalloproteinase expression (Funahashi et al., 2011). In addition, Dll4 expression is induced by hypoxia, presenting a tendency to correlate with VEGF levels (Mailhos et al., 2001; Patel et al., 2006). Dll4 is highly expressed in the tumor microvessels and small arteries while poorly detectable in venules and larger tumor vessels and in the adjacent normal tissue vessels (Gale, 2004). Studies indicated that inhibition of Dll4/Notch represses the tumor growth by promoting dysfunctional and immature tumor angiogenesis in a variety of xenograft and autochthonous models (Djokovic et al., 2010; Noguera-Troise et al., 2006; Ridgway et al., 2006; Scehnet et al., 2007). Tumors responsive to anti-Dll4 therapy include those that are resistant to inhibition with anti-VEGF, highlighting the potential utility of this approach (J. L. Li et al., 2011). However, in rodents Dll4 inhibition or loss of function has been associated with certain adverse events including vascular hyperproliferation in the liver and non-malignant vascular neoplasms (Djokovic et al., 2010; Minhong Yan et al., 2010). At least three anti-DLL4 antibodies have entered clinical testing (OMP-21M18 from OncoMed, REGN421 from Regeneron and MEDI0639 from MedImmune) to treat several types of cancer, including CRC. To date there have not been reported incidents of either liver toxicity or vascular neoplasms in these clinical programs. Ongoing clinical studies will determine if these anti-DLL4 agents can be developed into effective therapeutics.

In the gastrointestinal tract Dll4 seems to have redundant functions with Dll1 during intestinal development and maintaining homeostasis (Pellegrinet et al., 2011). In CRC, inhibition of DLL4 was shown to have synergistic activity with various chemotherapeutic agents in reducing tumor volume and cancer stem cells (CSCs) frequency in xenografts (Hoey et al., 2009). Additionally, it up-regulates markers of more differentiated colon cells (as ATOH1 and Chromogranin A) (Hoey et al., 2009). Therefore, as CSCs are frequently resistant to conventional cancer treatments including chemotherapy, the promotion of differentiation by Dll4/Notch pathway inhibition may sensitize tumor cells to chemotherapeutic drugs. Accumulating evidence has shown that CSCs depend on a functional angiogenesis (Zhao et al., 2011). Thus, Dll4/Notch signaling may have an effect on these cells by regulating the tumor angiogenesis. However, a study using a xenograft model indicated that this pathway could have a direct role on these cells (Hoey et al.,

2009). More recent studies indicated that anti-DLL4 therapy is also active in colorectal tumors xenografts harboring KRAS mutations, which are unresponsive to anti-EGFR therapy (M. Fischer et al., 2010). Additionally, another work indicated that anti-Dll4 therapy associated with radiotherapy and ultrasound-stimulated microbubble impaired colorectal tumor xenograft growth (El Kaffas et al., 2014; S. K. Liu et al., 2011). Therefore, in CRC the association of anti-Dll4/Notch therapy with standard therapy seems beneficial, even when KRAS mutations are present, and may function through various mechanisms of action.

3.2.3 TGF-β pathway

TGF-β ligand initiates signaling by binding to and bringing together type I and type II receptor serine/threonine kinases on the cell surface. This allows receptor II to phosphorylate the receptor I kinase domain, which then propagates the signal through phosphorylation of the Smad proteins (Shi & Massague, 2003).

Deregulation of TGF-β signaling, which is generally considered a tumor-suppressor pathway in the colon, occurs in the majority of colorectal cancers (Chittenden et al., 2008) Inactivating mutations have been observed in receptor genes (TGFBR2 and TGFBR1), post-receptor signaling pathway genes (SMAD2, SMAD4), and TGF-β superfamily members (ACVR2) (Deacu et al., 2004; Eppert et al., 1996; Grady & Carethers, 2008; Grady et al., 1999).

3.2.4 EGFR signaling

EGFR is a transmembrane tyrosine kinase receptor that belongs to the ErbB family. In addition to EGFR (also known as HER1 and ErbB-1), other receptors in this family include HER2/c-neu (ErbB-2), HER3 (ErbB-3), and HER4 (ErbB-4). Several ligands can bind the ErbB family of receptors, including EGF and TGF-α (Hynes & Lane, 2005). Ligand binding induces dimerization of the receptor with formation of homodimers and heterodimers, which leads to the activation of tyrosine kinase. The intracellular tyrosine kinase residues then become autophosphorylated, inducing activation of multiple signal transduction pathways, such as the mitogen-activated protein kinase (MAPK) and the PI3K/AKT. These pathways lead to the activation of transcription factors that regulate cell proliferation, migration, differentiation and apoptosis (Citri & Yarden, 2006).

EGFR is overexpressed in 70-80% of CRCs. There are contradictory results regarding the association of EGFR overexpression with tumor grade and prognosis (Goldstein & Armin, 2001; McKay et al., 2002; Resnick, Routhier, Konkin, Sabo, & Pricolo, 2004; Spano et al., 2005). *EGFR* mutations are uncommon in CRC (Barber, Vogelstein, Kinzler, & Velculescu, 2004; J. W. Lee et al., 2005) and some studies indicated that *EGFR* gene amplification is also rare (Shia et al., 2005; Spindler et al., 2006), while others observed it frequently

(Cappuzzo et al., 2008). In addition, activation of EGFR downstream effectors through mutations in KRAS (in 30-50% of CRCs), BRAF (in 5-10% of CRCs) and phosphatidylinositol-4,5-bisphosphate 3-kinase, catalytic subunit alpha (PIK3CA), inactivation of phosphatase and tensin homolog (PTEN) and activation of AKT can lead to tumor formation and progression (Krasinskas, 2011). Most of these alterations are predictive markers of resistance to EGFR-targeted therapy (Bardelli & Siena, 2010). This therapy can be based on inhibition of EGFR extracellular domain, of the RAS-RAF-MEK-ERK pathway or the PI3-AKT-mTOR pathway (Merla & Goel, 2012).

3.2.5 VEGF/VEGFR signaling

VEGF or VEGFA is a protein secreted by a wide variety of cells, including tumor cells. It was originally described as an inducer of vascular leakage (and then was named vascular permeability factor) (Dvorak, Brown, Detmar, & Dvorak, 1995; Ferrara, Houck, Jakeman, & Leung, 1992; Neufeld, Cohen, Gengrinovitch, & Poltorak, 1999; Plouet, Schilling, & Gospodarowicz, 1989). VEGFA is a member of a family of potent angiogenesis and/or lymphangiogenesis positive regulators that also includes VEGFB, VEGFC, VEGFD, placental growth factor (PlGF), Orf virus' VEGFE, and *Trimeresurus flavoviridis* (T. f.) svVEGFs (Ferrara, Gerber, & LeCouter, 2003; Junqueira de Azevedo, Farsky, Oliveira, & Ho, 2001; Lyttle, Fraser, Fleming, Mercer, & Robinson, 1994). There are three tyrosine kinase receptors, named Flt-1 (VEGFR1) (de Vries et al., 1992), KDR/Flk-1 (VEGFR2) (Klagsbrun, 1991) and Flt-4 (VEGFR3) (Pajusola et al., 1992), and the receptors Neuropilins (Soker, Takashima, Miao, Neufeld, & Klagsbrun, 1998). Binding of VEGFA to VEGFR2 leads to the activation of a cascade of downstream pathways that generates the main signals for sprouting angiogenesis (Shibuya, 2006). VEGFR1, however, has ten times higher affinity for the growth factor than VEGFR2, but very weak tyrosine kinase activity, serving as a VEGFA trapper (Shibuya, 2006).

In 1971 Folkman advanced the hypothesis that tumor growth is angiogenesis-dependent (Folkman, 1971). It was established that the angiogenic activation (angiogenic switch) is essential for the growth of almost every solid tumors (Folkman & Hanahan, 1991) and for invasion and metastasis (Zetter, 1998). The angiogenic induction may occur as a response to increased tumoral hypoxia that promotes VEGF expression, directly expression of VEGF and other pro-angiogenic factors by tumor cells and by recruiting bone marrow-derived endothelial progenitors (Dass, 2004). The formation of new blood vessels is controlled by pro- and anti-angiogenic factors, matrix-degrading proteases, and cell-extracellular matrix interactions (Folkman, 1992; Khosravi Shahi & Fernandez Pineda, 2008; Liekens, De Clercq, & Neyts, 2001; Sharma, Sharma, & Sarkar, 2005). VEGF is the predominant angiogenic factor in CRC and is associated with metastization and poor prognosis (Abdou, Aiad, Asaad, Abd El-Wahed, & Serag El-Dien, 2006; Ellis, 2003, 2004;

Ellis, Takahashi, Liu, & Shaheen, 2000; Takeda et al., 2000). Thus, inhibiting angiogenesis through VEGF/VEGFR inhibition is now regarded as an important approach in CRC treatment (Ferrarotto & Hoff, 2013).

3.3 Colorectal cancer

CRC is the third most common type of cancer with one million new cases diagnosed per year worldwide. About half a million people die of this disease per year (Jemal et al., 2011). The World Health Organization estimates an increase of 77% in the number of newly diagnosed cases of CRC and an increase of 80% in deaths from CRC by 2030 (Binefa, Rodriguez-Moranta, Teule, & Medina-Hayas, 2014; Karsa, Lignini, Patnick, Lambert, & Sauvaget, 2010). CRC is more frequent and causes more deaths in men than in women worldwide (Binefa et al., 2014). Is commonly regarded as a Western lifestyle disease and it is the second leading cause of cancer-related death in the Western world (Jemal et al., 2011).

3.3.1 Etiology

CRC is a very heterogeneous disease that is caused by the interaction of genetic and environmental factors (Binefa et al., 2014).

The majority of CRCs are sporadic (70-80%), which begin with benign lesions and eventually lead to fully metastatic tumors (Fearon & Vogelstein, 1990). Patients develop this disease based on risk factors, such as diet low in fruit and vegetables and excessive red meat and saturated fat, alcohol intake, sedentary lifestyle, tobacco and being overweight (Gonzalez & Riboli, 2010). However, the main risk factor is age > 50 years (Amersi, Agustin, & Ko, 2005).

Only a small proportion of cases are due to inherited forms, named autosomal dominant hereditary non-polyposis CRC (HNPCC) or Lynch syndrome (2%-5%), FAP (< 1%) and MYH-gene associated polyposis (MAP) (< 1%) (Farrington et al., 2005). An additional 20%-25% of cases are associated with a hereditary component not well established and are known as familial CRC (Pinol et al., 2005). HNPCC is an autosomal dominant genetic condition caused by a germline mutation in one of several mismatch repair genes (*MSH2, MLH1, MSH6, PMS1* and *PMS2*) that cause microsatellite instability in the genome (Yuan, Huang, & Zheng, 1999). This syndrome predisposes to multiple primary cancers, mainly CRC and endometrial cancer, without intestinal polyposis, that occur at the age of 40-45 years (Jass, 1998). FAP syndrome is inherited in an autosomal dominant matter by a germline mutation in the tumor suppressor *APC* gene (Powell et al., 1993), which inactivation also occurs in a large percentage of sporadic CRC (Kinzler et al., 1991; Nakamura et al., 1992; Powell et al., 1993; Solomon et al., 1987). Patients with FAP develop large numbers of benign adenomatous polyps of the colorectal epithelium early in

adulthood (Haggitt & Reid, 1986). Although adenomas are generally considered as benign, the large number of polyps prone to acquiring additional mutations confers FAP patients a 100% chance of developing CRC by the age of 40 (Bisgaard, Fenger, Bulow, Niebuhr, & Mohr, 1994). MAP is an autosomal disorder caused by a biallelic germline mutation in the base-excision-repair (BER) gene *MYH* (Half, Bercovich, & Rozen, 2009). Patients will develop polyps/adenomas in the gastrointestinal tract, but no extra-intestinal manifestations are seen (Half et al., 2009). Patients have an 80% risk of developing CRC by the age of 40-60 years (Theodoratou et al., 2010).

CRC can also be associated to chronic inflammation (colitis associated cancer or CAC) as a long-term complication of CD (Ekbom et al., 1990) and UC (Svartz & Ernberg, 1949), the two main forms of IBD. Though patients with IBD represent only a small fraction of CRC cases (1–2%), these patients are among those at greatest risk of developing this disease (Lakatos & Lakatos, 2008; Munkholm, 2003). However, UC patients have a higher risk of developing CAC than CD patients and these diseases are characterized by different immune responses. Specifically, UC is caused by an atypical Th2-mediated response (Roda et al., 2011), while CD is characterized by activation of Th1 and Th17 cells, where Th17 cell-derived IL-17 rather than Th1 cells may sustain inflammation and promote CAC (Rizzo, Pallone, Monteleone, & Fantini, 2011).

3.3.2 CRC carcinogenesis

The multistep process of carcinogenesis is characterized by the canonical phases of initiation, promotion, and progression. Vogelstein and colleagues were the first to describe a series of molecular events that turn normal mucosa first into hyperplastic epithelium, then into adenomatous polyps with dysplastic cells and then into malignant carcinoma with invasion of the basement membrane and metastasis (adenoma-carcinoma sequence) (Cho & Vogelstein, 1992; Kinzler & Vogelstein, 1996; Su et al., 1992; Vogelstein & Kinzler, 2004) (Fig. 5).

Although every adenoma has the capacity of malignant evolution, only few adenomas actually develop into invasive cancer (progressive adenomas), while the rest stabilizes or regress (Risio, 2010). The neoplastic transformation time is considered approximately 10-15 years. Colorectal tumors arise as a result of activating mutations in oncogenes, coupled with loss-of-function alterations in tumor suppressor genes. Up to 7 genetic and histological alterations have been suggested to be required for the progression from adenoma to carcinoma (Kinzler & Vogelstein, 1996). Although some genetic alterations appear to occur in a preferential order, it is rather the total accumulation of genetic changes that seems to be critical (Rustgi, 1994). At least four kinds of genomic or epigenetic instability have been described in CRCs: chromosomal instability (CIN), microsatellite instability (MSI), CpG island methylator phenotype (CIMP), and global DNA

hypomethylation (Pritchard & Grady, 2011). CIN involves the accumulation of mutations that leads to oncogene activation (*KRAS*) and tumor suppressor gene inactivation (*deleted in CRC (DCC), APC, SMAD4, p53*) (Fearon & Vogelstein, 1990). MSI is caused by the accumulation of errors during DNA replication in repetitive DNA fragments (microsatellites) due to the presence of mutations in genes responsible for its repair (*MSH2, MLH1, MSH6, PMS2, MLH3, MSH3, PMS1* and *Exo1*). CIMP includes aberrant hypermethylation, a mechanism to silence gene function, while a global decrease in methylation has also been identified in many CRCs and is tightly associated with CIN tumors (Pritchard & Grady, 2011). Premalignant serrated polyps are associated with MSI and CIMP, whereas conventional adenomas arise via biallelic inactivation of the *APC* tumor-suppressor gene and display CIN (Noffsinger, 2009). Just as important as genomic and epigenomic instability for the pathogenesis of CRC is the accumulation of mutations in specific genes and the resulting deregulation of specific signaling pathways that control the hallmark behaviors of cancer: cell proliferation, differentiation, apoptosis, immortalization, angiogenesis, and invasion (Pritchard & Grady, 2011).

Figure 5 - Model of the sequence of events in CRC development. *In* (Fearon & Vogelstein, 1990)

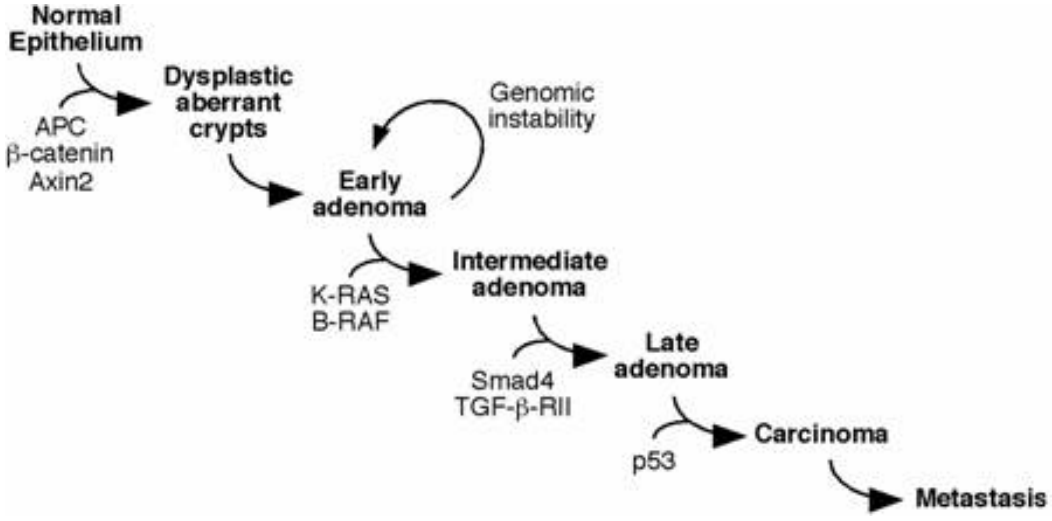

In the adenoma-carcinoma sequence, the smallest identifiable lesion is an aberrant crypt focus (ACF). The aberrant crypt foci are characterized by crypts with altered luminal openings, thickened epithelia and being larger than the adjacent normal crypts (Bird & Good, 2000). The majority of malignant dysplastic ACF bears *APC* mutations, whereas non-malignant hyperplastic ACF are proposed to arise from activating mutations in *KRAS* (Nucci, Robinson, Longo, Campbell, & Hamilton, 1997). There are also dysplastic β-catenin-accumulated crypts (BCAC). It is not clear whether BCAC represents a subgroup of ACF or can be clearly delineated as a separate entity (Y. Yamada et al., 2000).

Another frequent early event is the development of precancerous colorectal polyps, mucosal lesions that project into the lumen of the bowel. Experts estimate that about 85% of CRCs begin as precancerous polyps (Gopalappa, Aydogan-Cremaschi, Das, & Orcun, 2011). The colorectal polyps can be histologically classified in neoplastic (adenomas), non-neoplastic (hyperplastic, hamartomatous, or inflammatory) and premalignant serrated. In addition, polyps are generally described as being either sessile (flat) or pedunculated (having a stalk). Adenomatous polyps have different grades of dysplasia (abnormal differentiated phenotype) and are considered precursors for CRC. Histologically these polyps are either villous, tubular or tubulovillous. The risk of malignancy increases with the polyp size, the degree of villous component and if it is a flat adenoma (Shussman & Wexner, 2014). In addition, in patients with IBD we also can find a dysplasia-associated lesion or mass (DALM). The transition of a DALM to CRC is much faster than the classic adenoma-carcinoma sequence (Shussman & Wexner, 2014).

In sporadic colorectal adenomas, the initiating event seems to be loss of heterozygosity (LOH) of the *APC* gene, followed by a second hit in the same gene. Additionally, both sporadic and FAP adenomas appear to start as unicryptal adenomas and grow initially by fission of the crypt. Later there is growth down into adjacent crypts. (Preston et al., 2003). However, two models have been proposed. In the 'top-down' model, mutant cells appear in the intra-cryptal zone between crypt openings (Shih et al., 2001). There are two possibilities within this model. In one hand, mutant cells at the surface of the mucosa spread laterally and downward to form new crypts, eventually replacing them. On the other hand, a cell derived from a mutated stem cell may migrate to that area and expand with a second genetic hit that activates its growth potential. The 'bottom-up' model proposes that the malignant transformation process takes place among the stem cell population at the crypt base, and then the transformed stem cell migrates to the apex of the crypt where it expands. (Preston et al., 2003).

Additionally, two possible models of colorectal cancer carcinogenesis are currently described: a stochastic model, where any cell has an equal capacity of cancer initiation and promotion, and a cancer stem cell (CSC) model, where tumors are organized in a certain hierarchical degree and only CR-CSCs have cancer-initiating potential and the ability to sustain tumor growth (Vaiopoulos, Kostakis, Koutsilieris, & Papavassiliou, 2012). These CSCs are considered to have a capacity for self-renewal and ability to give rise to the heterogeneous lineages of cancer cells that comprise a tumor (Tan, Park, Ailles, & Weissman, 2006) and its presence within CRC has been widely reported (Dalerba et al., 2007; O'Brien, Pollett, Gallinger, & Dick, 2007; Ricci-Vitiani et al., 2007).

3.3.3 CAC carcinogenesis

The pathogenesis of IBD is still unclear, but both autoimmune and immune-mediated phenomena are involved (Wen & Fiocchi, 2004). It is currently believed that loss of tolerance against the indigenous enteric flora is the central event in IBD pathogenesis (Wen & Fiocchi, 2004). High levels of inflammatory mediators then contribute to the development and progression of CAC (Kraus & Arber, 2009), following an inflammation–dysplasia–carcinoma sequence (De Robertis et al., 2011). Specifically excessive inflammation, expansion of bacteria with genotoxic capabilities such as *Helicobacter* and *Bacteroides spp* and chronic oxidative stress by the generation of reactive oxygen and nitrogen species, pose a constant mutational challenge for the intestinal epithelium and create a tumor-promoting microenvironment (Arthur et al., 2012; Chichlowski, Sharp, Vanderford, Myles, & Hale, 2008; Ferguson, 2010; Hofseth et al., 2003; Hussain, Hofseth, & Harris, 2003; Iliev et al., 2012; Philip, Rowley, & Schreiber, 2004; Westbrook, Wei, Braun, & Schiestl, 2009; S. Wu et al., 2009).

Although similar mutations occur in sporadic CRC and CAC, they appear in different stages of the disease (Kern et al., 1994). For example mutations and LOH of *p53* gene are observed early in CAC (Lashner, Shapiro, Husain, & Goldblum, 1999) and only in later stages in sporadic CRC (Fearon & Vogelstein, 1990). Additionally, while in sporadic CRC mutations in the *APC* gene were described to initiate tumorigenesis, this does not seem to be the case in CAC (Tarmin et al., 1995). Furthermore, analysis of β-catenin showed no alterations in most specimens of UC and CAC (Leedham et al., 2009).

Moreover IBD and CAC development are mediated through the production of inflammatory mediators, such as the proinflammatory enzymes cyclooxygenase-2 (COX-2) and iNOS (Chichlowski, Westwood, Abraham, & Hale, 2010; T. Tanaka et al., 2003), cytokines, chemokines, growth- and transcription factors. The release of cytokines such as IL-6 and TNF-α during IBD promote tumor growth, while low expression of immunossupressive cytokines like TGF-β and IL-10 exacerbate this process (Rizzo et al., 2011). Although TNF-α has been classically considered as an anticancer agent, it is currently recognized that chronically elevated TNF-α may promote tumor growth, invasion and metastasis (Popivanova et al., 2008; Szlosarek, Charles, & Balkwill, 2006). The protumoral effect of TNF-α signaling in CAC is mostly due to the intracellular activation of NF-κB (Hacker & Karin, 2006). NF-κB is a pleiotropic transcription factor with a crucial role in innate and adaptive immunity and is required for the expression of various proinflammatory factors (Hacker & Karin, 2006). Additionally, in CAC the prosurvival signals provided by NF-κB in epithelial cells play a role in tumor initiation independent of the inflammation severity (Greten et al., 2004). NF-κB can support carcinogenesis by increasing cell proliferation, angiogenesis, invasion and metastasis, and inhibiting apoptosis (Naugler & Karin, 2008). One of the NF-κB-dependent tumor growth factors released by myeloid cells is IL-6, a

multifunctional cytokine important for immune responses, cell survival, apoptosis and proliferation (Kishimoto, 2005). With regard to CAC, IL-6 expressed during colitis was shown to promote tumor growth in mice (Becker et al., 2004). Moreover, in a similar model, IL-6 expressed by *lamina propria* myeloid cells protected normal and transformed epithelial cells from apoptosis in a STAT3-dependent manner (Grivennikov et al., 2009). In addition, other studies indicated the presence of a negative feedback loop between IL-6 expression and TGF-β signaling (Becker et al., 2004; Jenkins et al., 2005). The pivotal function of TGF-β in the immune system is to maintain tolerance via the regulation of lymphocyte proliferation, differentiation, and survival. In addition, TGF-β controls the initiation and resolution of inflammatory responses through the regulation of chemotaxis, activation, and survival of innate and adaptive immune cells (M. O. Li, Wan, Sanjabi, Robertson, & Flavell, 2006). The inhibition of TGF-β signaling causes IBD by upregulating the intracellular inhibitor of Smad signaling Smad7 (Monteleone, Boirivant, Pallone, & MacDonald, 2008). Additionally, blocking TGF-β signaling using Smad3-deficient mice leads to CAC development dependent on the presence of *Helicobacter* infection (Maggio-Price et al., 2006). However, TGF-β signaling has been demonstrated to act, under certain conditions, as a tumor promoter. Indeed, TGF-β signaling suppresses tumor-specific CD8+ T cell cytotoxicity (Chen et al., 2005), promotes tumor cell proliferation and metastasis (Massague, 2008). In addition, TGF-β induces the differentiation and activation of Treg cells, suppresses INF-γ production and in the presence of IL-6 induces the differentiation of IL-17-producing Th17 cells (Flavell, Sanjabi, Wrzesinski, & Licona-Limon, 2010). Furthemore, the excess amount of TGF-β in the tumor microenvironment may contribute to the alternative activation of M2 macrophages by downregulating NF-κB expression (Flavell et al., 2010). The other main immunomodulatory cytokine is IL-10. Patients carrying loss-of-function mutations of IL-10 receptor develop more aggressive IBD and CAC (Rizzo et al., 2011). Moreover, IL-10-deficient mice spontaneously develop chronic enterocolitis (Kuhn, Lohler, Rennick, Rajewsky, & Muller, 1993) and CAC (Berg et al., 1996). Analogous to IL-6, IL-10 activates STAT3 in target cells. However, the final effect is inhibition of NF-κB activation (Hoentjen, Sartor, Ozaki, & Jobin, 2005; Schottelius, Mayo, Sartor, & Baldwin, 1999) and reduction of the expression of proinflammatory cytokines such as TNF-α, IL-6 and IL-12 (Moore, de Waal Malefyt, Coffman, & O'Garra, 2001). Moreover, in a melanoma model, IL-10 seems to inhibit macrophages-derived angiogenic factors, and hence, tumor growth and metastasis (Huang, Xie, Bucana, Ullrich, & Bar-Eli, 1996).

Macrophages are usually the most abundant immune population in the tumor-microenvironment (Tavazoie et al., 2008). Tumor-derived IL-6, IL-10, TGF-β and PGE_2 promote the polarization into M2-like macrophages with protumor functions. These include the production of growth factors (e.g. EGF, FGF, VEGF, IL-6) and matrix-degrading

enzymes (MMPs) that favor angiogenesis, tumor cell proliferation and invasion, and the secretion of chemokines (e.g CCL17, CCL18 and CCL22) to recruit naïve and Th2 lymphocytes, ineffective in mounting a protective anti-tumor immune response (Tavazoie et al., 2008).

Cells of the innate immune system have been regarded mainly as pro-tumorigenic, as they facilitate an unspecific inflammatory response (M. J. Waldner & Neurath, 2009). The role of cells of the adaptive immune system however is more complex. Although T cell responses fuel the inflammatory process that promotes carcinogenesis, they also inhibit the tumor growth and progression by a process of recognition and rejection of malignant cells called immunosurveillance (Danese, Malesci, & Vetrano, 2011). In a CAC model, RAG1-deficient mice that do not have B and T cells did not develop tumors even in the presence of colitis (Becker et al., 2004). With regard to Th cell subsets, Osawa *et al.* compared *Il4*$^{-/-}$ and *Ifn-γ*$^{-/-}$ deficient mice in a CAC model and concluded that Th2-derived cytokines, and not IFN-γ, promoted the tumor growth (Osawa et al., 2006). Indeed, IFN-γ (the main marker of Th1 responses) has been shown to be involved in the activation of CD8+ T cells and natural killer (NK) cells (Senik, Stefanos, Kolb, Lucero, & Falcoff, 1980; Street, Trapani, MacGregor, & Smyth, 2002) and these and NKT cells have been shown to play a role in antitumor immunity. After being activated they release different cytotoxic molecules responsible for target cell killing (Rizzo et al., 2011). However, the role of CD8+ T cells in CAC seems to be controversial as they also contribute to intestinal inflammation and thereby might promote tumor growth (M. J. Waldner & Neurath, 2009). Other study indicated that Th17 cell response may be implicated, as IL-17 ablation reduced the number and mean tumor size and decreased inflammation and proliferation in CAC (Hyun et al., 2012). Indeed, IL-17 is known to induce the expression of proinflammatory factors such as TNF-α, IL-6, IL1, iNOS, metalloproteinases and chemokines, which play a role in CAC (Fouser, Wright, Dunussi-Joannopoulos, & Collins, 2008). Additionally, Th17 cell activation and infiltration in the tumor microenvironment inhibits IL-12 while enhancing IL-23 transcription. This shifts the balance from Th1 to Th17 (Danese et al., 2011). Moreover Tregs have been shown to have a protective effect on chronic inflammation and in CAC (Blat, Zigmond, Alteber, Waks, & Eshhar, 2014; Pastille et al., 2014; M. J. Waldner & Neurath, 2009). However, the expression of FOXP3 has been associated with a poor prognosis in several types of cancer, and Tregs have been shown to reduce the host antitumor immune response mediated by CD8+ T cells (Ishibashi, Tanaka, Tajima, Yoshida, & Kuwano, 2006; Wolf et al., 2005). Nevertheless, in the *Apc*$^{Min/+}$ model, Tregs were shown to reduce the intestinal tumor growth by increasing the apoptotic rate of tumor cells and reducing the expression of COX-2 (Erdman et al., 2005), indicating that the anti-inflammatory role of Tregs may exceed the suppression of tumor immunosurveillance.

3.4 Mouse models of colorectal cancer

3.4.1 The *Apc*$^{Min/+}$ model

The *Apc*$^{Min/+}$ mouse is regarded as a good model to study the multistage carcinogenesis of human FAP and sporadic CRC (Yasuhiro Yamada & Mori, 2007). Originally, this lineage was established from an ethylnitrosourea-treated C57BL/6 mouse, and its phenotype is an autosomal dominant trait (Moser, Pitot, & Dove, 1990). The *Apc*$^{Min/+}$ mouse has a dominant point mutation at the recessive tumor suppressor *Apc* gene that results in truncation of the gene product at amino acid 850 (Su et al., 1992). This mouse is therefore predisposed to multiple intestinal neoplasms (Min), where *Apc* LOH is necessary for tumor formation (Luongo, Moser, Gledhill, & Dove, 1994). In this model there are at least two distinct stages of carcinogenesis, where additional events are required for the transition of microadenomas (one to six dysplastic crypts, with loss of *Apc* and β-catenin accumulation like BCAC) to macroscopic tumors (Yasuhiro Yamada & Mori, 2007). The vast majority of *Apc*$^{Min/+}$ tumors develop in the small intestine, with a few developing in the colon (Moser, Dove, Roth, & Gordon, 1992; Moser et al., 1990). Most tumors in the *Apc*$^{Min/+}$ mouse are benign polypoidal, sessile or papillary adenomas and do not demonstrate either aggressive invasion or metastasis (Boivin et al., 2003).

3.4.2 The azoxymethane plus dextran sulfate sodium chemically induced model

A chronic inflammation-related mouse model of colorectal cancer combines the carcinogen azoxymethane (AOM) and the pro-inflammatory agent dextran sulfate sodium (DSS) salt (Clemens Neufert et al., 2007). AOM is a mutagenic agent that exerts colonotropic carcinogenicity by promoting DNA alkylation, which facilitates base mispairings (Papanikolaou, Wang, Delker, & Rosenberg, 1998). AOM is a tumor-initiating agent, but some tumor-promoting activity has also been reported (Bissahoyo et al., 2005). DSS is a non-genotoxic carcinogen that causes defects in the colonic epithelial barrier integrity, whereby increasing the mucosal permeability (Kitajima, Takuma, & Morimoto, 1999). Hence, it induces colonic inflammation and nitrosative stress and therefore promotes colonic dysplasia and neoplasms (T. Tanaka et al., 2003). Chronic colitis may be induced by DSS through continuous treatment in low concentration or cyclical administration (Perse & Cerar, 2012). Histological changes seen in mouse DSS-induced colitis are the features of IBD (UC and CD) in man (Perse & Cerar, 2012). They consist of mononuclear leucocytes infiltration, crypt architectural disarray, increasing the distance between crypt bases and *muscularis mucosae* and erosion (Perse & Cerar, 2012). CAC is thought to develop by a multistep process in which normal crypts are initiated to form ACF that proliferate by crypt fission to form microadenoma. The microadenomas enlarge to give macroscopic adenomas, adenomatous polyps, and eventually adenocarcinomas. Usually, 3–10 macroscopic tumors develop in 80%–100% of the mice, with adenomas infiltrated by

T lymphocytes and other immune cells, low- and high-grade dysplasia, and colitis with mucosal ulceration being present at week 12 from the start of the treatment (Becker et al., 2005; Bissahoyo et al., 2005). Such tumors display increased levels of COX-2 and iNOS Takahashi, 2000 #4201}. Development of cancer in this model closely mirrors the pattern seen in humans even at the molecular level. However, AOM-DSS induced tumors often lack mucosal invasiveness (Boivin et al., 2003).

4 EXPERIMENTAL WORK

4.1 Chapter I - Delta-like 4/Notch signaling promotes *Apc*$^{Min/+}$ tumor initiation through angiogenic and non-angiogenic related mechanisms

Badenes, M., Trindade, A., Pissarra, H., Costa, L., Duarte, A.

4.1.1 Abstract

Delta like 4 (Dll4)/Notch signaling is a key regulator of tumor angiogenesis. Additionally the role of Dll4 has been studied on tumor stem cells. However, as these cells are implicated in tumor angiogenesis, it is conceivable that the effect of Dll4 on these cells may be a consequence of its angiogenic function. Our aim was to evaluate the expression and dissect the functions of Dll4 in the *Apc*$^{Min/+}$ model of colorectal cancer. For that we analysed the protein expression pattern of Dll4 and other Notch members in the *Apc*$^{Min/+}$ tumors relatively to the normal gut and compared endothelial-specific with ubiquitous Dll4 knockout mice on an *Apc*$^{Min/+}$ background. We found that all Notch pathway members were present in the normal small and large intestine and also, but mainly Dll4 and Jagged1, in the intestinal adenomas. Dll4, all Notch receptors and Hes1 expression seemed upregulated in the tumors, with some regional differences. The same members and Hes5, instead of Hes1, presented ectopic expression in the tumor parenchyma. Dll4 expression was most pronounced in the tumor cells but it was also present in the tumor blood vessels and in other stromal cells. Ubiquitous and endothelial-specific Dll4 deletion led to a similar reduction of tumor growth because of a similarly marked tumoral angiogenic phenotype promoting non-productive vasculature and consequently hypoxia and apoptosis. The ubiquitous Dll4 inhibition led to a stronger decrease of tumor multiplicity than the endothelial-specific deletion by further reducing tumor proliferation and tumor stem cell density through upregulation of the cyclin-dependent kinase inhibitors 1C and 1B and downregulation of Myc, Cyclin D1 and D2 independently of β-catenin activation. This phenotype was associated to the observed increased epithelial differentiation deviated towards the secretory lineages by Atoh1 and Klf4 upregulation only in the ubiquitous Dll4 mutants. Therefore, Dll4 seems to promote *Apc*$^{Min/+}$ tumorigenesis through both angiogenic and non-angiogenic related mechanisms.

Keywords: Notch expression, Dll4, ubiquitous knockout, endothelial-specific knockout, tumor stem cells, angiogenesis, *Apc*$^{Min/+}$ mouse

4.1.2 Introduction

Colorectal cancer (CRC), one of the most frequent malignancies in the Western world, is commonly associated with mutations in the tumor suppressor *Adenomatous polyposis coli (APC)* gene both in hereditary (Powell et al., 1993) and in sporadic CRC (Payne, 1990). Mutations of this gene constitutively activate β-catenin target genes causing tumorigenesis (Fearnhead, Britton, & Bodmer, 2001). The $Apc^{Min/+}$ mouse, which spontaneously develops multiple intestinal neoplasms (Min) in the small and large intestine, is considered a good model to study CRC (McCart, Vickaryous, & Silver, 2008; Su et al., 1992).

Studies revealed that all of the Notch receptors, their ligands and some of their effectors (Hes1, 5, 6, 7 and Atoh1) are expressed in the normal intestinal crypts, the main niche for stem cells. Dll1 and Dll4 interact with Notch1 and 2 in the normal gut to maintain the homeostasis of intestinal stem cells (Pellegrinet et al., 2011) by repressing the cyclin-dependent kinase inhibitors *Cdkn1b and Cdkn1c* (Riccio et al., 2008). The Notch signaling pathway also promotes the enterocyte/colonocyte differentiation (Stanger, Datar, Murtaugh, & Melton, 2005; van Es et al., 2005), while Atoh1 and Klf4, which are transcriptionally repressed by Hes1, specify secretory (goblet, enteroendocrine, and Paneth) cell differentiation (Vooijs, Liu, & Kopan, 2011; Yang, Bermingham, Finegold, & Zoghbi, 2001).

Activation of Notch1 together with Wnt signalling seems to be essential to trigger CRC initiation by maintaining the self-renewal of tumor stem cells (Fre et al., 2009; Sikandar et al., 2010). These cells share some characteristics with normal stem cells but have accumulated oncogenic mutations and lost growth control. They possess the strongest tumor-initiating potential of all tumor cells and promote tumor growth and resistance to many current therapies, including chemo and radiotherapy (Rosen & Jordan, 2009). Several intestinal stem cell markers have been investigated, such as the leucine-rich repeat-containing G-protein-coupled receptor 5 (Lgr5) and the B cell–specific Moloney murine leukemia virus insertion site 1 (Bmi1) (Maynard et al., 2014). These two markers are also present in the normal gut in two functionally different intestinal stem cell populations; Lgr5 is present in mitotically active stem cells that are sensitive to irradiation and Wnt modulation, while Bmi1 is a marker for a reserve population of resistant quiescent injury-inducible stem cells (Yan et al., 2012). In CRC both Lgr5 and Bmi1 positive stem cell populations are associated with cancer initiation and progression (Espersen et al., 2015; Fre et al., 2005; Schepers et al., 2012) and are regulated by the Notch pathway in the normal gut (Lopez-Arribillaga et al., 2015; VanDussen et al., 2012).

Accumulating evidence has shown that tumor stem cells promote tumor angiogenesis and that their maintenance depends upon functional angiogenesis (Zhao et al., 2011). It is currently widely recognized that tumor growth and maintenance is dependent on the expansion of the individual's vasculature to the center of the tumor (Folkman, 1990). Previous work showed that the inhibition of Dll4/Notch represses tumor growth by promoting

dysfunctional an immature tumoral angiogenesis in a variety of xenograft and autochthonous mouse models (Djokovic et al., 2010; Noguera-Troise et al., 2006; Ridgway et al., 2006; Scehnet et al., 2007). In xenograft models of CRC anti-Dll4 therapy seems to additionally reduce the frequency of tumor stem cells (M. Fischer et al., 2010; T. Hoey et al., 2009).

Thus, we set out to characterize the expression pattern of Dll4 and other Notch members in the *Apc*$^{Min/+}$ tumors relatively to the normal intestine and compare endothelial-specific with ubiquitous *Dll4* loss-of-function mutants to address the role of Dll4 in intestinal tumor development in the *Apc*$^{Min/+}$ model. In particular, we aimed to assess whether an effect of Dll4 signaling on the *Apc*$^{Min/+}$ tumor stem cells was solely a consequence of its action on tumor angiogenesis or if other, more direct, mechanisms might be involved.

4.1.3 Methods

4.1.3.1 Experimental animals

All animal-involving procedures in this work were approved by the Faculty of Veterinary Medicine of Lisbon Ethics and Animal Welfare Committee (Approval ID: PTDC/CVT/71604/2006).

Mutant C57BL/6J-*Apc*$^{Min/+}$/J (*Apc*$^{Min/+}$) mice were purchased from the Jackson Laboratory (Bar Harbor, ME).

Wild type C57BL/6J mice were used to analyse Notch pathway expression in the normal intestine and *Apc*$^{Min/+}$ mice were used to characterize their expression in intestinal tumors.

Apc$^{Min/+}$ mice were crossed with *Dll4* conditional homozygous mice (*Dll4*$^{lox/lox}$). The resulting *Apc*$^{Min/+}$; *Dll4*$^{lox/lox}$ progeny was crossed with *VE-cadherin-Cre-ERT2* mice to produce endothelial-specific inducible *Dll4* loss-of-function (endo*Dll4*$^{-/-}$) or with *Cag-Cre-ERT2* mice to produce ubiquitous inducible loss-of-function (ubiq*Dll4*$^{-/-}$). When these mice reached 6 weeks, recombinase cre activity was induced by daily i.p. tamoxifen administration (50 mg/kg in 10% ethanol plus 90% cremophor), during 5 days. Tamoxifen treated cre-negative mice were used as controls.

In all experiments we used 12 animals per group.

4.1.3.2 Macroscopic analysis of the intestine

At 18 weeks of age the animals were sacrificed and the small and large intestine were excised, flushed and opened longitudinally. The macroscopic small and large intestine tumors of *Apc*$^{Min/+}$ *Dll4* mutant mice and controls were counted and measured with a calliper under the dissection microscope. Tumor volume was calculated assuming a hemispherical shape for the small bowel tumors and a spherical shape for large intestine tumors. The volumes of all tumors from each mouse were added to give the overall tumor burden per animal. Normal WT small and large intestine and the tumors of these regions from *Apc*$^{Min/+}$ Dll4 mutant mice and controls were collected.

4.1.3.3 Histopathological analysis

The collected samples were fixed in 10% formalin solution for 48h, dehydrated in alcohol, cleared in xylene, embedded in paraffin, sectioned at 4µm and stained with hematoxylin (Fluka AG Buchs SG Switzerland) and eosin Y (Sigma, St. Louis, MO) for histopathological analysis. The lesions observed on the H&E sections from *Apc*$^{Min/+}$ mice were classified as hyperplasias, when only an increase of the number of cells was observed, or as adenomas with low and high-grade dysplasia based on the alterations of the shape of the nucleus, the nucleus to cytoplasm ratio, cell polarity, chromatin pattern, and changes in gland architecture.

Periodic Acid-Schiff (PAS) staining (Sigma, St. Louis, MO) was used to mark the intestinal goblet cells. These cells were counted in the intestine PAS stained sections using a 400x magnification.

4.1.3.4 Immunohistochemical analysis

After dewaxing and rehydration, endogenous peroxidase activity was quenched (15 minutes, 1% H_2O_2) and antigen retrieval was performed (20 minutes at 95°C in 10mmol/L sodium citrate buffer, pH 6). The primary antibodies to mark Dll1 (ab76655), Dll4 (ab7280), Notch1 (ab27526), Notch2 (ab8926), Notch3 (ab23426), Hes1 (ab71559) and 5 (ab25374) (Abcam, Cambridge, UK) and Jagged1 (sc-8303), Jagged2 (sc-8157), Dll3 (sc-67270) and Notch4 (sc-5594) (Santa Cruz Biothecnology, California, USA) were diluted in PBS containing 2% bovine serum albumin, and incubated overnight at 4ºC with the tissue sections. These antibodies have been previously validated (Murta et al., 2013; Murta et al., 2014; Murta et al., 2015). The following morning, the tissue sections were incubated with goat anti-rabbit (12-348, Merck Millipore, Massachusetts, USA) or rabbit anti-goat (sc-2768, Santa Cruz Biothechnology, California, USA) horseradish peroxidase–labeled secondary antibody and the staining was revealed with ImmPACT DAB Peroxidase Substrate (100µl, Vector Laboratories, Burlingame, USA). The sections were examined under an Olympus Bx51 microscope with the objective 40x/0.75 (UPlanfL). The images were captured with a camera Olympus DP21.

4.1.3.5 Immunofluorescence analysis

Small and large intestine tumors were fixed in a 4% (w/v) paraformaldehyde in PBS solution at 4ºC for 1h, cryoprotected in 15% (w/v) sucrose in PBS solution, embedded in 7.5% (w/v) gelatin in PBS solution, snap frozen in liquid nitrogen and cryosectioned in 10 and 20µm-thick sections. The following primary antibodies were used: anti-PECAM-1 (557355), anti-E-cadherin (560061) (BD Biosciences, San Jose, USA), anti-α-SMA (ab5694), anti-PCNA (ab18197), anti-Lgr5 (ab75732), anti-HIF1α (ab85866), anti-Cyclin D1 (ab21699) (Abcam, Cambridge, UK), anti-Dll4 (AF1389, R&D Systems, Minneapolis, USA), anti-lysozyme

(A009902-2, Dako, Glostrup, Denmark), anti-non-phospho (active) β-catenin (8814, Cell Signaling Technology, Danvers, USA). Species-specific secondary antibodies conjugated with Alexa Fluor 488 and 594 (Invitrogen, Carlsbad, CA) were used to reveal primary antibody binding. Tissue sections were incubated with primary antibody overnight at 4°C and with secondary antibody for 1 hour at room temperature. Nuclei were counterstained with 4´, 6-diamidino-2-phenylindole dihydrochloride hydrate (DAPI; Molecular Probes, Eugene, OR).
Fluorescent immunostained sections were examined under a Leica DMRA2 fluorescence microscope with a Leica HC PL Fluotar 10 and 20X/0.5 NA dry objective, captured using Photometrics CoolSNAP HQ, (Photometrics, Friedland, Denmark), and processed with Metamorph 4.6-5 (Molecular Devices, Sunnyvale, CA, US). Morphometric analyses were performed using the NIH ImageJ 1.37v program. After transforming the RGB images into binary files, the percentage of white pixels per field was defined as a positive signal.
Under the effect of 2-2-2 tribromoethanol anaesthesia, biotin-conjugated lectin from *Lycopersicon esculentum* (100µg/100µl of PBS) or 1% Evans' Blue solution (Sigma, St. Luis, MO, US) were administered in the caudal vein to mark vessel perfusion and extravasation, respectively. Both solutions were allowed to circulate for 5 minutes before the vasculature was transcardially perfused with 4% (w/v) paraformaldehyde in PBS solution for 3 minutes. Tumor samples were collected and processed as described above. Tissue sections were stained and tumor perfusion was quantified by determining the percentage of red PECAM-positive structures that were co-localized with Streptavidin-Alexa 488 (Invitrogen, Carlsbad, CA, US) signals. Evans' Blue is red fluorescent and extravasation was visualized in contrast to green fluorescent vascular structures.
Apoptosis was measured using the TUNEL assay (Roche, Mannheim, Germany).

4.1.3.6 Quantitative transcriptional analysis

Intestinal tumors were snap frozen in liquid nitrogen until RNA extraction (Qiagen RNeasy). Using the SuperScript® III First-Strand Synthesis SuperMix for qRT-PCR (Invitrogen, Carlsbad, CA, USA), first-strand cDNA was synthesized from total RNA. Real-time PCR analysis was performed using specific primers. Primer pair sequences are reported on Annex II. Gene expression was normalized to *β-actin* and in the case of genes expressed in the vasculature it was additionally normalized to *Pecam-1*.

4.1.3.7 Statistical analysis

To compare measurements between control and test groups, the Mann-Whitney-Wilcoxon test was performed using the Statistical Package for the Social Sciences v15.0 (Chicago, IL). Results are presented as relative average ± SEM. *P*-values <0.05 and <0.01 were considered significant (*) and highly significant (**), respectively.

4.1.4 Results

4.1.4.1 Notch pathway is upregulated in *Apc*$^{Min/+}$ small and large intestine tumors relatively to the normal intestine

Previous RNA-based studies described the expression pattern of the Notch pathway components in the normal gut (Sander & Powell, 2004; Schroder & Gossler, 2002). However, there is still limited information about its expression in the *Apc*$^{Min/+}$ mouse intestinal tumors. The only existing studies in the *Apc*$^{Min/+}$ adenomas indicated that the expression of Notch receptors and ligands was similar to that observed in the crypts, Hes1 was detected uniformly (van Es et al., 2005) and Jagged1 was overexpressed in the tumor tissue with concomitant Notch1 and 2 activation (Rodilla et al., 2009). A more complete overview has not been produced. Therefore we evaluated the protein expression pattern of the ligands (Dll1, 3 and 4 and Jagged1 and 2), receptors (Notch1-4) and chosen effectors (Hes1 and 5) in the normal WT gut. We analysed the presence of these components in the crypts and villi of the small intestine, in the bottom and top of the crypts of the large intestine and in the *lamina propria* of both regions as summarized in Tables 1 and 2. Then we evaluated the expression pattern of Notch components in the *Apc*$^{Min/+}$ mouse small and large intestine adenomas and compared it with that of normal WT gut.

In the normal small intestine crypts our protein expression analysis revealed that all Notch members, except Dll3, were present (Fig. 6A and 6D, and Fig. 7A and 7D). Most pathway members were expressed at the bottom of the crypts, where the proliferative and Paneth cells are located (Fig. 6A and 6D, and Fig. 7A and 7D). Jagged1, however, was expressed throughout the crypts, but absent in Paneth cells (Fig. 6A), whereas Notch4 was only present in goblet cells (Fig. 6D).

In the normal small intestine villi, Dll1, Dll4 and seldom Notch4 were expressed in differentiated goblet cells (Fig. 6B and 6E). Dll3 and mainly Jagged1 and Hes5 were found diffusely in enterocytes (Fig. 6B and Fig. 7E), while Jagged2, Notch1 and 3 and Hes1 were only present in some of these cells (Fig. 6B and 6E, and Fig. 7B). Notch2 seemed absent in this region (Fig. 6E).

In the bottom of the crypts of the normal large intestine, Jagged1 and Hes5 were diffusely expressed in the epithelium (Fig. 6G and Fig. 7J). Jagged2, Notch1-4 and Hes1 were found in scattered cells within the lower part of the crypts (Fig. 6G and 6J, and Fig. 7G). Dll1, 3 and 4 seemed mostly absent in this region (Fig. 6G).

In the top of the crypts of the normal large intestine, Dll1, Dll4 and Notch4 were expressed in goblet cells (Fig. 6H and 6K). Dll3, Jagged1, Hes5, and to a lesser extent Hes1, were expressed diffusely in colonocytes (Fig. 6H, and Fig. 7H and 7K). Jagged2, Notch1, 2 and 3 seemed absent in this region (Fig. 6H and 6K).

All of the members were also present in some cells in the small and large intestine *lamina propria*, mainly Hes5 in the villi and upper part of the large intestine crypts (Fig. 7E and 7K) and Dll3 diffusely in the large intestine (Fig. 6G and 6H).

We observed that in the normal small and large intestine the protein expression of most of the Notch pathway components analysed was similar to their previously described gene expression pattern (Sander & Powell, 2004; Schroder & Gossler, 2002). However, we found the presence of Notch2 in the bottom of the crypts in the large intestine (Fig. 6J), Notch3 and 4 in the small and large intestine epithelium (Fig. 6D-E and 6J-K) and Hes1 in a diffuse pattern both in the small and large intestine (Fig. 7A-B and 7G-H), which was not previously reported.

In the $Apc^{Min/+}$ intestinal adenomas, the Notch pathway members were mostly expressed in some stromal cell populations, such as neutrophils, and in tumor cells, mainly at the periphery of the tumor mass (Fig. 6C, 6F, 6I and 6L, and Fig. 7C, 7F, 7I and 7L).

Compared with the normal small bowel, in the adenomas of the same region, Dll1, Dll3, Jagged1 and Notch3 presented a similar expression pattern (Fig. 6A-F). Jagged2 seemed less expressed (Fig. 6A-C), and Dll4, Notch1, 2 and 4, and Hes1 appeared upregulated (Fig. 6A-F and Fig. 7A-C). We observed ectopic expression of Dll4, Notch1, 2 and 4 and Hes5 in the tumor epithelium (Fig. 6C and 6F, and Fig. 7F). Dll4 also appeared in other tumor cells, besides goblet cells (Fig. 6C). Notch1 appeared diffusely in the tumor epithelium (Fig. 6F). Notch2 and Hes5 were present in the goblet cells (Fig. 6F and Fig. 7F). Notch4 was not detected in the goblet cells, being present in other epithelial cell types (Fig. 6F).

Compared with the normal large intestine, in the adenomas of the same region, Dll1 and Jagged1 had a similar expression pattern (Fig. 6G-I). Dll3 and Jagged2 seemed less expressed in the tumor epithelium (Fig. 6G-I), and Dll4, all Notch receptors, and Hes1 seemed upregulated (Fig. 6G-L and Fig. 7G-I). We observed ectopic expression of Dll4, Notch1 and 4, and Hes5 in the tumor epithelium (Fig. 6I and 6L, and Fig. 7L), which was similar to that described above for the small intestine adenomas. In this region Notch3 was also ectopically expressed, appearing diffusely in the tumor epithelium (Fig. 6L).

Table 1 - Summary of sites of Notch pathway protein expression in the normal small intestine

	small intestine					
	crypts			villi		*lamina propria*
	undifferentiated cells	Paneth cells	goblet cells	enterocytes	goblet cells	
Dll1	X	X			X	X
Dll3				X (diffusely)		X
Dll4	X	X			X	X
Jag1	X (diffusely)			X (diffusely)		X
Jag2	X			X		X
Notch1	X	X		X		X
Notch2	X	X				X
Notch3	X			X		X
Notch4			X		X	X
Hes1	X	X		X		X
Hes5	X	X		X (diffusely)		X

Dll1, 3 and 4 Jagged1 and 2, Notch1-4, Hes1 and 5 protein expression pattern (indicated by an x) in the crypts and villus epithelium and in the *lamina propria* of the normal WT small intestine of C57BL/6 mice at 18 weeks of age. One experiment with n = 2 per group and 2 fields per animal.

Table 2 - Summary of sites of Notch pathway protein expression in the normal large intestine

	large intestine			
	crypts bottom	crypts top		*lamina propria*
		colonocytes	goblet cells	
Dll1			X	X
Dll3		X (diffusely)		X (diffusely)
Dll4			X	X
Jag1	X (diffusely)	X (diffusely)		X
Jag2	X			X
Notch1	X			X
Notch2	X			X
Notch3	X			X
Notch4	X		X	X
Hes1	X	X (diffusely)		X
Hes5	X (diffusely)	X (diffusely)		X

Dll1, 3 and 4 Jagged1 and 2, Notch1-4, Hes1 and 5 protein expression pattern (indicated by an x) in the bottom and top of the crypts and in the *lamina propria* of the normal WT large intestine of C57BL/6 mice at 18 weeks of age. One experiment with n = 2 per group and 2 fields per animal.

Figure 6 - Notch pathway expression pattern in the small and large intestine and in *Apc*$^{Min/+}$ intestinal adenomas

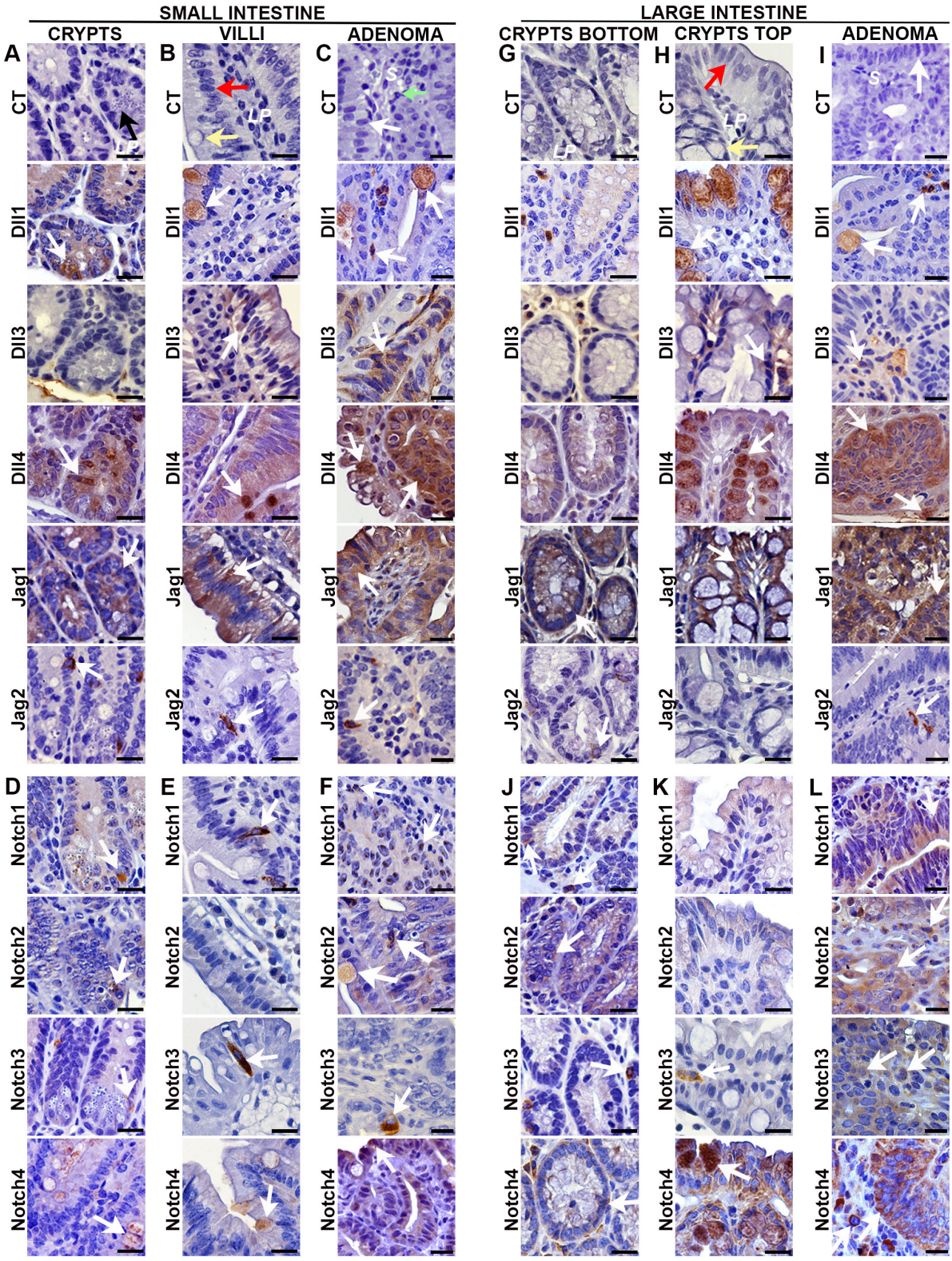

(A-L) Immunohistochemical analysis of Notch ligands and receptors expression (indicated by a white arrow) in the normal small and large intestine of C57Bl/6 mice, and in *Apc*$^{Min/+}$ small and large intestine adenomas (n=2 per group). Control staining was performed with the specific species IgG. Notch ligands (A-C) and receptors (D-F) expression in the small intestine crypts (A, D), villi (B, E) and

adenomas (C, F). Notch ligands (G-I) and receptors (J-L) expression in the large intestine in the bottom (G, J) and top (H, K) of the crypts and in adenomas (I, L). Scale bar = 20μm. Black arrow indicates a Paneth cell (A). Red arrow points to an enterocyte (B) or colonocyte (H); Yellow arrow indicates a goblet cell (B, H); White arrow in (C, I) indicates the tumor epithelium; Green arrow points out a neutrophil (C). *LP, lamina propria*; S, stroma.

Figure 7 - Hes1 and Hes5 expression pattern in the small and large intestine and in *Apc*$^{Min/+}$ intestinal adenomas

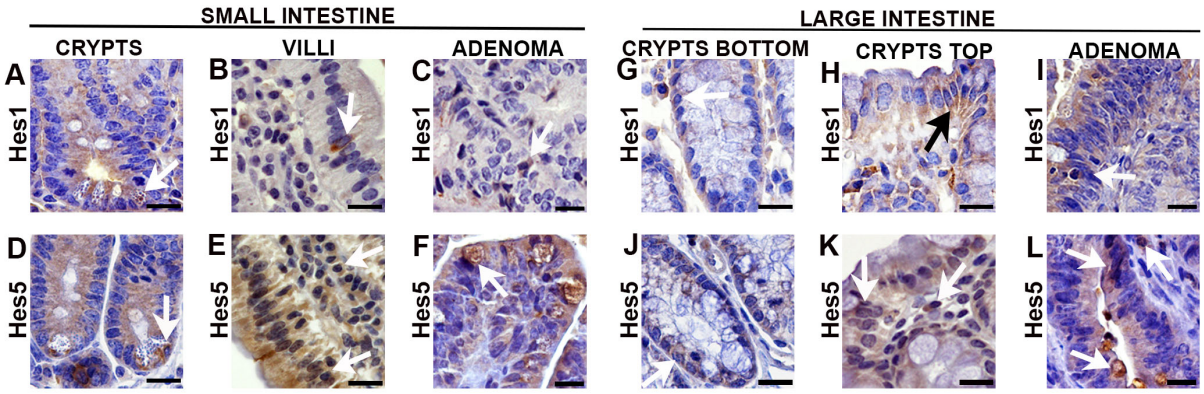

(A-L) Immunohistochemical analysis of Notch effectors Hes1 and Hes5 expression (indicated by an arrow) in the normal small and large intestine of C57BL/6 mice, and in *Apc*$^{Min/+}$ small and large intestine adenomas at 18 weeks of age. One experiment with n = 2 per group and 2 fields per animal. Hes1 (A-C) and Hes5 (D-F) expression in the small intestine crypts (A, D), villi (B, E) and adenomas (C, F). Hes1 (G-I) and Hes5 (J-L) expression in the large intestine in the bottom (G, J) and top (H, K) of the crypts and in adenomas (I, L). Scale bar = 20μm.

4.1.4.2 Endothelial-specific but mainly ubiquitous inhibition of Dll4 function delays the development of intestinal tumors in *Apc*$^{Min/+}$ mouse

Notch signaling activation promotes intestinal tumorigenesis mediated by *Apc* loss of function (Fre et al., 2009). In the present study, Dll4 and Jagged1 ligands appear to be the Notch pathway components with greater expression in the small and large *Apc*$^{Min/+}$ adenomas (Fig. 6C and 6I). Previous authors found that the inhibition of Jagged1-mediated Notch signaling is sufficient to reduce the size of the *Apc*$^{Min/+}$ intestinal tumors (Rodilla et al., 2009). However, Dll4/Notch signaling blockade was never evaluated in the *Apc*$^{Min/+}$ model of CRC. It was previously shown that Dll4/Notch signaling is important to maintain the normal gut homeostasis (Pellegrinet et al., 2011) and therefore may also regulate the process of intestinal tumorigenesis. Studies using a xenografted model of CRC suggested that Dll4, besides promoting a dysfunctional vasculature, could have an additional role maintaining the proliferative cancer stem cells (M. Fischer et al., 2010; Hoey et al., 2009). However, this was never studied in premalignant lesions, the initiating event of CRC. We found that in the *Apc*$^{Min/+}$ small and large intestine, Dll4 is strongly expressed in the tumor epithelium, including

in the goblet and Paneth cell lineages (Fig. 6C and 6I and Fig. 8A-B), and it is also present in the tumor endothelium (Fig. 8C-D). In addition, it is present near the Lgr5 positive stem cells in the normal gut and in the intestinal *Apc*$^{Min/+}$ adenomas (Fig. 8E-H). Therefore, we decided to elucidate if Dll4 inhibition could be effective in blocking *Apc*$^{Min/+}$ tumor initiation and development through angiogenic and/or non-angiogenic mechanisms. To that end, *Apc*$^{Min/+}$ mice with endothelial-specific (endo*Dll4*$^{-/-}$) and ubiquitous (ubiq*Dll4*$^{-/-}$) *Dll4* loss-of-function were analysed. At 18 weeks of age both Dll4 mutants had fewer and smaller tumors than the controls (Fig. 9A-E). Endothelial-specific and ubiquitous Dll4 deletion were more effective reducing tumor number than individual tumor growth, both in the small and large intestine (Fig. 9A-B). Intestinal tumorigenesis, but not the size of the tumors, was more affected in the ubiq*Dll4*$^{-/-}$ than in the endo*Dll4*$^{-/-}$ mutants (Fig. 9A-B). Therefore, the overall intestinal tumor burden of the ubiq*Dll4*$^{-/-}$ mice was reduced 6.4-fold, while in the endo*Dll4*$^{-/-}$ mice it was reduced 4.7-fold (Fig. 9C).

In the endo*Dll4*$^{-/-}$ tumors, the efficacy of the endothelial-specific *Dll4* deletion was evaluated through the expression level of the Notch target gene *Hey2* (A. Fischer, Schumacher, Maier, Sendtner, & Gessler, 2004) that was found to be decreased by 3.9-fold relatively to the controls. For the ubiq*Dll4*$^{-/-}$ mutants we measured *Dll4* expression, which was reduced 3.4-fold relatively to the controls (Fig. 10).

Figure 8 - Dll4 is expressed in tumoral Paneth cells and endothelium, and near tumoral and normal Lgr5+ cells

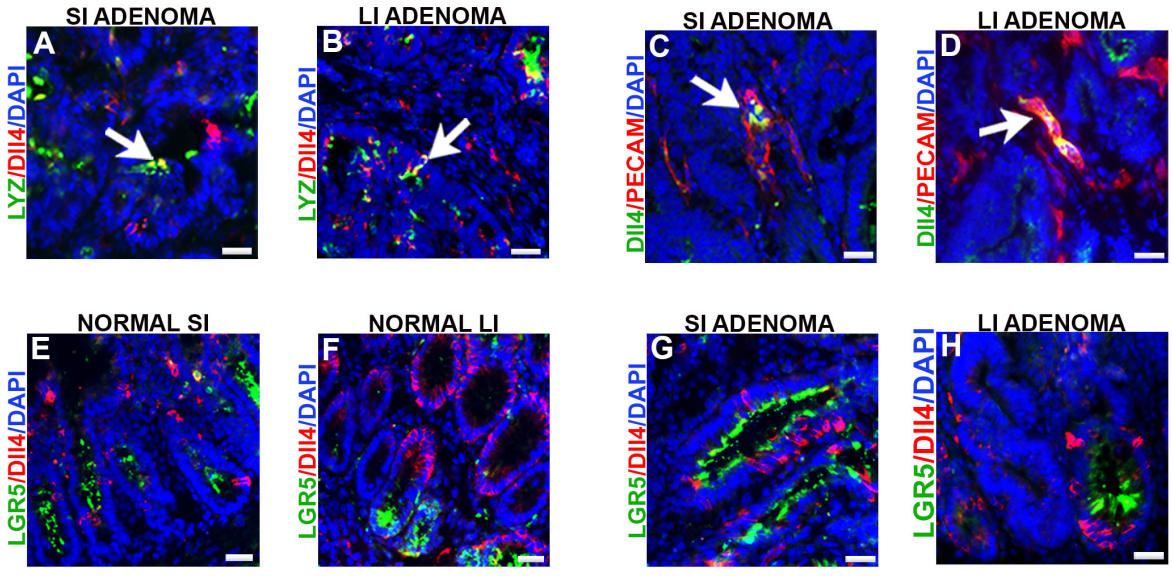

(A, B) Representative images of the immunofluorescence co-staining of Dll4 (in red) with lysozyme (produced by Paneth cells and stained in green) in the *Apc*$^{Min/+}$ small (A) and large (B) intestinal adenomas at 18 weeks of age. (C, D) Representative images of the immunofluorescence co-staining of Dll4 (in green) with PECAM-1 (in red) in the small (C) and large (D) intestinal adenomas. (E-H) Representative images of the immunofluorescence co-staining of Dll4 (in red) with the Lgr5 stem cell

marker (in green) in the normal small (E) and large (F) intestine and in adenomas from the small (G) and large (H) intestine. Nuclei were counterstained with DAPI (in blue). One experiment with n = 2 per group and 6 fields per animal. Scale bar = 50µm. SI, small intestine; LI, large intestine.

Figure 9 - Endothelial-specific and ubiquitous Dll4 loss-of-function inhibits the *Apc*$^{Min/+}$ small and large intestine tumor development

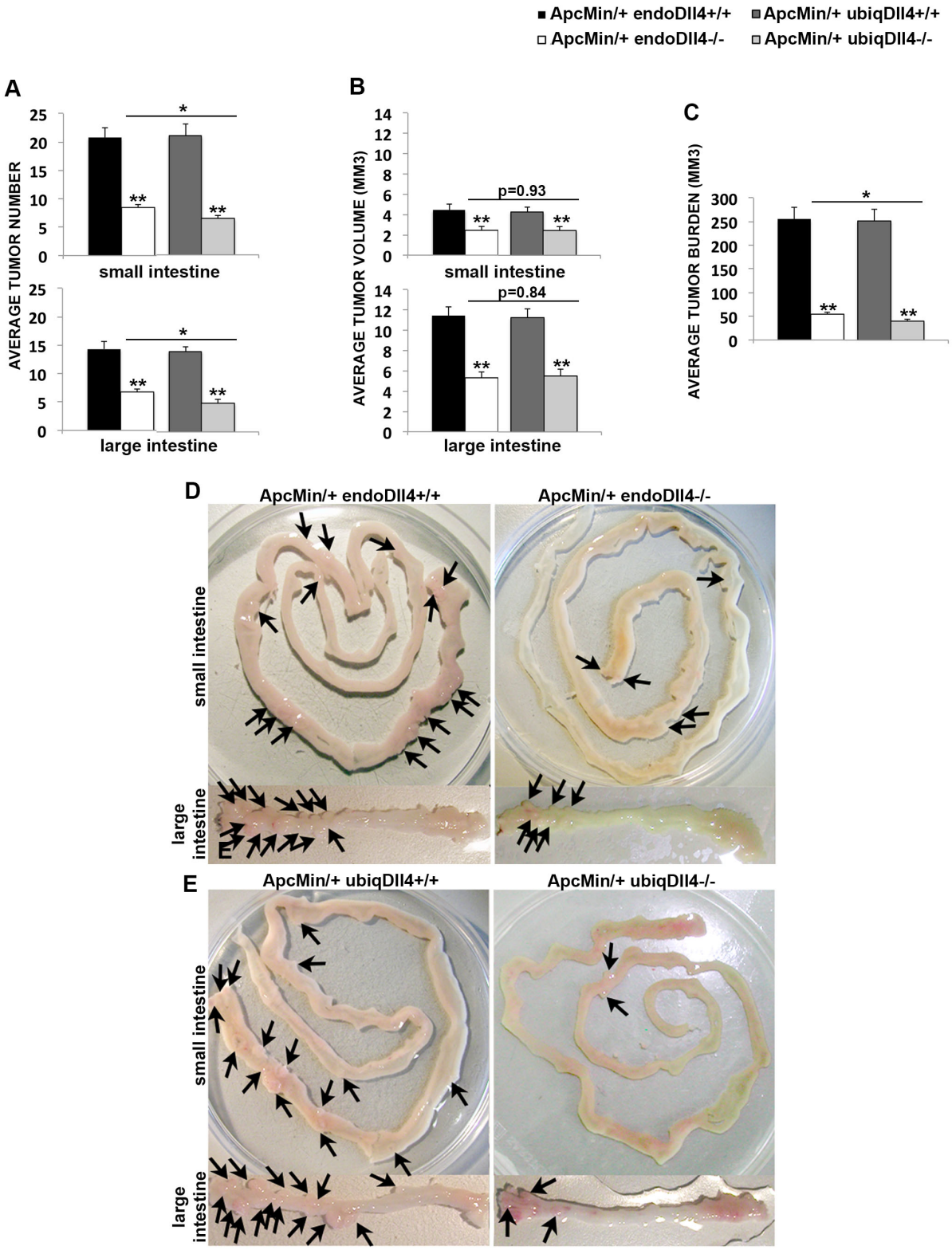

(A-B) Graphic bars represent the average ± SEM tumor number (A) and volume (B) (mm^3) in the small and large intestine of induced *Apc*$^{Min/+}$ endo*Dll4*$^{-/-}$ and *Apc*$^{Min/+}$ ubiq*Dll4*$^{-/-}$ mice *versus* their controls (*Apc*$^{Min/+}$ endo*Dll4*$^{+/+}$ and *Apc*$^{Min/+}$ ubiq*Dll4*$^{+/+}$) at 18 weeks of age. (C) Graphic bars represent the average ± SEM tumor burden (mm^3) in the whole intestine of the animals described above. One experiment with n = 12 per group. **P*<0.05; ***P*<0.01. (D-E) Photographs of the small and large intestines (tumors indicated by arrows) collected from the endothelial-specific mutants (D) and from the ubiquitous mutants (E) *versus* the respective controls.

Figure 10 - Confirmation of Dll4 knockout in endothelial-specific and ubiquitous Dll4 *Apc*$^{Min/+}$ mutant tumors

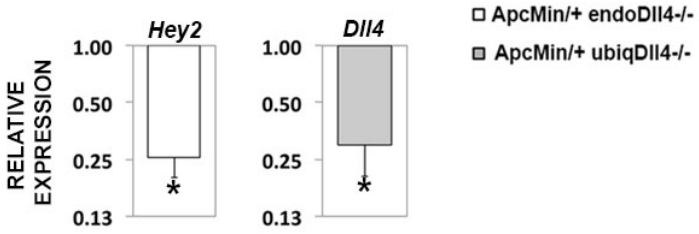

RT-PCR analysis of the Dll4/Notch effector *Hey2* relative expression in the *Apc*$^{Min/+}$ endo*Dll4*$^{-/-}$ intestinal tumors and of *Dll4* relative expression in the *Apc*$^{Min/+}$ ubiq*Dll4*$^{-/-}$ intestinal tumors, both from mice at 18 weeks of age. One experiment with n = 3 per group. The expression of *Hey2* and *Dll4* was normalized to *Pecam-1*. **P*<0.05.

4.1.4.3 Endothelial-specific and ubiquitous Dll4 deletion have similar negative impact in the tumor vasculature, promoting hypoxia and apoptosis in the *Apc*$^{Min/+}$ tumors

Given the critical role of Dll4 on tumor angiogenesis (Djokovic et al., 2010; Noguera-Troise et al., 2006; Ridgway et al., 2006; Scehnet et al., 2007), we analysed the tumor vasculature, hypoxia and apoptosis in the endothelial and ubiquitous mutants. The vascular density of the tumors from the small and large intestine was increased similarly in the endo*Dll4*$^{-/-}$ and ubiq*Dll4*$^{-/-}$ mice (Fig. 11A-C). The tumor vascular maturity was evaluated as the density of smooth muscle cells surrounding the wall of the tumor vessels. In the endo*Dll4*$^{-/-}$ and ubiq*Dll4*$^{-/-}$ mice there was a similar reduction of these smooth muscle cells in the blood vessels of both small and large intestine tumors (Fig. 11A-B and 11D). The functionality of the tumoral vasculature was evaluated by measuring vessel perfusion and extravasation. In the endo*Dll4*$^{-/-}$ and ubiq*Dll4*$^{-/-}$ mice the tumors presented a similar reduction of the vascular perfusion (Fig. 11E-G) and an equivalent increase of the vascular extravasation in both small and large intestine (Fig. 11H-I).

To evaluate tumor hypoxia, tumoral HIF1α density was measured. Both endo*Dll4*$^{-/-}$ and ubiq*Dll4*$^{-/-}$ tumors had an equivalent increase of the hypoxia level in the small and large intestine (Fig. 12A-C).

The apoptotic index, measured using the TUNEL assay, was similarly increased in the tumors of the small and large intestine in endo*Dll4*$^{-/-}$ and ubiq*Dll4*$^{-/-}$ mutants (Fig. 12D-F).

Figure 11 - Endothelial-specific and ubiquitous Dll4 deregulation affects similarly the *Apc*$^{Min/+}$ tumor angiogenesis

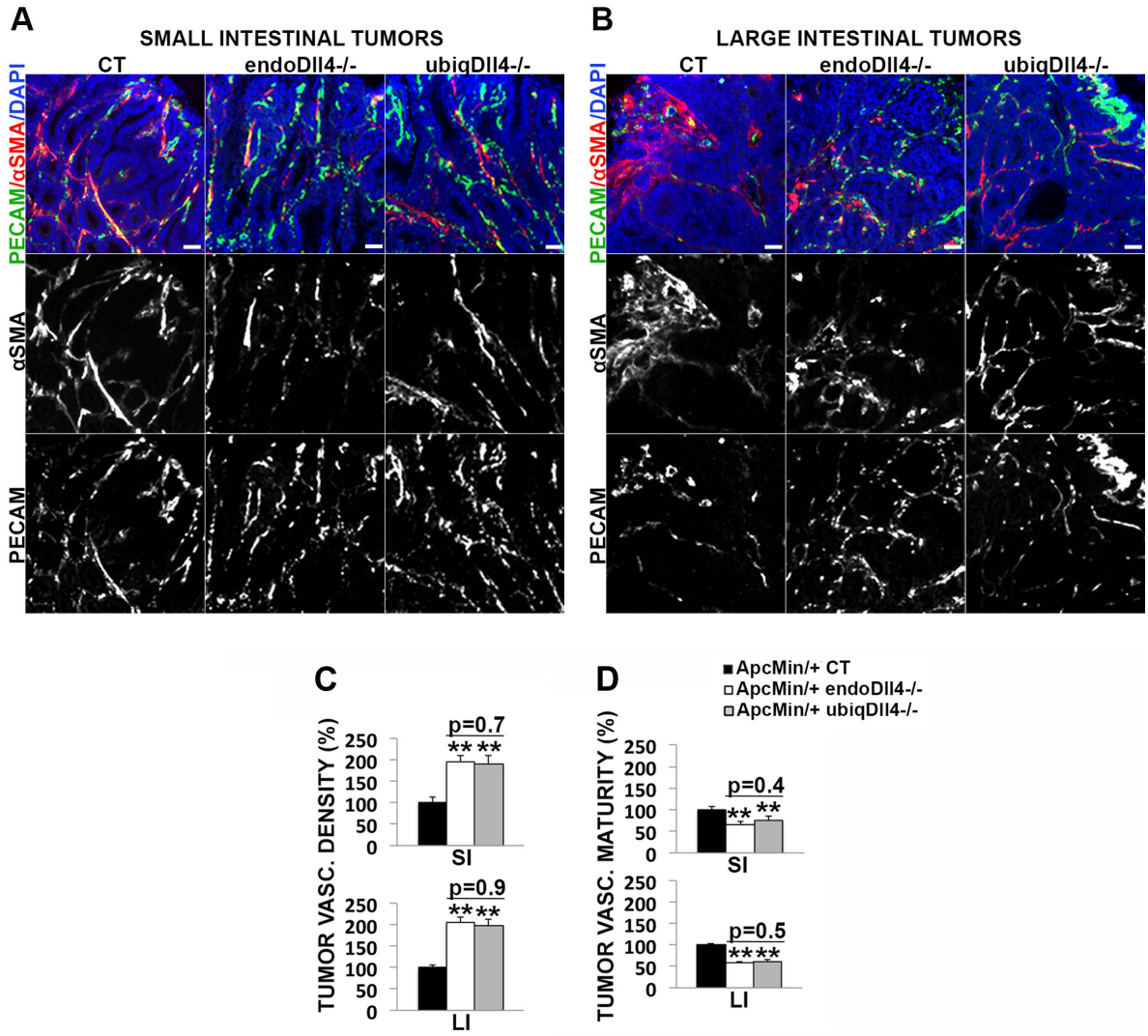

Figure 11 (continuation) - Endothelial-specific and ubiquitous Dll4 deregulation affects similarly the *Apc*$^{Min/+}$ tumor angiogenesis

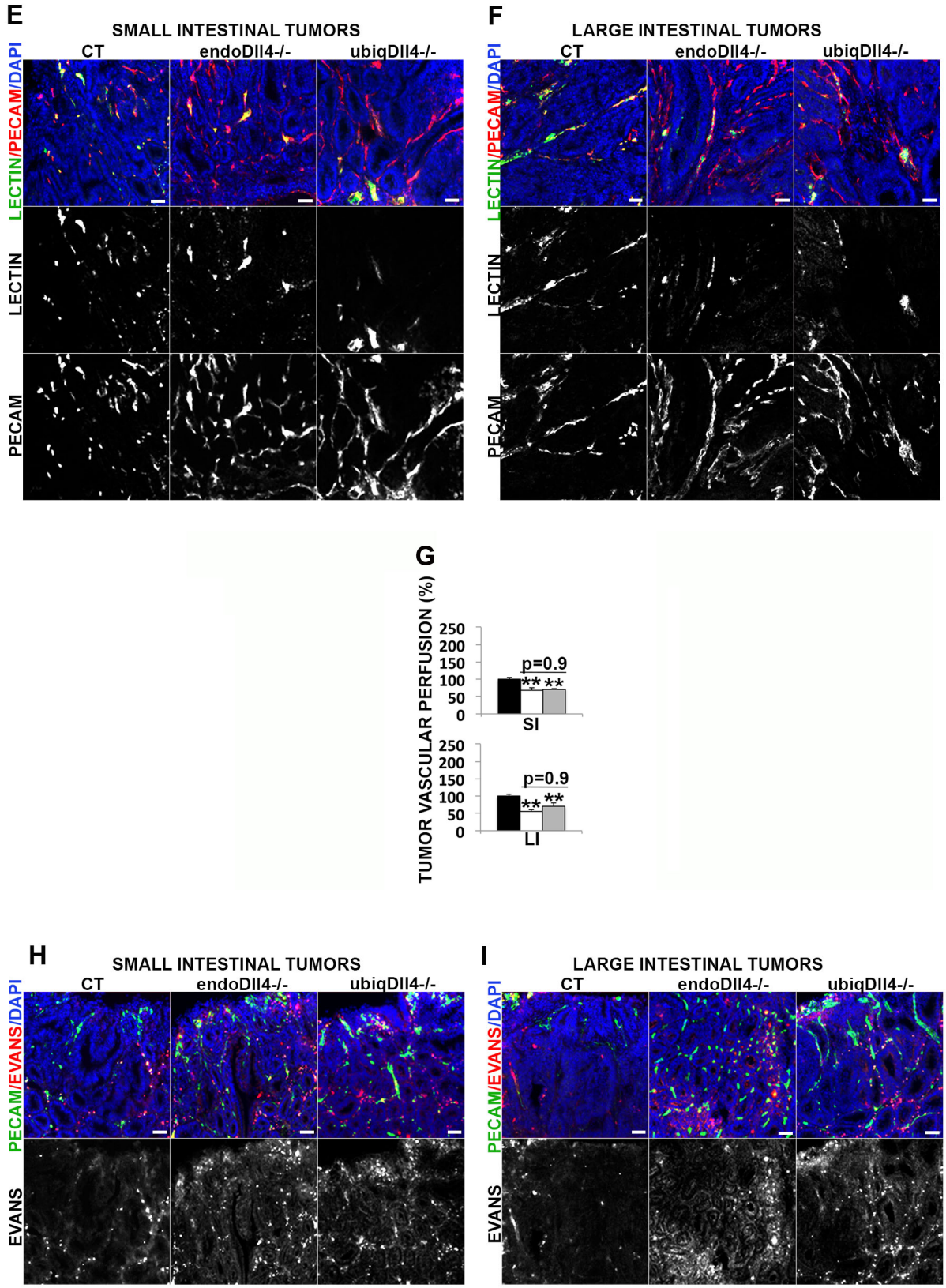

Figure 11 (continuation 2) - Endothelial-specific and ubiquitous Dll4 deregulation affects similarly the *Apc*$^{Min/+}$ tumor angiogenesis

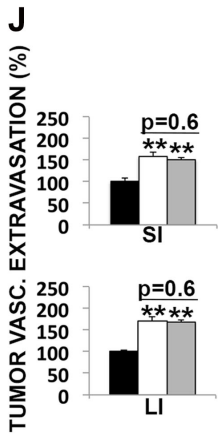

(A, B, E, F, H, I) Immunofluorescence stainings of 20µm small (A, E, H) and large (B, F, I) intestinal tumor cryosections from *Apc*$^{Min/+}$ endo*Dll4*$^{-/-}$, *Apc*$^{Min/+}$ubiq*Dll4*$^{-/-}$ mice and controls (CT) at 18 weeks of age. Scale bars = 100µm. Representative images of staining density for PECAM-1 (in green) and α-SMA (in red) (A, B), for lectin (in green) and PECAM-1 (in red) (E, F), and for PECAM-1 (in green) and Evans blue (in red) (H, I). The nuclei were counterstained with DAPI (in blue). (C, D, G, J) Graphic bars represent the relative (%) ± SEM small (SI) and large (LI) intestinal tumor vascular density (C), maturity (D), perfusion (G) and extravasation (J) in the animals described above**.** One experiment with n = 6 per group and 6 fields per animal. **P*<0.05; ***P*<0.01.

Figure 12 - Endothelial-specific and ubiquitous Dll4 deregulation promotes equally hypoxia and apoptosis in *Apc*$^{Min/+}$ tumors

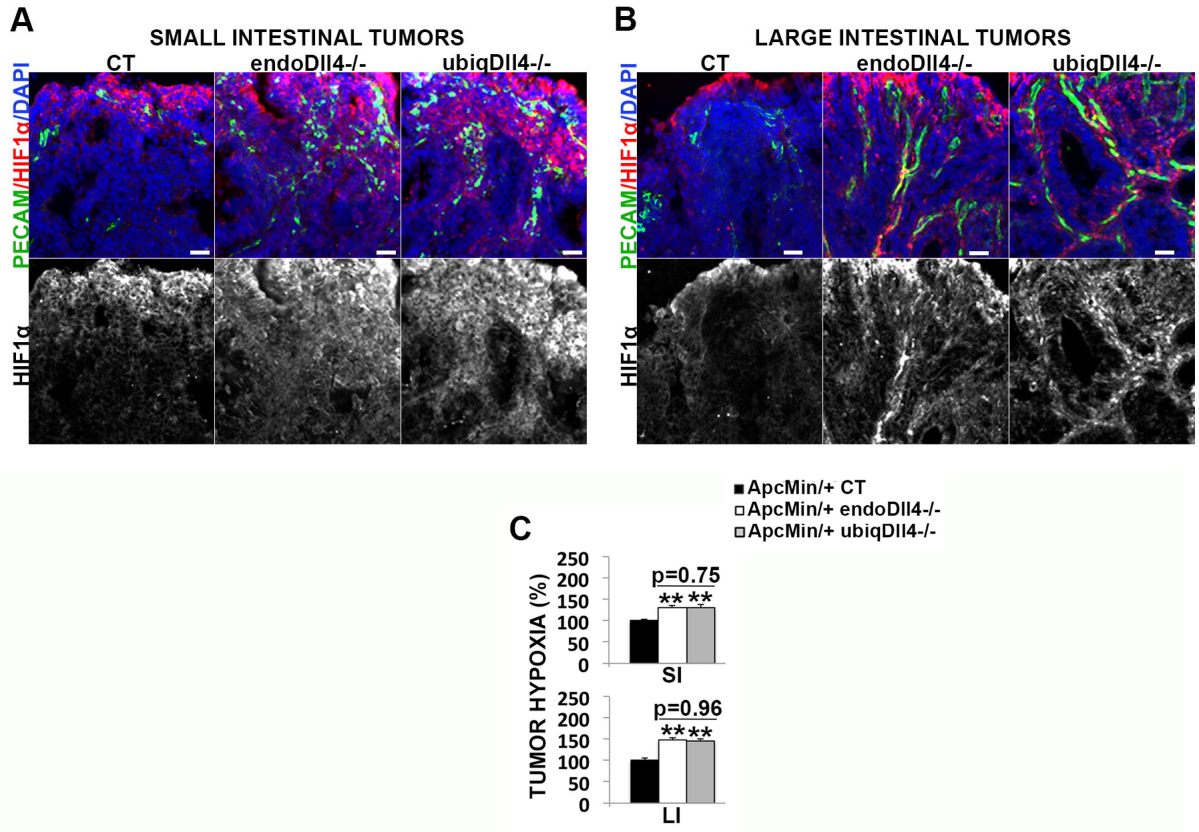

Figure 12 (continuation) - Endothelial-specific and ubiquitous Dll4 deregulation promotes equally hypoxia and apoptosis in *Apc*$^{Min/+}$ tumors

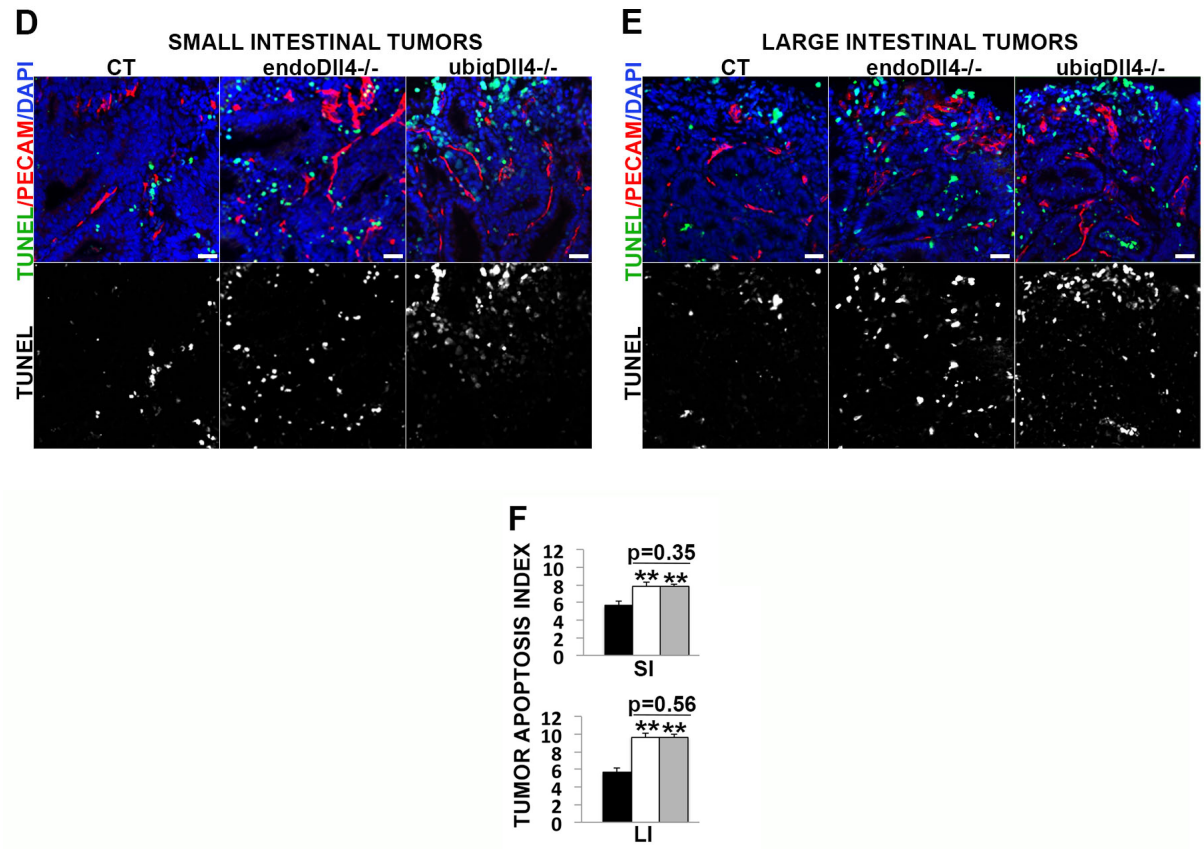

(A, B, D, E) Immunofluorescence stainings of 20µm (A, B) and 10µm (D, E) cryosections of small (A, D) and large (B, E) intestinal tumors collected from *Apc*$^{Min/+}$ endo*Dll4*$^{-/-}$, *Apc*$^{Min/+}$ ubiq*Dll4*$^{-/-}$ and control (CT) mice at 18 weeks of age. Scale bars = 100µm. Representative images of staining density for PECAM-1 (in green) and HIF1α (in red) (A, B), and for TUNEL (in green) and PECAM-1 (in red) (D, E). The nuclei were counterstained with DAPI (in blue). (C, F) Graphic bars represent the relative (%) ± SEM small (SI) and large intestine (LI) tumor hypoxia (C) and tumor apoptotic index (F) in the mice described above One experiment with n = 6 per group and 6 fields per animal. **P*<0.05; ***P*<0.01.

4.1.4.4 Ubiquitous deletion of Dll4 has a significantly stronger effect than endothelial-specific Dll4 deletion in the inhibition of *Apc*$^{Min/+}$ tumor proliferation and neoplastic transformation

In addition to its angiogenic effect, Dll4/Notch seems to regulate the intestinal cancer cells through other mechanisms (T. Hoey et al., 2009). Therefore, we analysed the effect of endothelial-specific *versus* ubiquitous *Dll4* deletion on tumor proliferation. We observed that the small and large intestine tumor cell proliferation was reduced in the endo*Dll4*$^{-/-}$ and mainly in the ubiq*Dll4*$^{-/-}$ mice (Fig. 13A-C). The ubiq*Dll4*$^{-/-}$ mice exhibited a statistically significant stronger reduction of tumor proliferation than the endo*Dll4*$^{-/-}$ mice both in the small and large intestine (Fig. 13A-C).

Additionally, we analysed if Dll4 deregulation was affecting the *Apc*$^{Min/+}$ neoplastic transformation. The samples were histopathologically classified in hyperplasia, adenoma with low-grade dysplasia and adenoma with high-grade dysplasia (Fig. 14). No adenocarcinoma lesions were detected. The *Apc*$^{Min/+}$ small and large intestine neoplastic transformation seemed to be only delayed in the ubiq*Dll4*$^{-/-}$ mice, as they presented substantially more lesions of hyperplasia and less adenomas with high-grade dysplasia comparative to the controls in the large and, mainly, in the small intestine (Fig. 13D-E). Thus, in the controls and endo*Dll4*$^{-/-}$ mice the majority of the small and large intestine lesions where adenomas with high-grade dysplasia, while in the ubiq*Dll4*$^{-/-}$ mice most of the lesions were hyperplasias and adenomas with low-grade dysplasia in the small and large intestine, respectively (Fig. 13D-E).

4.1.4.5 Ubiquitous deletion of *Dll4* has a stronger inhibitory effect than the endothelial-specific blockade on *Apc*$^{Min/+}$ tumor stem cell maintenance independently of β-catenin activation

Recent studies showed that the mitotically active Lgr5-positive and the quiescent Bmi1-positive stem cells are responsible for intestinal tumorigenesis (Espersen et al., 2015; Maynard et al., 2014; Schepers et al., 2012) and that this is regulated by Notch signaling (Lopez-Arribillaga et al., 2015; VanDussen et al., 2012). Therefore, given the observed reduction in the *Apc*$^{Min/+}$ small and large intestine tumor number in the *Dll4* knock-out mice compared with the controls, we decided to analyse if Dll4 reduction was affecting the Lgr5+ and/or Bmi1+ stem cell expression in the tumors. Compared with the controls, Lgr5 protein and gene expression was reduced in the small and large intestine tumors from both mutants, but mainly in those from ubiq*Dll4*$^{-/-}$ mice (Fig. 13F-J). Additionally, as previously shown by Pellegrinet et al., we did not observe differences in the density of Lgr5-positive stem cells in the adjacent normal intestine of the mutants (Pellegrinet et al., 2011) (data not shown). In the case of the Bmi1 stem cell marker, its expression was only reduced in the ubiq*Dll4*$^{-/-}$ mice, in both small and large intestine tumors (Fig. 13I-J). The differences between the two types of *Dll4* mutants in the expression of Lgr5 and Bmi1 markers in the small and large intestine tumors were statistically significant (Fig. 13F-J).

Previous reports indicated that Notch signaling seems to maintain the intestinal stem cells by transcriptionally repressing the cyclin-dependent kinase inhibitors 1B *(Cdkn1b)* and 1C *(Cdkn1c)* (Riccio et al., 2008). Accordingly, we observed an increase of *Cdkn1b and Cdkn1c* gene expression only in the ubiq*Dll4*$^{-/-}$ small and large intestine tumors relatively to the controls and to the endo*Dll4*$^{-/-}$ mice (Fig. 13I-J).

Myc and cyclin D1 and D2 are important regulators of intestinal stem cells and are implicated in tumor initiation and progression (Cole et al., 2010; Hulit et al., 2004; Ignatenko et al., 2006). We observed they were all downregulated only in the ubiq*Dll4*$^{-/-}$ small and large

intestine tumors, mainly in the first region, relatively to the controls and to the endo*Dll4*$^{-/-}$ mice (Fig. 13I-M).

Given the central role of the Wnt signaling in *Apc*$^{Min/+}$ tumorigenesis (Sansom, 2004), we measured the tumor density of the Wnt pathway-derived non-phosphorylated (active) β-catenin to understand if Dll4 ubiquitous and/or endothelial-specific inhibition was affecting this pathway. We did not observe statistically significant differences in either of the mutants (Fig. 15A-B).

Figure 13 - Ubiquitous deletion of Dll4 has a greater inhibitory effect in the *Apc*$^{Min/+}$ tumorigenesis and neoplastic transformation than the endothelial-specific deletion

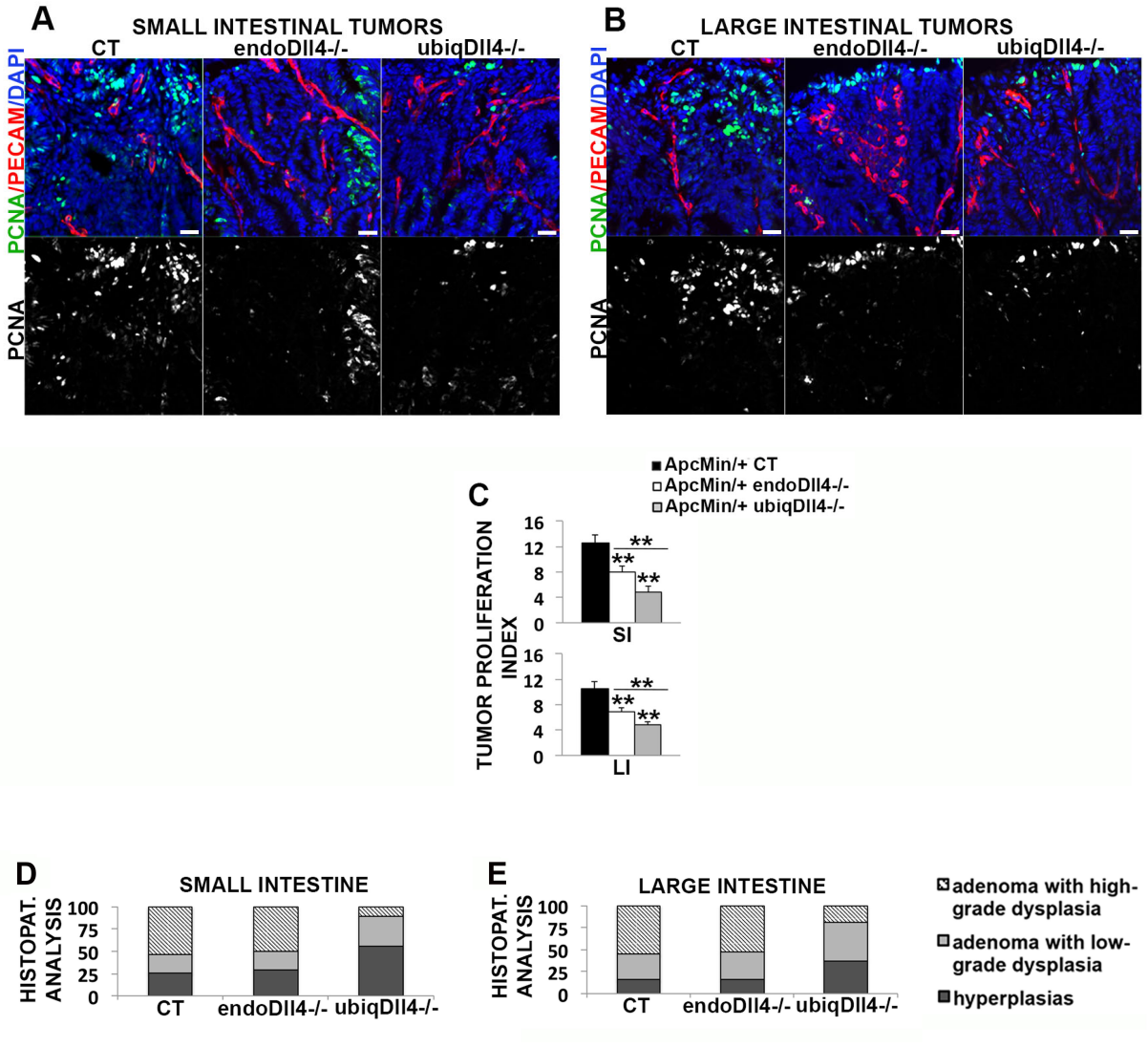

Figure 13 (continuation) - Ubiquitous deletion of Dll4 has a greater inhibitory effect in the *Apc*$^{Min/+}$ tumorigenesis and neoplastic transformation than the endothelial-specific deletion

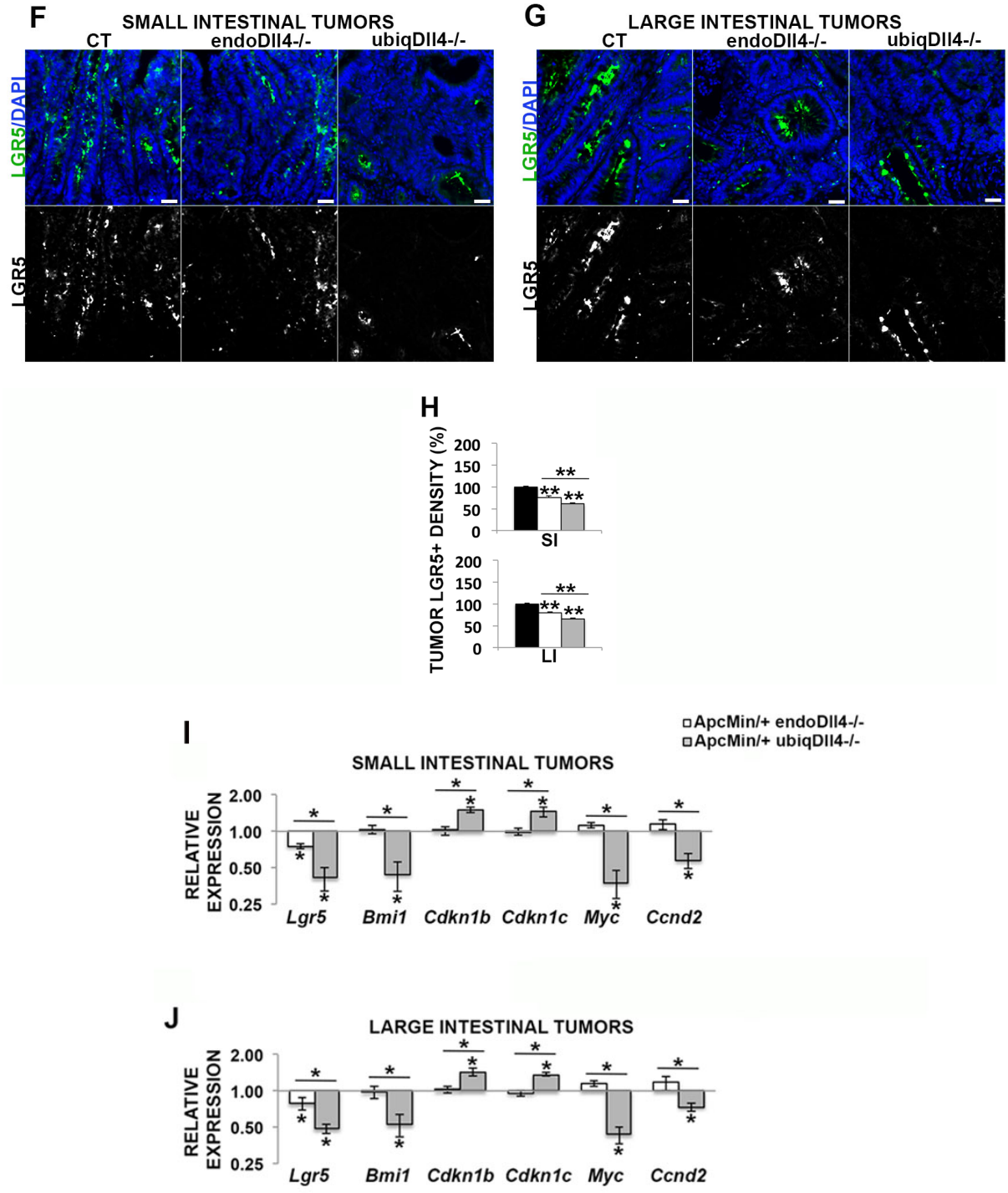

Figure 13 (continuation 2) - Ubiquitous deletion of Dll4 has a greater inhibitory effect in the *Apc*$^{Min/+}$ tumorigenesis and neoplastic transformation than the endothelial-specific deletion

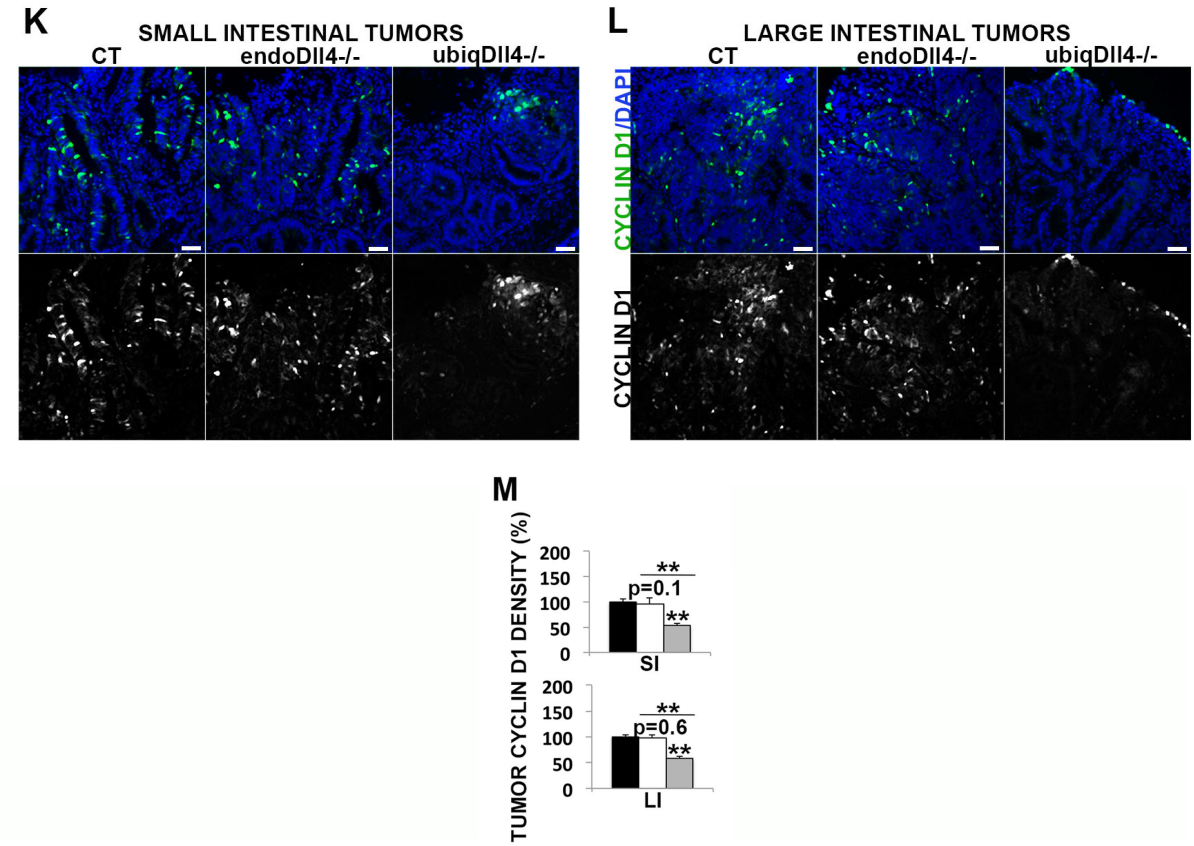

(A, B, F, G, K, L) Immunofluorescence stainings of small (A, F, K) and large (B, G, L) intestinal tumor cryosections (10µm) from *Apc*$^{Min/+}$ endo*Dll4*$^{-/-}$ and ubiq*Dll4*$^{-/-}$ mice *versus* the controls (CT) at 18 weeks of age. Representative images of staining density for PCNA (in green) and PECAM-1 (in red) (A, B), for Lgr5 (in green) (F, G), and for Cyclin D1 (in green) (K, L). The nuclei were counterstained with DAPI (in blue). Scale bars = 100µm. (C, H, M) Graphic bars represent the small (SI) and large intestine (LI) tumor proliferation index (C), and the relative tumor Lgr5 (H) and Cyclin D1 (M) density (%) ± SEM in the animals described above. One experiment with n = 6 per group and 6 fields per animal. (D, E) Graphic bars represent the proportion (%) of hyperplasias and adenomas with low and high-grade dysplasia obtained in the histopathological analysis (H&E) of the macroscopic small (D) and large (E) intestinal lesions from *Apc*$^{Min/+}$ endo*Dll4*$^{-/-}$, ubiq*Dll4*$^{-/-}$ and control (CT) mice at 18 weeks of age. One experiment with n = 12 per group. (I, J) RT-PCR analysis of *Lgr5*, *Bmi1, Cdkn1b, Cdkn1c, Myc, Ccnd2* relative expression in the *Apc*$^{Min/+}$ endo*Dll4*$^{-/-}$ and ubiq*Dll4*$^{-/-}$ small (I) and large (J) intestinal tumor samples from mice at 18 weeks of age. One experiment with n = 3 per group. **P*<0.05; ***P*<0.01.

Figure 14 - Histopathological classification of the *Apc*$^{Min/+}$ small and large intestine lesions

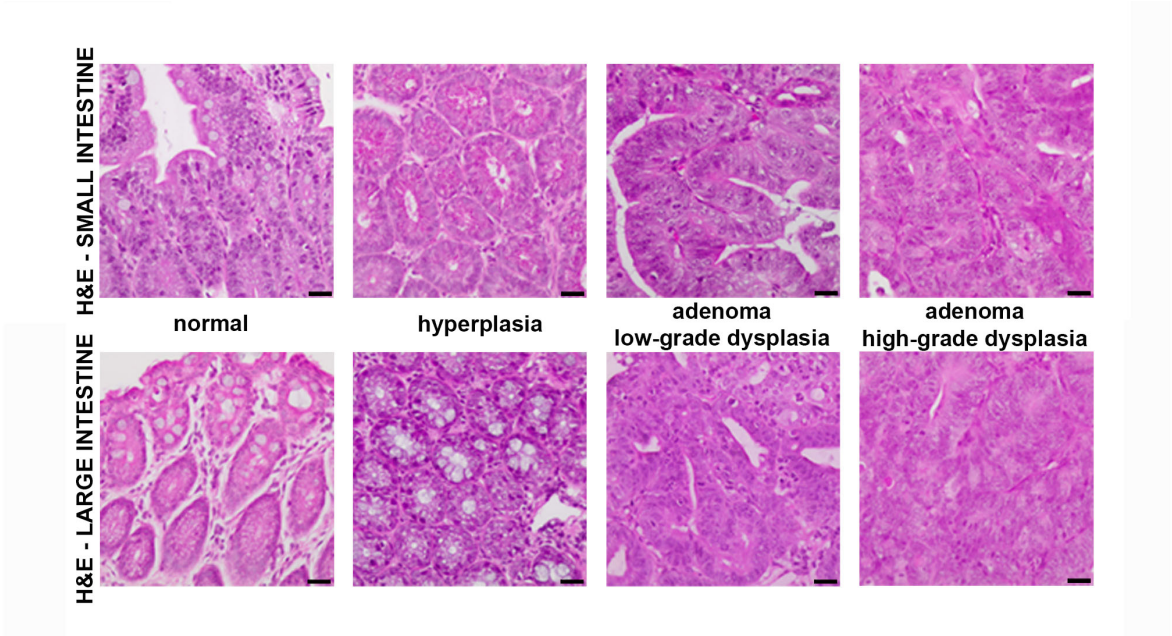

H&E images of the normal small and large intestine, and of a hyperplasia and adenomas with low and high-grade dysplasia from these regions, the lesions found in the *Apc*$^{Min/+}$ endo*Dll4*$^{-/-}$, *Apc*$^{Min/+}$ ubiq*Dll4*$^{-/-}$ and controls at 18 weeks of age. One experiment with n = 12 per group. Scale bars = 100μm.

Figure 15 - Dll4 endothelial-specific and ubiquitous deregulation does not affect the intestinal *Apc*$^{Min/+}$ associated β-catenin activation

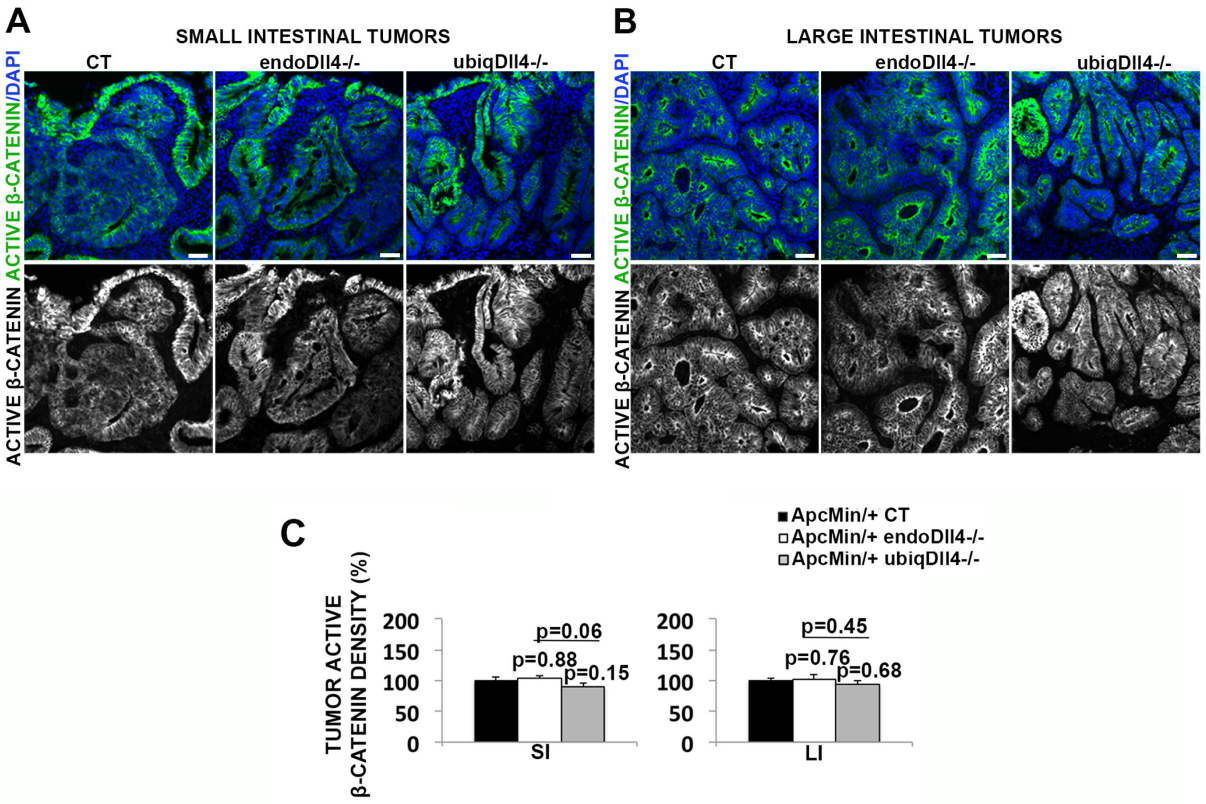

(A, B) Representative images of the immunofluorescence staining density for non-phosphorylated (active) β-catenin (in green) of the small (A) and large (B) intestine tumor cryosections (10μm) from *Apc*$^{Min/+}$ endo*Dll4*$^{-/-}$ and *Apc*$^{Min/+}$ ubiq*Dll4*$^{-/-}$ mice *versus* controls (CT) at 18 weeks of age. The nuclei were counterstained with DAPI (in blue). Scale bars = 100μm. (C) Graphic bars represent the small and large intestine relative tumor non-phosphorylated (active) β-catenin density ± SEM in the animals described above. One experiment with n = 6 per group and 6 fields per animal.

4.1.4.6 Ubiquitous, but not endothelial-specific deletion of Dll4, promotes epithelial differentiation and secretory lineage commitment in the *Apc*$^{Min/+}$ tumors

It has been reported that Notch signaling is required for repression of secretory cell differentiation in colon cancer (Sikandar et al., 2010). Blocking this pathway by removal of its transcription factor *RBP-J*$_k$ or by treatment with gamma-secretase inhibitors, causes a complete conversion of normal and tumoral intestinal proliferative cells into post-mitotic goblet cells (van Es, van Gijn, et al., 2005). This raises the possibility that the observed reduction of tumoral stem cells might be related to differentiation towards the secretory cell lineages. Therefore we evaluated the density of the epithelial differentiation marker E-cadherin (Tsanou, Peschos, Batistatou, Charalabopoulos, & Charalabopoulos, 2008) and determined the density of Paneth cells in the tumors, by measuring the level of lysozyme (which is produced by these cells) and the proportion of goblet cells. Paneth cells are normally present only in the small intestine, but previous reports showed Paneth cell metaplasia in large intestine adenomas (Wada et al., 1992).

Relatively to the controls, we found a moderate increase of tumor epithelial differentiation in the ubiq*Dll4*$^{-/-}$, but not in the endo*Dll4*$^{-/-}$, small and large intestine (Fig. 16A-C). Additionally, the density of Paneth cells and mainly the proportion of goblet cells were increased only in the ubiq*Dll4*$^{-/-}$ small and large intestine tumors (Fig. 16D-J). The differences between the two Dll4 mutants in the level of epithelial differentiation and specifically in the density of Paneth and goblet cells were statistically significant (Fig. 16A-J).

We also measured the relative transcription in the tumors of *Akp3, Muc2, Lyz1* and *Neurog3* markers for the enterocyte, goblet, Paneth and neuroendocrine cell populations, respectively, and also of the promoters of secretory lineage commitment *Atoh1* and *Klf4* (Katz et al., 2002;Yang et al., 2001). Compared with the controls, all the lineage markers evaluated were significantly increased in the ubiq*Dll4*$^{-/-}$ tumors, mainly *Muc2,* and *Lyz1* in the small intestine and *Muc2, Atoh1 and Klf4* in the large intestine (Fig. 16K-L). No significant differences were observed in the endo*Dll4*$^{-/-}$ small and large intestine tumors relatively to the controls (Fig. 16K-L).

Figure 16 - Ubiquitous, but not endothelial-specific, loss of Dll4 promotes intestinal differentiation towards the secretory lineages

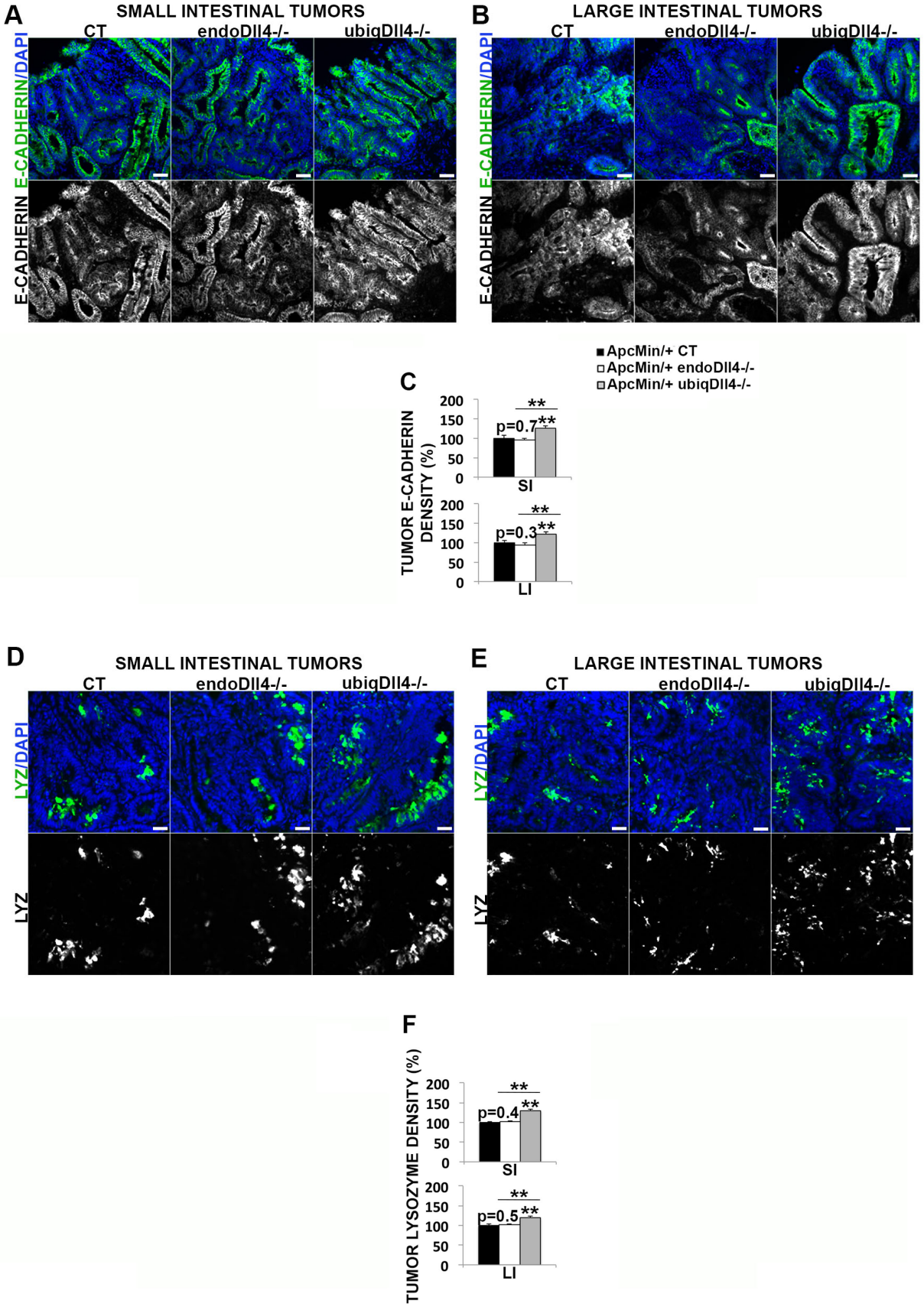

Figure 16 (continuation) - Ubiquitous, but not endothelial-specific, loss of Dll4 promotes intestinal differentiation towards the secretory lineages

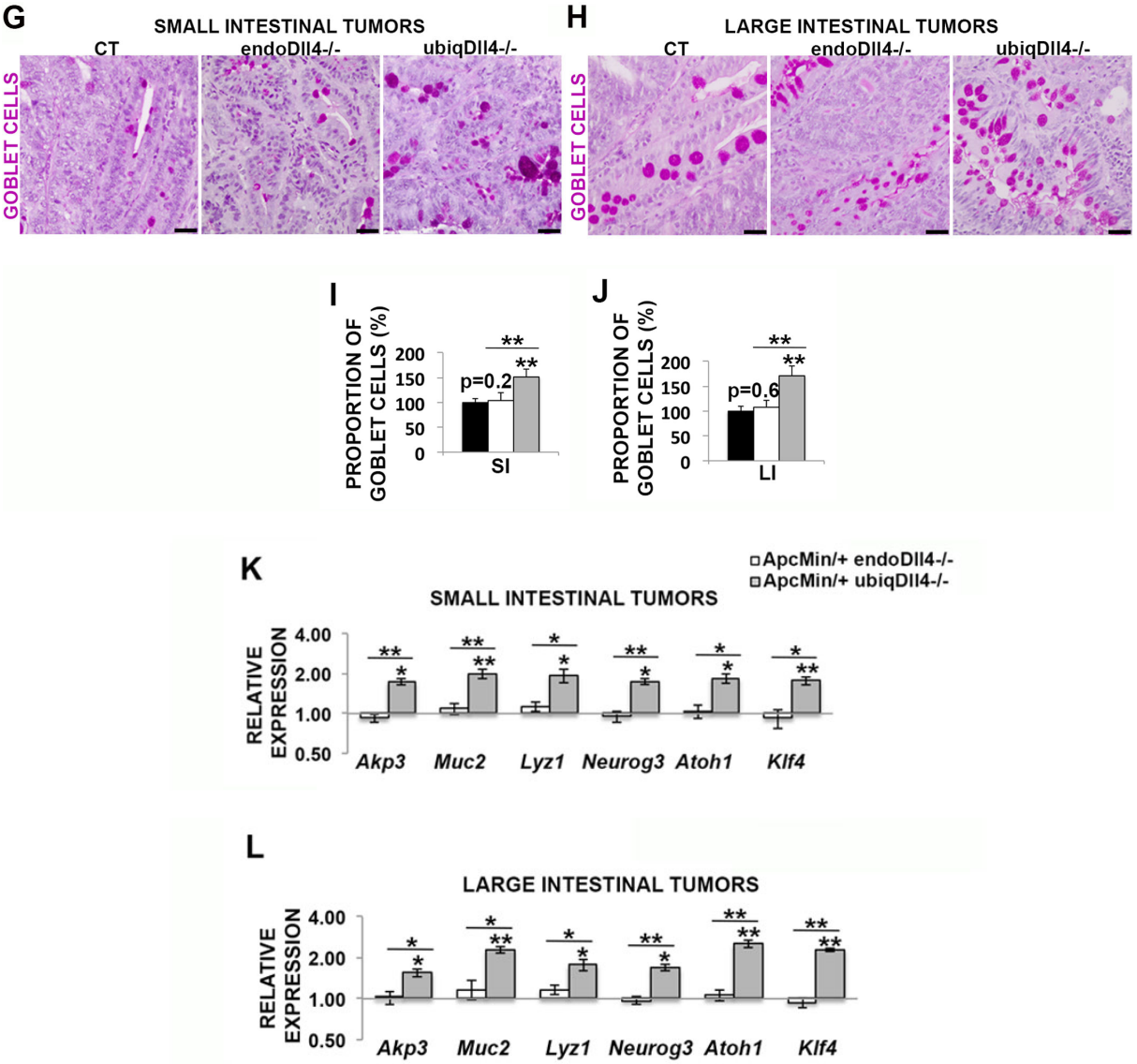

(A, B, D, E) Immunofluorescence stainings of small (A, D) and large (B, E) intestinal tumor cryosections (10µm) from *Apc*$^{Min/+}$ endo*Dll4*$^{-/-}$ and ubiq*Dll4*$^{-/-}$ mice *versus* controls (CT) at 18 weeks of age. Representative images of staining density for E-cadherin (in green) (A, B) and lysozyme (in green) (D, E). Nuclei were counterstained with DAPI (in blue). Scale bars = 100µm. (C, F) Graphic bars represent the tumor relative (%) ± SEM density of E-cadherin (C) and lysozyme (F) in the small (SI) and large (LI) intestinal tumors from the animals described above. One experiment with n = 6 per group and 6 fields per animal. (G, H) PAS staining (of goblet cells) of paraffin-embedded small (G) and large (H) intestinal tumor sections (4µm) from *Apc*$^{Min/+}$ endo*Dll4*$^{-/-}$ and ubiq*Dll4*$^{-/-}$ mice *versus* controls (CT) at 18 weeks of age. Scale bars = 100µm. (I, J) Graphic bars represent the relative proportion (%) ± SEM of goblet cells in the small (I) and large (J) intestinal tumor epithelium from the animals described above. One experiment with n = 6 per group and 6 fields per animal. (K, L) RT-PCR analysis of *Akp3, Muc2, Lyz, Neurog3, Atoh1, Klf4* relative expression in the *Apc*$^{Min/+}$ endo*Dll4*$^{-/-}$ and *Apc*$^{Min/+}$ ubiq*Dll4*$^{-/-}$ small (K) and large (L) intestinal tumor samples. One experiment with n = 3 per group. **P*<0.05; ***P*<0.01.

4.1.5 Discussion

Activation of Notch pathway seems to promote intestinal tumorigenesis induced by *Apc* loss (Fre et al., 2009) and Dll4 is one of the Notch signaling pathway components found to be upregulated in these tumors (Peignon et al., 2011). Reports have shown that Dll4 inhibition delays the tumor growth by deregulating the tumor angiogenic process (Djokovic et al., 2010; Noguera-Troise et al., 2006; Ridgway et al., 2006; Scehnet et al., 2007), but in CRC anti-DLL4 therapy may also reduce the cancer stem cell frequency (M. Fischer et al., 2010; Hoey et al., 2009). Despite the advances in the understanding of Dll4/Notch signaling in cancer, most of the previous reports were focused on role of Dll4 in the tumor angiogenic process and further studies are still needed to unveil all the mechanisms by which Dll4 affects the tumor initiation and development in the gut.

Reports have shown that all Notch receptors, ligands and some of the Notch target genes are expressed in the normal gut (Sander & Powell, 2004; Schroder & Gossler, 2002; van Es et al., 2005). However, in the $Apc^{Min/+}$ intestinal tumors their expression has been poorly described. A study indicated that expression of Notch receptors and ligands closely follows the expression in the normal crypts, while Hes1 expression was observed uniformly in the adenomas (van Es et al., 2005). Other report showed that Jagged1 is overexpressed in the tumor tissue with concomitant Notch1 and 2 activation (Rodilla et al., 2009). In the present work we analysed the protein expression pattern of most Notch pathway members in the $Apc^{Min/+}$ intestinal tumors compared with the normal WT gut. Regarding the previous gene expression analysis of Notch members in the normal gut (Sander & Powell, 2004; Schroder & Gossler, 2002), we observed some differences in our analysis. These included the presence of Notch2 in the bottom of the large intestine crypts, of Notch3 and 4 in the small and large intestine epithelium and Hes1 not only in the small intestine crypts (Schroder & Gossler, 2002), but diffusely expressed in the small and large intestine.

Our expression analysis in the $Apc^{Min/+}$ small and large intestine adenomas confirmed that the Notch pathway is present and activated in intestinal adenomas harbouring *Apc* mutations (Fre et al., 2009; Peignon et al., 2011; Rodilla et al., 2009; van Es et al., 2005). Dll4 and Jagged1 were more expressed in these tumors than the other members of this pathway. Comparing the adenomas with the normal WT gut we found that Jagged2 and Dll3 partially lose their expression (the last only in the large intestine). We observed a different expression pattern of Dll4, all Notch receptors (with regional variation) and Hes5 in the tumor epithelium. The same Notch members and Hes1, instead of Hes5, seemed upregulated in the adenomas (Notch3 only in the large intestine). Thus our expression analysis indicates that in the $Apc^{Min/+}$ small and large intestine adenomas, Dll4 is the most upregulated ligand and is present both in the tumor epithelium and endothelium.

In the normal gut Dll4 acts redundantly with Dll1 mediating the Notch signaling regulation of the intestinal stem cells proliferation and their commitment towards de secretory cell fate

(Pellegrinet et al., 2011). We found that Dll4 is expressed near the Lgr5+ stem cells also in the intestinal tumors, therefore indicating a possible role of this ligand in the maintenance of also the tumor stem cells. These stem cells are believed to be responsible for tumor initiation and progression (Barker et al., 2009; Boman & Wicha, 2008) and depend on proper angiogenesis to function and survive (Zhao et al., 2011). Therefore we intended to elucidate if Dll4 also regulates the fate of tumor stem cells beside its angiogenic effect in a spontaneous model of CRC, the $Apc^{Min/+}$ mouse. To address this question we compared ubiquitous with endothelial-specific Dll4 loss-of-function mouse mutants. Our results highlighted the importance of Dll4 angiogenic and epithelial effect during intestinal $Apc^{Min/+}$ tumor initiation and development rather than in maintaining the normal gut homeostasis. Pellegrinet el al. reported that in the normal gut, *Dll4* intestinal epithelial-specific inhibition alone is not sufficient to promote a phenotype due to redundant Dll1-mediated Notch signaling (Pellegrinet et al., 2011). This lack of intestinal effect after *Dll4* inhibition can also be related to the fact that in the normal gut simultaneous inhibition of *Notch1* and *2* is necessary to result in complete conversion of the crypt progenitors into postmitotic goblet cells (Riccio et al., 2008) and it is not known whether Dll4 can activate both receptors in the gut. Nevertheless, our results show that Dll4 seems at least partially responsible for the known effects of Notch activation during intestinal tumorigenesis, as Dll4 ubiquitous deletion led to a similar, but less pronounced, epithelial phenotype as the pan-Notch/*gamma*-secretase inhibition in the $Apc^{Min/+}$ tumors (van Es et al., 2005). However, as the alterations were moderated with no macroscopic repercussions (no observed increase of mucus secretion) in the ubiquitous Dll4 mutants' gut, Dll1 may partially compensate the lack of Dll4 in this setting and/or Dll4 may not activate both Notch1 and 2 receptors. In addition, as we only analysed the Lgr5 and Bmi1 positive stem cell populations, it is not certain if this pathway can affect similarly all the stem cells present in the intestinal tumors.

We found that ubiquitous and endothelial-specific Dll4 blockade led to a similar phenotype in the small and large intestine, but a stronger effect on tumor initiation was observed in the small intestine and a greater impact on tumor growth was seen in the large intestine.

By comparing the ubiquitous mutants with the endothelial-specific knockouts we found that the observed epithelial phenotype is probably caused by the deregulation of the tumor angiogenesis but also by other important mechanisms. Both ubiquitous and endothelial-specific mutants had a similar angiogenic phenotype, with similarly increased hypoxia and apoptosis leading to similar reduction of the tumor volume. Therefore, Dll4 deletion inhibited the intestinal tumor growth mainly by inducing a dysfunctional and immature angiogenesis that led to hypoxia and therefore apoptosis as previously reported in other tumor models (Djokovic et al., 2010; Noguera-Troise et al., 2006; Ridgway et al., 2006; Scehnet et al., 2007).

The multiplicity of tumors was also reduced in the mutants relatively to their controls and this effect was more pronounced in the ubiquitous than in the endothelial-specific mutants, associated to a stronger reduction of tumor cell proliferation and tumor stem cell density in the first mutants. The stronger inhibitory effect on tumor cell proliferation through Dll4 ubiquitous deletion may have therefore prevented the accumulation of more mutations that lead to tumor initiation, promote the transition of microadenomas to macroadenomas and favor the neoplastic transformation. Therefore in the intestinal adenomas, Dll4 seems to promote proliferation and maintain the stem cells through angiogenic, but also non-angiogenic related mechanisms. Indeed we observed decreased expression of Myc, cyclin D1 and D2, independently of β-catenin activation, only in the ubiq*Dll4*$^{-/-}$ tumors.

The Wnt signaling has been considered a crucial player in the initiation of CRC associated to inactive mutations in the *APC* gene (Fearnhead et al., 2001). Nuclear accumulation of β-catenin promotes neoplastic conversion by triggering the cell cycle-regulators Cyclin D1 and D2 and Myc and, consequently, uncontrolled cell proliferation contributing to tumor progression (Cole et al., 2010; He et al., 1998; Tetsu & McCormick, 1999). Notch signaling seems to cooperate with Wnt signaling to trigger intestinal tumorigenesis, as activation of Notch in *Apc* mutant mice led to a significant increase in the number of adenomas developed (Fre et al., 2009). Additionally, a previous study indicated that Jagged1 was the link between Wnt and Notch pathways in the *Apc*$^{Min/+}$ tumorigenesis, where β-catenin seems to transcriptionally activate Jagged1 (Rodilla et al., 2009). However, it has been shown that the Mastermind-like 1 co-activator of Notch pathway can bind to the promoters of Cyclin D1 and Myc in colon cancer cell lines (Alves-Guerra, Ronchini, & Capobianco, 2007) and these molecules are activated directly by Notch1 in other types of cancer (Efstratiadis, Szabolcs, & Klinakis, 2007) and possibly Cyclin D1 in CRC (Gopalakrishnan, Saravanakumar, Madankumar, Thiyagu, & Devaraj, 2014). It has been also demonstrated that Cyclin D2 and Myc are also induced by Notch1 to promote stem cell renewal in another setting (Satoh et al., 2004). Additionally, the overexpression of Dll4 in a leukemia cell line led to increased protein expression of Myc (Shi & Rui, 2011). Therefore, during *Apc*$^{Min/+}$ tumorigenesis Dll4/Notch signaling may directly upregulate the expression of Cyclin D1 and D2 and Myc. We observed that Dll4 deletion reduced tumorigenesis without affecting β-catenin nuclear accumulation and thus Wnt activation. Therefore, Dll4/Notch activation may promote intestinal tumorigenesis by angiogenic and non-angiogenic mediated mechanisms in a β-catenin independent manner. The non-angiogenic related regulation may include a synergistic effect of Dll4/Notch with Wnt signaling to promote tumorigenesis by increasing the transcription of important Wnt target genes.

In addition, Dll4 ubiquitous inhibition upregulated the zinc finger-containing transcription factor KLF4 in the *Apc*$^{Min/+}$ tumors. KLF4 is a cell proliferation inhibitor and can act as a tumor suppressor, being normally downregulated in *Apc*$^{Min/+}$ tumors and in early stages of human

CRC (Evans & Liu, 2008). The loss of one of its alleles increases *Apc*$^{Min/+}$ tumorigenesis, possibly by derepressing β-catenin mediated gene expression (Ghaleb et al., 2007). Another work indicated that Notch signaling supresses KLF4 expression in intestinal tumors and colorectal cancer cells (Ghaleb et al., 2008). Our results indicate that Dll4 seems to be the ligand responsible for this Notch-mediated phenotype. Therefore, Dll4/Notch may promote carcinogenesis by upregulating the transcription of Wnt target genes through KLF4 downregulation in the *Apc* mutated tumors. Previous work indicated that Hes1 downregulation by Notch inhibition derepresses Atoh1, which seems to induce KLF4 upregulation to promote goblet cell differentiation in a redundant manner (Ghaleb, Aggarwal, Bialkowska, Nandan, & Yang, 2008; Vooijs et al., 2011). However, it seems that Hes1 may act both upstream and downstream of Atoh1 to negatively regulate KLF4 (Vooijs et al., 2011). We found that in the ubiquitous, but not in the endothelial-specific, Dll4 knockouts, the reduction of Lgr5 and Bmi1 positive tumor stem cell density was accompanied with increased tumor epithelium differentiation with a moderate deviation towards the secretory lineages, probably due to the observed *Atoh1* and *Klf4* overexpression by *Hes1* downregulation as it occurs when Notch signaling is inhibited (Ghaleb et al., 2008; van Es et al., 2005). This indicates that besides the effect on angiogenesis, Dll4/Notch signaling seems to have an additional role maintaining the tumor stem cells undifferentiated.

Additionally, Dll4/Notch ubiquitous inhibition promoted the transcription of the cell cycle regulators cyclin-dependent kinase (CDK) inhibitors *Cdkn1b* and *Cdkn1c* in the *Apc*$^{Min/+}$ tumors. A previous report showed that inactivation of Notch1 and 2 in the normal gut is associated with derepression of these CDK inhibitors (Riccio et al., 2008). This phenotype was completely abrogated in the absence of Atoh1 (Kim & Shivdasani, 2011), a molecule that is also considered to act as a tumor suppressor in CRC (Kazanjian & Shroyer, 2011). Therefore, Dll4/Notch inhibition may also negatively affect the tumor stem cell populations through Atoh1 derepression-mediated upregulation of the CDK inhibitors *Cdkn1b* and *Cdkn1c*.

In summary, we show that Dll4 seems to be the ligand responsible, at least partially, for the previously reported Notch effects during intestinal tumor development. Dll4/Notch deletion seems to inhibit the initiation and development of intestinal tumorigenesis through angiogenic and non-angiogenic related mechanisms independently of β-catenin activation and without affecting the normal gut. The non-angiogenic associated effects mediated by this pathway blockade may include the inhibition of tumor cell proliferation, the neoplastic transformation, the maintenance of the tumor stem cells and the promotion of epithelial differentiation mainly towards the secretory cell lineages.

Thus, despite the need for further studies, Dll4/Notch blockade appears to be a good candidate strategy to prevent CRC in patients predisposed to this disease and should also be considered in the treatment of early stages of CRC.

4.2 Chapter II – Delta-like 4 endothelial overexpression decreases the vascularity of intestinal adenomas in *Apc*$^{Min/+}$ mice reducing tumor multiplicity and growth

Badenes, M., Trindade, A., Pissarra, H., Costa, L., Duarte, A.

4.2.1 Abstract

The growth of solid tumors depends on adequate angiogenesis, which is tightly regulated by Delta-like 4 (Dll4)/Notch signaling. Tumorigenesis is driven by the tumor stem cells, whose maintenance also requires functional angiogenesis within the tumors. Dll4 endothelial function has been shown to be extremely dependent on expression levels. The inhibition of Dll4/Notch signaling blocks tumor growth by deregulating angiogenesis, and tumor stem cell frequency in colorectal cancer (CRC). However, some side effects associated with chronic inactivation of this pathway have been described. Furthermore, there are concerns that its pro-angiogenic effect may reduce the effectiveness of chemotherapy and select for more malignant cells or that the nonfunctional vessels may normalize. Therefore, we tested how the alternative approach of genetically stimulating endothelial Dll4/Notch signaling would affect the intestinal tumor development in the *Apc*$^{Min/+}$ mouse model of CRC. We found that Dll4 endothelial overexpression led to reduced tumorigenesis and tumor growth, associated with reduced tumor proliferation, Lgr5 positive stem cell frequency and angiogenesis. The tumors presented more mature and functional vasculature, but the reduction of the vascular density resulted in increased hypoxia and promoted apoptosis. It did not, however, affect the neoplastic transformation. Therefore, promoting endothelial Dll4/Notch signaling may constitute a valid approach to add to the conventional treatment of CRC.

Keywords: Dll4 endothelial overexpression, CRC, *Apc*$^{Min/+}$ model, tumorigenesis, tumor growth

4.2.2 Introduction

Angiogenesis is tightly associated to tumor growth (Folkman, 1990). The angiogenic switch occurs in the early development of cancer, where vascular endothelial growth factor (VEGF) signaling promotes endothelial cell proliferation, migration and sprouting (Takahashi, Ellis, & Mai, 2003). Dll4/Notch signaling acts as a negative feedback regulator of VEGF-induced endothelial cell function, by reducing the expression of VEGFR2 and Neuropilin-1 and by modulating tip cell function (Hellstrom et al., 2007; Williams et al., 2006).

Inhibition of Dll4/Notch signaling is being tested as a novel molecular strategy to treat cancer, as the blockade of this pathway in several types of cancer, including CRC, leads to dysfunctional vessel proliferation that impairs tumor growth (Djokovic et al., 2010; Noguera-Troise et al., 2006; Ridgway et al., 2006; Scehnet et al., 2007). In CRC, anti-Dll4 therapy also reduced the frequency of tumor stem cells (M. Fischer et al., 2010; Hoey et al., 2009) that are responsible for tumor initiation, development and resistance to conventional therapy (Rosen & Jordan, 2009) and seem to interact closely with angiogenesis (Zhao et al., 2011). However, chronic inhibition of Dll4/Notch pathway has been shown to promote toxicity through pathological activation of endothelial cells, disruption of the normal organ homeostasis and induction of benign vascular tumors (Djokovic et al., 2010; J. L. Li et al., 2010; Minhong Yan et al., 2010). In addition, there is concern about that Dll4 inhibition-mediated angiogenic defects, namely an increase in density of non-functional blood vessels, that may eventually become normalized due to the known high plasticity of tumor vessels (Mancuso et al., 2006), which would then favour tumor expansion due to increased perfusion. Furthermore, the reduced vascular function caused by anti-Dll4 approaches may also impair the delivery of chemotherapeutics to the tumor site and the subsequent hypoxia can promote the selection of more malignant tumor cells (Hayden, 2009).

The activation of Dll4, that negatively regulates VEGF-induced angiogenesis (Williams et al., 2006), may therefore represent a beneficial alternative strategy to treat cancer by inhibiting angiogenesis, and as with anti-VEGF inhibitors, by possibly improving the delivery of chemotherapeutic drugs through normalization of the tumor vasculature (Jain, 2005). Indeed, a study demonstrated that overexpression of Dll4 in tumor cells inhibits the VEGF-mediated growth of co-cultured endothelial cells (Segarra et al., 2008). However there is contradictory information regarding the effect of Dll4/Notch pathway activation on tumor growth (J. L. Li et al., 2007; Segarra et al., 2008). While the upregulation of Dll4 in xenograft models of Burkitt lymphoma, plasmacytoma and myelomonocytic leukemia reduced tumor growth (Segarra et al., 2008), in glioblastoma and prostate cancer xenografts it had the opposite effect on tumor growth by decreasing hypoxia and apoptosis (J. L. Li et al., 2007). Therefore, we wanted to evaluate if endothelial activation of Dll4 could be beneficial as an anti-tumor strategy, particularly in CRC, as this was never studied in this type of cancer. For that we analyzed endothelial-specific Dll4 gain-of-function in the widely used *Apc*$^{Min/+}$ mouse model of CRC

(McCart, Vickaryous, & Silver, 2008; Su et al., 1992). We decided to use Dll4 gain-of-function mice specifically in the endothelium and not in tumor cells, because previous studies indicate that in the gut epithelium Dll4 may promote cancer rather than inhibit it (Hoey et al., 2009)

4.2.3 Methods

4.2.3.1 Experimental animals

Mutant C57BL/6J-*Apc*$^{Min/+}$ (*Apc*$^{Min/+}$) mice were purchased from the Jackson Laboratory (Bar Harbor, ME).

The endoDll4OE mutants were obtained by crossing *Apc*$^{Min/+}$ mice with Tet$_{O7}$-Dll4 mice crossed with *Tie2-rtTA* mice (*Apc*$^{Min/+}$ Tet$_{O7}$-Dll4+:*Tie2-rtTA*+). Doxycycline (2mg/ml in drinking water with 1% of sugar from week 13) was given to double transgenic offspring throughout the experiment, inducing endothelial-specific transgene expression. The control mice used were *Apc*$^{Min/+}$ Tet$_{O7}$-Dll4- *Tie2-rtTA*+ and were induced with doxycycline as reported above.

4.2.3.2 Macroscopic analysis

The mice were sacrificed at 18 weeks of age and their small and large intestine was excised, flushed and opened longitudinally. The macroscopic small and large intestine tumors were counted and measured with a calliper under the dissection microscope. Tumor volume was calculated assuming a hemispherical shape for the small bowel tumors and a spherical shape for large intestine tumors. The volumes of all tumors from each mouse were added to give the overall tumor burden per animal. The small and large intestine tumors and livers were collected.

4.2.3.3 Histopathological analysis

The collected samples were fixed in 10% formalin solution for 48h, dehydrated in alcohol, cleared in xylene, embedded in paraffin, sectioned at 4µm and stained with hematoxylin (Fluka AG Buchs SG Switzerland) and eosin Y (Sigma, St. Louis, MO) for histopathological analysis. The lesions observed on the H&E sections from *Apc*$^{Min/+}$ mice were classified as hyperplasias, when only an increase of the number of cells was observed, or as adenomas with low and high-grade dysplasia based on the alterations of the shape of the nucleus, the nucleus to cytoplasm ratio, cell polarity, chromatin pattern, and changes in gland architecture. Periodic Acid-Schiff (PAS) staining (Sigma, St. Louis, MO) was used to mark the intestinal goblet cells. These cells were counted in the intestine PAS stained sections using a 400x magnification.

4.2.3.4 Immunofluorescence analysis

Small and large intestine tumors were fixed in a 4% (w/v) paraformaldehyde in PBS solution at 4ºC for 1h, cryoprotected in 15% (w/v) sucrose in PBS solution, embedded in 7.5% (w/v) gelatin in PBS solution, snap frozen in liquid nitrogen and cryosectioned in 10 and 20µm-thick sections. The following primary antibodies were used: anti-PECAM-1 (557355), anti-E-cadherin (560061) (BD Biosciences, San Jose, USA), anti-α-SMA (ab5694), anti-PCNA (ab18197), anti-Lgr5 (ab75732), anti-HIF1α (ab85866), anti-Cyclin D1 (ab21699) (Abcam, Cambridge, UK), anti-lysozyme (A009902-2, Dako, Glostrup, Denmark), anti-non-phospho (active) β-catenin (8814, Cell Signaling Technology, Danvers, USA). Species-specific secondary antibodies conjugated with Alexa Fluor 488 and 594 (Invitrogen, Carlsbad, CA) were used to reveal primary antibody binding. Tissue sections were incubated with primary antibody overnight at 4°C and with secondary antibody for 1h at room temperature. Nuclei were counterstained with 4´, 6-diamidino-2-phenylindole dihydrochloride hydrate (DAPI; Molecular Probes, Eugene, OR).

Fluorescent immunostained sections were examined under a Leica DMRA2 fluorescence microscope with Leica HC PL Fluotar 10 and 20X/0.5 NA dry objective, captured using Photometrics CoolSNAP HQ, (Photometrics, Friedland, Denmark), and processed with Metamorph 4.6-5 (Molecular Devices, Sunnyvale, CA, US). Morphometric analyses were performed using the NIH ImageJ 1.37v program. After transforming the RGB images into binary files, the percentage of white pixels per field was defined as a positive signal.

Under the effect of 2-2-2 tribromoethanol anaesthesia, biotin-conjugated lectin from *Lycopersicon esculentum* (100µg/100µl of PBS) or 1% Evans' Blue solution (Sigma, St. Luis, MO, US) were administered in the caudal vein to mark vessel perfusion and extravasation, respectively. Both solutions were allowed to circulate for 5 minutes before the vasculature was transcardially perfused with 4% (w/v) paraformaldehyde in PBS solution for 3 minutes. Tumor samples were collected and processed as described above. Tissue sections were stained and tumor perfusion was quantified by determining the percentage of red PECAM-positive structures that were co-localized with Streptavidin-Alexa 488 (Invitrogen, Carlsbad, CA, US) signals. Evans' Blue is red fluorescent and extravasation was visualized in contrast to green fluorescent vascular structures.

Apoptosis was measured using the TUNEL assay (Roche, Mannheim, Germany).

4.2.3.5 Quantitative transcriptional analysis

Intestinal tumors from the mutant mice were snap frozen in liquid nitrogen until RNA extraction (Qiagen RNeasy). Using the SuperScript® III First-Strand Synthesis SuperMix for qRT-PCR (Invitrogen, Carlsbad, CA, USA), first-strand cDNA was synthesized from total RNA. Real-time PCR analysis was performed using specific primers. Primer pair sequences

are reported on Annex II. Gene expression was normalized to *β*-actin and in the case of genes expressed in the vasculature it was additionally normalized to *Pecam-1*.

4.2.3.6 Statistical analysis

To compare measurements between control and test groups, the Mann-Whitney-Wilcoxon test was performed using the Statistical Package for the Social Sciences v15.0 (Chicago, IL). Results are presented as relative average ± SEM. *P*-values <0.05 and <0.01 were considered significant (*) and highly significant (**), respectively.

4.2.4 Results

4.2.4.1 Endothelial Dll4 overexpression inhibits the *Apc*$^{Min/+}$ tumor initiation and development

One of the strategies being used to treat cancer, including CRC, is based on targeting the tumoral angiogenesis (Kubota, 2012). However, anti-angiogenic therapies have been associated with side effects and lack of efficacy due to the development of treatment resistance (Vasudev & Reynolds, 2014). Therefore there is a great need to improve anti-cancer angiogenesis targeting therapies. Anti-Dll4 therapeutic approaches have been demonstrated to cause a non-productive pro-angiogenic effect that delays tumor growth (Djokovic et al., 2010; Noguera-Troise et al., 2006; Ridgway et al., 2006; Scehnet et al., 2007). However safety concerns have been raised about this therapeutic strategy (Djokovic et al., 2010; J. L. Li et al., 2010; Minhong Yan et al., 2010). Thus we explored the alternative approach of stimulating Dll4/Notch signaling. A report showed that Dll4 endothelial overexpression reduces the vascular density during physiological angiogenesis (Alexandre Trindade et al., 2012), which may also occur in a tumoral setting. Therefore we analysed the effect of Dll4 endothelial gain-of-function (endoDll4OE) in *Apc*$^{Min/+}$ mouse model that mimics human CRC (McCart et al., 2008; Su et al., 1992; Yasuhiro Yamada & Mori, 2007). We found that, interestingly, Dll4 endothelial upregulation inhibited both the *Apc*$^{Min/+}$ intestinal tumorigenesis and tumor growth (Fig. 17A-D). Specifically, compared with the controls, the endoDll4OE mice had a 2.5- and 1.7-fold reduction of the tumor number in the small and large intestine, respectively and a 1.7- and 2.2-fold reduction of the tumor volume, respectively (Fig. 17A and B). Therefore, they had a 4.2-fold reduction of the overall tumor burden (Fig. 17C).

We found no macroscopic toxic effect in the endoDll4OE mice or vascular lesions in the liver, which have been reported after chronic Dll4 blockade (Djokovic et al., 2010; J. L. Li et al., 2010; Minhong Yan et al., 2010).

To confirm the endothelial-specific *Dll4* gain-of-function we evaluated the expression of *Hey2* normalized to *Pecam-1* and observed that *Hey2* expression had a 6-fold increase in the endoDll4OE mice (Fig. 18).

Figure 17 - *Dll4* endothelial-specific overexpression delays the tumor initiation and development in *Apc*$^{Min/+}$ mouse

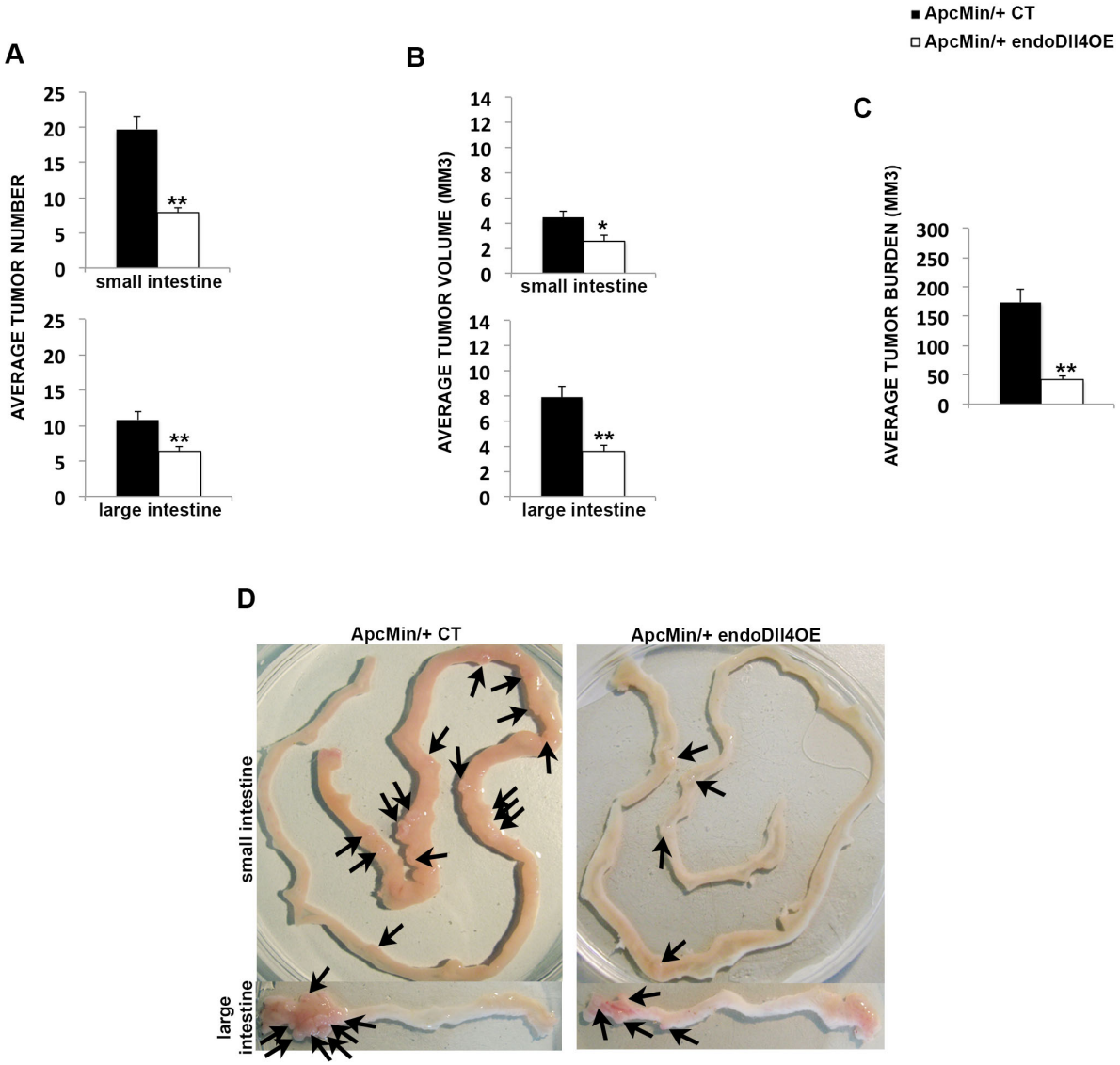

(A-B) Graphic bars represent the average ± SEM tumor number (A) and volume (mm^3) (B) in the small and large intestine of induced *Apc*$^{Min/+}$ endoDll4OE mice *versus* controls (CT) at 18 weeks of age. (C) Graphic bars represent the average ± SEM tumor burden (mm^3) in the whole intestine of the animals described above. One experiment with n = 12 per group. **P*<0.05; ***P*<0.01. (D) Photographs of the small and large intestines (tumors indicated by arrows) of the same mice.

Figure 18 - Confirmation of Dll4/Notch mediated *Hey2* overexpression in *Apc*$^{Min/+}$ endoDll4OE tumors

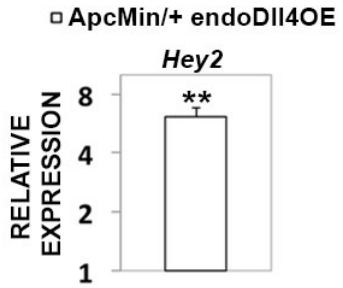

Graphic bars represent the relative expression of the Dll4/Notch pathway effector *Hey2* ± SEM, analyzed by RT-PCR and normalized to *Pecam-1*, in the tumors of *Apc*$^{Min/+}$ endoDll4OE mice at 18 weeks of age. One experiment with n = 3 per group. ***P*<0.01.

4.2.4.2 Endothelial overexpression of Dll4 promotes apoptosis by inhibiting angiogenesis in the *Apc*$^{Min/+}$ tumors

We evaluated the endothelial phenotype and the level of hypoxia and apoptosis in the endoDll4OE tumors relatively to their controls. As expected, endoDll4OE led to the opposite effect of Dll4 inhibition on tumor angiogenesis (Djokovic et al., 2010; Noguera-Troise et al., 2006; Ridgway et al., 2006; Scehnet et al., 2007). Dll4 endothelial overexpression had an anti-angiogenic effect, reducing the endothelial proliferation and new vessel formation, but promoted individual vessel maturity and functionality in the *Apc*$^{Min/+}$ small and large intestine tumors. In the endoDll4OE tumors the vascular density was strongly decreased in the small and large intestine, while the vascular maturity was mildly increased in both regions (Fig. 19A-D). The vascular perfusion was also mildly increased in the small and large intestine, respectively (Fig. 19E-G) and the vascular extravasation was strongly decreased in both regions (Fig. 19H-J). However, we observed that the endoDll4OE mice had also increased tumor hypoxia and apoptosis despite their improved vessel competence both in the small and large intestine (Fig. 20A-F).

Figure 19 - Dll4 endothelial-specific overexpression inhibits angiogenesis, despite increasing the vessels maturity and functionality in *Apc*$^{Min/+}$ tumors

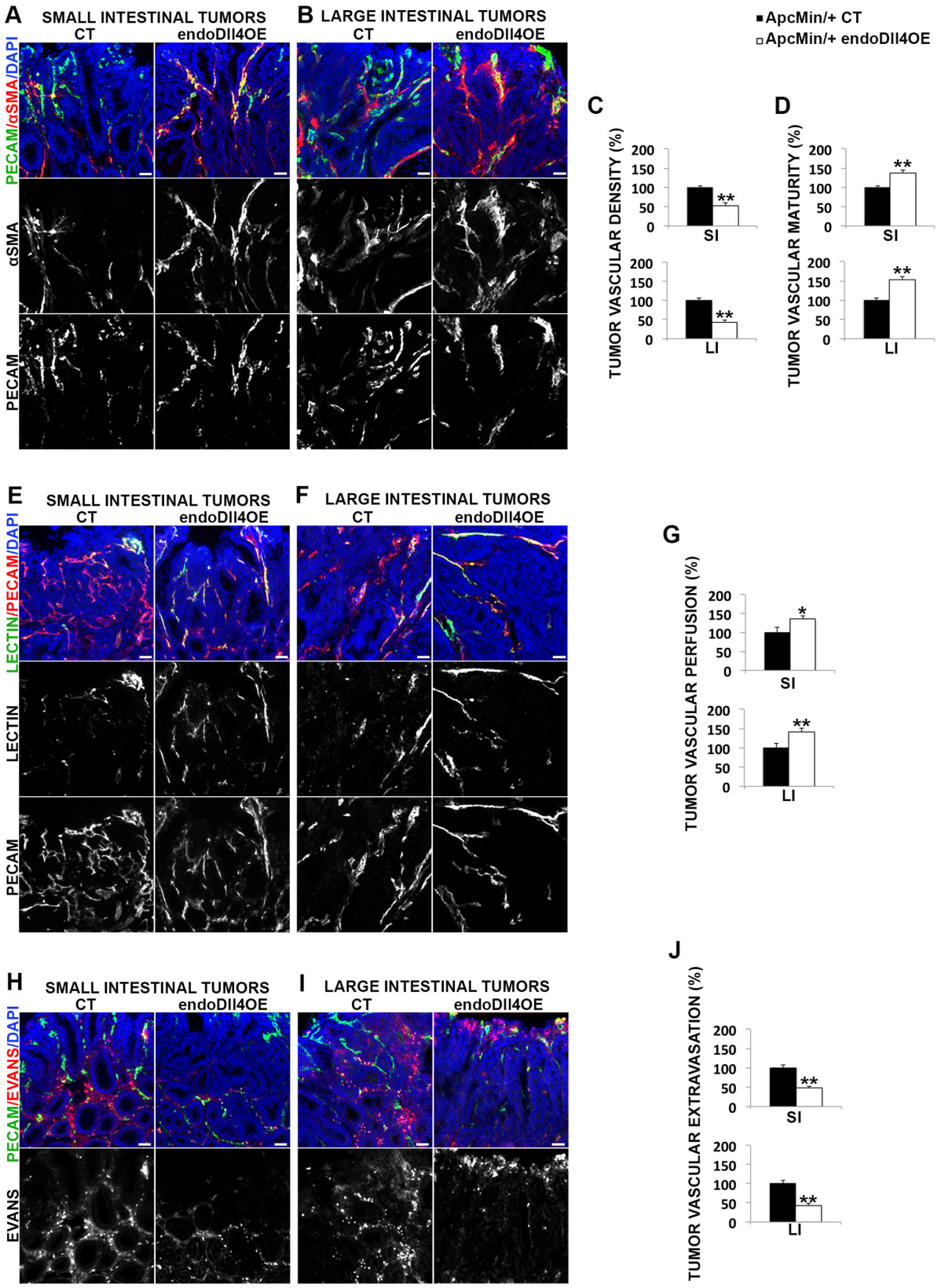

(A, B, E, F, H, I) Immunofluorescence stainings of 20µm small (A, E, H) and large (B, F, I) intestine tumor cryosections from *Apc*$^{Min/+}$ endoDll4OE mice *versus* controls (CT) at 18 weeks of age. The cell

nuclei were stained with DAPI (in blue). Scale bars = 100μm. Representative images of staining density for PECAM-1 (in green) and α-SMA (in red) (A, B), for lectin, (in green) and PECAM-1 (in red) (E, F), and for PECAM-1 (in green) and Evans' blue (in red) (H, I). (C, D, G, J) Graphic bars represent the relative tumor vascular density (C), maturity (D), perfusion (G) and extravasation (J) ± SEM in the animals described above. One experiment with n = 6 per group and 6 fields per animal. **P*<0.05; ***P*<0.01.

Figure 20 - Dll4 endothelial-specific activation promotes hypoxia and apoptosis in *Apc*$^{Min/+}$ tumors

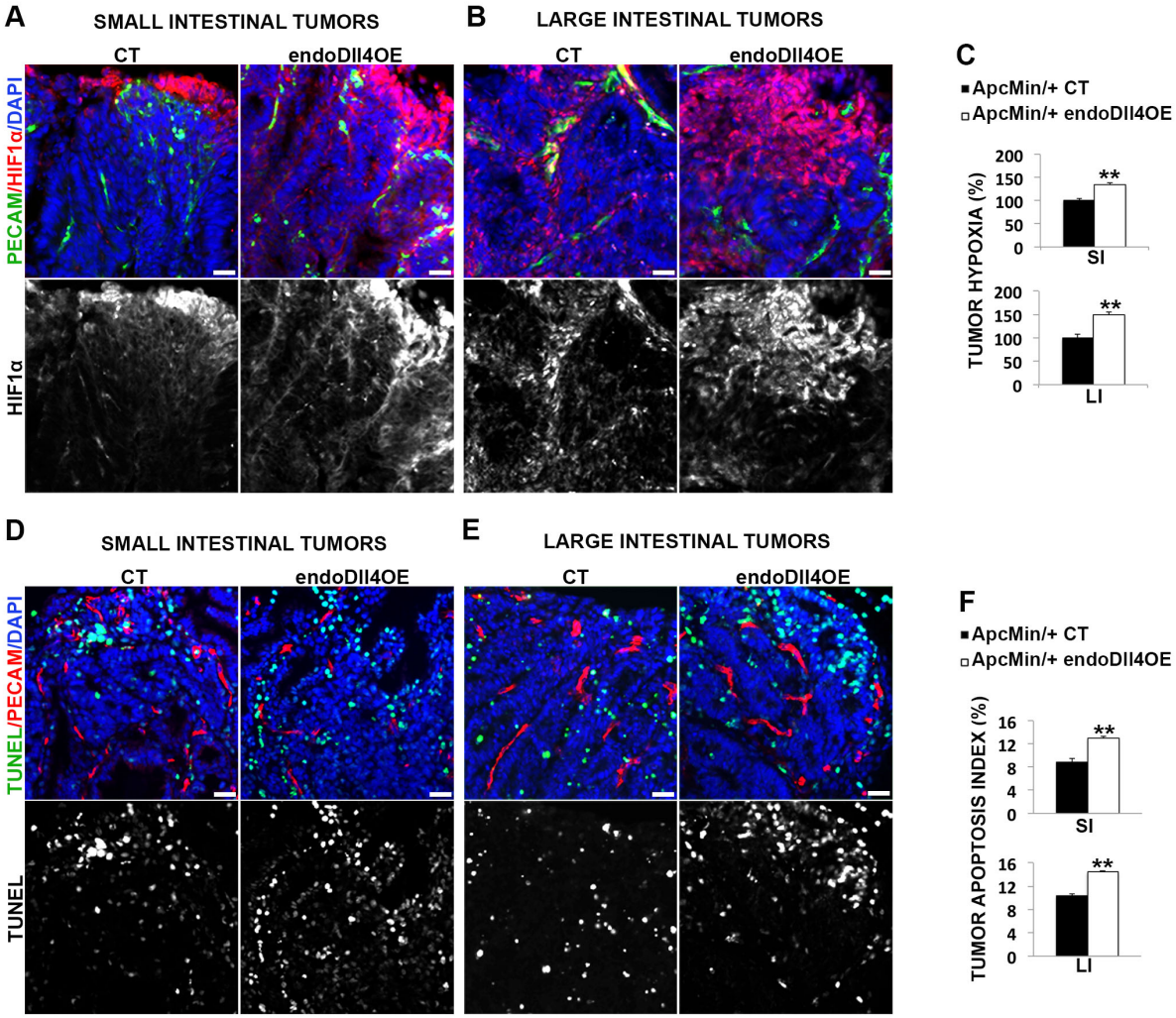

(A, B, D, E) Immunofluorescence stainings of 20μm (A, B) and 10μm (D, E) small (A, D) and large (B, E) intestine tumor cryosections from *Apc*$^{Min/+}$ endoDll4OE mice *versus* controls (CT) at 18 weeks of age. Nuclei were counterstained with DAPI (in blue). Scale bars = 100μm. Representative images of staining density for PECAM-1 (in green) and HIF1α (in red) (A, B), and for TUNEL (in green) and PECAM-1 (in red) (D, E). (C, F) Graphic bars represent the relative tumor hypoxia (C) and apoptosis index (F) ± SEM in the animals described above. One experiment with n = 6 per group and 6 fields per animal. **P*<0.05; ***P*<0.01.

4.2.4.3 Endothelial overexpression of Dll4 decreases proliferation and Lgr5+ stem cell density, without affecting the neoplastic transformation and differentiation, in the *Apc*$^{Min/+}$ tumors

As endothelial Dll4 overexpression reduced Apc$^{Min/+}$ intestinal tumor initiation, we decided to evaluate if it affected the *Apc* loss-of-function mediated activation of protumorigenic β-catenin (Fearnhead, Britton, & Bodmer, 2001). We also measured the level of tumor proliferation and the density of tumor stem cells expressing the marker leucine-rich repeat-containing G-protein-coupled receptor 5 (Lgr5), as these cells have been described to be associated with CRC initiation and progression (Schepers et al., 2012).

The activation of β-catenin in the small and large intestine tumors was not affected by endothelial overexpression of Dll4 (Fig. 21A-B). Nevertheless, the level of tumor proliferation was mildly reduced in the *endoDll4OE* small and large intestine, (Fig. 22A-C) and the level of Lgr5+ tumor stem cells was also slightly decreased in both regions (Fig. 22D-F).

As a previous report indicated that Notch1 signaling may regulate the Cyclin D1-mediated colon cancer cell proliferation (Gopalakrishnan, Saravanakumar, Madankumar, Thiyagu, & Devaraj, 2014), we also measured the expression of this cell cycle regulator. We found no differences in the expression of Cyclin D1 in the *endoDll4OE* small and large intestine tumors (Fig. 23A-B).

We also performed a histopathological analysis and measured in the *Apc*$^{Min/+}$ tumors the density of the epithelial differentiation marker E-cadherin (Tsanou et al., 2008) that revealed no differences in the neoplastic transformation/tumor differentiation of the *endoDll4OE* tumors compared with the controls (Fig. 22G-I). In addition, as Dll4/Notch signaling promotes enterocyte/colonocyte differentiation commitment (Pellegrinet et al., 2011) we evaluated if the differentiation was being deviated towards the secretory lineages in the *endoDll4OE* *Apc*$^{Min/+}$ tumors, by measuring the density of Paneth cells and the proportion of goblet in the small and large intestine tumor epithelium, but we did not find any differences relatively to the controls (data not shown).

Figure 21 - Dll4 endothelial-specific overexpression does not affect the activation of β-catenin in *Apc*$^{Min/+}$ intestinal tumors

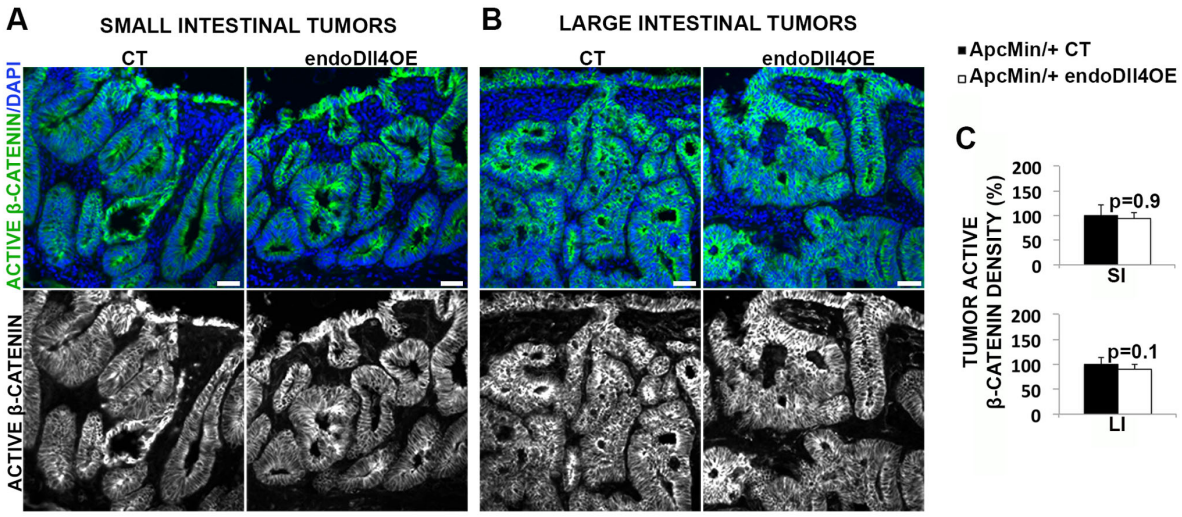

(A, B) Immunofluorescence stainings of the small (A) and large (B) intestine tumor cryosections (10μm) from *Apc*$^{Min/+}$ endoDll4OE mice *versus* controls (CT) at 18 weeks of age. Representative images of staining density for active β-catenin (in green). Nuclei were counterstained with DAPI (in blue). Scale bars = 100μm. The level of tumor active β-catenin was similar in the two groups both in the small (A) and large (B) intestine. (C) Graphic bars represent the relative tumor active β-catenin density ± SEM in the animals described above. One experiment with n = 6 per group and 6 fields per animal.

Figure 22 - Endothelial overexpression of Dll4 decreases proliferation and Lgr5+ stem cell density, not affecting the neoplastic progression and differentiation, in the *Apc*$^{Min/+}$ tumors

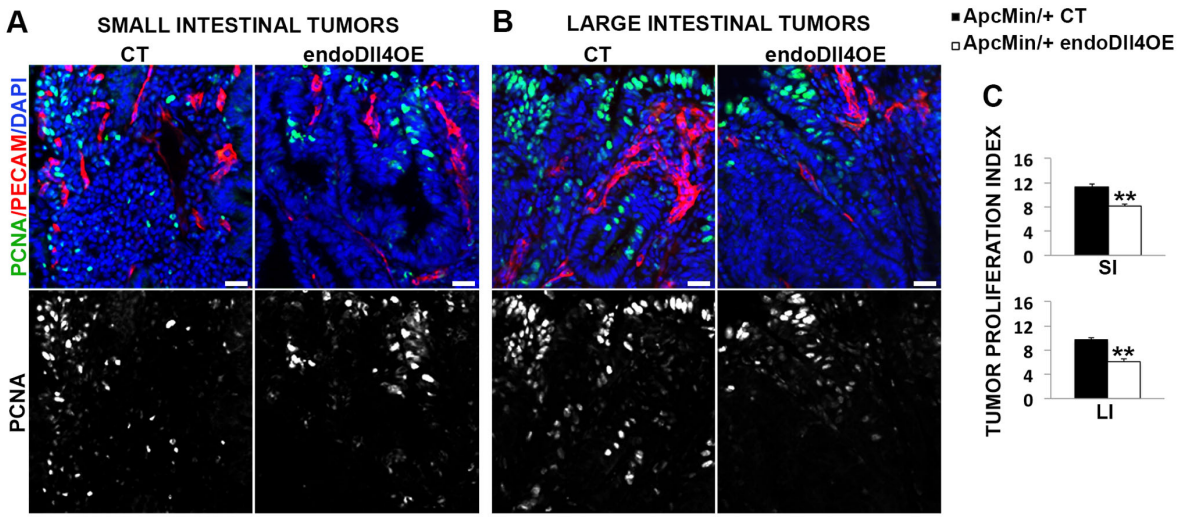

Figure 22 (continuation) - Endothelial overexpression of Dll4 decreases proliferation and Lgr5+ stem cell density, not affecting the neoplastic progression and differentiation, in the *Apc*$^{Min/+}$ tumors

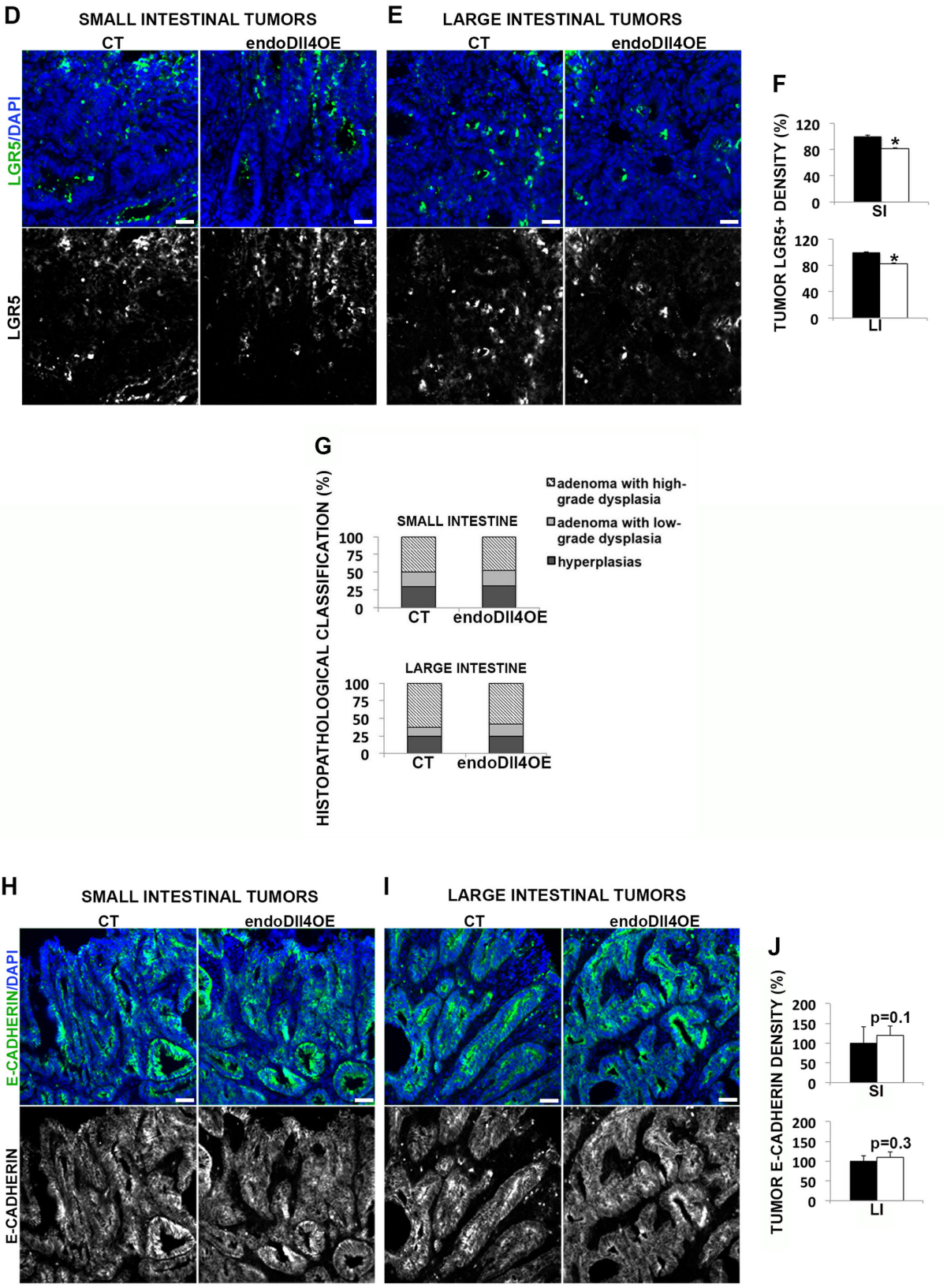

(A, B, D, E, H, I) Immunofluorescence stainings of the small (A, D, H) and large (B, E, I) intestine tumor cryosections (10μm) from *Apc*$^{Min/+}$ endoDll4OE mice *versus* controls (CT) at 18 weeks of age.

Nuclei were counterstained with DAPI (in blue). Scale bars = 100µm. Representative images of staining density for PCNA (in green) and PECAM-1 (in red) (A, B), for Lgr5 (in green) (D, E), and for E-cadherin (in green) (H, I). (C, F, J) Graphic bars represent the small and large intestine tumor proliferation index (%) ± SEM (C) and the relative tumor Lgr5 (F) and E-cadherin (J) density (%) ± SEM in the animals described above. One experiment with n = 6 per group and 6 fields per animal. **P*<0.05; ***P*<0.01. (G) Graphic bars represent the proportion (%) of hyperplasias and adenomas with low and high-grade dysplasia obtained in the histopathological analysis (H&E) of the macroscopic small and large intestine lesions from *Apc*$^{Min/+}$ endoDll4OE mice *versus* their controls (CT) at 18 weeks of age. One experiment with n = 12 per group.

Figure 23 - Endothelial Dll4 overexpression seems independent of Cyclin D1 protein expression in *Apc*$^{Min/+}$ intestinal tumors

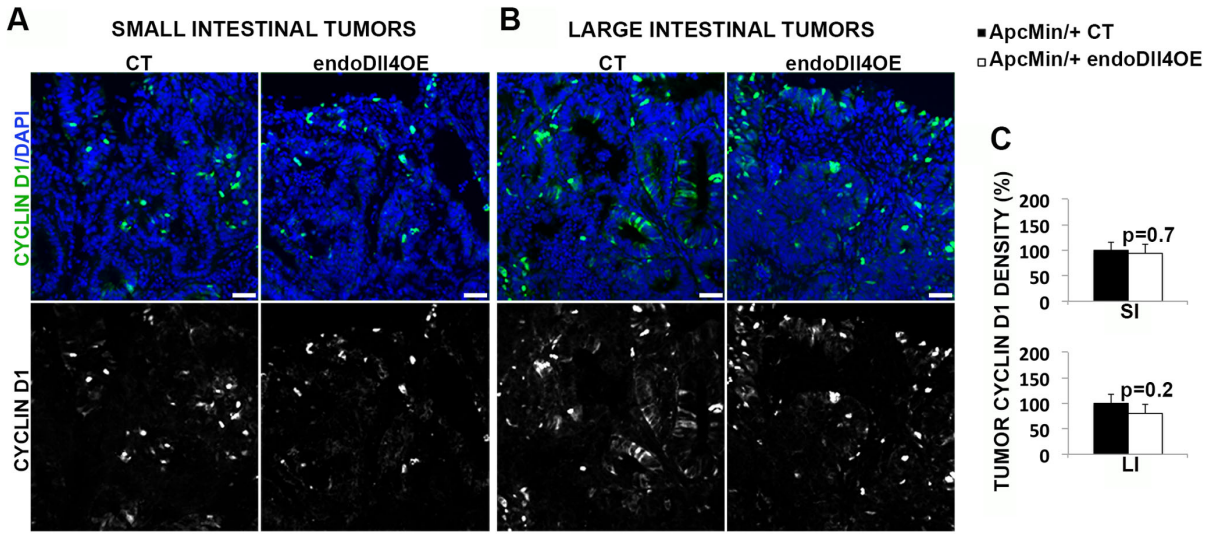

(A, B) Immunofluorescence stainings of the small (A) and large (B) intestine tumor cryosections (10µm) from *Apc*$^{Min/+}$ endoDll4OE mice *versus* controls (CT) at 18 weeks of age. Representative images of staining density for Cyclin D1 (in green). Nuclei were counterstained with DAPI (in blue). Scale bars = 100µm. The tumor Cyclin D1 density was similar in both groups in the small (A) and large (B) intestine. One experiment with n = 6 per group and 6 fields per animal.

4.2.5 Discussion

VEGF-targeting anti-angiogenic therapy is being successfully used as an adjuvant in metastatic CRC therapeutic protocols (J. J. Lee & Chu, 2014). However, this strategy is associated with the development of some toxic effects and treatment resistance (Vasudev & Reynolds, 2014). Furthermore, it has failed in the adjuvant setting in non-metastatic CRC (Allegra et al., 2013; de Gramont et al., 2012). Therefore, there is a need for improved angiogenesis targeting therapies. The Notch ligand Dll4 is a known critical regulator of tumor angiogenesis (Djokovic et al., 2010; Noguera-Troise et al., 2006; Ridgway et al., 2006; Scehnet et al., 2007) and its function seems to be extremely dose-dependent (Duarte, 2004; Alexandre Trindade et al., 2012). The inhibition of Dll4 has been proven to promote immature

and dysfunctional vessel proliferation that results in poor blood supply and therefore tumor growth inhibition in several types of cancer, including CRC (Djokovic et al., 2010; Hoey et al., 2009; Noguera-Troise et al., 2006; Ridgway et al., 2006; Scehnet et al., 2007). However, concerns were raised concerning the long-term safety of Dll4 blockade-based therapies as they can lead to potentially significant toxicity (Djokovic et al., 2010; J. L. Li et al., 2010; Minhong Yan et al., 2010), hypoxia-induced increased tumor malignancy (Hayden, 2009), limited concomitant chemotherapy effectiveness by reducing the vessel competence, and therapy resistance by vascular defect self-repair and reperfusion.

It was demonstrated that Dll4 upregulation blocks VEGF-induced endothelial cell function (Williams et al., 2006). This introduced the idea that Dll4 overexpression could be exploited therapeutically to modulate angiogenesis. A previous study indicated that tumoral Dll4 overexpression reduces the vascular density in cancer (J. L. Li et al., 2007; Segarra et al., 2008). However, this approach can have opposite effects on tumor growth in different types of cancer by reducing or increasing the tumor hypoxia and apoptosis, by affecting differently the tumor vascular competence. As this strategy was never studied in CRC, we decided to evaluate if Dll4 endothelial activation could be beneficial to treat it, using the *Apc*$^{Min/+}$ mouse model.

We found that in the *Apc*$^{Min/+}$ small and large intestine Dll4 endothelial-specific overexpression inhibited the tumor growth as demonstrated previously by Dll4 overall activation in a xenograft model of blood related cancer types (Segarra et al., 2008). Interestingly, we also found some effect reducing the *Apc*$^{Min/+}$ small and large intestine tumorigenesis. We found that the phenotype was similar in the small and large intestine, but affected more the tumor multiplicity in the small intestine and the tumor growth in the large intestine. A previous work showed that in colon cancer the activation of Notch1 may promote Cyclin D1-mediated proliferation (Gopalakrishnan et al., 2014). However, this effect was not observed after Dll4 activation in the endothelium. On the contrary, we found reduced tumor cell proliferation and mild inhibition of Lgr5 positive tumor stem cell maintenance, that are responsible for CRC initiation (Schepers et al., 2012), and these effects seemed independent of Wnt/β-catenin activation. As previous reports have shown that tumor stem cells depend on competent angiogenesis (Zhao et al., 2011), probably an endothelial Dll4 overexpression VEGF-mediated anti-angiogenic effect impaired the blood supply needed to support and maintain the tumor stem cells and the proliferative capacity of tumor cells. However, it was demonstrated that VEGF signaling could also contribute for the maintenance of tumor stem cells and for tumor initiation independently of angiogenesis (Goel & Mercurio, 2013). Nevertheless, a previous report indicated that anti-VEGF therapy only reduced the *Apc*$^{Min/+}$ tumor size through inhibition of angiogenesis, but not the number of tumors, indicating that VEGF signaling in the *Apc*$^{Min/+}$ model is not important in the establishment of early adenomas before the angiogenic switch (Korsisaari et al., 2007). Therefore, further studies are needed

to identify how Dll4 expressed in the tumor endothelium modulates tumorigenesis in this model of CRC and which signaling pathways are implicated.

As expected, endothelial Dll4 overexpression led to the opposite effect of Dll4 inhibition on tumor angiogenesis (Djokovic et al., 2010; Noguera-Troise et al., 2006; Ridgway et al., 2006; Scehnet et al., 2007). The activation of Dll4 in the endothelium inhibited vascular proliferation, probably by downregulating VEGF signaling, but increased the vascular maturity and competence. As we observed more hypoxia and increased apoptosis in the *endoDll4OE* small and large intestine tumors, this indicates that probably the observed increase of the vessel competence was not sufficient to balance the negative effect caused by a decreased number of vessels, leading to impaired overall tumor blood supply suppressing tumor expansion. In addition, improved vessel competence may be beneficial to promote the delivery of cytostatic and other drugs to the tumor site and the enhanced vessel wall maturation may avoid the intravasation of malignant cells into the circulation and their dissemination. However, tumor invasiveness can be promoted by hypoxia (Hayden, 2009) that was increased in the *endoDll4OE* tumors. Nevertheless, we did not find any differences in the neoplastic progression and tumor differentiation caused by endothelial Dll4 overexpression. However, we must bear in mind that we only evaluated premalignant lesions and therefore studies in more advanced stages of CRC are needed to evaluate the safety of this therapeutic approach. In the meantime, we can conclude by the overall effects of endothelial Dll4 overexpression that this strategy may be considered in the treatment of CRC.

4.3 Chapter III - Delta-like 4/Notch inhibition has a synergistic effect with anti-Egfr therapy on *Apc*$^{Min/+}$ tumorigenesis

Badenes, M., Trindade, A., Pissarra, H., Liu, R., Krasperonov, V., Gill, S.P., Costa, L., Duarte, A.

4.3.1 Abstract

Colorectal cancer (CRC) is the third most common malignancy in humans. Mutations in the *Adenomatous polyposis coli* (*APC*) gene are needed for the initiation of hereditary and for most of sporadic cases of CRC. One of the currently used approaches to treat CRC is the blockade of epidermal growth factor receptor (EGFR) signaling. Notch signaling is another important pathway in CRC. Previous studies revealed a cross talk between Notch and EGFR signaling in cancer development. However, this was never demonstrated in CRC. Previous reports revealed that in CRC Dll4/Notch blockade reduces tumor growth by reducing the tumor stem cell frequency, as well as by promoting non-productive angiogenesis. However, this angiogenic effect may also be responsible for the impairment of the delivery of other anti-cancer drugs to the tumor. The aims of this work were to elucidate how Dll4/Notch signaling inhibition affects the intestinal tumor development in the *Apc*$^{Min/+}$ mouse model of CRC and evaluate the effects of the combination therapy with Dll4 and Egfr inhibitors in this setting. We used Dll4-Fc, a soluble fusion protein containing the extracellular domain of Dll4 that binds to Notch receptors acting as dominant-negative, and the EGFR-specific tyrosine kinase inhibitor erlotinib. We found that, in the intestine, Dll4-Fc therapy alone reduced tumorigenesis by reducing proliferation and promoting differentiation of the tumor stem cells towards the secretory lineages. Additionally, the observed deregulation of the tumor vasculature was also responsible for delayed tumor growth and neoplastic progression. The association of Dll4-Fc to erlotinib had a synergistic effect blocking *Apc*$^{Min/+}$ tumorigenesis independently of β-catenin activation and promoted unspecific tumor epithelial differentiation. Therefore, targeting DLL4/Notch and EGFR simultaneously may be beneficial in the treatment of CRC.

Keywords: Dll4, Egfr**,** Dll4-Fc and erlotinib, tumorigenesis, *Apc*$^{Min/+}$ mouse

4.3.2 Introduction

Colorectal cancer (CRC) is the third most common malignancy and the second leading cause of cancer-related death in the West. Mutations in the recessive tumor suppressor gene *Adenomatous polyposis coli (APC)* lead to hereditary CRC familial adenomatous polyposis (FAP) syndrome (Powell et al., 1993) and are a common early event in sporadic CRC development (Payne, 1990). The $Apc^{Min/+}$ mouse has a mutation in the *Apc* gene and spontaneously develops multiple intestinal neoplasms (Min) in the small and large intestine (Su et al., 1992).

Dll1 and Dll4-mediated Notch activation together with Wnt signaling have been shown to be crucial for maintaining the intestinal progenitors undifferentiated and proliferating (Pellegrinet et al., 2011) and to have an additional role promoting the absorptive lineage differentiation (Fre et al., 2005). Activation of Notch1 is implicated in the establishment of adenomas in $Apc^{Min/+}$ mutant mice (Fre et al., 2009; van Es, van Gijn, et al., 2005) by regulating the differentiation of tumor stem cells (Sikandar et al., 2010). The inhibition of Dll4/Notch signaling appears to reduce these cells frequency in xenograft models of CRC (M. Fischer et al., 2010; Hoey et al., 2009). Interestingly, this seems to occur even when KRAS mutations, which are associated with resistance to EGFR targeted therapy, are present (M. Fischer et al., 2010). However, it was never demonstrated how Dll4/Notch inhibition affects the intestinal adenoma formation, the precursor lesion of CRC. In addition, several reports indicated that Dll4/Notch signaling is crucial for tumor development by regulating the angiogenic process. In these studies, the inhibition of Dll4/Notch signaling delayed tumor growth by promoting a non-productive vasculature (Djokovic et al., 2010; Noguera-Troise et al., 2006; Ridgway et al., 2006; Scehnet et al., 2007). These findings raised the important question of whether the impairment of the tumor angiogenesis caused by Dll4 inhibition could hamper the concomitant delivery of other anti-cancer drugs to the tumors, in contrast to anti-VEGF therapies that seem to improve the delivery of anti-cancer drugs by “normalizing” the tumor vasculature (Jain, 2005).

Targeted therapies are currently used to improve the efficacy of standard CRC treatment (Rolfo et al., 2014). One of these strategies consists in the blockade of EGFR signaling, which is overexpressed and involved in the development and progression of CRC through activation of the ras-raf mitogen activated protein kinase (MAPK)/ERK and AKT-PI3-kinase (phosphatidylinositol 3-kinase) pathways (Spano et al., 2005; Vokes & Chu, 2006). In the $Apc^{Min/+}$ model Egfr activation is increased both in the enterocytes and mainly in the intestinal adenomas (Moran et al., 2004), being required for the initiation and subsequent expansion of these tumors (Roberts et al., 2002).

A cross talk between the Notch and EGFR pathways has been described in tumors of the lung, breast, skin and glia (Baker, Zlobin, & Osipo, 2014; H. Yamaguchi et al., 2014). As the components of these two pathways are overexpressed in CRC this may be also true in this

type of cancer (Qiao & Wong, 2009). Therefore, the aim of this work was to evaluate the pharmacological inhibition of Dll4/Notch signaling in the *Apc*$^{Min/+}$ model and to analyse how anti-Dll4 therapy would affect the delivery and/or efficacy of anti-EGFR treatment in this model. Thus, we tested the blockade of Dll4/Notch signaling with a dominant-negative fusion protein containing the extracellular domain of Dll4 fused to the Fc fraction of IgG (Dll4-Fc) (Scehnet et al., 2007). Dll4-Fc therapy was given alone and in combination with erlotinib, an EGFR-specific tyrosine kinase inhibitor, to identify any potential therapeutic benefit of this association.

4.3.3 Methods

4.3.3.1 Experimental animals

All animal-involving procedures in this work were approved by the Faculty of Veterinary Medicine of Lisbon Ethics and Animal Welfare Committee (Approval ID: PTDC/CVT/71604/2006).

Mutant C57BL/6 J-*Apc*$^{Min/+}$/J (*Apc*$^{Min/+}$) mice were purchased from the Jackson Laboratory (Bar Harbor, ME).

Dll4-Fc was administered to male *Apc*$^{Min/+}$ mice by i.p. injection from 13 to 18 weeks of age (10mg/kg in PBS, 3x a week). Dll4-Fc was produced as previously described (Scehnet et al., 2007). Erlotinib was administered to *Apc*$^{Min/+}$ mice by oral gavage from 13 to 18 weeks of age (100mg/Kg in PBS with 0,5% (v/v) Tween 80, daily). *Apc*$^{Min/+}$ control mice received only the vehicle in the same regimen.

In all therapeutic trials 12 animals per group were used.

4.3.3.2 Macroscopic analysis of the intestine

After 5 weeks of therapy the mice were humanely sacrificed by cervical dislocation and the small and large intestine were excised, flushed and opened longitudinally. The macroscopic small and large intestine tumors of *Apc*$^{Min/+}$ treated and control mice were counted and measured with a calliper under the dissection microscope. Tumor volume was calculated assuming a hemispherical shape for the small bowel tumors and a spherical shape for large intestine tumors. The volumes of all tumors from each mouse were added to give the overall tumor burden per animal. The intestinal tumors and livers were collected.

4.3.3.3 Histopathological analysis

The collected samples were fixed in 10% formalin solution for 48h, dehydrated in alcohol, cleared in xylene, embedded in paraffin, sectioned at 4µm and stained with hematoxylin (Fluka AG Buchs SG Switzerland) and eosin Y (Sigma, St. Louis, MO) for histopathological analysis. The lesions observed on the H&E sections from *Apc*$^{Min/+}$ mice were classified as hyperplasias, when only an increase of the number of cells was observed, or as adenomas

with low and high-grade dysplasia based on the alterations of the shape of the nucleus, the nucleus to cytoplasm ratio, cell polarity, chromatin pattern, and changes in gland architecture.

Periodic Acid-Schiff (PAS) staining (Sigma, St. Louis, MO) was used to mark the intestinal goblet cells. These cells were counted in the intestine PAS stained sections using a 400x magnification.

4.3.3.4 Immunofluorescence analysis

Tumors were fixed in a 4% (w/v) paraformaldehyde in PBS solution at 4ºC for 1h, cryoprotected in 15% (w/v) sucrose in PBS solution, embedded in 7.5% (w/v) gelatin in PBS solution, snap frozen in liquid nitrogen and cryosectioned in 10 and 20µm-thick sections. The following primary antibodies were used: anti-PECAM-1 (557355), anti-E-cadherin (560061) (BD Biosciences, San Jose, USA), anti-α-SMA (ab5694), anti-PCNA (ab18197), anti-Lgr5 (ab75732), anti-HIF1α (ab85866), anti-Cyclin D1 (ab21699) (Abcam, Cambridge, UK), anti-Dll4 (AF1389, R&D Systems, Minneapolis, USA), anti-lysozyme (A009902-2, Dako, Glostrup, Denmark), anti-phospho-Egfr (Tyr1068) (3777), anti-phospho-p44/42 MAPK (Erk1/2) (Thr202/Tyr204) (4370), anti-phospho-Akt (Ser473) (4060), N1ICD (4147), anti-non-phospho (active) β-catenin (8814) (Cell Signaling Technology, Danvers, USA). Species-specific secondary antibodies conjugated with Alexa Fluor 488 and 594 (Invitrogen, Carlsbad, CA) were used to reveal primary antibody binding. Tissue sections were incubated with primary antibody overnight at 4°C and with secondary antibody for 1h at room temperature. Nuclei were counterstained with 4´, 6-diamidino-2-phenylindole dihydrochloride hydrate (DAPI; Molecular Probes, Eugene, OR).

Fluorescent immunostained sections were examined under a Leica DMRA2 fluorescence microscope with Leica HC PL Fluotar 10 and 20X/0.5 NA dry objective, captured using Photometrics CoolSNAP HQ, (Photometrics, Friedland, Denmark), and processed with Metamorph 4.6-5 (Molecular Devices, Sunnyvale, CA, US). Morphometric analyses were performed using the NIH ImageJ 1.37v program. Positive signal was determined by the percentage of white pixels per field after transforming the RGB images into binary files.

Under the effect of 2-2-2 tribromoethanol anaesthesia, biotin-conjugated lectin from *Lycopersicon esculentum* (100µg/100µl of PBS) or 1% Evans' Blue solution (Sigma, St. Luis, MO, US) were administered in the caudal vein to mark vessel perfusion and extravasation, respectively. Both solutions were allowed to circulate for 5 minutes before the vasculature was transcardially perfused with 4% (w/v) paraformaldehyde in PBS solution for 3 minutes. Tumor samples were collected and processed as described above. Tissue sections were stained and tumor perfusion was quantified by determining the percentage of red PECAM-positive structures that were co-localized with Streptavidin-Alexa 488 (Invitrogen, Carlsbad,

CA, US) signals. Evans' Blue is red fluorescent and extravasation was visualized in contrast to green fluorescent vascular structures.
Apoptosis was measured using the TUNEL assay (Roche, Mannheim, Germany).

4.3.3.5 Quantitative transcriptional analysis

Intestinal tumors from the therapy trials were snap frozen in liquid nitrogen until RNA extraction (Qiagen RNeasy). Using the SuperScript® III First-Strand Synthesis SuperMix for qRT-PCR (Invitrogen, Carlsbad, CA, USA), first-strand cDNA was synthesized from total RNA. Real-time PCR analysis was performed using specific primers. Primer pair sequences are reported on Annex II. Gene expression was normalized to *β*-actin and in the case of genes expressed in the vasculature it was additionally normalized to *Pecam-1*.

4.3.3.6 Statistical analysis

To compare measurements between control and test groups, the Mann-Whitney-Wilcoxon test was performed using the Statistical Package for the Social Sciences v15.0 (Chicago, IL). Results are presented as relative average ± SEM. *P*-values <0.05 and <0.01 were considered significant (*) and highly significant (**), respectively.

4.3.4 Results

4.3.4.1 Dll4-Fc potentiates the inhibitory effect of erlotinib in the small intestine tumor multiplicity of *Apc*$^{Min/+}$ mice

Previous work showed that Dll4 blockade inhibits the tumor growth by deregulating the angiogenic process (Djokovic et al., 2010; Noguera-Troise et al., 2006; Ridgway et al., 2006; Scehnet et al., 2007). It has also been shown that anti-DLL4 therapy reduces the cancer stem cell frequency in CRC (M. Fischer et al., 2010; Hoey et al., 2009). However, it has never been demonstrated if Dll4 inhibition can be beneficial in initial stages of CRC. This led us to carry out a therapeutic trial using the Dll4 antagonist, Dll4-Fc, in the *Apc*$^{Min/+}$ mouse model of CRC. We observed that Dll4-Fc therapy reduced the number of tumors by 3.4- and 2.9-fold in the small and large intestine, respectively (Fig. 24A and 24D-E). The individual tumor volume was also reduced by 2- and 2.4-fold, respectively (Fig. 24B and 24D-E). Therefore, the Dll4-Fc therapy resulted in a 7-fold reduction of the intestine overall tumor burden (Fig. 24C-E).
The Egfr pathway is important in the establishment of adenomas in the *Apc*$^{Min/+}$ CRC mouse model (Roberts et al., 2002) and Notch signaling seems to interact with this pathway in other types of cancer (Baker et al., 2014; H. Yamaguchi et al., 2014). Therefore, we tested if the combination of Dll4-Fc with the anti-Egfr tyrosine kinase inhibitor erlotinib, could have some benefit in this model of CRC. Our main concern was to assess if the previously described Dll4-Fc effect on tumor angiogenesis would allow the effective delivery of erlotinib to the

tumors. We observed that the combination of these therapies had an additive effect by further reducing the small and large intestine tumor number (Fig. 24A and 24D-E), when compared with the monotherapies. However, in the large intestine this was only significantly altered relatively to erlotinib monotherapy (Fig. 24A and 24D-E). Relatively to the controls, the mice treated with erlotinib alone showed no statistically significant differences in average tumor volume, whereas those treated with the combined therapy had smaller tumors, similar to those observed in mice receiving Dll4-Fc monotherapy (Fig. 24B and 24D-E). Thus, while in the erlotinib treatment the overall tumor burden was reduced by 3.2-fold, in the combinatory intervention trial this parameter was reduced by 11.4-fold (Fig. 24C-E).
Importantly, the therapies tested did not cause any toxic effects in the liver (data not shown).

Figure 24 - Dll4-Fc therapy promotes the anti-tumoral activity of erlotinib treatment by reducing the *Apc*$^{Min/+}$ tumor number and volume

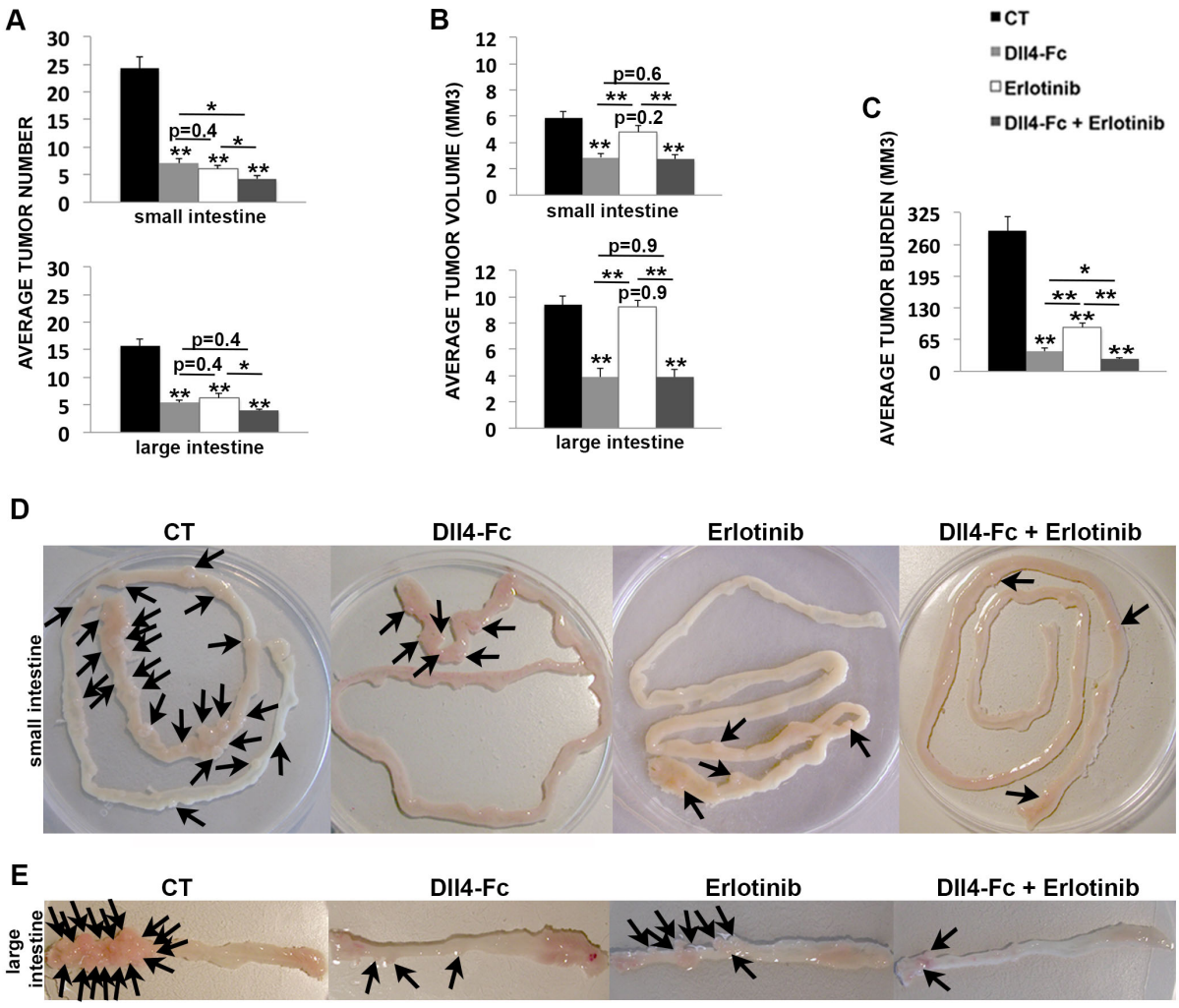

(A-B) Graphic bars represent average ± SEM tumor number (A) and volume (mm^3) (B) in the small and large intestine of Dll4-Fc, erlotinib and Dll4-Fc plus erlotinib-treated *Apc*$^{Min/+}$ mice *versus* their controls (CT) at 18 weeks of age. (C) Graphic bars represent the average ± SEM tumor burden (mm^3) in the whole intestine of the animals described above. One experiment with n = 12 per group. (D-E)

Photographs of the small (D) and large (E) intestine (tumors indicated by arrows) collected from the animals described above.

4.3.4.2 The inhibition of Egfr pathway activation in *Apc*$^{Min/+}$ intestinal tumors is one of the mechanisms responsible for the observed additive effect of Dll4-Fc and erlotinib therapy

We evaluated the effect of the therapies tested on the activation of Egfr pathway by measuring the levels of phosphorylated Egfr and also the phosphorylation status of its downstream targets extracellular regulated kinase (Erk) and Akt (Grant, Qiao, & Dent, 2002) in the tumor samples.

We found that, relatively to the controls, the protein expression of phosphorylated Egfr, Erk and Akt in the erlotinib-treated small and large intestine tumors was strongly reduced, especially the first (Fig. 25A, Fig. 26A-C and Fig. 27A-C).). Interestingly, we observed that Dll4-Fc had some inhibitory effect on the Egf/Egfr pathway, suggesting a possible crosstalk between the two pathways (Fig. 25A, Fig. 26A-C and Fig. 27A-C). Accordingly, the combinatory therapy had a cumulative negative effect on the Egfr/Akt pathway in the small and large intestine tumors (Fig. 25A, Fig. 26A-C and Fig. 27A-C).

4.3.4.3 Erlotinib treatment induces Notch1 activation in *Apc*$^{Min/+}$ intestinal tumors

To confirm the effect of the therapies tested in the Notch signaling pathway, the gene expression of *Hes1, Hes5* and *Hey2, Dll4, Dll1* and *Jagged1* and *Notch1-4* in the tumor samples was evaluated by RT-PCR.

Dll4-Fc-treated tumors presented a strong decrease of *Hes1, Hes5* and mainly of *Hey2* RNA levels in the small and large intestine (Fig. 25C-D). Additionally, these tumors had a statistically significant increase of *Dll4, Dll1, Jagged1* and *Notch1* and *4* RNA transcription in the small and large intestine (Fig. 25C-D).

Interestingly, in the erlotinib-treated tumors we also found a statistically significant increase of *Notch1*, *Hes1* and *Hes5* RNA transcription in the small and large intestine (Fig. 25C-D).

In the combinatory trial, *Hes1*, *Hes5* and *Hey2* RNA transcription in the small and large intestine tumors was less decreased than in the Dll4-Fc trial (Fig. 25C-D). In these tumors we also found a statistically significant increase of the RNA transcription of all the analysed ligands and receptors, with the exception of *Notch3* (Fig. 25C-D). Comparing the transcription levels of Notch pathway members in the combination trial with each of the monotherapies, we found statistically significant differences only relatively to the erlotinib treatment, specifically in the expression of the analysed effectors and ligands in the small and large intestine (*Jagged1* only in the last) (Fig. 25C-D).

As *Notch1* expression was found to be upregulated in the erlotinib-treated tumors, we measured Notch1 intracellular domain (N1ICD) protein density in the intestinal tumors of the treated groups to assess Notch1 signaling. Interestingly, we found that N1ICD was increased

in the tumoral epithelium of the small intestine, while it was mostly observed in the stroma of the tumors collected from the large intestine (Fig. 25E and 25G), in all three therapeutic groups and controls. As expected, Dll4-Fc-treated mice showed decreased N1ICD levels in small and large intestine tumors (Fig. 25E-H). In contrast, erlotinib-treated tumors presented increased nuclear N1ICD staining (Fig. 25E-H). In the combinatory trial, the levels of nuclear N1ICD were similar to that measured in Dll4-Fc-treated tumors from both small and large intestine (Fig. 25E-H).

Figure 25 - Both Dll4-Fc and erlotinib treatments affect the EGFR and Notch pathways in the *Apc*$^{Min/+}$ tumors

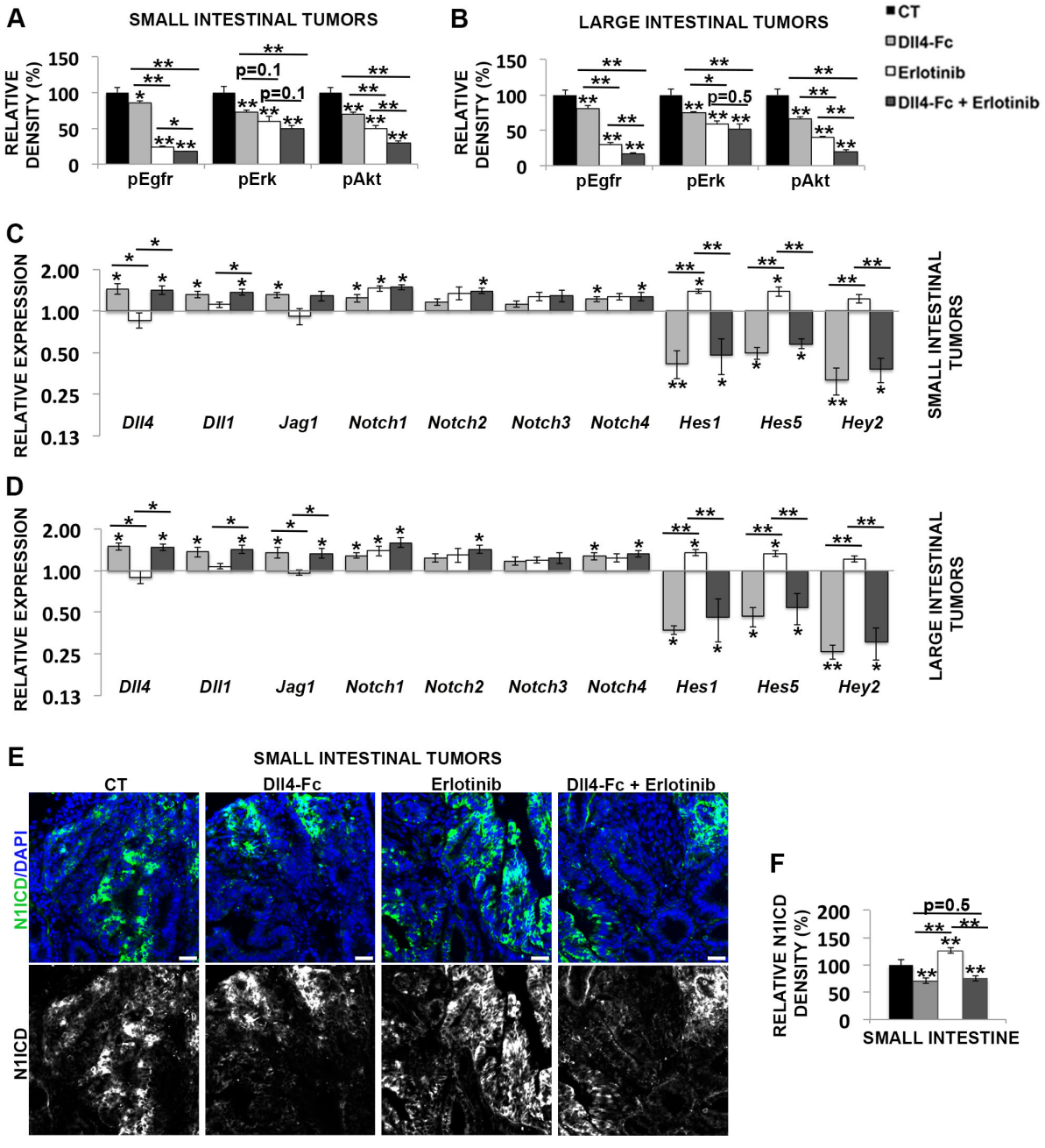

Figure 25 (continuation) - Both Dll4-Fc and erlotinib treatments affect the EGFR and Notch pathways in the *Apc*$^{Min/+}$ tumors

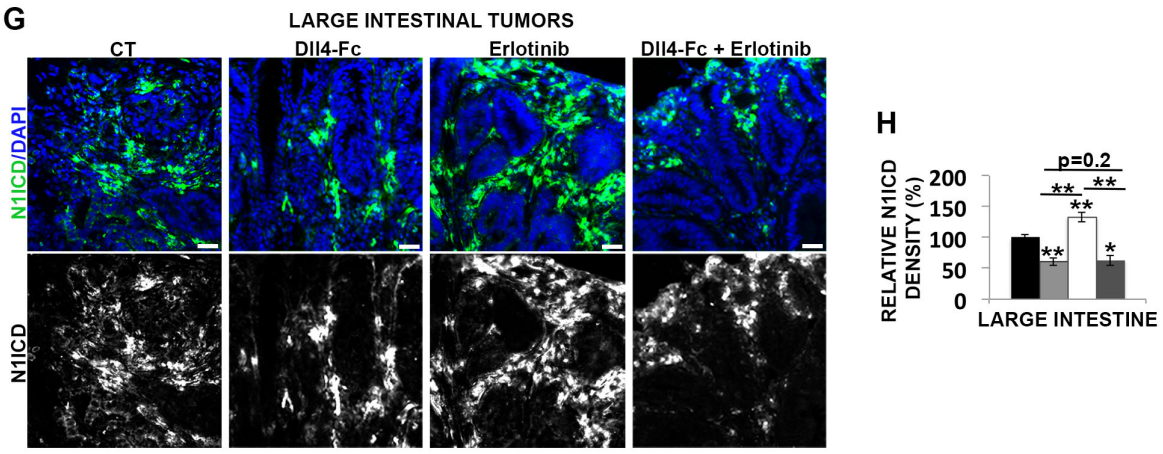

(A-B) Graphic bars represent the relative density (%) ± SEM of phosphorylated Egfr, Erk and Akt, respectively, analyzed by immunofluorescence, in the small (A) and large (B) intestine tumors of Dll4-Fc, erlotinib and Dll4-Fc plus erlotinib-treated *Apc*$^{Min/+}$ mice *versus* controls (CT) at 18 weeks of age. One experiment with n = 6 per group and 6 fields per animal. (C-D) RT-PCR analysis of *Dll4, Dll1, Jag1, Notch1-4, Hes1* and *5* and *Hey2* relative expression normalized to *Pecam-1* in the same animals small (C) and large (D) intestine tumors. One experiment with n = 3 per group. (E-G) Immunofluorescence staining representative images for N1ICD density (green) in the small (E) and large (G) intestine tumor cryosections (10µm) of the animals mentioned above. The nuclei were counterstained with DAPI (in blue). Scale bars = 100µm. (F-H) Graphic bars represent the relative density (%) ± SEM of N1ICD in the small (F) and large (H) intestine tumors. One experiment with n = 6 per group and 6 fields per animal. *P<0.05; **P<0.01.

Figure 26 - Impact of erlotinib and Dll4-Fc treatments, alone and in combination, on the activation of Egfr pathway in *Apc*$^{Min/+}$ small intestine tumors

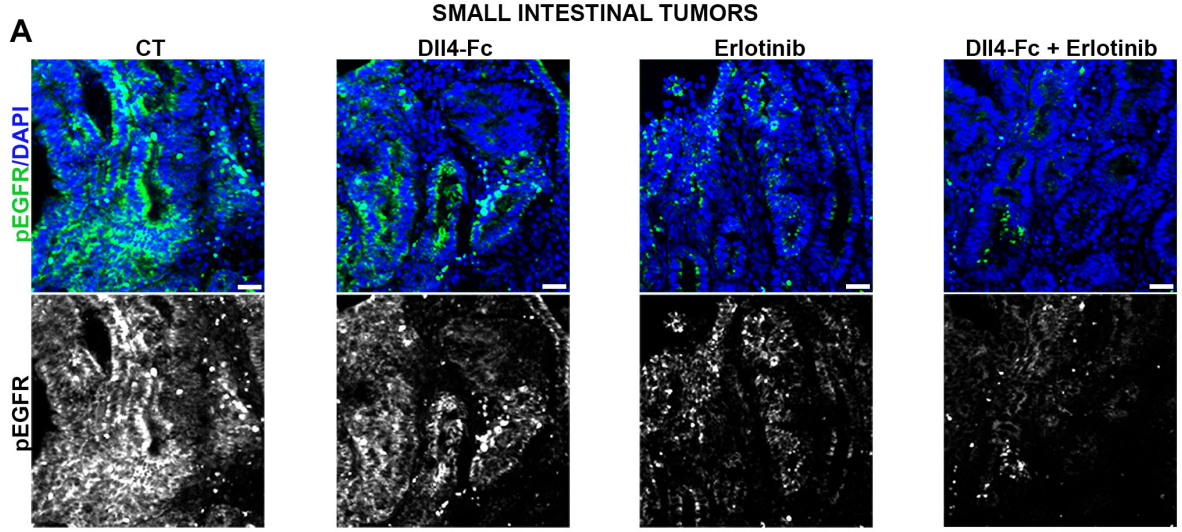

Figure 26 (continuation) - Impact of erlotinib and Dll4-Fc treatments, alone and in combination, on the activation of Egfr pathway in *Apc*$^{Min/+}$ small intestine tumors

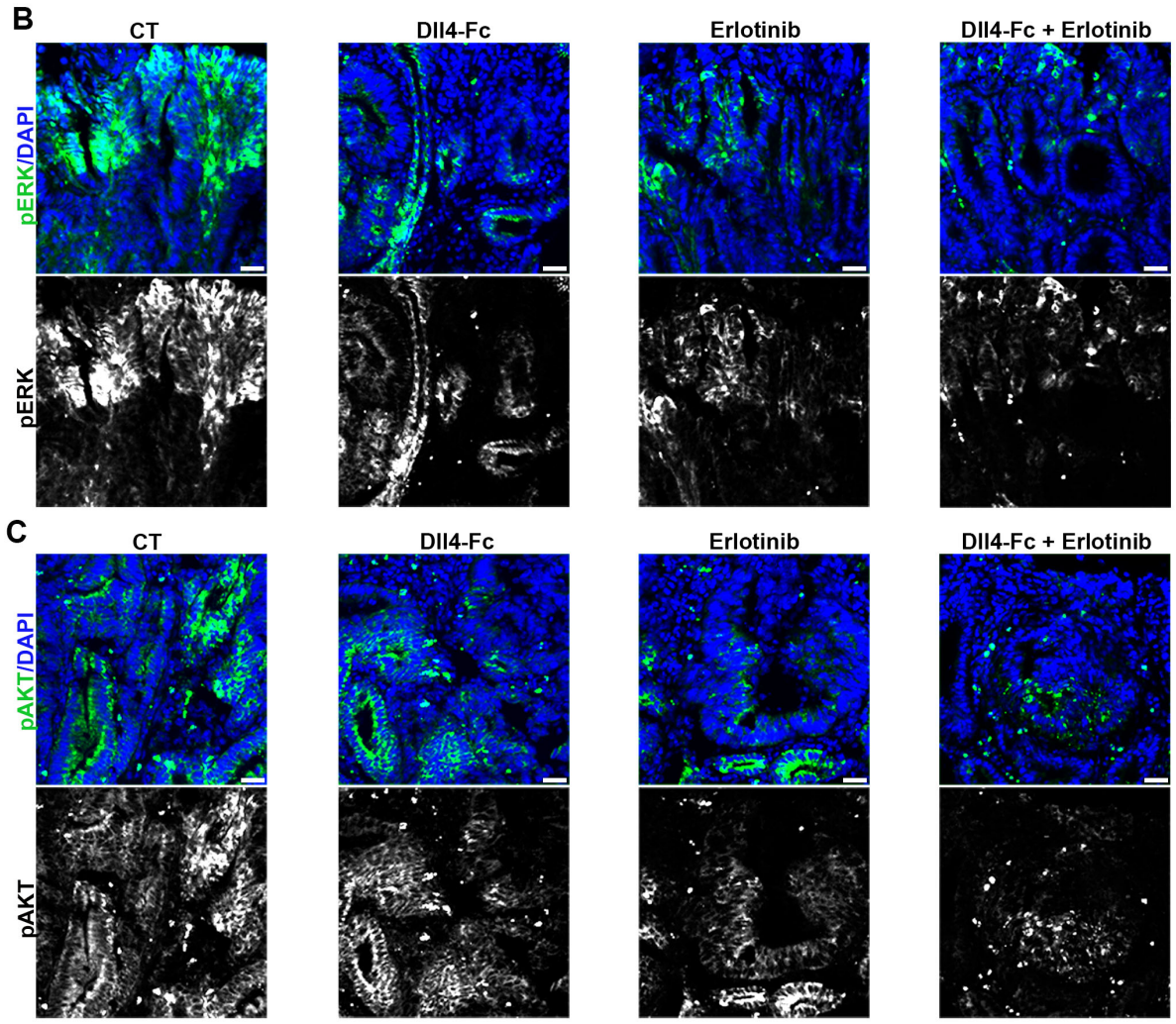

(A-C) Representative images of immunofluorescence staining density for phosphorylated Egfr (A), Erk (B) and Akt (C) (in green) with the nuclei counterstained by DAPI (in blue) in the small intestine tumor cryosections (10µm) from Dll4-Fc, erlotinib and Dll4-Fc plus erlotinib-treated *Apc*$^{Min/+}$ mice *versus* controls (CT) at 18 weeks of age. Scale bars = 100µm. One experiment with n = 6 per group and 6 fields per animal.

Figure 27 - Effect of erlotinib and Dll4-Fc therapies, alone and in combination, on Egfr pathway activation in *Apc*$^{Min/+}$ large intestine tumors

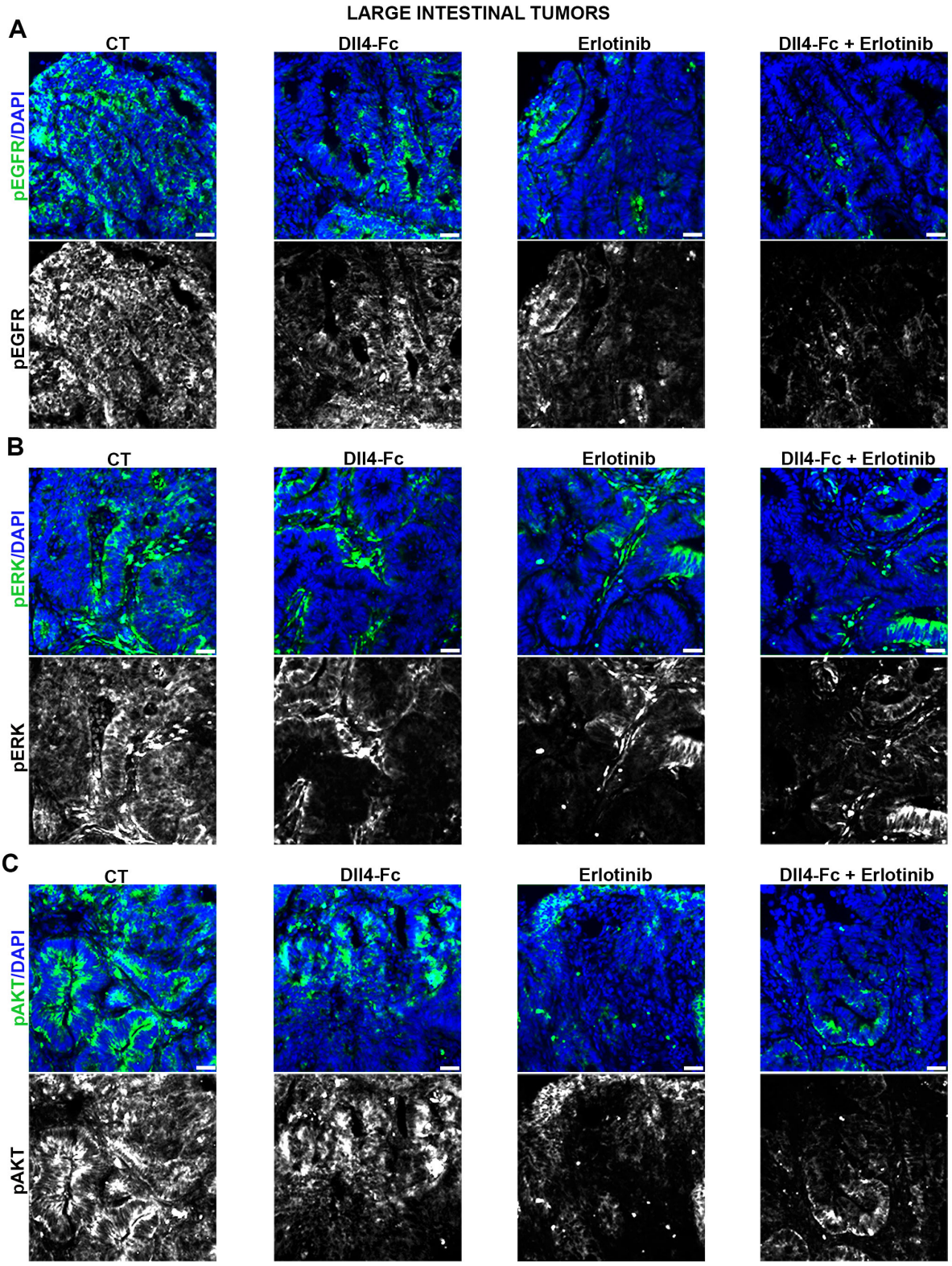

(A-C) Representative images of immunofluorescence staining density for Egfr (A), Erk (B) and Akt (C) (in green) with the nuclei counterstained by DAPI (in blue) in the large intestine tumor cryosections (10μm) from Dll4-Fc, erlotinib and Dll4-Fc plus erlotinib-treated *Apc*$^{Min/+}$ mice *versus* controls (CT) at 18 weeks of age. Scale bars = 100μm. One experiment with n = 6 per group and 6 fields per animal.

4.3.4.4 Dll4-Fc promotes an intestinal tumor dysfunctional and immature pro-angiogenic phenotype with increased hypoxia and apoptosis, even when associated to erlotinib therapy

Previous work, using other models, described how Dll4-Fc acts on tumor angiogenesis (Djokovic et al., 2010; Noguera-Troise et al., 2006; Ridgway et al., 2006; Scehnet et al., 2007). Predictably, we found the same therapeutic effect in the $Apc^{Min/+}$ model. Specifically, the Dll4-Fc treated animals had an approximately 2-fold increase of vascular density in the small and large intestine tumors (Fig. 28A-B and Fig. 29A-B). Accordingly, in these animals the gene expression of *Vegfa* and *c*, *Vegfr2* and *3* and *Pecam-1* in the small and mainly large intestine tumors was increased, while the level of *Vegfr1* transcripts was decreased (Fig. 30A-B). These tumors also had a reduction of smooth muscle cell coverage in the newly formed vessel walls (Fig. 28A and 28C, and Fig. 29A and 29C). Regarding vascular functionality, we observed that the vessels of the tumors collected from the small and large intestine, were poorly perfused (Fig. 28D-E and Fig. 29D-E). In addition, these vessels were very leaky, displaying an increase in the levels of Evans' Blue extravasation in the small and large intestine tumors (Fig. 28F-G and Fig. 29F-G). We also found increased HIF1α protein expression, an indicator of hypoxia, (Fig. 31A-D) and increased apoptosis in these tumors (Fig. 31E-H).

The animals treated with erlotinib alone displayed reduced vascular density in the tumors of the small and large intestine (Fig. 28A-B and Fig. 29A-B), as previously reported in pancreatic cancer (Starling, Neoptolemos, & Cunningham, 2006). In these animals the expression of *Vegfa* and *c* and *Pecam-1* was strongly reduced and that of *Vegfr1* was mildly increased in the large and mainly in the small intestine, while that of the other genes was not significantly altered (Fig. 30A-B). Additionally, the wall of the newly formed vessels displayed slightly more smooth muscle cell coverage than that of controls, in the small and large intestine tumors (Fig. 28A and 28C, and Fig. 29A and 29C). Moreover, the erlotinib treated mice displayed increased vascular perfusion and reduced vascular extravasation in the tumors collected from both small and large intestine (Fig. 28D-G and Fig. 29D-G). These vascular changes were accompanied by decreased protein expression of HIF1α in the tumors of both regions (Fig. 31A-D), but the tumor apoptotic level was not significantly altered (Fig. 31E-H).

In the combinatory trial, the vascular density of the small and large intestine tumors was increased, but not as much as in the Dll4-Fc treatment (Fig. 28A-B and Fig. 29A-B). The vascular related gene expression analysis confirmed this result (Fig. 30A-B). The effect of Dll4-Fc on vascular maturity was maintained when in combination with erlotinib (Fig. 28A and 28C, and Fig. 29A and 29C). Interestingly, in this trial the tumor vessels were not as dysfunctional as in the Dll4-Fc treated animals, but still presented less perfusion and more extravasation than the controls (Fig. 28D-G and Fig. 29D-G). Accordingly, the protein

expression of HIF1α in the Dll4-Fc plus erlotinib-treated tumors was less increased than in the Dll4-Fc trial in the small and large intestine (Fig. 30A-D). In addition, the combination therapy led to a slight reduction of the level of tumor apoptosis compared to Dll4-Fc alone that was only statistically significant for the large intestine (Fig. 30E-H).

Figure 28 - Dll4-Fc promotes dysfunctional angiogenesis, even when associated with erlotinib treatment, in *Apc*$^{Min/+}$ small intestine tumors

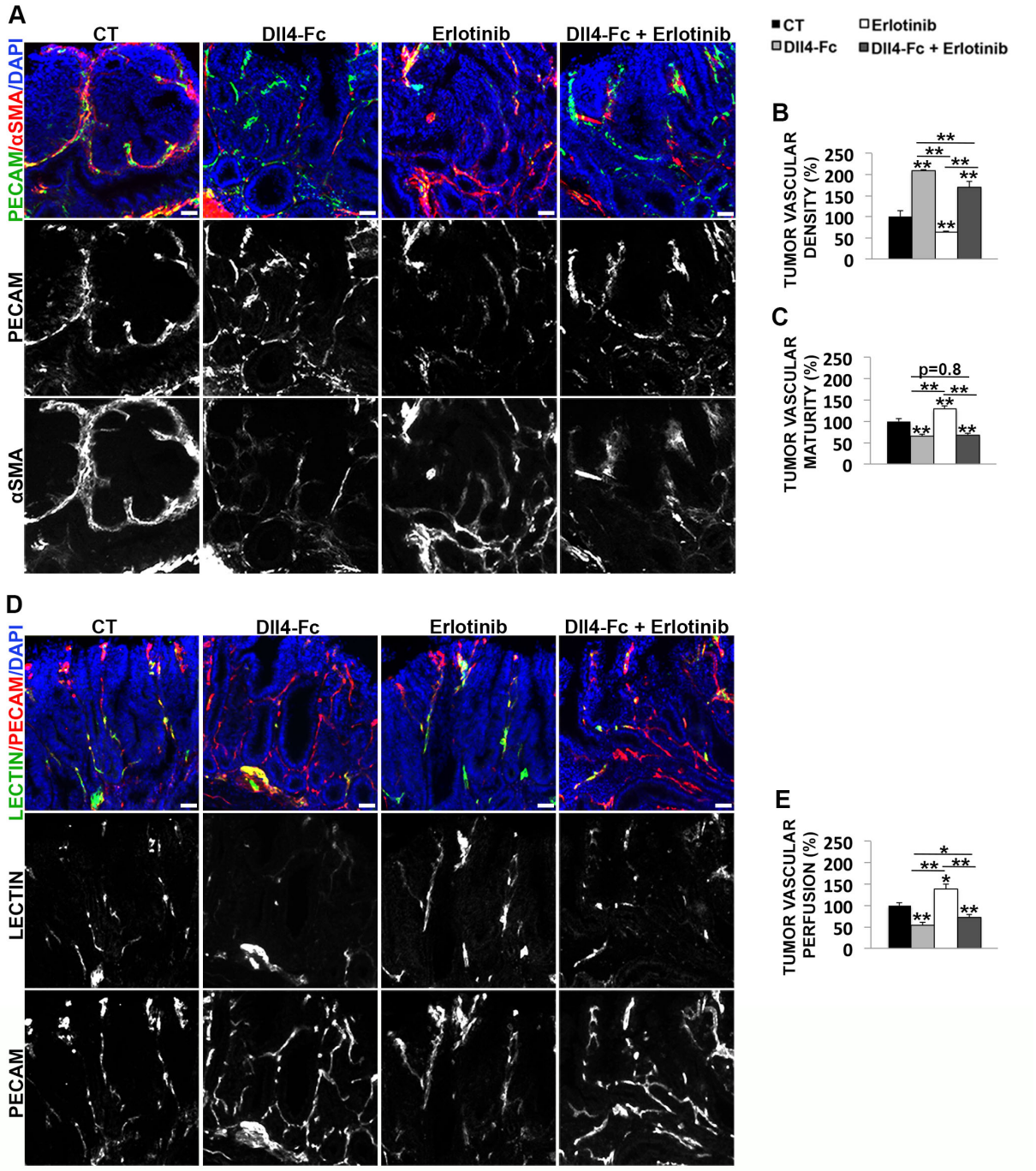

Figure 28 (continuation) - Dll4-Fc promotes dysfunctional angiogenesis, even when associated with erlotinib treatment, in *Apc*$^{Min/+}$ small intestine tumors

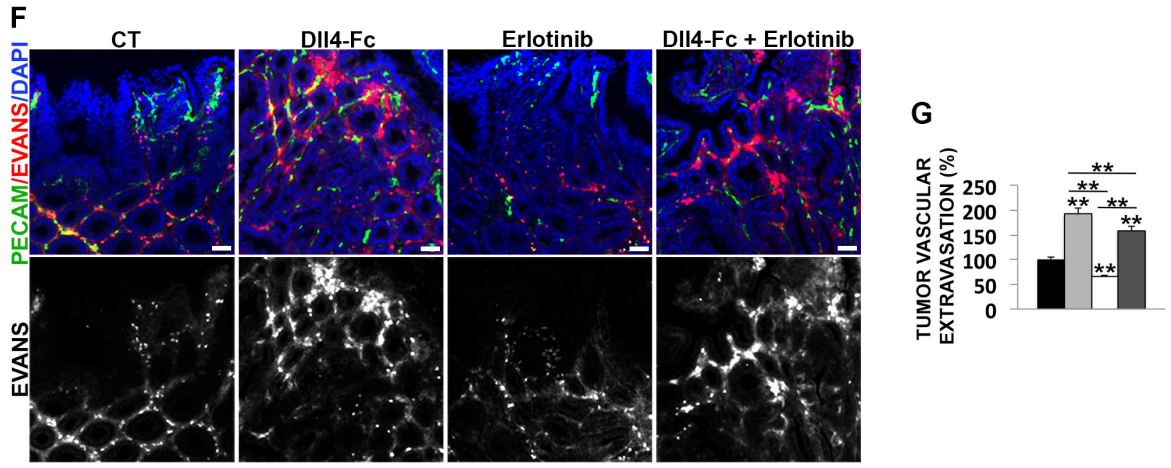

(A, D, F) Immunofluorescence stainings of 20µm small intestine tumor cryosections from Dll4-Fc, erlotinib and Dll4-Fc plus erlotinib-treated *Apc*$^{Min/+}$ mice *versus* controls (CT) at 18 weeks of age. Scale bars = 100µm. The nuclei were counterstained with DAPI (in blue). Representative images of staining density for PECAM-1 (in green) and α-SMA (in red) (A), for lectin (in green) and PECAM-1 (in red) (D), and for PECAM-1 (in green) and Evans blue (in red) (F). (B, C, E, G) Graphic bars represent the relative (%) ± SEM tumor vascular density (B), maturity (C), perfusion (E) and extravasation (G) in the small intestine of the animals described above (n=6 per group). **P*<0.05; ***P*<0.01.

Figure 29 - Dll4-Fc promotes dysfunctional angiogenesis, even with concomitant erlotinib therapy, in *Apc*$^{Min/+}$ large intestine tumors

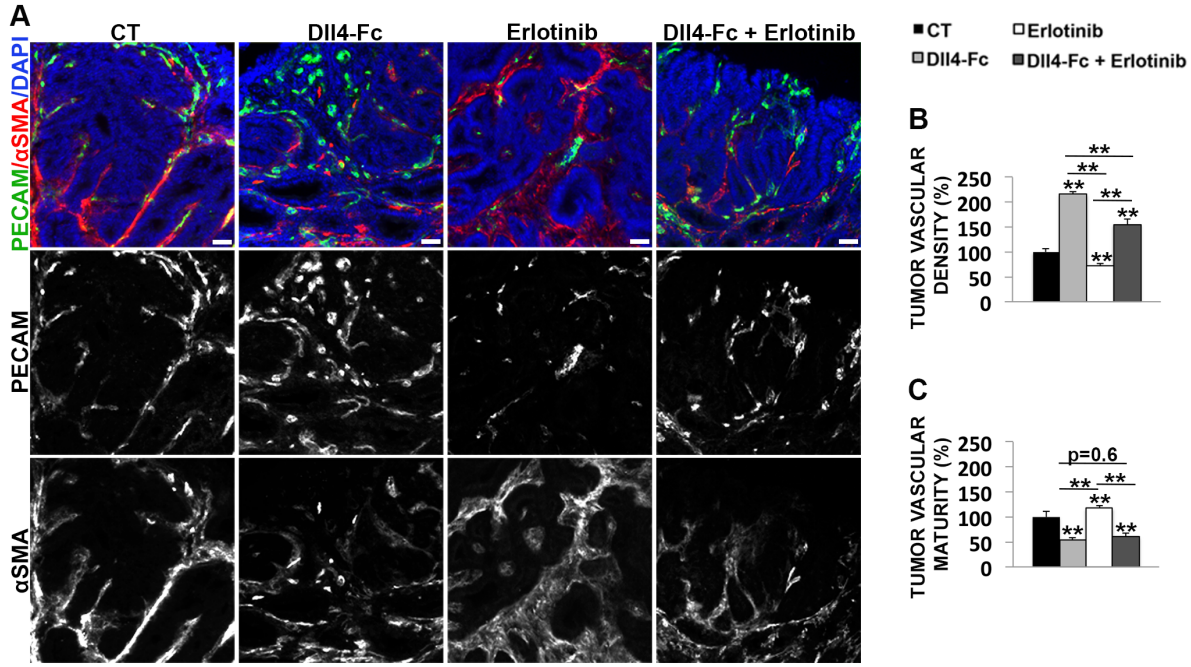

Figure 29 (continuation) - Dll4-Fc promotes dysfunctional angiogenesis, even with concomitant erlotinib therapy, in *Apc*$^{Min/+}$ large intestine tumors

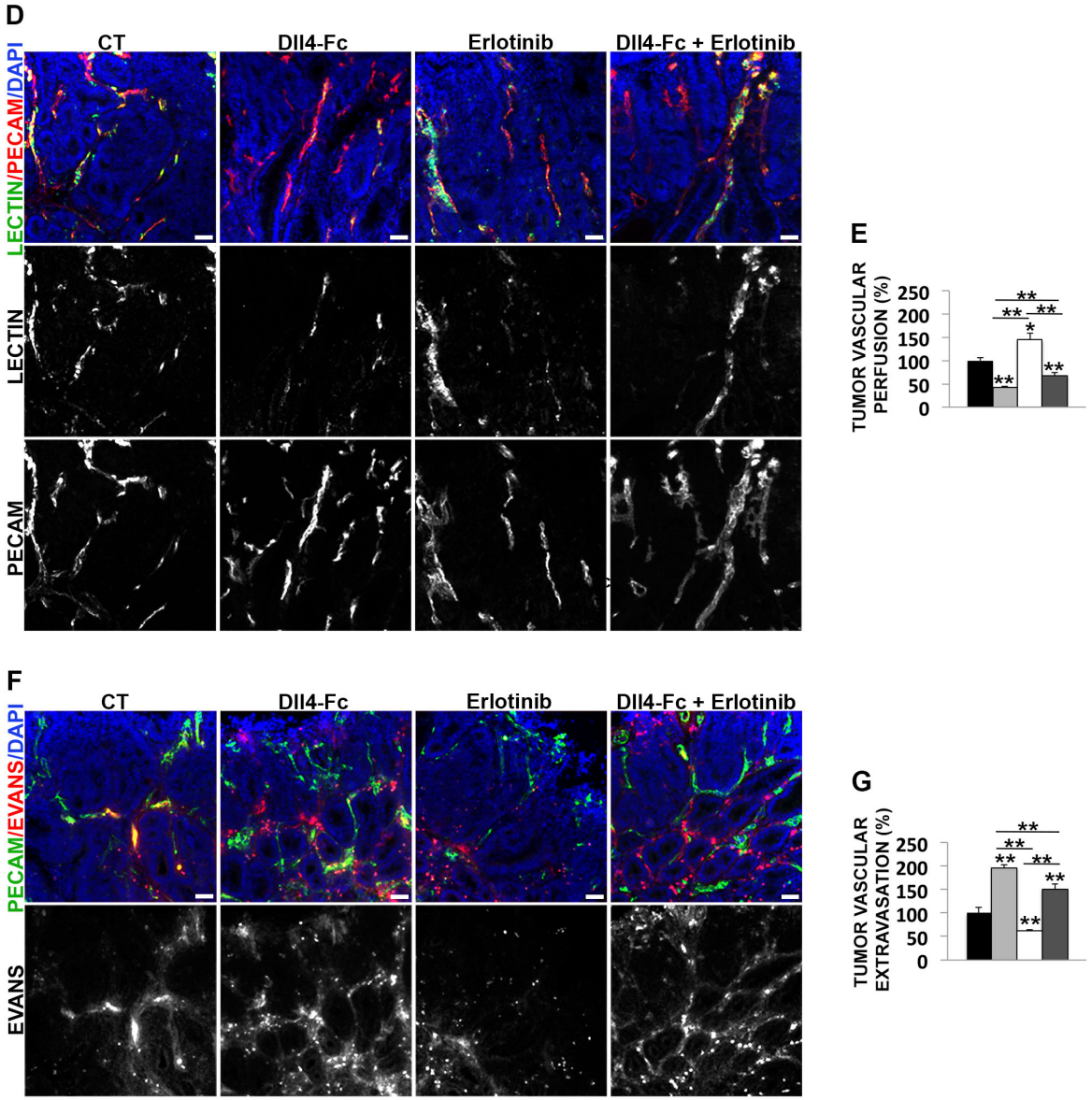

(A, D, F) Immunofluorescence stainings of 20μm large intestine tumor cryosections from Dll4-Fc, erlotinib and Dll4-Fc plus erlotinib-treated *Apc*$^{Min/+}$ mice *versus* controls (CT) at 18 weeks of age. Scale bars = 100μm. The nuclei were counterstained with DAPI (in blue). Representative images of staining density for PECAM-1 (in green) and α-SMA (in red) (A), for lectin (in green) and PECAM-1 (in red) (D), and for PECAM-1 (in green) and Evans blue (in red) (F). (B, C, E, G) Graphic bars represent the relative (%) ± SEM tumor vascular density (B), maturity (C), perfusion (E) and extravasation (G) in the large intestine of the animals described above. One experiment with n = 6 per group and 6 fields per animal. **P*<0.05; ***P*<0.01.

Figure 30 - Dll4-Fc promotes *Vegf/Vegfr* gene expression in *Apc*$^{Min/+}$ tumors, even when associated with erlotinib treatment

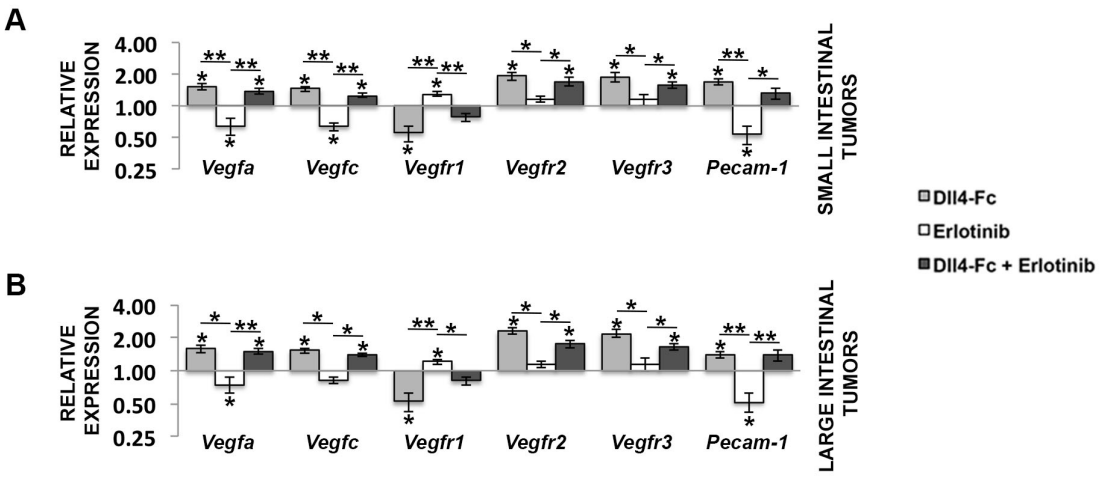

(A, B) RT-PCR analysis of *Vegfa* and *c*, *Vegfr1-3* and *Pecam-1* relative expression in Dll4-Fc, erlotinib and Dll4-Fc plus erlotinib-treated small (A) and large (B) intestine *Apc*$^{Min/+}$ tumors at 18 weeks of age. One experiment with n = 3 per group. **P*<0.05; ***P*<0.01.

Figure 31 - Dll4-Fc promotes hypoxia and apoptosis, even with concomitant erlotinib therapy, in *Apc*$^{Min/+}$ small and large intestine tumors

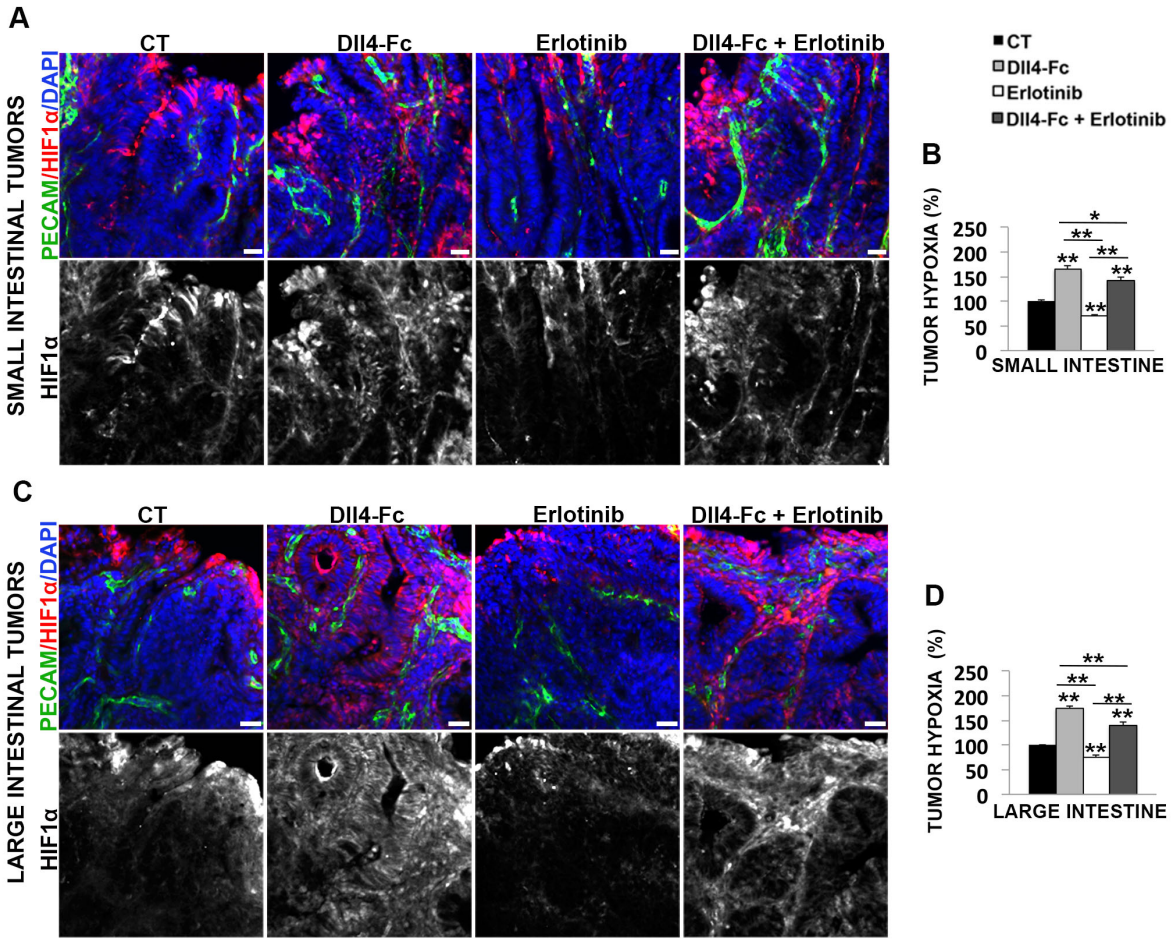

Figure 31 (continuation) - Dll4-Fc promotes hypoxia and apoptosis, even with concomitant erlotinib therapy, in *Apc*$^{Min/+}$ small and large intestine tumors

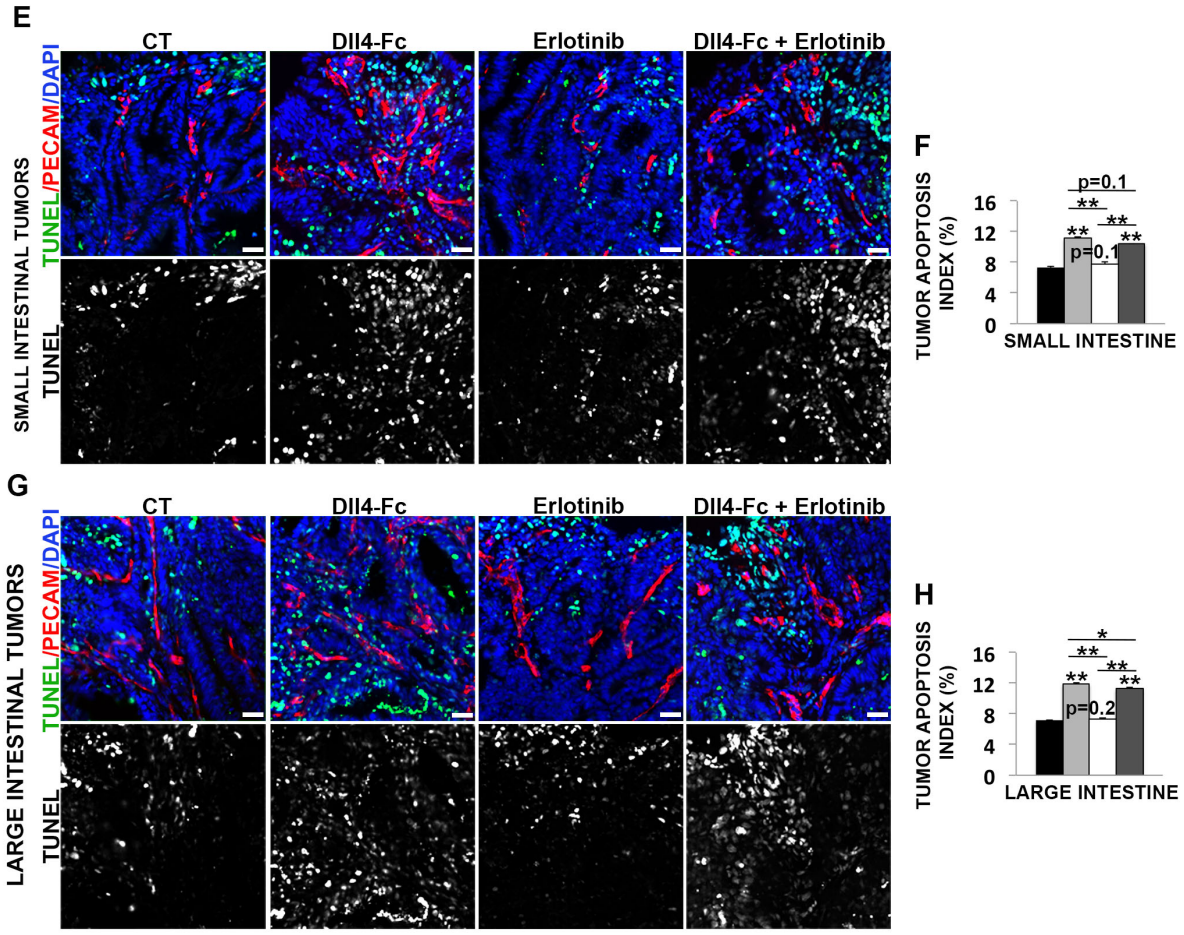

(A, C, E, G) Immunofluorescence stainings of 20µm small (A, E) and large (C, G) intestine tumor cryosections from Dll4-Fc, erlotinib and Dll4-Fc plus erlotinib-treated *Apc*$^{Min/+}$ mice *versus* controls (CT). Scale bars = 100µm. The nuclei were counterstained with DAPI (in blue). Representative images of staining density for PECAM-1 (in green) and HIF1α (in red) (A, C), and for TUNEL (in green) and PECAM-1 (in red) (E, G). (B, D, F, H) Graphic bars represent the relative tumor hypoxia (%) ± SEM (B, D) and apoptosis index (%) ± SEM (F, H) in the small (B, F) and large (D, H) intestine of the animals described above. One experiment with n = 6 per group and 6 fields per animal. **P*<0.05; ***P*<0.01.

4.3.4.5 Association of Dll4-Fc to erlotinib has a synergistic effect inhibiting the tumor cell proliferation and tumor stem cell maintenance

As both Dll4-Fc and erlotinib treatments led to a significant reduction of the *Apc*$^{Min/+}$ tumor multiplicity, we evaluated if these therapies were affecting the tumor proliferation, neoplastic transformation or tumor stem cell maintenance.

Indeed, the cellular proliferation in the tumors of Dll4-Fc and erlotinib treated mice was decreased in the large and mainly in the small intestine (Fig. 32A-B and Fig. 33A-B). Dll4-Fc alone had a significantly more pronounced effect than erlotinib in both intestinal regions (Fig.

32A-B and Fig. 33A-B). The combination therapy further decreased the cellular proliferation in the small and large intestine tumors (Fig. 32A-B and Fig. 33A-B). However, the differences found between Dll4-Fc alone and the combination therapies were not statistically significant in the large intestine (Fig. 33A-B).

Neoplastic progression in the treated-mice was characterised by histopathological classification. In the control group the majority of the lesions in the small and large intestine were adenomas with high-grade dysplasia (Fig. 32C and Fig. 33C). In the Dll4-Fc treated mice the small and large intestine lesions were mainly hyperplasias and adenomas with low-grade dysplasia (Fig. 32C and Fig. 33C). In the erlotinib-treated animals the lesions were similar to the controls, both in the small and large intestine (Fig. 32C and Fig. 33C). In the combination trial the lesions were mainly adenomas with low-grade dysplasia in the small and large intestine (Fig. 32C and Fig. 33C). Therefore Dll4-Fc alone and in combination with erlotinib, but not erlotinib alone, seemed to delay the neoplastic transformation.

Tumor stem cells expressing leucine-rich repeat-containing G-protein-coupled receptor 5 (Lgr5) and the B cell–specific Moloney murine leukemia virus insertion site 1 (Bmi1) are responsible for neoplastic initiation and development (Espersen, Olsen, Linnemann, Hogdall, & Troelsen, 2015; Fre et al., 2005; Schepers et al., 2012).

In the tumors of the small and large intestine, Dll4-Fc and erlotinib had a cumulative effect in the reduction of the protein and gene expression of Lgr5, but only Dll4-Fc was able to reduce the gene expression of *Bmi1* (Fig. 32D-F and Fig. 33D-F). We found that these effects were more pronounced in the small than in the large intestine (Fig. 32D-F and Fig. 33D-F). Moreover, no differences in the density of Lgr5-positive stem cells in the adjacent normal intestine of the three treated mouse groups were observed relatively to the controls (data not shown).

We also analysed the tumor gene expression of the cyclin-dependent kinase inhibitors 1B *(Cdkn1b)* and 1C *(Cdkn1c)*, which are mediators of crypt progenitor cells maintenance, downstream of Notch-Hes1 signaling (Riccio et al., 2008). *Cdkn1b and c* expression was significantly increased only in the Dll4-Fc and in the combination treated small and large intestine tumors (Fig. 32F and Fig. 33F).

Next we analysed *Myc* and *Ccnd2* gene expression and Cyclin D1 protein levels, which are important factors for tumor initiating cell maintenance and proliferation in the $Apc^{Min/+}$ mouse model (Cole et al., 2010; Hulit et al., 2004; Ignatenko et al., 2006). All the treatments led to a significant downregulation of *Myc* and *Ccnd2 RNA* expression and also to decreased Cyclin D1 protein levels, especially the combinatory trial, particularly in the small intestine (Fig. 32F-G and Fig. 33F-G). However no statistically significant differences were found between the therapy groups (Fig. 32F-G and Fig. 33F-G).

To confirm if this effect on tumor initiating cells and tumor proliferation was Wnt related, the levels of the Wnt pathway-derived non-phosphorylated (active) β-catenin density were

analysed. We observed only a slight reduction in the combination-treated small intestine tumors (Fig. 34A-D).

Figure 32 - Dll4-Fc plus erlotinib have a cumulative negative effect on tumor proliferation and tumor stem cell maintenance in the *Apc*$^{Min/+}$ small intestine

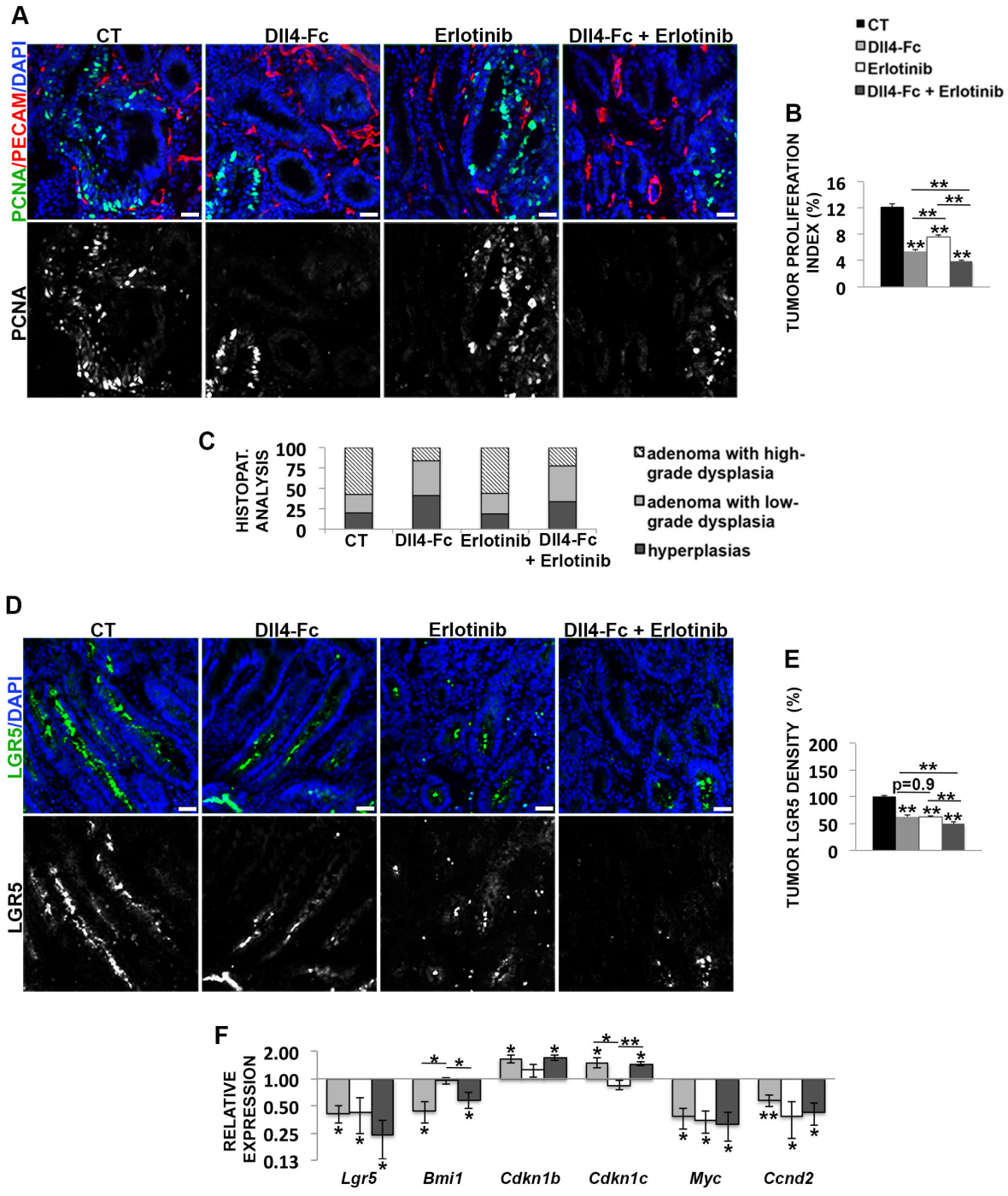

Figure 32 (continuation) - Dll4-Fc plus erlotinib have a cumulative negative effect on tumor proliferation and tumor stem cell maintenance in the *Apc*$^{Min/+}$ small intestine

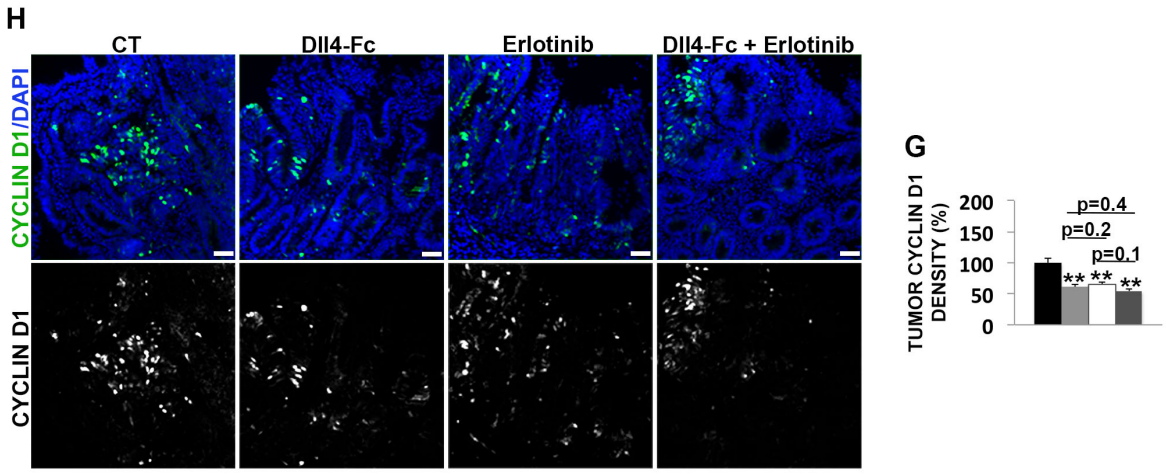

(A, D, H) Immunofluorescence stainings of the small intestine tumor cryosections (10µm) from Dll4-Fc, erlotinib and Dll4-Fc plus erlotinib-treated *Apc*$^{Min/+}$ mice *versus* their controls (CT). Scale bars = 100µm. The nuclei were counterstained with DAPI (in blue). Representative images of staining density for PCNA (in green) and PECAM-1 (in red) (A), for lgr5 (in green) (D), and for Cyclin D1 (in green) (H). (B, E, G) Graphic bars represent the small intestine tumor proliferation index (%) ± SEM (B), and the relative tumor Lgr5 (E) and Cyclin D1 (G) density (%) ± SEM in the animals described above. One experiment with n = 6 per group and 6 fields per animal. (C) Graphic bars represent the proportion (%) of hyperplasias and adenomas with low and high-grade dysplasia in the macroscopic small intestine lesions from the mice described above. One experiment with n = 12 per group. (F) RT-PCR analysis of *Lgr5*, *Bmi1, Cdkn1b, Cdkn1c, Myc, Ccnd2* relative expression in the Dll4-Fc, erlotinib and Dll4-Fc plus erlotinib-treated *Apc*$^{Min/+}$ small intestine tumors One experiment with n = 3 per group. **P*<0.05; ***P*<0.01.

Figure 33 - Dll4-Fc plus erlotinib have a cumulative negative effect on tumor proliferation and tumor stem cell maintenance in the *Apc*$^{Min/+}$ large intestine

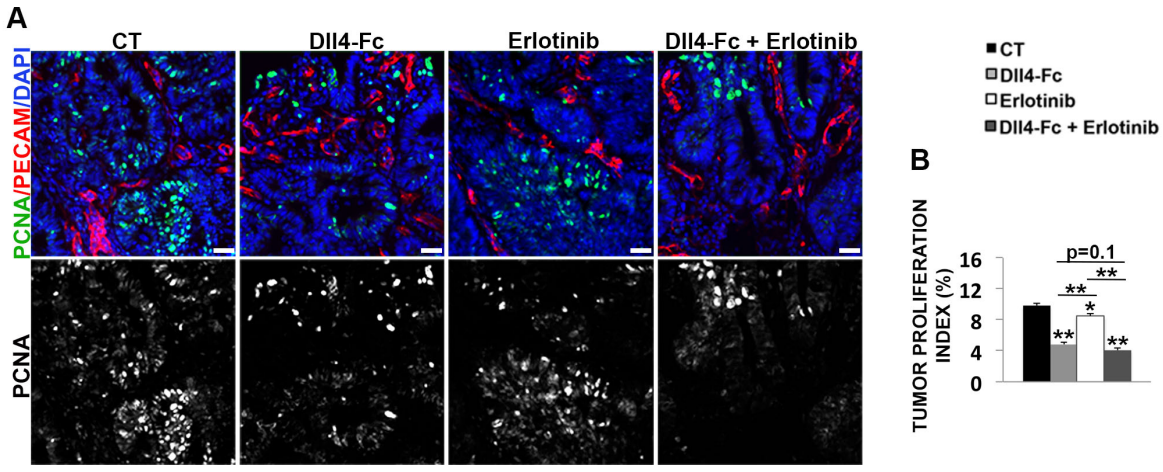

Figure 33 (continuation) - Dll4-Fc plus erlotinib have a cumulative negative effect on tumor proliferation and tumor stem cell maintenance in the *Apc*$^{Min/+}$ large intestine

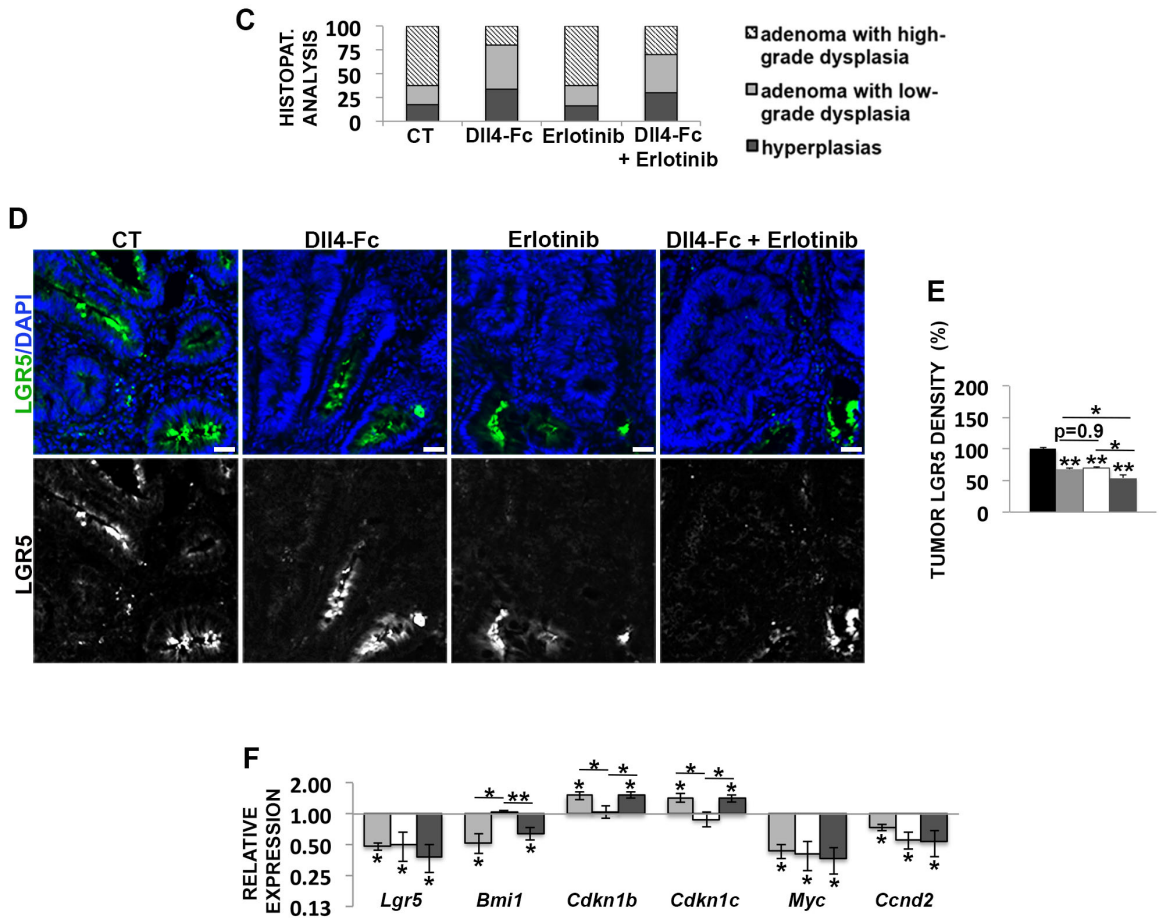

(A, D, H) Immunofluorescence stainings of the large intestine tumor cryosections (10µm) from Dll4-Fc, erlotinib and Dll4-Fc plus erlotinib-treated *Apc*$^{Min/+}$ mice *versus* their controls (CT). Scale bars = 100µm. The nuclei were counterstained with DAPI (in blue). Representative images of staining density for PCNA (in green) and PECAM-1 (in red) (A), for Lgr5 (in green) (D), and for Cyclin D1 (in green) (H). (B, E, G) Graphic bars represent the large intestine tumor proliferation index (%) ± SEM (B), and the relative tumor density (%) ± SEM of Lgr5 (E) and Cyclin D1 (G) in the animals described above (n=6 per group). (C) Graphic bars represent the proportion (%) of hyperplasias and adenomas with low and high-grade dysplasia obtained in the histopathological analysis (H&E) of the macroscopic large intestine lesions from the mice described above. One experiment with n = 12 per group. (F) RT-PCR analysis of *Lgr5*, *Bmi1, Cdkn1b, Cdkn1c, Myc, Ccnd2* relative expression in the Dll4-Fc, erlotinib and Dll4-Fc plus erlotinib-treated *Apc*$^{Min/+}$ large intestine tumors (n=3 per group). **P*<0.05; ***P*<0.01.

Figure 34 - Dll4-Fc and erlotinib therapies seem to be independent from associated β-catenin activation in the small and large intestine *Apc*$^{Min/+}$ tumors

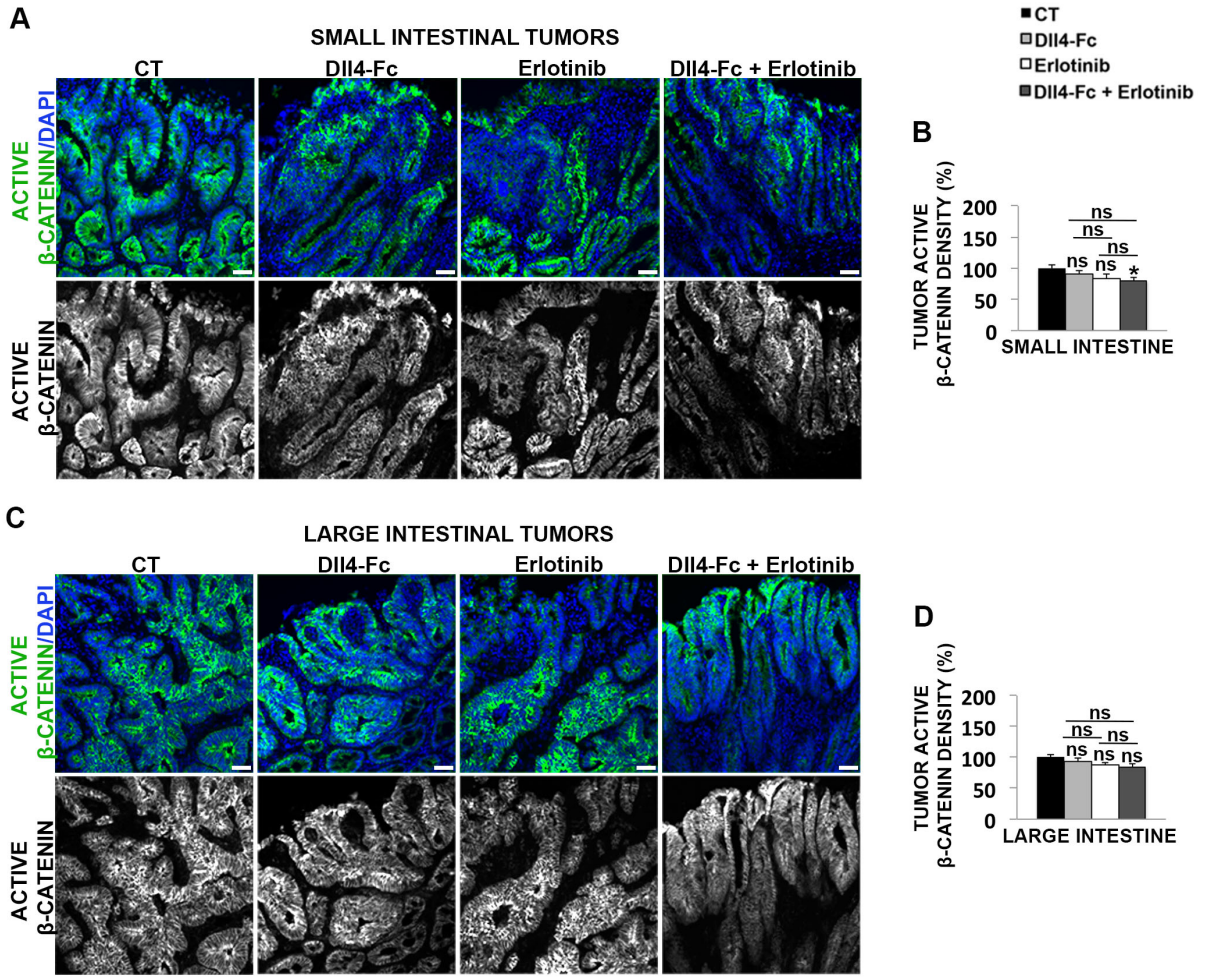

(A, C) Representative images of immunofluorescence staining density for non-phosphorylated (active) β-catenin (in green) of the small (A) and large (C) intestine tumor cryosections (10µm) from Dll4-Fc, erlotinib and Dll4-Fc plus erlotinib-treated *Apc*$^{Min/+}$ mice *versus* their controls (CT). Nuclei were counterstained by DAPI (in blue). Scale bars = 100µm. (B, D) Graphic bars represent the small (B) and large (D) intestine relative tumor non-phosphorylated (active) β-catenin density (%) ± SEM in the mice described above (n=6 per group). *P<0.05; ns, not significant.

4.3.4.6 Association of Dll4-Fc to erlotinib promotes unspecific intestinal lineage differentiation of proliferative tumor stem cells

Next we analysed the levels of differentiation of the tumor stem cells and if their differentiation was predominantly towards the secretory or the absorptive lineages. We started by measuring the density of the epithelial differentiation marker E-cadherin (Tsanou et al., 2008) in the *Apc*$^{Min/+}$ untreated and treated tumors. In the Dll4-Fc and in the combination treated tumors, we observed a moderate increase of the tumor epithelial differentiation both in the small and large intestine relatively to the controls, whereas the

erlotinib treated tumors presented no statistically significant differences (Fig. 35A-B and Fig. 36A-B).

To identify into which intestinal epithelial lineages the tumor stem cells were differentiating, we analysed the protein expression of lysozyme (produced by Paneth cells), the proportion of goblet cells in the tumor parenchyma, and the expression of several epithelial lineage markers.

Normally, Paneth cells are only present in the small intestine (Garabedian, Roberts, McNevin, & Gordon, 1997), but metaplasia of these cells was observed in the adenomas of the large intestine collected from all mouse groups. Relatively to the control group, the number of these cells was moderately increased in the Dll4-Fc treated small and large intestine tumors (Fig. 35C-D and Fig. 36C-D). In contrast, in the erlotinib-treated group, the number of Paneth cells in the tumors from these regions was just slightly reduced (Fig. 35C-D and Fig. 36C-D). In the small and large intestine tumors treated with the combination therapy, the proportion of these cells was increased as in those collected from the Dll4Fc treated animals (Fig. 35C-D and Fig. 36C-D).

On the other hand, in the Dll4-Fc treated animals both small and large intestine tumors presented a moderate increase in the proportion of the goblet cells (Fig. 35E-F and Fig. 36E-F). The erlotinib-treated group had a mild decrease in the proportion of these cells in both small and large intestine tumors and, in the tumors subjected to the combination therapy, the proportion of these cells was no different from that of the controls (Fig. 35E-F and Fig. 36E-F).

Then we measured the relative gene expression of *Akp3, Muc2, Lyz1* and *Neurog3* markers for the enterocyte, goblet, Paneth and neuroendocrine cell populations, respectively, and of the secretory-specific transcription factors *Atoh1* and *Klf4* (Katz et al., 2002; Yang et al., 2001). These were all significantly upregulated in the small and large intestine tumors subjected to the Dll4-Fc and combination treatments (Fig. 35G and Fig. 36G). In the erlotinib-treated small and large intestine tumors, the expression of genes from the different epithelial lineages was downregulated, especially of those related with the secretory fates (Fig. 35G and Fig. 36G). *Muc2* and *Atoh1* were the most upregulated genes in the Dll4-Fc treated tumors in the small and mostly in the large intestine (Fig. 35G and Fig. 36G). *Muc2* was the gene most downregulated in erlotinib treated small and large intestine tumors (Fig. 35G and Fig. 36G). However, in the small and large intestine tumors subjected to the combination therapy, all the analysed genes were similarly expressed (Fig. 35G and Fig. 36G).

Figure 35 - Dll4-Fc increases the epithelial differentiation, even when associated with erlotinib, and promotes the secretory cell fate in *Apc*$^{Min/+}$ small intestine tumors

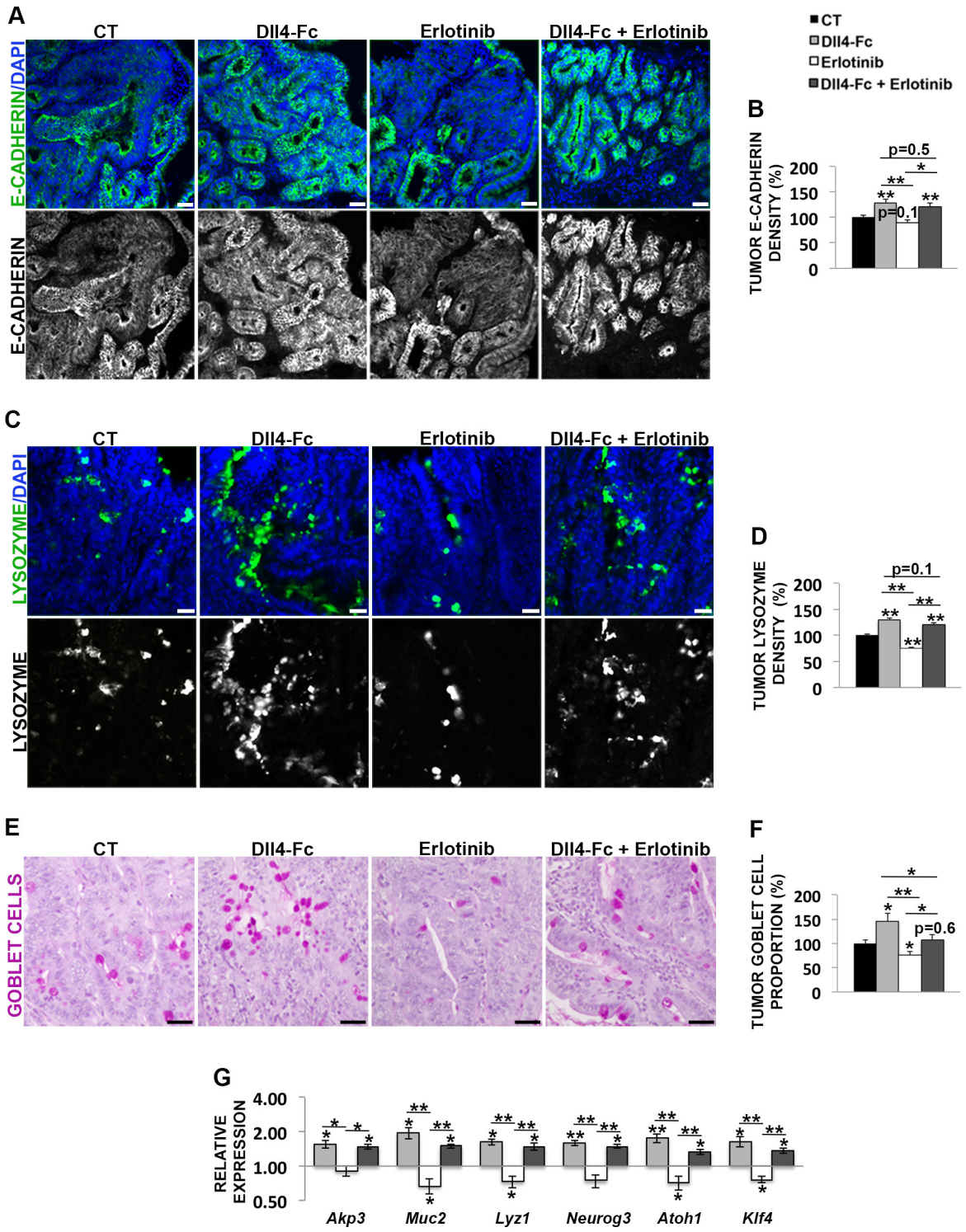

(A, C) Immunofluorescence stainings of small intestine tumor cryosections (10µm) from Dll4-Fc, erlotinib and Dll4-Fc plus erlotinib-treated *Apc*$^{Min/+}$ mice *versus* their controls (CT). Scale bars = 100µm. The nuclei were counterstained with DAPI (in blue). Representative images of staining density for E-cadherin (in green) (A), and for lysozyme (in green) (C). (B, D) Graphic bars represent the relative density (%) ± SEM of E-cadherin (B) and lysozyme (D) in the small intestine tumors of the animals described above (n=6 per group). (E) PAS staining of paraffin-embedded small intestine tumor sections (4µm) from the animals mentioned above. Scale bars = 100µm. (F) Graphic bars

represent the relative proportion of goblet cells (%) ± SEM in the small intestine tumor epithelium of the same animals (n=6 per group). (G) RT-PCR analysis of *Akp3, Muc2, Lyz, Neurog3, Atoh1, Klf4* relative expression in the Dll4-Fc, erlotinib and Dll4-Fc plus erlotinib-treated $Apc^{Min/+}$ small intestine tumors (n=3 per group). **P*<0.05; ***P*<0.01.

Figure 36 - Dll4-Fc increases the epithelial differentiation, even when associated with erlotinib, and promotes the secretory cell fate in $Apc^{Min/+}$ large intestine tumors

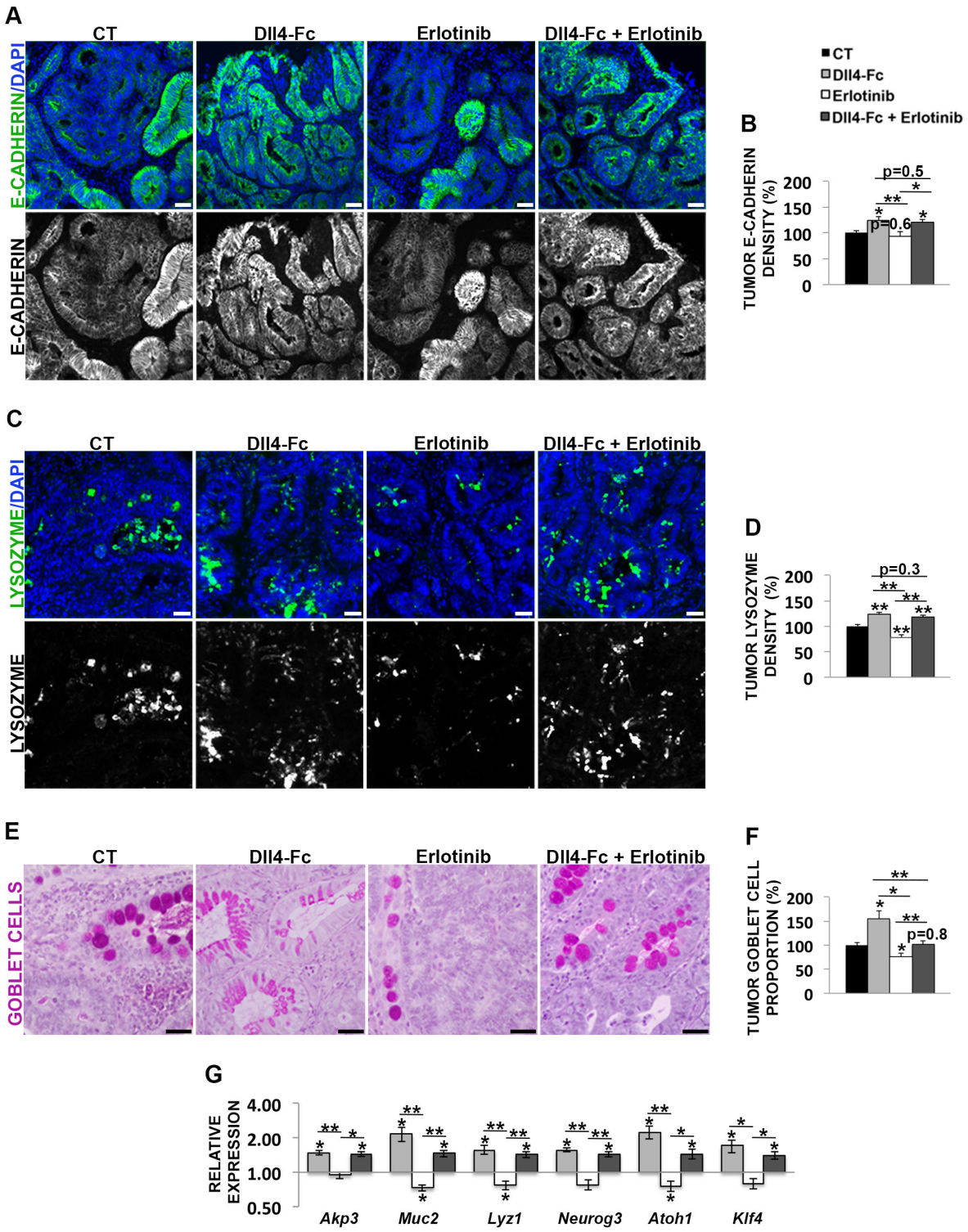

(A, C) Immunofluorescence stainings of large intestine tumor cryosections (10µm) from Dll4-Fc, erlotinib and Dll4-Fc plus erlotinib-treated *Apc*$^{Min/+}$ mice *versus* their controls. Scale bars = 100µm. The nuclei were counterstained with DAPI (in blue). Representative images of staining density for E-cadherin (in green) (A), and for lysozyme (in green) (C). (B, D) Graphic bars represent the relative density (%) ± SEM of E-cadherin (B) and lysozyme (D) in the large intestine tumors of the animals described above (n=6 per group). (E) PAS staining of paraffin-embedded large intestine tumor sections (4µm) from the animals mentioned above. Scale bars = 100µm. (F) Graphic bars represent the relative proportion of goblet cells (%) ± SEM in the large intestine tumor epithelium of the same animals (n=6 per group). (G) RT-PCR analysis of *Akp3, Muc2, Lyz, Neurog3, Atoh1, Klf4* relative expression in the Dll4-Fc, erlotinib and Dll4-Fc plus erlotinib-treated *Apc*$^{Min/+}$ large intestine tumors (n=3 per group). **P*<0.05; ***P*<0.01.

4.3.5 Discussion

Blockade of a single target or pathway promotes limited benefit for cancer patients and therefore new combination treatment strategies are being extensively explored (Yap, 2015). Notch signaling has been studied as a novel molecular target therapy approach to treat CRC (Qiao & Wong, 2009). Anti-Dll4/Notch therapy seems to reduce tumor growth and tumor stem cell frequency in xenograft models of CRC (Hoey et al., 2009) even when associated to KRAS mutations, which confer resistance to anti-EGFR therapy (M. Fischer et al., 2010). In lung, breast, skin and glial cancers, Notch and EGFR pathways seem to crosstalk (Baker et al., 2014; H. Yamaguchi et al., 2014). This may also occur in CRC as both pathways are overexpressed in this type of cancer (Qiao & Wong, 2009). Hence a combination strategy targeting both Dll4/Notch and EGFR pathways may be beneficial. However, as anti-Dll4 therapy promotes the establishment of a non-productive vasculature with poor perfusion (Djokovic et al., 2010; Noguera-Troise et al., 2006; Ridgway et al., 2006; Scehnet et al., 2007), this may impair the delivery to the tumor site and consequently the efficacy of anti-EGFR and other anti-cancer drugs. Therefore, in this work we tried to elucidate how Dll4-Fc affects the *Apc*$^{Min/+}$ intestinal tumor development and if Dll4-Fc could be beneficially associated to anti-Egfr therapy in CRC.

Dll4-Fc therapy, alone and in the combinatory trial, delayed the tumor growth by promoting immature and dysfunctional angiogenesis. Dll4-Fc treatment led to reduced tumor vascular perfusion, which could impair the delivery of erlotinib and other anti-cancer drugs to the tumors. However, it also increased vascular extravasation in the tumor, which could promote the exit of these drugs from the newly formed vessels and their accumulation in the tumoral stroma. In our experiment this paradoxically negative effect on the tumor vasculature functionality caused by Dll4-Fc treatment probably did not affect the delivery of erlotinib to the tumors, as erlotinib therapy administered in combination with Dll4-Fc indeed blocked the activation of Egfr pathway and inhibited tumorigenesis. Therefore, anti-Dll4 therapy may not improve the delivery of anti-cancer drugs to the tumors as the anti-VEGF therapies seem to

accomplish by “normalizing” the tumor vasculature (Jain, 2005), but it appears that it does not impair it either. Importantly, in this setting, an anti-Dll4 approach may be more beneficial than anti-VEGF targeting, as Dll4-Fc delayed the *Apc*$^{Min/+}$ tumor growth just as much an anti-VEGF therapy (Alferez et al., 2008), but in addition reduced the establishment of these tumors.

Interestingly, contrary to Dll4-Fc, anti-Egfr therapy did not affect the tumor volume and had no significant effect on tumor apoptosis, differentiation and neoplastic transformation. This lack of anti-Egfr effect on the tumor volume was previously shown by Roberts *et al*., who believe that Egfr activity is required only in the formation of microadenomas and may then be necessary only for later stages of tumor progression (Roberts et al., 2002). This could explain why we did not find increased epithelial differentiation and delayed neoplastic transformation in the erlotinib-treated pre-malignant lesions respectively to the controls. The observed inefficacy of erlotinib treatment in reducing tumor volume may be associated to the lack of effect on apoptosis, which may be at least partially related to its angiogenic phenotype. Erlotinib therapy inhibited tumor angiogenesis, as previously described in pancreatic cancer (Mendelsohn & Baselga, 2003), by downregulating *Vegfa* and *c* expression and by upregulating the expression of *Vegfr1*, a decoy receptor that sequesters VEGFA (Hiratsuka, Minowa, Kuno, Noda, & Shibuya, 1998). However, the tumor vessels were more mature and functional, which led to reduced tumor hypoxia and therefore allowed tumor growth. There are probably several mechanisms implicated in this erlotinib-associated phenotype. It has been demonstrated that erlotinib regulates the Vegf/Vegfr pathway through Akt-mediated production of endothelial nitric oxide synthase (Fulton et al., 1999) and may directly inhibit HIF-1α expression (Peng et al., 2006), therefore regulating VEGF expression (Y. Liu, Cox, Morita, & Kourembanas, 1995). In addition, this may also be associated to the observed increase of Notch1 activation in erlotinib-treated tumors, as Notch signaling has been extensively shown to be a critical regulator of tumor angiogenesis (Dufraine et al., 2008). The observed Notch1 upregulation may also be directly associated with the lack of apoptotic effect in the tumors (Qiao & Wong, 2009). This activation of Notch1 signaling after Egfr inhibition was previously observed in breast cancer, while the EGFR signaling-mediated inhibition of *Notch1* gene transcription was shown in skin cancer (H. Yamaguchi et al., 2014). Therefore, in this setting, erlotinib may activate Notch signaling and this could be, at least in part, responsible for the observed lack of efficacy on tumor growth of erlotinib therapy. Additionally, this could be Dll4-mediated as a previous work indicated that Dll4, when expressed in the tumor cells, activates Notch in the endothelium and negatively regulates tumor angiogenesis but it can promote tumor growth by improving the vascular function and by reducing hypoxia and apoptosis in the tumors (J. L. Li et al., 2007), as observed in the erlotinib-treated tumors.

Interestingly, Dll4-Fc had some inhibitory effect on the Egfr pathway, downregulating phosphorylated Egfr, Erk and mainly Akt, and in association with the anti-Egfr therapy it had a synergistic effect in the reduction of the *Apc*$^{Min/+}$ tumor multiplicity in the small intestine. Therefore, this suggests the existence of a crosstalk between the Notch and Egfr pathways to induce intestinal tumorigenesis. This inhibitory effect on adenoma formation by anti-Egfr therapy had been previously reported (Roberts et al., 2002), but not by an anti-Dll4 approach. However a previous work showed that Notch1 activation may be needed to trigger tumorigenesis in the *Apc* mutated intestine (Fre et al., 2009) and we observed that Dll4-Fc therapy inhibited Notch1 activation in the *Apc*$^{Min/+}$ small and large intestine tumors.

Anti-Dll4 and anti-Egfr therapies had a cumulative effect downregulating factors related to proliferation and maintenance of Lgr5 positive tumor stem cells, which seemed mostly unrelated to β-catenin activation. Only Dll4-Fc treatment led to an increase of the CDK inhibitors 1B and 1C, as observed upon Notch inactivation in the normal gut (Riccio et al., 2008), and decreased Bmi1 expression. These effects could explain why Dll4-Fc had a more pronounced effect reducing the tumor proliferation than erlotinib. Additionally, this can also be related to the Dll4-Fc-derived increase of intestinal differentiation in the tumors, as *Cdkn1b* seems to be important in this process (Deschenes, Vezina, Beaulieu, & Rivard, 2001).

Dll4-Fc promoted the intestinal differentiation towards the secretory lineages, but not as drastically as previously tested pan-Notch inhibitors (van Es, van Gijn, et al., 2005). It seems that blockade of both Notch1 and Notch2 is necessary to promote a complete conversion of intestinal stem cells to differentiated goblet cells (Riccio et al., 2008). Therefore, the less accentuated deviation towards the secretory lineages in Dll4-Fc treated tumors may be explained by the gene expression analysis we carried out, which indicated that Dll4 may signal mainly through Notch1 and Notch4, rather than Notch2, in the intestinal tumors. In addition, Dll1, whose expression is increased in Dll4-Fc treated tumors, may also be implicated in this process by attenuating the secretory differentiation as previously described in the normal gut (Pellegrinet et al., 2011). Nevertheless, when we combined Dll4-Fc with erlotinib the increase of differentiation was not deviated into any specific lineage. This was probably due to the observed smaller increase of tumor Atoh1 and Klf4 expression in the combinatory trial, as erlotinib seemed to have a negative effect on Atoh1 expression, which may be related to Notch1 activation.

Thus, in this work we have shown that in the *Apc*$^{Min/+}$ small and large intestine Dll4-Fc therapy inhibited tumorigenesis and tumor growth by affecting proliferation, stem cell maintenance, differentiation and angiogenesis.

When associated to erlotinib it had a cumulative effect in inhibiting tumor multiplicity, showing that the decreased functionality of the tumor vasculature caused by the anti-Dll4 therapy did not impair the appropriate delivery of erlotinib to the tumors. However, further studies are

needed to understand if the induction of Notch activation is responsible for the inefficacy of anti-Egfr therapy on tumor volume and transformation in this setting. Nevertheless, Dll4-Fc therapy is able to delay tumor growth and transformation, to inhibit tumor establishment and does not affect the delivery of erlotinib to the tumor, promoting instead its anti-cancer effect. Therefore, our results indicate that anti-DLL4 therapy can be beneficially associated with anti-EGFR treatment and possibly with other conventional therapies used to treat CRC.

4.4 Chapter IV - Delta-like 4/Notch signaling blockade inhibits the development of chronic colitis-associated colorectal cancer in a mouse model

Badenes, M., Trindade, A., Pissarra, H., Carinhas, J., Liu, R., Krasperonov, V., Gill, P.S, Costa, L., Duarte, A.

4.4.1 Abstract

Colorectal cancer (CRC), one of the most frequent cancers, can develop as a complication of inflammatory bowel diseases (IBD). Notch signaling plays a central role in intestinal homeostasis and in CRC development. Our objective was to analyze the Notch pathway expression pattern and the effect of Dll4/Notch inhibition in chronic colitis and in colitis-associated cancer (CAC). For that we analyzed the protein expression of most Notch pathway members and assessed the effect of Dll4 genetical (*Dll4*$^{+/-}$) and pharmacological (Dll4-Fc) blockade in the azoxymethane plus dextran sodium sulphate (AOM+DSS) CAC mouse model. We found high levels of expression of all Notch members in the inflamed large intestine and in CAC. Dll4 and Notch1 expression was more pronounced in the tumor than in the inflamed intestinal epithelium. The inhibition of Dll4 led to a significant reduction in the average number and volume of tumors by several mechanisms. Specifically, Dll4 blockade promoted apoptosis, dysfunctional tumoral angiogenesis and inhibited tumor cell proliferation. Additionally, it decreased the number of Leucine-rich G-protein coupled Receptor 5 (Lgr5) positive tumor stem cells and promoted Paneth and goblet cell differentiation. Furthermore, the observed inhibition of tumorigenesis was associated with reduced colitis and tumor inflammation by decreasing the number of immune cells (macrophages, dendritic cells, neutrophils and helper and cytotoxic T cells) and the expression of important inflammatory mediators, such as *iNos*, *Cox-2*, *Tnf-α*, *Il-6, Il-17a, Ifn-γ* and *Il-4*. Dll4 inhibition also led to a decrease in the expression of the CAC promoter *Nfkb2*, to the upregulation of the CAC inhibitor *Tgf-β,* to an increase in the number of regulatory T cells and to the abrogation of the proinflammatory M1 macrophage polarization in the tumors. Therefore, Dll4-Fc is likely to be beneficial in the treatment of CAC by deregulating tumor angiogenesis, proliferation, apoptosis, inflammation and stem cell maintenance.

Keywords: Notch expression; *Dll4*$^{+/-}$; Dll4-Fc; CAC; mouse model

4.4.2 Introduction

Colorectal cancer (CRC) is one of the leading causes of cancer death (Siegel, Desantis, & Jemal, 2014). Patients with inflammatory bowel diseases (IBD; Crohn's disease or ulcerative colitis) have high risk of developing CRC (Mattar, Lough, Pishvaian, & Charabaty, 2011). High levels of the proinflammatory cytokines IL-6 and TNF-α, inducible inflammatory enzymes (COX2, iNOS) and NF-$_K$B activation contribute to the development of CAC (Foersch & Neurath, 2014). Additionally, the cytokines IL-4 and IL-17A seem to promote tumor growth, while IFN-γ is critical for the activation of cytotoxic cells and antitumor activity (Rizzo et al., 2011). In general, cells of the innate and adaptive immune system seem to act as pro-tumorigenic in chronic colitis-associated cancer (CAC) (M. J. N. Waldner, M. F., 2015). However, regulatory T cells, which have been shown to attenuate tumor immunosurveillance, act as potent suppressors of chronic inflammation and thus can have protective effects in CAC (Blat et al., 2014; Pastille, Pohlmann, Wirsdorfer, Reib, & Flohe, 2015; M. J. Waldner & Neurath, 2009). In addition, tumor-associated macrophages can exert proinflammatory (M1 polarization state) or anti-inflammatory (M2 polarization state) effects (Wang et al., 2015). M1 macrophages are abundant at sites of chronic inflammation and in early tumors, but tend to switch to a M2-phenotype during tumor progression (Mantovani, Sozzani, Locati, Allavena, & Sica, 2002).

Molecular targeting of tumor-specific pathways is increasingly used in the treatment of CRC. Angiogenesis was identified as an attractive target (Folkman, 1971), leading to the development of anti-angiogenic agents such as the anti-VEGF monoclonal antibody bevacizumab, currently used in patients with metastatic CRC (Ranieri et al., 2006). However, side effects and development of tumor resistance have been reported for this type of drug (Vasudev & Reynolds, 2014). Therefore, there is a need for improved angiogenesis targeting therapies, which may be useful in CRC treatment.

Numerous studies revealed that Dll4/Notch signaling is involved in vascular development for arterial cell-fate determination and in the inhibition of both physiological and pathological angiogenesis (M. Yan & Plowman, 2007). Dll4 targeting agents like the Dll4-Fc fusion protein (Ridgway et al., 2006; Scehnet et al., 2007), or anti-Dll4 antibodies (Noguera-Troise et al., 2006; Ridgway et al., 2006) caused a pro-angiogenic effect in tumors grafted in mice that paradoxically leads to decreased tumor growth due to the formation of immature and dysfunctional vessels.

Notch signaling is also essential in maintaining the intestinal development and homeostasis (Vooijs et al., 2011). In the normal gut, Dll1 and Dll4-mediated Notch signaling are required for intestinal stem cell proliferation and maintenance and in lineage specification of absorptive cells (Pellegrinet et al., 2011). In addition, epithelial Notch1-mediated signaling regulates the intestinal mucosal immune responses by crosstalking with NF-$_K$B and MAPK pathways and therefore eliciting T-cell responses (Mathern et al., 2014). In CRC, it has been

shown that Dll4/Notch pathway promotes the tumor growth and maintains the cancer stem cell population (M. Fischer et al., 2010; Hoey et al., 2009). However, a putative role for Dll4 in the development of CAC has not yet been addressed. This led to used a well-established chemically induced CAC mouse model (Clemens Neufert et al., 2007) to characterize Dll4 and other Notch pathway members expression in CAC and to test if Dll4/Notch signaling could constitute a target for CAC therapy.

4.4.3 Methods

4.4.3.1 Chemical induction of CAC

A chemically induced model for chronic colitis-associated CRC was used (C. Neufert, C. Becker, & M. F. Neurath, 2007). At 8 weeks of age, CD-1 male mice were injected with the carcinogen azoxymethane (AOM) (Sigma-Aldrich, St. Luis, MO, USA) (7,5 mg/Kg, i.p.). One week later, 3% proinflammatory dextran sodium sulphate (DSS) (MP Biomedicals, Santa Ana, CA, USA) was added to their drinking water for one week, followed by two weeks of rest. This cycle was repeated 4 times.

4.4.3.2 Evaluation of anti-tumor efficacy of Dll4 blockade

All animal-involving procedures in this work were approved by the Faculty of Veterinary Medicine of Lisbon Ethics and Animal Welfare Committee (Approval ID: PTDC/CVT/71604/2006).

Dll4$^{+/-}$ (CD-1 background) mice (Duarte et al., 2004) were compared with control WT mice.

In the therapeutical trial wild type CD-1 mice were administered with either PBS or Dll4-Fc (Scehnet et al., 2007) (5 mg/Kg/day, i.p., 3x/wk). The treatment started 10 weeks after AOM+DSS administration (when the tumors start to appear macroscopically) and continued for 4 weeks.

In the two trials 12 animals per group were used.

4.4.3.3 Macroscopic analysis of the large intestine

At 14 weeks after AOM+DSS administration the animals were humanely sacrificed by cervical dislocation and the colon and rectum were excised, flushed and opened longitudinally. The tumors were counted and measured with a calliper under the dissection microscope. Tumor volume was calculated assuming a spherical shape. The volumes of all tumors from each mouse were added to give the overall tumor burden per animal. The inflamed intestine, intestinal tumors and livers were collected.

4.4.3.4 Histopathological analysis

The collected samples were fixed in 10% formalin for 48h, dehydrated in alcohol, cleared in xylene, embedded in paraffin, sectioned in 4µm-thick sections and stained with hematoxylin

(Fluka AG Buchs SG Switzerland) and eosin Y (Sigma, St. Louis, MO) for histopathological analysis. The lesions observed on the H&E large intestine sections were classified as hyperplasias, when only an increase of the number of cells was observed, or as adenomas with low and high-grade dysplasia based on the alterations of the shape of the nucleus, the nucleus to cytoplasm ratio, cell polarity, chromatin pattern, and changes in gland architecture.

The number of neutrophils was counted in the H&E stained tumor sections under 200x magnification.

Colitis lesions were recorded and scored according to the morphological criteria described by Cooper et al. (Cooper, Murthy, Shah, & Sedergran, 1993).

Periodic Acid-Schiff (PAS) staining (Sigma, St. Louis, MO) was used to mark the intestinal goblet cells. These cells were counted in the intestine PAS stained sections using a 400x magnification.

4.4.3.5 Immunohistochemical analysis

After dewaxing and rehydration, endogenous peroxidase activity was quenched (15 minutes, 1% H_2O_2) and antigen retrieval was performed (20 minutes at 95°C in 10mmol/L sodium citrate buffer, pH 6). The primary antibodies to mark Dll1 (ab76655), Dll4 (ab7280), Notch1 (ab27526), Notch2 (ab8926), Notch3 (ab23426), Hes1 (ab71559) and 5 (ab25374) (Abcam, Cambridge, UK) and Jagged1 (sc-8303), Jagged2 (sc-8157), Dll3 (sc-67270) and Notch4 (sc-5594) (Santa Cruz Biothecnology, California, USA) were diluted in PBS containing 2% bovine serum albumin, and incubated overnight at 4ºC with the tissue sections. These antibodies have been previously validated (Murta et al., 2013; Murta et al., 2014; Murta et al., 2015). The following morning, the tissue sections were incubated with goat anti-rabbit (12-348, Merck Millipore, Massachusetts, USA) or rabbit anti-goat (sc-2768, Santa Cruz Biothechnology, California, USA) horseradish peroxidase–labeled secondary antibody and the staining was revealed with ImmPACT DAB Peroxidase Substrate (100µl, Vector Laboratories, Burlingame, USA). The sections were examined under an Olympus BX51 microscope with a 40x/0.75 objective (UPlanfL). The images were captured with an Olympus DP21 camera.

4.4.3.6 Immunofluorescence analysis

Normal, inflamed intestine and intestinal tumors were fixed in 4% (w/v) paraformaldehyde in PBS solution at 4ºC for 1h, cryoprotected in 15% (w/v) sucrose in PBS solution, embedded in 7,5% (w/v) gelatin in PBS solution, snap frozen in liquid nitrogen and cryosectioned in 10 and 20µm-thick sections. The following primary antibodies were used: anti-PECAM-1 (557355), anti-CD4 (550280), anti-CD8 (550797), anti-CD11c (BD Pharmingen, San Jose, CA, USA), anti-α-SMA (ab5694), anti-PCNA (ab18197), anti-Lgr5 (ab75732), anti-HIF1α (ab85866),

anti-FOXP3 (ab54501), anti-IL-4 (ab11524), anti-IL-17A (ab79056), anti-iNOS (ab15323), anti-ArgI (ab91279), anti-CD19 (ab25232) (Abcam, Cambridge, UK), anti-IFN-γ (507801) (Biolegend, San Diego, CA, USA), anti-lysozyme (A009902-2), anti-CD3 (A0452) (Dako, Glostrup, Denmark), anti-F4/80 (MCA497, AbD Serotec, Kidlington, UK) and anti-Dll4 (AF1389, R&D Systems, Minneapolis, USA). Species-specific secondary antibodies conjugated with Alexa Fluor 488 and 594 (Invitrogen, Carlsbad, CA) were used to reveal primary antibody binding. Tissue sections were incubated with primary antibody overnight at 4°C and with secondary antibody for 1 hour at room temperature. Nuclei were counterstained with 4´, 6-diamidino-2-phenylindole dihydrochloride hydrate (DAPI; Molecular Probes, Eugene, OR, USA).

Under the effect of 2-2-2 tribromoethanol anaesthesia, biotin-conjugated lectin from *Lycopersicon esculentum* (100 µg/100µl of PBS) or 1% Evans' Blue solution (Sigma, St. Luis, MO, US) were administered in the caudal vein to mark vessel perfusion and extravasation, respectively. Both solutions were allowed to circulate for 5 minutes before the vasculature was transcardially perfused with 4% PFA for 3 minutes.

Apoptosis was measured using the TUNEL assay (Roche, Mannheim, Germany).

Fluorescent immunostained sections were examined under a Leica DMRA2 fluorescence microscope with a Leica HC PL Fluotar 10 and 20X/0.5 NA dry objective, captured using Photometrics CoolSNAP HQ, (Photometrics, Friedland, Denmark), and processed with Metamorph 4.6-5 (Molecular Devices, Sunnyvale, CA, USA). Morphometric analyses were performed using the NIH ImageJ 1.37v program. After transforming the RGB images into binary files, the percentage of white pixels per field was defined as a positive signal.

For co-localization and cell-counting analysis a Zeiss LSM 710 confocal microscope with a 40x/1.3 NA oil objective (EC Plan-Neofluar) was used, as well as the Zen software 2009 Light Edition (Carl Zeiss, Oberkochen, Germany), and a previously described software written in MATLAB (Mathworks, Natick, MA, USA) (Fernandes et al., 2014).

4.4.3.7 Quantitative transcriptional analysis

Intestine tumor samples were snap frozen in liquid nitrogen until RNA extraction (Qiagen RNeasy). Using the SuperScript® III First-Strand Synthesis SuperMix for qRT-PCR (Invitrogen, Carlsbad, CA, USA), first-strand cDNA was synthesized. Real-time PCR analysis was performed using specific primers and *β*-actin as endogenous control.

4.4.3.8 Statistical analysis

To compare measurements between control and test groups, the Mann-Whitney-Wilcoxon test was performed using the Statistical Package for the Social Sciences v15.0 (Chicago, IL). Results are presented as relative average ± SEM. *P*-values <0.05 and <0.01 were considered significant (*) and highly significant (**), respectively.

4.4.4 Results

4.4.4.1 Notch pathway members are strongly expressed in chronic colitis and CAC

Notch pathway members are expressed in the normal gut (Sander & Powell, 2004; Schroder & Gossler, 2002). Previous reports showed that in acute colitis Dll4, Notch1, NICD and Hes1 presence increases in the colonic crypts (Okamoto et al., 2009; Shimizu et al., 2014). However, there is yet no information about the expression of Notch pathway members in chronic colitis and in CAC. Therefore, we assessed the protein expression of all Notch pathway ligands and receptors and of two of its effectors, Hes1 and Hes5, in these settings.

In the intestine of mice affected by chronic colitis, we observed the presence of Dll1 in goblet cells (Fig. 37A), Dll3 was absent in the colorectal epithelium (Fig. 37A) and Dll4 was present in both absorptive and goblet cells (Fig. 37A). Jagged1 was observed diffusely through all the crypts, but mainly in their upper region (Fig. 37A) and Jagged2 was found at the bottom of the crypts, in the proliferative zone (Fig. 37A). Relatively to the receptors, Notch1 was present only in a few cells at the bottom of the crypts (Fig. 37C), while Notch2, 3 and 4 were observed at the top of the crypts (Fig. 37C). Notch2 and 3 were present in some colonocytes and Notch4 in differentiated goblet cells (Fig. 37C). The Notch effectors Hes1 and Hes5 were expressed mainly at the bottom of the crypts (Fig. 37E) All the Notch pathway members analyzed were also present in the *lamina propria*, mainly Dll1, 3 and 4, Jagged1 and Hes1 (Fig. 37A, 37C and 37E).

We compared the expression pattern of these Notch pathway components in chronic colitis with that obtained in the normal gut (unpublished data). We found that, relatively to the normal large intestine, Jagged1, Jagged2, Notch1 and Notch4 had a similar expression pattern. However, Dll1 was more expressed in the *lamina propria* and less expressed in the epithelium (goblet cells). Dll3 lost its expression in the epithelium. Dll4 was observed also in colonocytes and was more expressed in the *lamina propria*. Notch2 was less expressed in the bottom of the crypts and appeared in some colonocytes in the top of the crypts. Notch3 also appeared in the upper part of the crypts in some colonocytes. Hes1 was more expressed in the bottom of the crypts and *lamina propria* and less expressed in the upper part. Hes5 was less expressed through all the epithelium and *lamina propria*, mainly in the upper portion.

In CAC, the expression pattern of Dll1, Dll3, Jagged1, Notch2 and Notch4 was similar to that observed in chronic colitis (Fig. 37A-D). However, the expression of Dll4, Notch1 and Notch3 seemed increased in CAC, particularly that of Notch3 in the tumor stroma (Fig. 37A-D). Conversely, we observed decreased expression of Jagged2 in the tumor epithelium (Fig. 37A-B), and of Hes1 and 5 in the tumor stroma (Fig. 37E-F).

4.4.4.2 Dll4 blockade reduces the formation and size of colitis-driven CR tumors

Our expression analysis revealed that Dll4 and Notch1 are the components of Notch pathway that are more upregulated in CAC tumor cells relatively to the inflamed large intestine epithelial cells. In both settings Dll4 expression was found in the epithelium (Fig. 37A-B), including in a few metaplastic Paneth cells (Fig. 37I-J). Dll4 was also present in the vasculature (Fig. 37G-H), in macrophages (Fig. 37K-L) and in some dendritic cells (Fig. 37M-N) mainly in the inflamed intestine, as determined by co-staining for PECAM-1, F4/80, and CD11c, respectively. Given the increased expression of Dll4 in the tumors, we decided to evaluate the influence of genetic and pharmacologic Dll4/Notch pathway blockade in CAC. For that we compared Dll4 heterozygotes (*Dll4*$^{+/-}$) and Dll4-Fc treated mice with WT and PBS treated controls. At the endpoint, compared with the controls, the *Dll4*$^{+/-}$ animals showed a reduction of 86%, 49% and 93% in the average number, volume and burden of tumors in the intestine, respectively (Fig. 38A-D). The Dll4-Fc treated animals showed a reduction of 76%, 62% and 92% in the average number, volume, and burden of tumors, respectively (Fig. 38A-D).

To confirm the blockade of Dll4, we used RT-PCR to measure the transcript levels of *Hey2* and *Hes1*, two important downstream effectors of the Dll4/Notch pathway. Compared to WT controls, both were significantly downregulated in the *Dll4*$^{+/-}$ tumors by almost 50% and 40% respectively and in the Dll4-Fc treated tumors both were decreased by nearly 60% (Fig. 39).

Histopathological analysis revealed mainly hyperplasias, defined as benign lesions with reduced malignancy potential (Winawer et al., 1997) and tubulovillous adenomas with low and high-grade dysplasia (Fig. 38E). While in the controls, 49.6% and 17.4% of the lesions were adenomas with high- and low-grade dysplasia, respectively, and 33% were hyperplasias, in the *Dll4*$^{+/-}$ group the severity of the lesions was markedly reduced. In these animals only 29.9% of the tumors were adenomas with high-grade dysplasia, 38.1 % were adenomas with low-grade dysplasia and 32% were mere hyperplasias. In the Dll4-Fc treated group the severity of the lesions was even further reduced, with only 8.2% of the adenomas showing high-grade dysplasia, 34.8% low-grade dysplasia, and the remaining 57%, corresponding to hyperplasias (Fig. 38F).

Histopathological analysis of the livers revealed no evidence of induced lesions in either *Dll4*$^{+/-}$ animals or Dll4-Fc treated groups (data not shown).

Figure 37 - Notch pathway expression pattern in chronically inflamed CR and in CAC

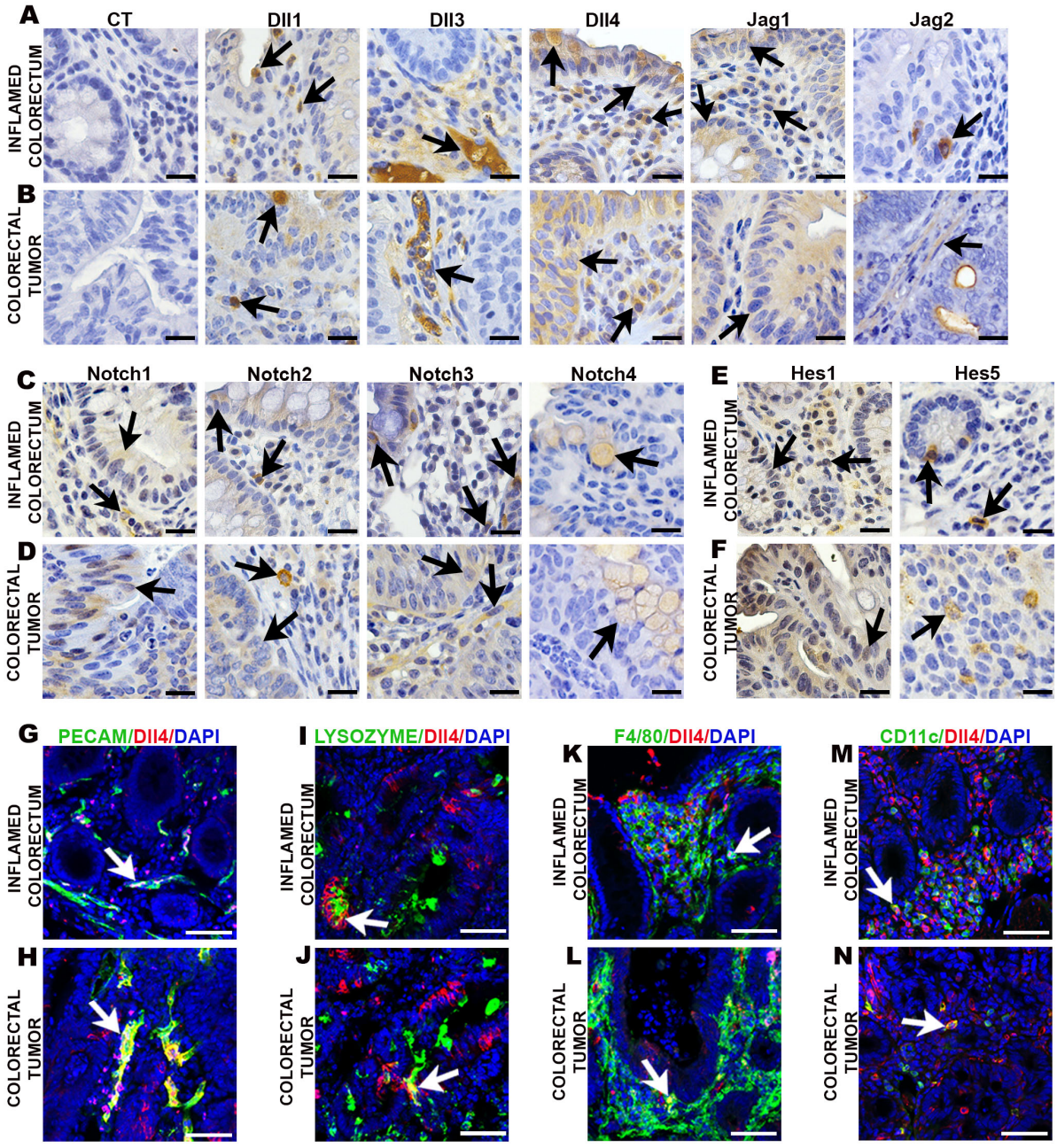

(A-F) Immunohistochemical analysis of Dll1, 3 and 4, Jagged1 and 2 (A-B), Notch1-4 (C-D), and Hes1 and 5 (E-F) expression (indicated by arrows) in paraffin-embedded 4µm sections of WT mice inflamed and tumor large intestine. Scale bar = 20µm. One experiment with n = 2 and 2 fields per animal. Control staining was performed with the specific species IgG. (G-N) Immunofluorescence co-stainings of the WT inflamed (G, I, K, M) and tumor (H, J, L, N) large intestine (10µm cryosections): Dll4 (G-N) in red, and PECAM-1 (G-H), lysozyme (I-J), F4/80 (K-L), and CD11c (M-N) in green. The nuclei were conterstained with DAPI (blue). Scale bar = 50µm. One experiment with n = 2 and 2 fields per animal.

Figure 38 - *Dll4*$^{+/-}$ and Dll4-Fc treated mice display a marked reduction in the number and size of colitis-driven CR tumors

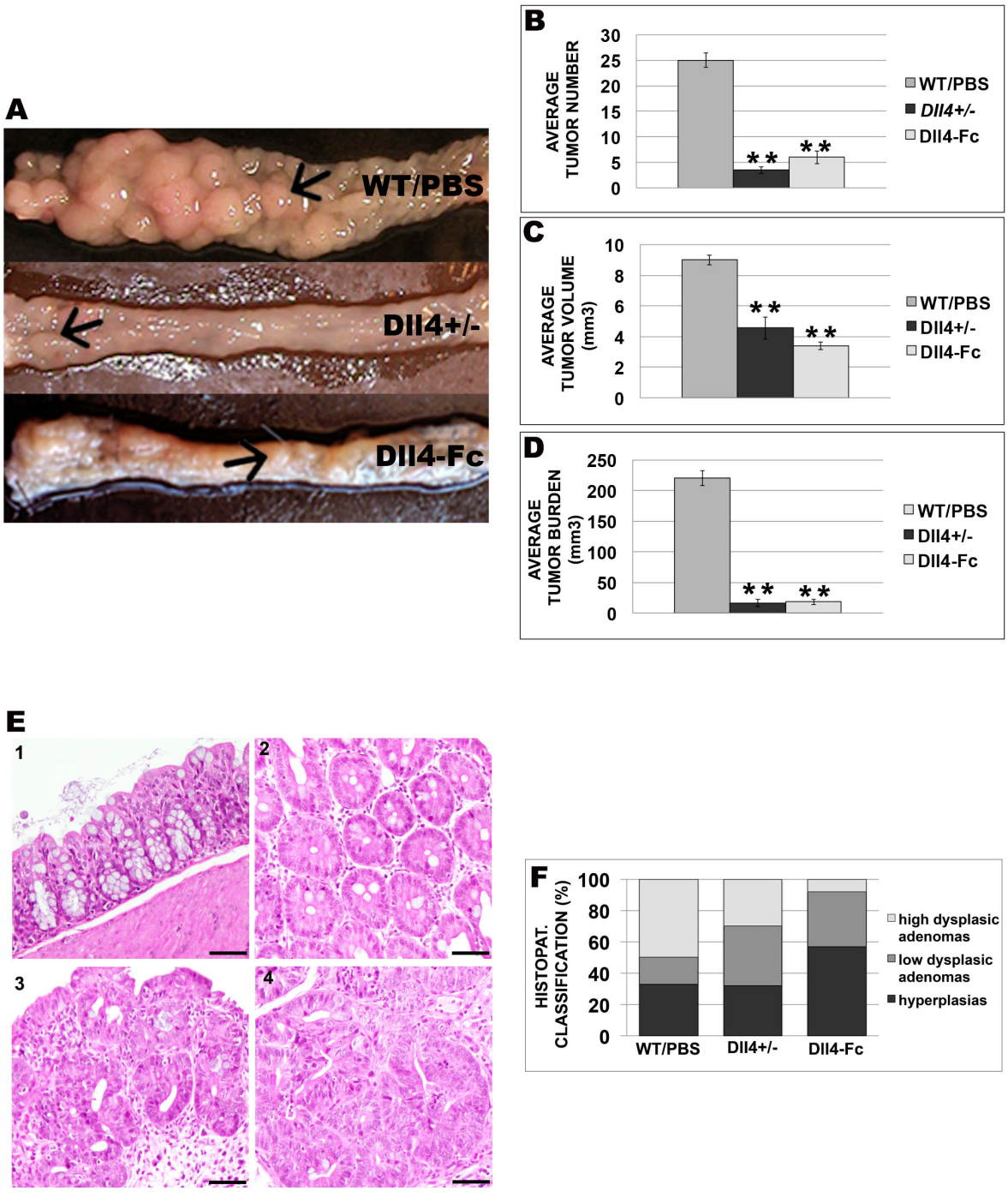

(A) Macroscopic colitis-driven CR tumor photographs of *Dll4*$^{+/-}$ and Dll4-Fc treated mice *versus* controls (WT/PBS treated mice). (B-D) Graphic bars represent the average ± SEM tumor number (B), volume (mm^3) (C), and burden (mm^3) (D) per group. One experiment with n = 12 per group. $^{**}P<0.01$. (E) H&E images of the normal rectum (1), and of rectal hyperplasia (2), and adenoma with low (3) and high (4) grade of dysplasia, the lesions found in the animals subjected to the CAC model. Scale bar = 50µm. (F) Graphic bars represent the proportion (%) of hyperplasias and adenomas with low or high-grade dysplasia in the macroscopic large intestine lesions from the experimental groups (*Dll4*$^{+/-}$ and Dll4-Fc) and the controls (WT/PBS). One experiment with n = 12 per group.

Figure 39 - Confirmation of the efficacy of the Dll4/Notch pathway blockade

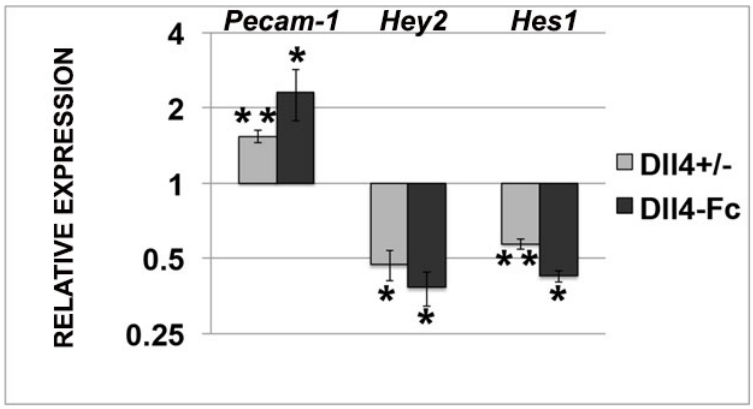

RT-PCR analysis of the Dll4/Notch effectors *Hey2* and *Hes1* relative expression, normalized to *Pecam-1*, in *Dll4*$^{+/-}$ and Dll4-Fc treated colitis-driven CR tumors relatively to the controls (WT/PBS treated mice). One experiment with n = 3 per group. **P*<0.05; ***P*<0.01.

4.4.4.3 Dll4 blockade deregulates angiogenesis in CAC

Given that blockade of Dll4 signaling is known to inhibit tumor growth by deregulating angiogenesis (Djokovic et al., 2010; Noguera-Troise et al., 2006; Ridgway et al., 2006; Scehnet et al., 2007) we performed indirect immunofluorescence to characterize the vasculature of the Dll4 deficient (*Dll4*$^{+/-}$/Dll4-Fc treated) CR tumors *versus* controls. Relatively to the controls, vascular density was increased in the *Dll4*$^{+/-}$ and in the Dll4-Fc treated mice by 43% and 127%, respectively (Fig. 40A-B). Furthermore, the wall of the tumor vessels presented a reduction in the smooth muscle cell coverage density of 14% and 53% respectively (Fig. 40A and 40C). In addition, the tumoral vasculature exhibited loss of functionality, with a 34% and 69% increase of vessel extravasation (Fig. 40D-E) and a 32% and 60% reduction of vessel perfusion in the *Dll4*$^{+/-}$ and Dll4-Fc treated mice, respectively (Fig. 40F-G).

HIF-1α is an important mediator of the hypoxic response (Ryan et al., 2000). In this setting we found that the tumors of *Dll4*$^{+/-}$ and Dll4-Fc treated mice exhibited a 32% and 66% increase in the expression of HIF-1α, respectively (Fig. 40H-I).

Figure 40 - Colitis-driven CR tumors of *Dll4*$^{+/-}$ and Dll4-Fc treated mice display increased vascular density and impaired vascular functionality

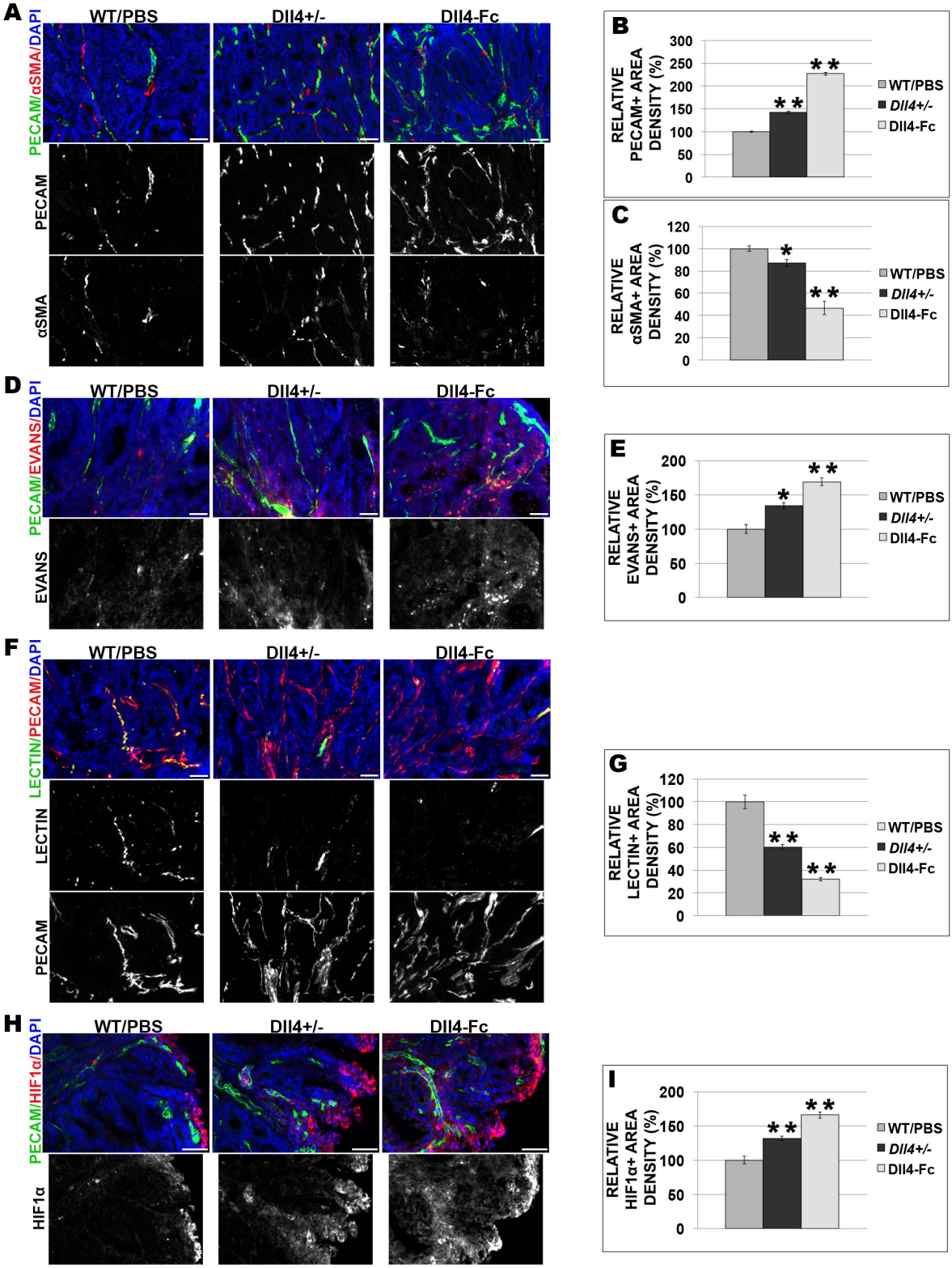

(A, D, F, H) Immunofluorescence stainings of colitis-driven CR tumors 20µm cryosections from *Dll4*$^{+/-}$ and Dll4-Fc treated mice *versus* controls (WT/PBS treated mice). Representative images of staining density for PECAM-1 (in green) and α-SMA (in red) (A), for PECAM-1 (in green) and Evans' Blue (in red) (D), for lectin (in green) and PECAM-1 (in red) (F), and for PECAM-1 (in green) and HIF-1α (in

red) (H). The nuclei were conterstained with DAPI (blue). Scale bar = 100μm. (B, C, E, G, I) Graphic bars represent the relative (%) ± SEM CR tumor vascular density (B), maturity (C), extravasation (E) and perfusion (G), and the relative (%) ± SEM hypoxia (I) in the animals described above. One experiment with n = 6 per group and 6 fields per animal. *P<0.05; **P<0.01.

4.4.4.4 Dll4 inhibition reduces chronic colitis and CR tumor inflammation

Chronic colitis is associated with elevated risk of CRC, as inflammatory cells have a major role in promoting neoplastic transformation (T. Tanaka et al., 2003). Therefore we scored the colitis severity (from grade 1 to 3) in the large intestine of Dll4 deficient (*Dll4*$^{+/-}$/Dll4-Fc treated) and control mice. The analysis revealed that *Dll4*$^{+/-}$ but mainly Dll4-Fc treated mice had less severe colitis lesions than the controls (Fig. 41A-B). While in the latter, the majority of the lesions found were grade 2 and a few grade 3, in the *Dll4*$^{+/-}$ but mainly in the Dll4-Fc treated mice, most of the lesions found were grade 1 and, most importantly, no grade 3 lesions were observed (Fig. 41A-B).

Additionally, we analyzed by immunofluorescence or H&E staining the immune cell infiltration and the gene expression of specific cytokines and inflammatory mediators in the Dll4 deficient (*Dll4*$^{+/-}$/Dll4-Fc treated) and control CR tumors.

We observed that, in this model of CAC, the tumors were mainly infiltrated by F4/80 positive macrophages, the majority being of the M2 subtype (where the M1 and M2 macrophages were determined by co-staining of F4/80 with iNOS or Arginase I, respectively) (Fig. 42A and 42C). Several CD11c+ dendritic cells (Fig. 42D) were also present, mainly at the base of the tumors, along with a few neutrophils (identified in H&E-stained sections) (Fig. 42H).

Additionally we observed high expression of IFN-γ and IL-17A and lower expression of IL-4 in the tumors (Fig. 43A-C). These were also infiltrated by many helper, cytotoxic and regulatory T cells (by marking the CD3+CD4+, CD3+CD8+ and FOXP3+ cells, respectively) (Fig. 44A, 44C and 44E) and by only a few CD19+ B cells (Fig. 44G).

We found that, relatively to the controls, *Dll4*$^{+/-}$ and mainly Dll4-Fc treated mice had less infiltrating macrophages (Fig. 42A-C), dendritic cells (Fig. 42D-G) and neutrophils (Fig. 42H-I) in the CR tumors. Interestingly, the proportion of proinflammatory M1 macrophages was significantly reduced (Fig. 42F). The M2 subset, however, was not significantly altered (Fig. 42F).

Furthermore, Dll4 inhibition decreased the relative expression of several cytokines involved in inflammation (*Il-2, Ifn-γ, Tnf-α, Il-4, Il-10, Il-13, Il-17a, Il-6*) in the tumors (Fig. 42J). Importantly, the relative expression of the proinflammatory and protumoral *Tnf-α and Il-6* cytokines (Rizzo et al., 2011) was reduced by 31% and 40% in the *Dll4*$^{+/-}$ tumors, respectively, and by 64% and 69% in Dll4-Fc treated tumors, respectively (Fig. 42J). The transcription of the inflammatory enzymes *Cox-2* and *iNos* (Fig. 42J) and the protein level of iNOS (Fig. 42E) were also reduced in the *Dll4*$^{+/-}$ and mainly in Dll4-Fc treated tumors. The CAC promoter *Nfkb2* (Rizzo et al., 2011) was reduced by 44% and 52% in the *Dll4*$^{+/-}$ and

Dll4-Fc treated tumors, respectively, while the CAC inhibitor *Tgf-β* (Rizzo et al., 2011) was increased by 62% and 70% in these same tumors, respectively (Fig. 42J). Interestingly, the relative expression of the proinflammatory cytokines *Il-2, Ifn-γ* and *Il-17a* was more reduced than the relative expression of the anti-inflammatory cytokines *Il-4, Il-10 and Il-13* in the *Dll4*$^{+/-}$ and Dll4-Fc treated tumors (Fig. 42J). Accordingly, the number of cells positive to IFN-γ and IL-17A was more reduced than those positive to IL-4 in these same tumors relatively to the controls (Fig. 43A-D).

Regarding the adaptive immunity, the number of helper and mainly cytotoxic T cells was significantly decreased in the *Dll4*$^{+/-}$ and Dll4-Fc treated tumors (Fig. 44A-D). However, FOXP3, a marker of regulatory T cell differentiation (Korn et al., 2009), was slightly increased in these tumors (Fig. 44E-F). In the case of B cells, these were relatively few in all tumors without significant variation among groups (Fig. 44G-H).

Figure 41 - *Dll4*$^{+/-}$ and Dll4-Fc treated mice display reduced colitis

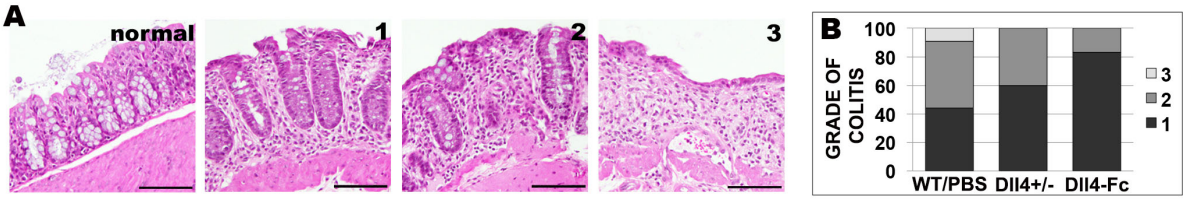

(A) H&E staining of paraffin-embedded large intestine 4μm sections from *Dll4*$^{+/-}$ and Dll4-Fc treated mice *versus* controls (WT/PBS treated mice). Representative images of the normal large intestine and of colitis with severity of grade 1 to 3. Scale bar = 100μm. (B) Graphic bars represent the proportion (%) of each classification of colitis severity (1-3) in the samples from the animals described above. One experiment with n = 12 per group and 2 fields per animal.

Figure 42 - Dll4 blockade downregulates innate immunity, M1 macrophage polarization and inflammatory mediators in colitis-driven CR tumors

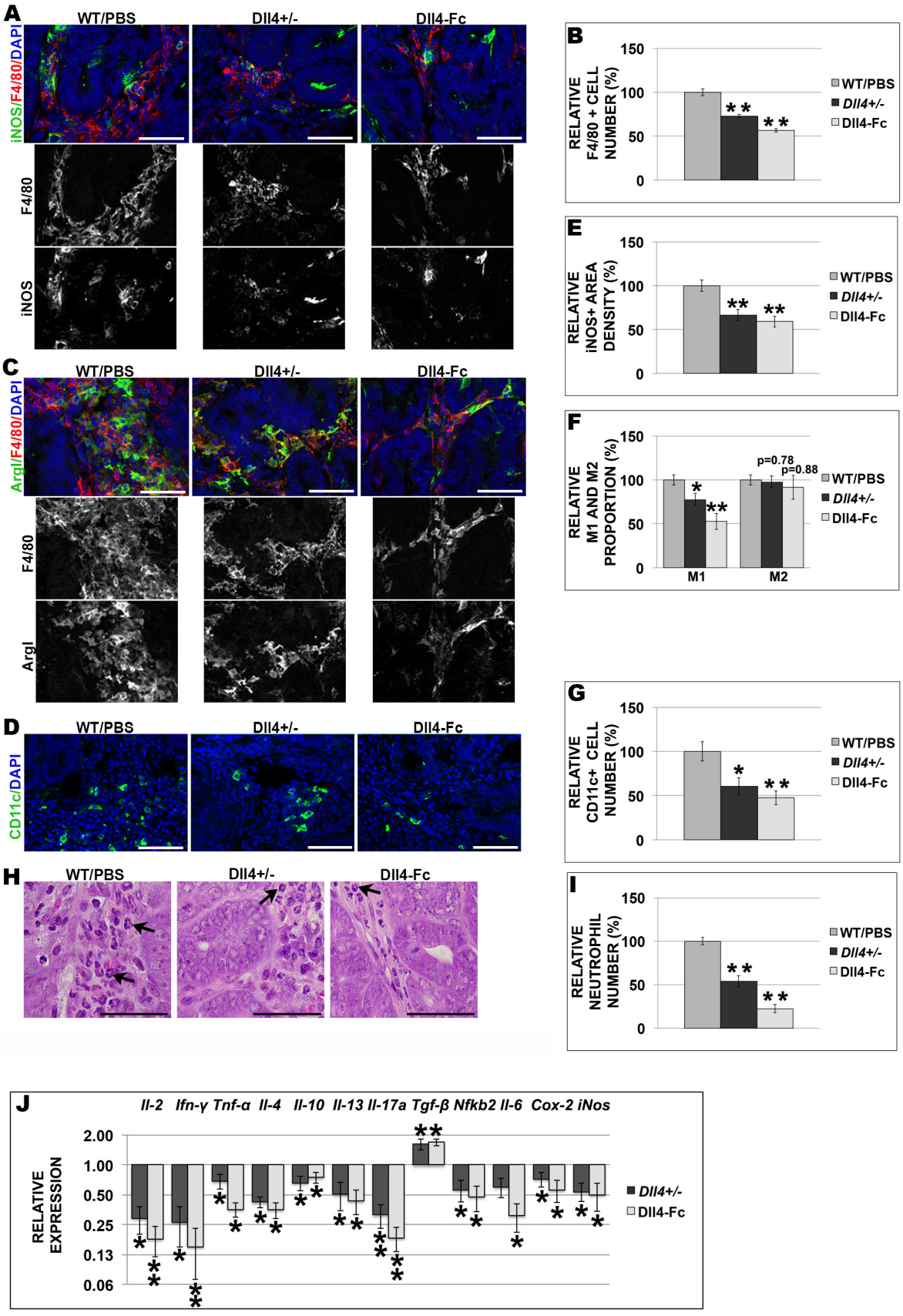

(A, C, D) Immunofluorescence stainings of colitis-driven CR tumor 10µm cryosections from *Dll4*$^{+/-}$ and Dll4-Fc treated mice *versus* controls (WT/PBS treated mice). Representative images of staining density for F4/80 (in red) and iNOS (in green) (A), for F4/80 (in red) and Arginase I (in green) (C), and for CD11c (in green) (D). The nuclei were counterstained with DAPI (in blue). Scale bar = 50µm. (B, E, F, G) Graphic bars represent the relative (%) ± SEM number of F4/80+ macrophages (B), density of iNOS (E), F4/80+iNOS+ M1 and F4/80+Arginase I+ M2 macrophage proportion (F), and number of CD11c+ dendritic cells (G) in the CR tumors from the animals described above. One experiment with n = 6 per group and 6 fields per animal. (H) H&E staining of paraffin-embedded CR tumor sections (4µm) from *Dll4*$^{+/-}$ and Dll4-Fc treated mice compared to controls (WT/PBS treated mice). Representative images of neutrophils (indicated by arrows) in the CR tumors. Scale bar = 20µm. (I) Graphic bars represent the relative (%) ± SEM number of neutrophils. (J) RT-PCR analysis of *Il-2, Ifn-γ, Tnf-α*, *Il-4, Il-10, Il-13, Il-17a, Tgf-β, Nfkb2, Il-6, Cox-2* and *iNos* relative expression in the *Dll4*$^{+/-}$ and Dll4-Fc treated tumors *versus* controls (WT/PBS treated tumors). One experiment with n = 3 per group. **P*<0.05; ***P*<0.01.

Figure 43 - Dll4 blockade reduces the number of cells positive to IL-4 and mainly to IL-17A and IFN-γ in colitis-driven CR tumors

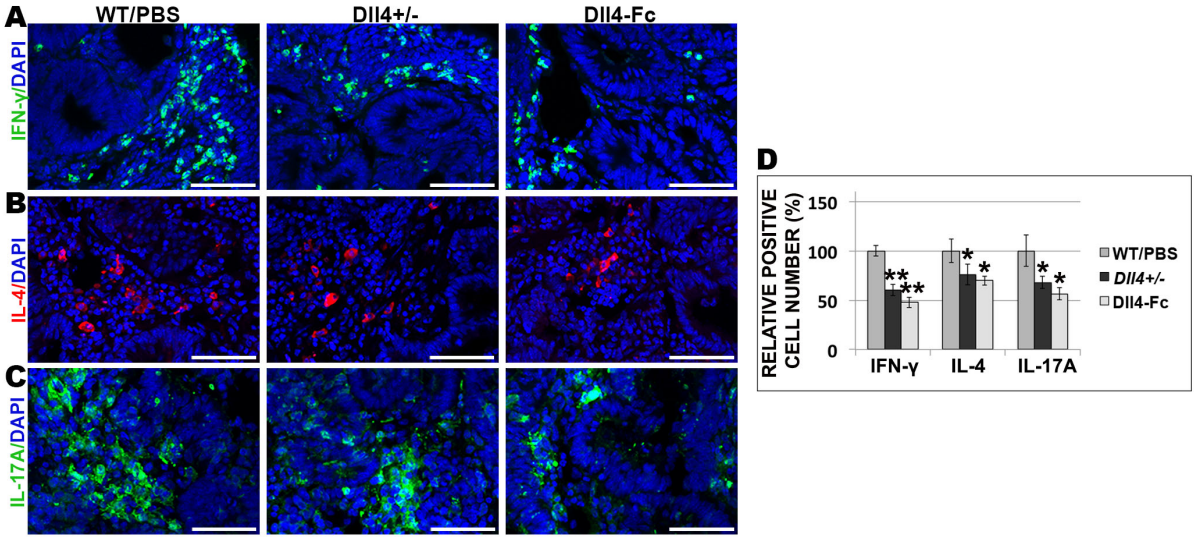

(A-C) Immunofluorescence stainings of colitis-driven CR tumor 10µm cryosections from *Dll4*$^{+/-}$ and Dll4-Fc treated mice *versus* controls (WT/PBS treated mice). Representative images of staining density for IFN-γ (in green) (A), for IL-4 (in red) (B), and for IL-17A (in green) (C). Nuclei were counterstained with DAPI (in blue). Scale bar = 50µm. (D) Graphic bars represent the relative percentage ± SEM of cells positive to IFN-γ, IL-4 and IL-17A in the CR tumors from the animals described above. One experiment with n = 6 per group and 6 fields per animal. **P*<0.05; ***P*<0.01.

Figure 44 - Dll4 blockade inhibits helper and cytotoxic T cell, but not B cell, accumulation and elevates the number of regulatory T cells in colitis-driven CR tumors

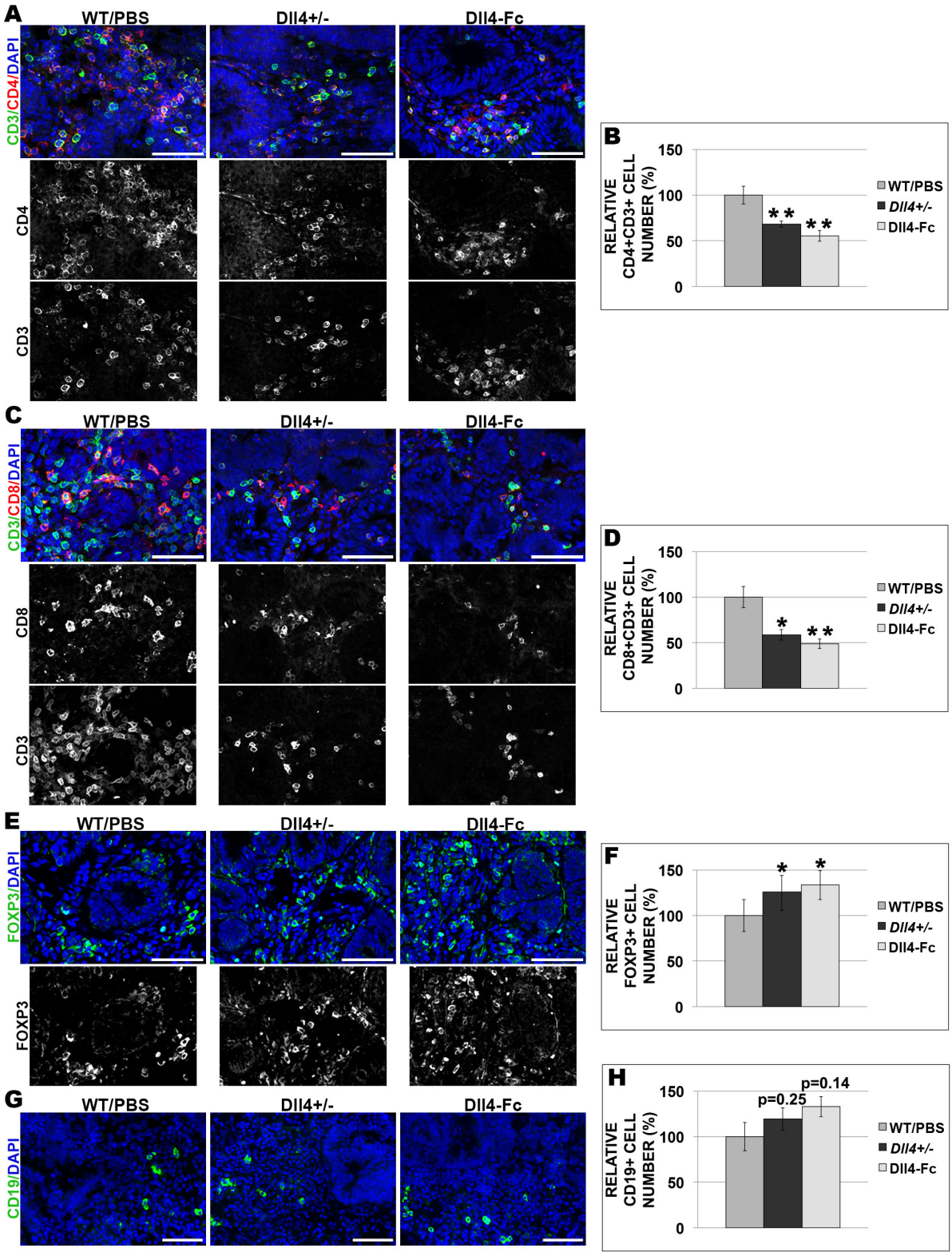

(A, C, E, G) Immunofluorescence stainings of CR tumor 10µm cryosections from *Dll4*$^{+/-}$ and Dll4-Fc treated mice *versus* controls (WT/PBS treated mice). Representative images of staining density for CD3 (in green) and CD4 (in red) (A), for CD3 (in green) and CD8 (in red) (C), for FOXP3 (in green)

(E), and for CD19 (in green) (G). Nuclei were counterstained with DAPI (blue). Scale bar = 50μm. (B, D, F, H) Graphic bars represent the relative percentage ± SEM of cells positive to CD4 and CD3 (B), to CD8 and CD3 (D), to FOXP3 (F), and to CD19 (H) in the CR tumors from the animals described above. One experiment with n = 6 per group and 6 fields per animal. *P<0.05; **P<0.01.

4.4.4.5 Dll4 blockade decreases the number of Lgr5 positive stem cells and increases secretory lineage differentiation in the large intestine inflammatory and tumoral lesions

Tumors are characterized by deregulated cell proliferation and suppression of apoptosis, two hallmarks critical for neoplastic progression (Hanahan & Weinberg, 2000). We assessed if the Dll4 inhibition affected tumor cell apoptosis and proliferation. Compared with the controls, a significant increase in the number of apoptotic cells in the *Dll4*$^{+/-}$ and Dll4-Fc treated tumors (54% and 82%, respectively) was observed (Fig. 45A-B). Additionally, both *Dll4*$^{+/-}$ and Dll4-Fc treated tumors presented less proliferating cells than the controls (52% and 61%, respectively) (Fig 45C-D). As Dll4 loss-of-function decreased the tumor number, we assessed its effect on the number of Lgr5+ stem cells. We found that in the *Dll4*$^{+/-}$ and Dll4-Fc treated animals these cells were decreased by 39% and 31%, respectively, in the tumors (Fig. 45E-F), but not in the inflamed large intestine (Fig. 46A-B).

We observed the presence of Paneth cell metaplasia in the tumors of all groups, mainly in the *Dll4*$^{+/-}$ and Dll4-Fc treated groups. Specifically, relatively to controls, in the *Dll4*$^{+/-}$ and Dll4-Fc treated inflamed large intestine, the number of Paneth cells was increased by 29% and 20%, respectively (Fig. 46C-D), while in the tumors these cells were increased by 42% and 31% respectively (Fig. 45G-H). We also observed that the proportion of goblet cells was increased by 36% and 24% in the inflamed colorectal epithelium (Fig. 46E-F) and by 50% and 36% in the tumor epithelium of *Dll4*$^{+/-}$ and Dll4-Fc treated mice, respectively (Fig. 45I-J). Therefore the inhibition of Dll4/Notch signaling in the inflamed large intestine and mainly in CAC seems to lead the Lgr5+ stem cells to differentiate towards the Paneth and goblet cell secretory lineages. However, this was not observed in the normal large intestine of *Dll4*$^{+/-}$ and of Dll4-Fc treated mice (data not shown).

Figure 45 – Colitis-driven CR tumors with Dll4 inhibition show increased apoptosis, reduced proliferation, decreased number of Lgr5 positive stem cells, and induction of secretory differentiation

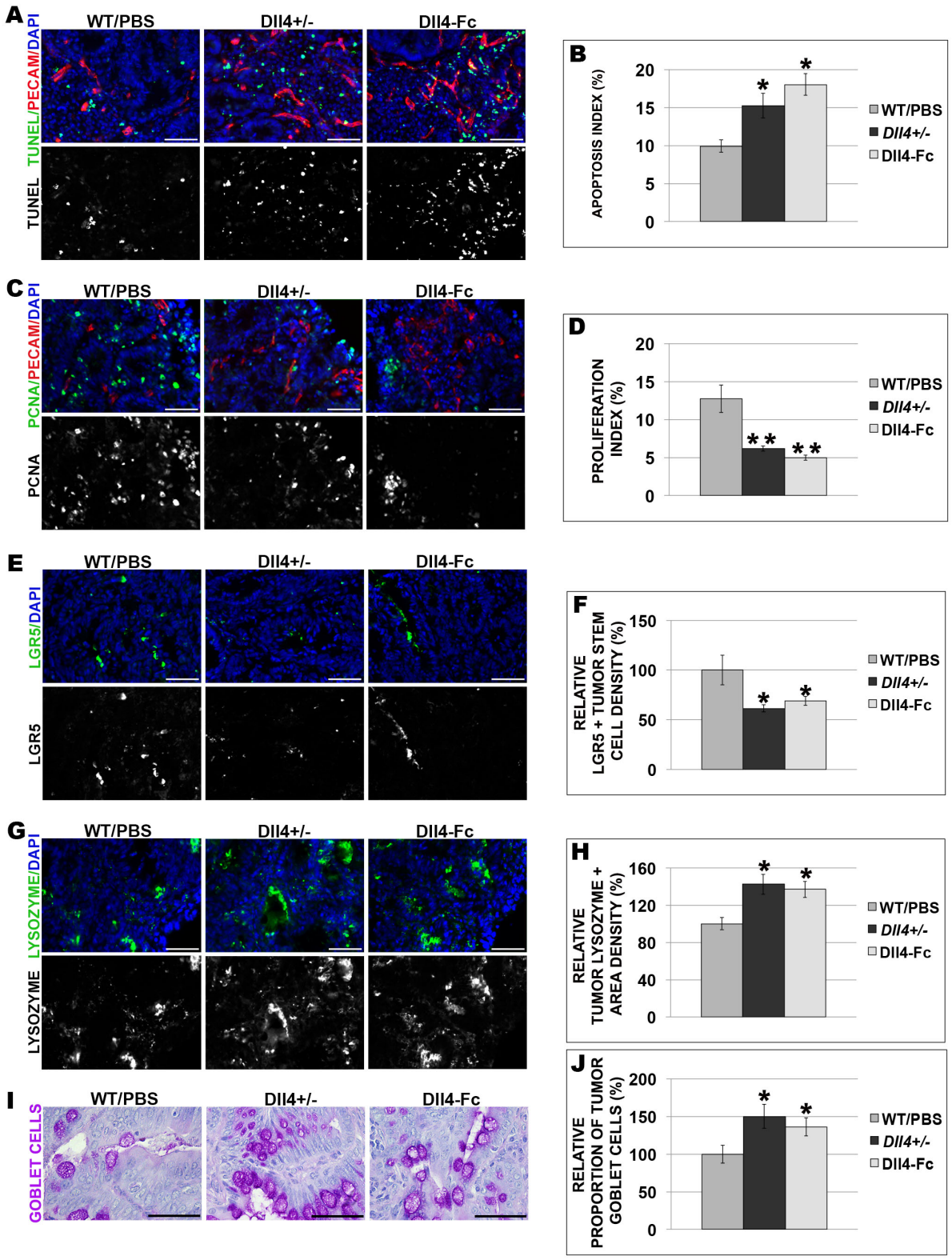

(A, C, E, G) Immunofluorescence staining of colitis-driven CR tumor 10µm cryosections from *Dll4*$^{+/-}$ and Dll4-Fc treated mice *versus* controls (WT/PBS treated mice). Representative images of staining density for TUNEL (in green) and PECAM-1 (in red) (A), for PCNA (in green) and PECAM-1 (in red)

(C), for Lgr5 (in green) (E), and for lysozyme (in green) (G). Nuclei were counterstained with DAPI (in blue). Scale bar = 100µm. (B, D, F, H) Graphic bars represent the index (%) ± SEM of apoptosis (B) and proliferation (D), and of the relative density (%) ± SEM of Lgr5 (F) and lysozyme (H) in the CR tumors of the animals mentioned above. (I) Representative images of PAS staining of goblet cells in colitis-driven CR tumors (paraffin-embedded 4µm sections) from *Dll4*$^{+/-}$ and Dll4-Fc treated mice *versus* controls (WT/PBS treated mice). Scale bar = 50µm. (J) Graphic bars represent the proportion (%) ± SEM of goblet cells in the CR tumor epithelium of the animals described above. One experiment with n = 6 per group and 2 to 6 fields per animal. **P*<0.05; ***P*<0.01.

Figure 46 - In inflamed large intestine Dll4 inhibition does not affect the number of Lgr5 positive cells, but slightly increases secretory lineages differentiation

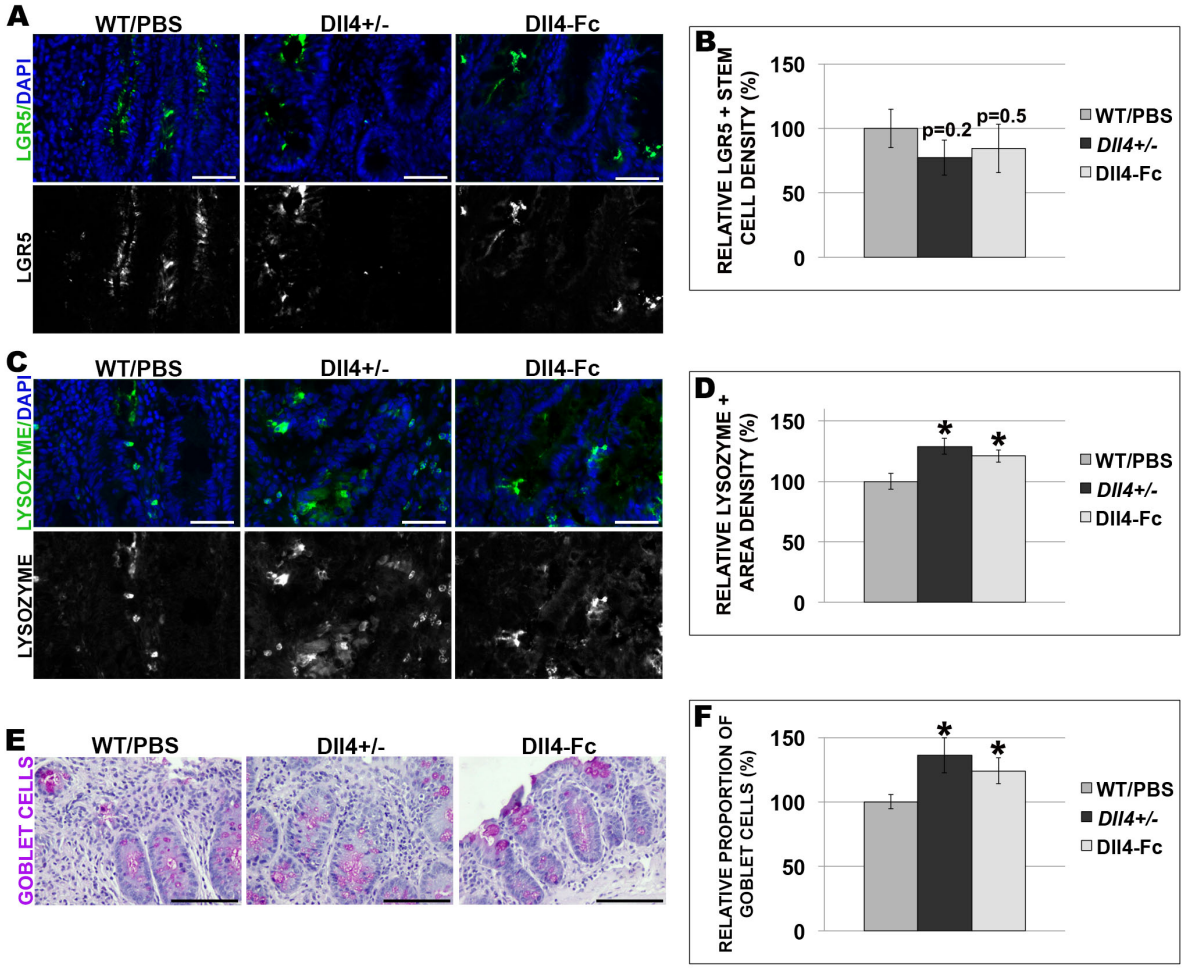

(A, C) Immunofluorescence stainings of inflamed large intestine 10µm cryosections from *Dll4*$^{+/-}$ and Dll4-Fc treated mice *versus* controls (WT/PBS treated mice). Representative images of staining density for Lgr5 (in green) (A) and for lysozyme (in green) (C). Nuclei were counterstained with DAPI (in blue). Scale bar = 50µm. (B, D) Graphic bars represent the Lgr5 (B) and lysozyme (D) relative density (%) ± SEM in the inflamed large intestine of the animals mentioned above. (E) PAS staining of goblet cells in the inflamed large intestine (paraffin-embedded 4µm sections) from *Dll4*$^{+/-}$ and Dll4-Fc treated mice *versus* controls (WT/PBS treated mice). Scale bar = 50µm. (F) Graphic bars represent

the proportion of goblet cells (%) ± SEM in the inflamed large intestine epithelium of the animals described above. One experiment with n = 6 per group and 2 to 6 fields per animal. *P<0.05.

4.4.5 Discussion

Patients with IBD have high probability of developing CRC. Currently available therapies for this type of cancer are still insufficient (Jemal, Thomas, Murray, & Thun, 2002).

Dll4/Notch signaling has been proposed as a target for cancer therapy due to its crucial role on tumor angiogenesis (Djokovic et al., 2010; Noguera-Troise et al., 2006; Ridgway et al., 2006; Scehnet et al., 2007). Additionally, this pathway is constitutively active in CRC (Qiao & Wong, 2009). Previous studies have shown that anti-Dll4 therapy inhibits the colorectal cancer growth and the frequency of cancer stem cells (M. Fischer et al., 2010; Hoey et al., 2009). Furthermore, there are several reports indicating that Notch signaling regulates immune responses in the gut (Mathern et al., 2014; Obata et al., 2012; Okamoto et al., 2009; Shinoda et al., 2010). Additionally, this pathway seems to crosstalk with NF-$_K$B and MAPK pathways to promote T-cell responses (Mathern et al., 2014). We may therefore speculate that Dll4/Notch signaling activation may be crucial in the development of CAC. In the present work we assessed for the first time the effect of Dll4 inhibition on IBD and on CAC. A previous report showed that in the normal human colon Dll4 is present in occasional cells in the superficial surface mucosa, being absent in goblet cell (Jubb et al., 2009). Other members of the Notch pathway are also present in this region (Sander & Powell, 2004). In acute colitis, upregulation of Dll4, Notch1, NICD and Hes1 expression has already been described (Okamoto et al., 2009; Shimizu et al., 2014). However, the expression pattern of Notch pathway members in chronic colitis and in CAC remained unknown. We started by evaluating the expression of Dll4 and other Notch pathway members in the inflamed large intestine and in CAC. We found a strong presence of Notch pathway components in both chronic colitis and CAC. Among these, Dll4 and Notch1 seemed to be the most upregulated in tumor cells compared with the inflamed colorectal epithelium. Jubb et al. described that in human colon cancer samples, Dll4 was highly expressed mainly in the endothelium and in the neoplasic cells with goblet cell differentiation (Jubb et al., 2009). However, we found that in chronic colitis and in CAC Dll4 is present in goblet cells, but also in colonocytes and other tumor cells, respectively. In these settings we also observed Dll4 expression in some metaplastic Paneth cells and in some cells of the *lamina propria*, including macrophages and dendritic cells.

Given the marked upregulation of Dll4 in CAC, we analyzed the impact of its allelic loss on CAC development. As it inhibited the tumor formation and growth, we then tested a pharmacological blockade of Dll4 using Dll4-Fc. We observed that Dll4 inhibition reduced mainly the tumor number, suggesting that Dll4 could have a role in the initiation of CAC. Interestingly, the decrease in the tumor number upon Dll4 blockade was associated with a reduction in the density of Lgr5+ tumor stem cells, which appeared to differentiate more into

the Paneth and goblet cells secretory lineages. Therefore, Dll4/Notch signaling seems to have a role in maintaining the undifferentiated state of the tumor stem cells and in favoring colonocyte lineage differentiation. Remarkably, Dll4 blockade, in contrast with previously tested γ-secretase inhibitors (van Es, van Gijn, et al., 2005), caused no discernible impact on normal intestinal goblet cell differentiation. Radtke's group had already previously identified Dll1 as a key regulator of the mouse intestine (Pellegrinet et al., 2011) and showed that intestine-specific inactivation of either *Dll4 or Jag1* had no phenotype, while the loss of *Dll1* resulted in a moderate increase in goblet cell numbers. Additionally, *Dll1-Dll4* double knockout mice developed even more intestinal abnormalities (Pellegrinet et al., 2011). Therefore, it is likely that Dll1 may compensate for the lack of Dll4 in the healthy intestine. However, during chronic colitis and especially in CAC, the differentiation towards the secretory lineages was favored upon Dll4 blockade. Nevertheless, this increase in differentiation did not result in a macroscopic effect, indicating that the intestinal inhibition of Dll4 may be used without causing the severe side effects associated with γ-secretase inhibitors.

Additionally, Dll4 blockade caused a reduction in tumor volume, presumably associated with its crucial role on the regulation of angiogenesis. The analysis of the vasculature of Dll4 deficient tumors showed an increase in vascular density. As previously reported, these newly formed vessels were defective, presenting reduced smooth muscle coverage, increased extravasation and reduced perfusion. This caused hypoxia-limited tumor growth. Consequently, an increase in tumor cell death and a decrease in tumor cell proliferation were detected. However, it seems that this is not the only mechanism responsible for the observed reduction of tumor growth. In fact, a recent report showed that the knockdown of Notch1, probably the main Dll4 receptor, significantly inhibited the proliferation, colony and tumorsphere formation of SW480 and HT-29 cells, induced apoptosis and cell cycle arrest at G0/G1 phase, and mitigated the development and growth of implanted colon cancers *in vivo* (Zhang, Li, Ji, & Zheng, 2010). Therefore a potential direct pro-apoptotic and anti-proliferative effect of Dll4 inhibition should also be considered.

Dll4 blockade reduced the severity of colitis and CR tumor inflammation. As in colitis and in CAC Dll4 is expressed in some macrophages and dendritic cells, it may therefore regulate tumor and non-tumor CR inflammation through these cells. Additionally, Dll4 is expressed in some antimicrobial metaplastic Paneth cells, whose density increases after Dll4 blockade. Thus, Dll4 inhibition may decrease the CR inflammation in part by promoting Paneth cell metaplasia. Furthermore, Dll4 blockade inhibitory effect on vascular perfusion may also help restrain the immune cell influx to the inflammation site.

Osawa and colleagues showed that in the AOM plus trinitrobenzene sulfonic acid (TNBS) CAC model, the disease is mediated by IL-4 rather than IFN-γ (Osawa et al., 2006). However, a study that used the AOM+DSS model, indicated that IL-17A ablation resulted in the

reduction of the number and average tumor size and decreased the inflammatory mediators IL-6, IFN-γ and TNF-α and the tumor cell proliferation (Hyun et al., 2012). In the present work we also used the AOM+DSS model. Our protein expression analysis indicated that the CAC condition is mediated mainly by IL-17A and IFN-γ rather than IL-4. Furthermore, IL-17A rather than IFN-γ might sustain inflammation and promote CAC development as previously suggested (Rizzo et al., 2011).

We found that Dll4 blockade reduced the accumulation of cells of both the innate and adaptive immune system, which is probably interrelated, as antigen-presenting cells are important T cell stimulators (Sprent, 2005). In addition, it inhibited the proinflammatory M1 macrophage polarization. The effect of Dll4 inhibition on macrophage accumulation and polarization was similar to that previously described in atherosclerosis (Fukuda et al., 2012; Fung et al., 2007). Specifically, these studies showed that Dll4 blockade attenuated atherosclerosis by reducing the accumulation of macrophages and the level of NF-$_{K}$B activation (Fukuda et al., 2012; Fung et al., 2007) and by inhibiting the proinflammatory M1 phenotype (Fukuda et al., 2012).

Additionally, Dll4 inhibition led to increased accumulation of regulatory T cells in the tumors. This effect on regulatory T cell differentiation was previously described in autoimmune diseases, where the inhibition of Dll4/Notch signaling decreased the severity of the disease and the inflammation by increasing the pool of these cells (Bassil et al., 2011; Jiao et al., 2014; Takeichi et al., 2010; Tran et al., 2013). Furthermore, the transcription of *Tgf-β* was increased in Dll4 deficient tumors and may have promoted the innate and adaptive immunity phenotypes observed in CAC. It is known that tumor-derived TGF-β represses the activation, maturation and differentiation of the innate immune cells and CD4 and CD8 T-cells and induces the recruitment and differentiation of regulatory T cells (Flavell et al., 2010). TGF-β signaling was also shown to inhibit IFN-γ production and to promote the differentiation of IL-17 producing cells in the presence of IL-6 (Flavell et al., 2010). We found that Dll4 inhibition led to a stronger decrease of the expression of the proinflammatory cytokines *Il-2, Ifn-γ* and *Il-17a* than of the anti-inflammatory cytokines *Il-4, Il-10 and Il-13*. As the transcription of *Il-6* was decreased in Dll4 deficient tumors, this may have blocked IL-17A producing cell differentiation despite the increased transcription of *Tgf-β*. In turn, the decreased *Il-6* gene expression may have been caused by *Nfkb2* downregulation in the same tumors, as it was demonstrated that *Il-6* transcription results from NF-$_{K}$B activation (Grivennikov et al., 2009). This, in turn, depends on *Tnf-α* expression, which was also downregulated in these tumors (Rizzo et al., 2011). Furthermore, *Il-6* decreased gene expression was also probably associated with the decreased number of IL-6 producing dendritic cells, macrophages and T cells (Grivennikov et al., 2009) in Dll4 deficient tumors.

Nevertheless, the observed inflammatory profile in Dll4 deficient mice was concordant with previous reports, indicating that Dll4 inhibition seems to restrain the abnormal and excessive

immune response that characterizes IBD and eventually promotes CAC (Kraus & Arber, 2009). In addition, we observed that the immunomodulatory cytokine IL-10 was only slightly reduced in Dll4 deficient tumors; thereby IL-10 function is probably maintained in these animals. Therefore, our results showed that besides promoting dysfunctional tumoral angiogenesis, Dll4 blockade seems to also inhibit intestinal tumor initiation and development, in part by reducing inflammation and the expression of important promoters of CAC, such as the antiapoptotic and proliferation inducer *Tnf-α*/*Nfkb2*/*Il-6* pathway (Karin, 2009; Rizzo et al., 2011) and by increasing the expression of the CAC inhibitor *Tgf-β* (Rizzo et al., 2011).

To further understand the effect of Dll4 inhibition on CAC, we performed a microscopic analysis of the Dll4 deficient tumors *versus* controls. Although the number of adenomas *versus* hyperplasias seemed similar between heterozygous and control mice, the grade of adenomatous dysplasia was reduced in the $Dll4^{+/-}$ group. As dysplasia is a precursor of CRC in IBD (Itzkowitz & Harpaz, 2004), this result indicates that the blockade of Dll4 seemed to promote some delay in the neoplasic transformation. The phenotype observed in $Dll4^{+/-}$ mice may be associated to the observed reduced inflammation and angiogenic dysfunction. This and the promotion of stem cell differentiation may have, in this case, prevented the abnormal proliferation and accumulation of mutations that normally leads to neoplasic development. In the case of Dll4-Fc therapy, the Dll4 inhibition significantly reduced the number of neoplasias. Therefore, the majority of the Dll4-Fc treated lesions were hyperplasias, benign lesions that have no potential for malignancy (Winawer et al., 1997). Thus, Dll4-Fc therapy had an important role in reducing the neoplasic development. This could be associated to the fact that Dll4-Fc therapy seems to have a more significant effect on the tumor and non-tumor inflammation and also in tumor angiogenesis than the genetic Dll4 deletion. This and the Dll4/Notch gene effectors level, suggests that the dosage of Dll4-Fc used is capable of reducing Dll4 signaling activity below the 50% level expected in $Dll4^{+/-}$ mice (Duarte, 2004). Nevertheless, despite the differences in the level and period of Dll4 blockade between the genetic and pharmacological experiments, in both models Dll4/Notch signaling inhibition blocked the initiation and progression of colitis-associated CRC, confirming each other results.

In conclusion, we described for the first time the mechanisms by which Dll4 blockade could be beneficial in the treatment of CAC. We believe that this therapy could also be useful to treat IBD and therefore to prevent CRC formation. Our findings have important implications as they show that, in addition to the effect on tumor angiogenesis, Dll4 blockade also seems to inhibit CAC initiation and progression by reducing inflammation and proliferation and, conversely, by promoting stem cell differentiation and apoptosis. Despite further studies being needed, these multifactorial Dll4-Fc mechanisms of action could be beneficial to avoid the development of tumor resistance to the therapy and to reduce tumor recurrence.

5 CONCLUSIONS

CRC remains the second leading cause of cancer-related death in the Western world (Jemal et al., 2011). Most cases are sporadic (Bogaert & Prenen, 2014) and a small proportion is hereditary, such as familial adenomatous polyposis (FAP) syndrome (Bogaert & Prenen, 2014), and associated to the inflammatory bowel diseases ulcerative colitis (Svartz & Ernberg, 1949) and Crohn's disease (Ekbom et al., 1990). The development of novel therapeutic and preventive strategies that can target critical CRC-related pathways is needed. Studies have indicated that Notch signaling is expressed and constitutively activated in CRC (Reedijk et al., 2008) and its inhibition is able to suppress CRC initiation and growth (Ghaleb et al., 2008; van Es & Clevers, 2005; van Es, van Gijn, et al., 2005), and sensitize the cancer cells to the standard therapies (Akiyoshi et al., 2008; Meng et al., 2009). However, Notch signaling is also required to maintain the normal gut homeostasis by regulating stem cell proliferation and survival as well as cell lineage differentiation (Fre et al., 2005). Therefore, successful targeting of Notch signaling in CRC will require a considerable refinement of our understanding of the regulation of this pathway and its effects in both normal and cancer intestinal cells. Indeed, treatment with GSIs that inhibit the cleavage of Notch receptors has been found to result in severe gastrointestinal toxicity, limiting their therapeutic utility (Milano et al., 2004). Thus, chronic, long-term suppression of Notch signaling is likely to require more selective agents, such as DLL4 inhibitors that have been shown to block tumor growth by promoting nonproductive angiogenesis and reduce tumor stem cell frequency in cancer (Djokovic et al., 2010; M. Fischer et al., 2010; Hoey et al., 2009; Ridgway et al., 2006; Scehnet et al., 2007). Nevertheless, there are some concerns about Dll4 blockade-based therapies as they can lead to potentially significant toxicity (Djokovic et al., 2010; J. L. Li et al., 2010; Minhong Yan et al., 2010), promote hypoxia-mediated malignancy (Hayden, 2009), limit the delivery of concomitant therapies, and lead to tumor regrowth through normalization of anti-Dll4 mediated vascular defects. Therefore, the opposite approach, activating Dll4, has being considered as a novel anti-angiogenic therapy strategy. However, this can lead to tumor growth or shrinkage in different types of tumors by reducing or increasing the tumor hypoxia and apoptosis, respectively (J. L. Li et al., 2007; Segarra et al., 2008).

The effect of Dll4/Notch signaling on tumor angiogenesis and therefore tumor growth has been extensively studied and dissected (Djokovic et al., 2010; Hoey et al., 2009; Noguera-Troise et al., 2006; Ridgway et al., 2006; Scehnet et al., 2007). In CRC this signaling may also regulate the tumor initation by affecting the cancer stem cell frequency (M. Fischer et al., 2010; Hoey et al., 2009). However, the role of Dll4/Notch pathway in precancerous intestinal lesions, the initiating event of CRC development, has never been studied.

Therefore we explored, by modulating Dll4/Notch signaling genetically and pharmacologically, how it affects the establishment and growth of adenomas in the *Apc*$^{Min/+}$

model and in the AOM+DSS model of chronic-colitis associated cancer (CAC). Additionally, we evaluated if the nonfunctional vasculature caused by anti-Dlll4 therapy affected the delivery of the anti-CRC EGFR-specific tyrosine kinase inhibitor (TKI) erlotinib in the *Apc*$^{Min/+}$ *model.*

We first evaluated the expression pattern of Notch components in the *Apc*$^{Min/+}$ small and large intestine tumors, and during DSS-induced chronic colitis and in AOM+DSS derived CAC, as this has been poorly studied. We compared the expression of Notch components in these settings with the one in the normal gut. Our results complemented the already published data of Notch pathway expression pattern in the normal gut (Sander & Powell, 2004; Schroder & Gossler, 2002). Thus we found that all Notch receptors, and not only Notch1 and 2, and all their ligands are expressed in the small and large intestine epithelium. We confirmed that this pathway is strongly present and is being activated, at least, through Hes1 and 5 Notch target genes in the gut in all the analyzed settings. Additionally, we observed numerous changes in the expression pattern of Notch members relatively to the normal gut. The most upregulated components in CAC were Dll4, Notch1 and Notch3, whereas in *Apc*$^{Min/+}$ tumors these were Dll4, all Notch receptors and Hes1, with some regional differences. Therefore, in both models Dll4 was the most upregulated ligand. It acquired ectopic expression in absorptive cells in all the settings and its expression was increased mainly in the *lamina propria* in chronic colitis and in the tumor epithelium in CAC and *Apc*$^{Min/+}$ tumors. Furthermore, it was expressed in the vasculature as expected and near the Lgr5+ stem cells in all these settings.

Given the increased expression of Dll4 in chronic colitis and in the tumors, we evaluated the influence of *Dll4* blockade in CAC and in the *Apc*$^{Min/+}$ model. In addition, as there are some concerns about the safety of anti-Dll4 therapies, we also analyzed the alternative approach of stimulating Dll4/Notch signaling in the *Apc*$^{Min/+}$ model. For this we used endothelial-specific *Dll4* gain-of-function mice, because Dll4 in the epithelium may promote CRC rather than inhibit it (Hoey et al., 2009).

When we inhibited Dll4 genetically and pharmacologically, we observed that in the normal gut, despite being present, Dll4 is not essential to maintain its homeostasis. This is due to Dll1/Notch signaling compensation, as a previous work demonstrated that Dll4 and mainly Dll1 are essential for intestinal stem cell maintenance and enterocyte differentiation in the normal gut (Pellegrinet et al., 2011). However, when we deregulated Dll4 in CAC and in the *Apc*$^{Min/+}$ mice we observed a strong phenotype that was similar in both models, indicating that Dll4 is important in the development of intestinal adenomas, acting through similar mechanisms of action in both colitis-related and *Apc* mutated tumors. In addition, in the *Apc*$^{Min/+}$ model the Dll4 blockade associated phenotype was similar in the small and large intestine tumors, but the inhibition of Dll4/Notch signaling was more effective in the large

intestine. However, it was more successful reducing the tumor number in the small intestine and more effective reducing the tumor volume in the large intestine. This could be related to the observed different regional distribution of N1ICD, as in the small intestine tumors N1ICD was observed primarily in the epithelium, while in the large intestine tumors it was mostly observed in the stroma.

In both CAC and *Apc*$^{Min/+}$ models Dll4/Notch signaling seems to promote mainly the tumor initiation, by maintaining the tumor stem cells undifferentiated and promoting tumor cell proliferation. We found that Dll4/Notch signaling in the endothelium maintains mildly the *Apc*$^{Min/+}$ tumor proliferation and the Lgr5+, but not the Bmi1+, stem cell frequency, and this is inhibited by the presence of nonfunctional or reduced angiogenesis caused by the blockade or activation of Dll4 in the endothelium, respectively. Thus, paradoxically, endothelial Dll4 overexpression inhibited the *Apc*$^{Min/+}$ tumor initiation almost as much as endothelial *Dll4* loss-of-function. However, other mechanisms, probably through Dll4/Notch epithelial and other stromal signaling, are also involved in this, as the loss of Dll4 ubiquitously promotes a stronger tumorigenic phenotype than the inactivation of Dll4 specifically in the endothelium. Therefore, Dll4 may mediate the previously observed phenotype of epithelial Notch signaling on intestinal tumorigenesis (Fre et al., 2009; van Es, van Gijn, et al., 2005). We found that Dll4/Notch signaling in the intestinal tumor epithelium may maintain the tumor stem cell populations through Atoh1 repression-mediated downregulation of the CDK inhibitors *Cdkn1b and Cdkn1c* (Kim & Shivdasani, 2011; Riccio et al., 2008). Furthermore, this seems to be also associated to the increased expression of the Wnt targets c-Myc, and Cyclin D1 and D2 (Cole et al., 2010; He et al., 1998; J. Liu et al., 2001), possibly through *Klf4* downregulation (Ghaleb et al., 2007) by Dll4/Notch signaling, independently of Wnt/β-catenin activation by *Apc* loss-of-function. Therefore, Dll4/Notch signaling may have a synergistic epithelial effect with Wnt signaling to promote tumorigenesis.

Interestingly, in the intestinal tumor epithelium, Dll4 seems to also inhibit differentiation, neoplasic transformation, and the secretory lineage commitment by Hes1-mediated *Atoh1* and *Klf4* repression (Ghaleb et al., 2008; van Es, van Gijn, et al., 2005). This regulation of the secretory cell differentiation was not as pronounced as that seen with pan-Notch inhibitors (van Es, van Gijn, et al., 2005), because as the results of our Dll4-Fc trial in the *Apc*$^{Min/+}$ model suggest, Dll4 may signal mainly through Notch1 and also Notch4 in the intestinal tumor epithelium, and blocking Notch1 and 2 simultaneously is necessary to promote the complete conversion of intestinal stem cells into secretory cells (Riccio et al., 2008). Furthermore, as the expression of *Dll1* was induced by Dll4-Fc administration, Dll1/Notch signaling may also attenuate this secretory differentiation (Pellegrinet et al., 2011). Additionally, the comparison of endothelial-specific *versus* ubiquitous *Dll4* mutant mice allowed us to clarify that the observed increase of tumor apoptosis in Dll4 deficient tumors was mainly derived from the increased level of hypoxia associated to the Dll4

angiogenic phenotype. Therefore, it seems that Dll4 does not have a significant direct anti-apoptotic effect, at least in the *Apc*$^{Min/+}$ adenomas.

Furthermore, our studies indicated that in CAC and *Apc*$^{Min/+}$ adenomas, Dll4/Notch signaling leads to tumor growth by promoting the development of a competent tumor vascular network, through regulation of the VEGF/VEGFR pathway, as in malignant colorectal neoplasias (Hoey et al., 2009). Therefore, the inhibition of Dll4 promoted non-productive angiogenesis that delayed the intestinal tumor growth as previously reported (Djokovic et al., 2010; Hoey et al., 2009; Noguera-Troise et al., 2006; Ridgway et al., 2006; Scehnet et al., 2007). Consistently, endothelial Dll4 activation led to the opposite effect of the Dll4 loss-of-function on tumor angiogenesis. However, endothelial Dll4 overexpression also inhibited the *Apc*$^{Min/+}$ tumor expansion, almost as much as endothelial Dll4 loss-of-function. This anti-tumor growth effect by Dll4 endothelial overexpression was associated to the reduction of tumor vessel density as, despite the blood vessels being more mature and functional, hypoxia and apoptosis increased in the intestinal tumors of these mutants.

Interestingly, Dll4 inhibition was more effective in the CAC model, accentuating the importance of Dll4 during chronic inflammation, which is considered the driving mechanism for tumor development in CAC. Indeed, in this model, Dll4 seems to promote additionally chronic colitis and CAC by: enhancing the number of innate and adaptive immune cells in the mucosa, promoting macrophage polarization into pro-inflammatory M1 subset, inducing a protumoral and pro-inflammatory response mediated mainly by IL-17 producing cells, promoting excessive and deregulated inflammation by decreasing the number of the immunomodulators Treg cells by TGF-β downregulation, and upregulating the proinflammatory enzymes COX-2 and iNOS, and the antiapoptotic and proliferation inducer *Tnf-α*/*Nfkb2*/*Il-6* pathway (Karin, 2009; Rizzo et al., 2011).

When we associated Dll4-Fc to erlotinib treatment in the *Apc*$^{Min/+}$ model, Dll4-Fc therapy promoted nonfunctional angiogenesis, as in malignant tumors (Djokovic et al., 2010; Hoey et al., 2009; Noguera-Troise et al., 2006; Ridgway et al., 2006; Scehnet et al., 2007), but this did not seem to affect the delivery of erlotinib, and therefore probably other anti-cancer drugs, to the tumors. A possible explanation for this, that has to be further studied, is that Dll4-Fc mediated increase of the tumor vascular extravasation can lead to the accumulation of erlotinib in the tumor tissue. Dll4-Fc inhibited the tumor growth by its angiogenic effect, but erlotinib did not affect the adenoma size as previously described (Roberts et al., 2002). This inefficacy of erlotinib reducing the tumor growth was accompanied by unaltered level of tumor apoptosis and seemed also related to its angiogenic phenotype that reduced hypoxia by “normalizing the tumor vasculature”. Erlotinib promoted Notch1 activation in the tumors, which has been extensively shown to be a critical regulator of tumor angiogenesis (Dufraine et al., 2008) and apoptosis (Qiao & Wong, 2009) and therefore may be connected to the lack of efficacy in reducing tumor growth of erlotinib therapy. Nevertheless, when we associated

Dll4-Fc to erlotinib, the angiogenic effect of Dll4-Fc was stronger than the effect of erlotinib and therefore the treated tumors were smaller than the controls. More importantly, the combination of Dll4-Fc and erlotinib had an additive effect reducing the tumor number by inhibiting the tumor proliferation and maintenance of Lgr5 positive tumor stem cells through downregulation of the cell cycle regulators c-Myc, and Cyclin D1 and D2, mostly independently of β-catenin activation. Dll4-Fc had also a negative effect on *Bmi1* expression and a more pronounced effect in reducing tumor proliferation than erlotinib, which can be associated to the observed increase of the Cyclin-dependent kinase inhibitors *Cdkn1b and c* only in the Dll4-Fc treated tumors. the Dll4-Fc therapy alone inhibited the neoplastic transformation, and led to tumor differentiation, probably associated to *Cdkn1b* upregulation. This differentiation was moderately deviated towards the secretory cell fates. However, when Dll4-Fc was combined with erlotinib, the increase of differentiation was not deviated into any specific lineage, possibly because erlotinib caused the activation of Notch1 signaling and therefore repressed *Atoh1* expression.

In summary, in the present work we observed that Dll4/Notch signaling promotes the establishment and growth of inflammation-related and $Apc^{Min/+}$ dysplastic intestinal adenomas by regulating: angiogenesis, inflammation, proliferation, apoptosis, differentiation/ neoplastic transformation, and the maintenance of tumor stem cells. In addition, we dissected that most of these processes are regulated through angiogenic, but also by non-angiogenic related mechanisms. All the strategies used to inhibit Dll4/Notch signaling were greatly effective in reducing the intestinal tumor multiplicity and size, mainly in the colitis-driven tumors. Paradoxically, the anti-angiogenic phenotype induced by endothelial-specific activation of Dll4 was almost as effective inhibiting the tumor development as the dysfunctional vasculature promoted by endothelial *Dll4* loss-of-function. Furthermore, we found that Dll4-Fc therapy did not impair the delivery of erlotinib to the tumors, but instead these therapies had a synergistic effect on intestinal tumorigenesis without promoting toxicity. Therefore, either Dll4/Notch inactivation or activation-based therapeutic approaches, and mainly targeting DLL4/Notch and EGFR simultaneously, should be considered at initial stages of CRC and as chemoprevention on patients predisposed to this disease, such as FAP and IBD patients.

6 REFERENCES

Abdou, A. G., Aiad, H., Asaad, N., Abd El-Wahed, M., & Serag El-Dien, M. (2006). Immunohistochemical evaluation of vascular endothelial growth factor (VEGF) in colorectal carcinoma. *J Egypt Natl Canc Inst, 18*(4), 311-322.

Akiyoshi, T., Nakamura, M., Yanai, K., Nagai, S., Wada, J., Koga, K., . . . Katano, M. (2008). Gamma-secretase inhibitors enhance taxane-induced mitotic arrest and apoptosis in colon cancer cells. *Gastroenterology, 134*(1), 131-144. doi: 10.1053/j.gastro.2007.10.008

Alferez, D., Wilkinson, R. W., Watkins, J., Poulsom, R., Mandir, N., Wedge, S. R., . . . Goodlad, R. A. (2008). Dual inhibition of VEGFR and EGFR signaling reduces the incidence and size of intestinal adenomas in Apc(Min/+) mice. *Mol Cancer Ther, 7*(3), 590-598. doi: 10.1158/1535-7163.MCT-07-0433

Allegra, C. J., Yothers, G., O'Connell, M. J., Sharif, S., Petrelli, N. J., Lopa, S. H., & Wolmark, N. (2013). Bevacizumab in stage II-III colon cancer: 5-year update of the National Surgical Adjuvant Breast and Bowel Project C-08 trial. *J Clin Oncol, 31*(3), 359-364. doi: 10.1200/JCO.2012.44.4711

Amersi, F., Agustin, M., & Ko, C. Y. (2005). Colorectal cancer: epidemiology, risk factors, and health services. *Clin Colon Rectal Surg, 18*(3), 133-140. doi: 10.1055/s-2005-916274

Amsen, D., Antov, A., Jankovic, D., Sher, A., Radtke, F., Souabni, A., . . . Flavell, R. A. (2007). Direct regulation of Gata3 expression determines the T helper differentiation potential of Notch. *Immunity, 27*(1), 89-99. doi: 10.1016/j.immuni.2007.05.021

Amsen, D., Blander, J. M., Lee, G. R., Tanigaki, K., Honjo, T., & Flavell, R. A. (2004). Instruction of distinct CD4 T helper cell fates by different notch ligands on antigen-presenting cells. *Cell, 117*(4), 515-526.

Anastasi, E., Campese, A. F., Bellavia, D., Bulotta, A., Balestri, A., Pascucci, M., . . . Screpanti, I. (2003). Expression of activated Notch3 in transgenic mice enhances generation of T regulatory cells and protects against experimental autoimmune diabetes. *J Immunol, 171*(9), 4504-4511.

Andersen, P., Uosaki, H., Shenje, L. T., & Kwon, C. (2012). Non-canonical Notch signaling: emerging role and mechanism. *Trends Cell Biol, 22*(5), 257-265. doi: 10.1016/j.tcb.2012.02.003

Artavanis-Tsakonas, S., Rand, M. D., & Lake, R. J. (1999). Notch signaling: cell fate control and signal integration in development. *Science, 284*(5415), 770-776.

Arthur, J. C., Perez-Chanona, E., Muhlbauer, M., Tomkovich, S., Uronis, J. M., Fan, T. J., . . . Jobin, C. (2012). Intestinal inflammation targets cancer-inducing activity of the microbiota. *Science, 338*(6103), 120-123. doi: 10.1126/science.1224820

Aster, J. C. (2014). In brief: Notch signalling in health and disease. *J Pathol, 232*(1), 1-3. doi: 10.1002/path.4291

Bach, S. P., Renehan, A. G., & Potten, C. S. (2000). Stem cells: the intestinal stem cell as a paradigm. *Carcinogenesis, 21*(3), 469-476.

Baker, A. T., Zlobin, A., & Osipo, C. (2014). Notch-EGFR/HER2 Bidirectional Crosstalk in Breast Cancer. *Front Oncol, 4*, 360. doi: 10.3389/fonc.2014.00360

Barber, T. D., Vogelstein, B., Kinzler, K. W., & Velculescu, V. E. (2004). Somatic mutations of EGFR in colorectal cancers and glioblastomas. *N Engl J Med, 351*(27), 2883. doi: 10.1056/NEJM200412303512724

Bardelli, A., & Siena, S. (2010). Molecular mechanisms of resistance to cetuximab and panitumumab in colorectal cancer. *J Clin Oncol, 28*(7), 1254-1261. doi: 10.1200/JCO.2009.24.6116

Barker, N., van Es, J. H., Kuipers, J., Kujala, P., van den Born, M., Cozijnsen, M., . . . Clevers, H. (2007). Identification of stem cells in small intestine and colon by marker gene Lgr5. *Nature, 449*(7165), 1003-1007. doi: 10.1038/nature06196

Bassil, R., Zhu, B., Lahoud, Y., Riella, L. V., Yagita, H., Elyaman, W., & Khoury, S. J. (2011). Notch ligand delta-like 4 blockade alleviates experimental autoimmune encephalomyelitis by promoting regulatory T cell development. *J Immunol, 187*(5), 2322-2328. doi: 10.4049/jimmunol.1100725

Batlle, E., Henderson, J. T., Beghtel, H., van den Born, M. M., Sancho, E., Huls, G., . . . Clevers, H. (2002). Beta-catenin and TCF mediate cell positioning in the intestinal epithelium by controlling the expression of EphB/ephrinB. *Cell, 111*(2), 251-263.

Becker, C., Fantini, M. C., Schramm, C., Lehr, H. A., Wirtz, S., Nikolaev, A., . . . Neurath, M. F. (2004). TGF-beta suppresses tumor progression in colon cancer by inhibition of IL-6 trans-signaling. *Immunity, 21*(4), 491-501. doi: 10.1016/j.immuni.2004.07.020

Becker, C., Fantini, M. C., Wirtz, S., Nikolaev, A., Kiesslich, R., Lehr, H. A., . . . Neurath, M. F. (2005). In vivo imaging of colitis and colon cancer development in mice using high resolution chromoendoscopy. *Gut, 54*(7), 950-954. doi: 10.1136/gut.2004.061283

Benedito, R., & Duarte, A. (2005). Expression of Dll4 during mouse embryogenesis suggests multiple developmental roles. *Gene Expr Patterns, 5*(6), 750-755. doi: 10.1016/j.modgep.2005.04.004

Berg, D. J., Davidson, N., Kuhn, R., Muller, W., Menon, S., Holland, G., . . . Rennick, D. (1996). Enterocolitis and colon cancer in interleukin-10-deficient mice are associated with aberrant cytokine production and CD4(+) TH1-like responses. *J Clin Invest, 98*(4), 1010-1020. doi: 10.1172/JCI118861

Bienz, M., & Clevers, H. (2000). Linking colorectal cancer to Wnt signaling. *Cell, 103*(2), 311-320.

Binefa, G., Rodriguez-Moranta, F., Teule, A., & Medina-Hayas, M. (2014). Colorectal cancer: from prevention to personalized medicine. *World J Gastroenterol, 20*(22), 6786-6808. doi: 10.3748/wjg.v20.i22.6786

Bird, R. P., & Good, C. K. (2000). The significance of aberrant crypt foci in understanding the pathogenesis of colon cancer. *Toxicol Lett, 112-113*, 395-402.

Bisgaard, M. L., Fenger, K., Bulow, S., Niebuhr, E., & Mohr, J. (1994). Familial adenomatous polyposis (FAP): frequency, penetrance, and mutation rate. *Hum Mutat, 3*(2), 121-125. doi: 10.1002/humu.1380030206

Bissahoyo, A., Pearsall, R. S., Hanlon, K., Amann, V., Hicks, D., Godfrey, V. L., & Threadgill, D. W. (2005). Azoxymethane is a genetic background-dependent colorectal tumor initiator and promoter in mice: effects of dose, route, and diet. *Toxicol Sci, 88*(2), 340-345. doi: 10.1093/toxsci/kfi313

Bjerknes, M., & Cheng, H. (1999). Clonal analysis of mouse intestinal epithelial progenitors. *Gastroenterology, 116*(1), 7-14.

Blat, D., Zigmond, E., Alteber, Z., Waks, T., & Eshhar, Z. (2014). Suppression of murine colitis and its associated cancer by carcinoembryonic antigen-specific regulatory T cells. *Mol Ther, 22*(5), 1018-1028. doi: 10.1038/mt.2014.41

Bogaert, J., & Prenen, H. (2014). Molecular genetics of colorectal cancer. *Ann Gastroenterol, 27*(1), 9-14.

Boivin, G. P., Washington, K., Yang, K., Ward, J. M., Pretlow, T. P., Russell, R., . . . Coffey, R. J. (2003). Pathology of mouse models of intestinal cancer: consensus report and recommendations. *Gastroenterology, 124*(3), 762-777. doi: 10.1053/gast.2003.50094

Booth, C., & Potten, C. S. (2000). Gut instincts: thoughts on intestinal epithelial stem cells. *J Clin Invest, 105*(11), 1493-1499. doi: 10.1172/JCI10229

Brabletz, T., Jung, A., Dag, S., Hlubek, F., & Kirchner, T. (1999). beta-catenin regulates the expression of the matrix metalloproteinase-7 in human colorectal cancer. *Am J Pathol, 155*(4), 1033-1038.

Bray, S. J. (2006). Notch signalling: a simple pathway becomes complex. *Nat Rev Mol Cell Biol, 7*(9), 678-689. doi: 10.1038/nrm2009

Buczacki, S. J., Zecchini, H. I., Nicholson, A. M., Russell, R., Vermeulen, L., Kemp, R., & Winton, D. J. (2013). Intestinal label-retaining cells are secretory precursors expressing Lgr5. *Nature, 495*(7439), 65-69. doi: 10.1038/nature11965

Campese, A. F., Grazioli, P., Colantoni, S., Anastasi, E., Mecarozzi, M., Checquolo, S., . . . Screpanti, I. (2009). Notch3 and pTalpha/pre-TCR sustain the in vivo function of naturally occurring regulatory T cells. *Int Immunol, 21*(6), 727-743. doi: 10.1093/intimm/dxp042

Cappuzzo, F., Finocchiaro, G., Rossi, E., Janne, P. A., Carnaghi, C., Calandri, C., . . . Varella-Garcia, M. (2008). EGFR FISH assay predicts for response to cetuximab in

chemotherapy refractory colorectal cancer patients. *Ann Oncol, 19*(4), 717-723. doi: 10.1093/annonc/mdm492

Chen, M. L., Pittet, M. J., Gorelik, L., Flavell, R. A., Weissleder, R., von Boehmer, H., & Khazaie, K. (2005). Regulatory T cells suppress tumor-specific CD8 T cell cytotoxicity through TGF-beta signals in vivo. *Proc Natl Acad Sci U S A, 102*(2), 419-424. doi: 10.1073/pnas.0408197102

Cheng, H., & Bjerknes, M. (1983). Cell production in mouse intestinal epithelium measured by stathmokinetic flow cytometry and Coulter particle counting. *Anat Rec, 207*(3), 427-434. doi: 10.1002/ar.1092070305

Cheng, H., & Leblond, C. P. (1974). Origin, differentiation and renewal of the four main epithelial cell types in the mouse small intestine. V. Unitarian Theory of the origin of the four epithelial cell types. *Am J Anat, 141*(4), 537-561. doi: 10.1002/aja.1001410407

Chichlowski, M., Sharp, J. M., Vanderford, D. A., Myles, M. H., & Hale, L. P. (2008). Helicobacter typhlonius and Helicobacter rodentium differentially affect the severity of colon inflammation and inflammation-associated neoplasia in IL10-deficient mice. *Comp Med, 58*(6), 534-541.

Chichlowski, M., Westwood, G. S., Abraham, S. N., & Hale, L. P. (2010). Role of mast cells in inflammatory bowel disease and inflammation-associated colorectal neoplasia in IL-10-deficient mice. *PLoS One, 5*(8), e12220. doi: 10.1371/journal.pone.0012220

Chittenden, T. W., Howe, E. A., Culhane, A. C., Sultana, R., Taylor, J. M., Holmes, C., & Quackenbush, J. (2008). Functional classification analysis of somatically mutated genes in human breast and colorectal cancers. *Genomics, 91*(6), 508-511. doi: 10.1016/j.ygeno.2008.03.002

Cho, K. R., & Vogelstein, B. (1992). Suppressor gene alterations in the colorectal adenoma-carcinoma sequence. *J Cell Biochem Suppl, 16G*, 137-141.

Chu, D., Zhang, Z., Zhou, Y., Wang, W., Li, Y., Zhang, H., . . . Ji, G. (2011). Notch1 and Notch2 have opposite prognostic effects on patients with colorectal cancer. *Ann Oncol, 22*(11), 2440-2447. doi: 10.1093/annonc/mdq776

Citri, A., & Yarden, Y. (2006). EGF-ERBB signalling: towards the systems level. *Nat Rev Mol Cell Biol, 7*(7), 505-516. doi: 10.1038/nrm1962

Cole, A. M., Myant, K., Reed, K. R., Ridgway, R. A., Athineos, D., Van den Brink, G. R., . . . Sansom, O. J. (2010). Cyclin D2-cyclin-dependent kinase 4/6 is required for efficient proliferation and tumorigenesis following Apc loss. *Cancer Res, 70*(20), 8149-8158. doi: 10.1158/0008-5472.CAN-10-0315

Cooper, H. S., Murthy, S. N., Shah, R. S., & Sedergran, D. J. (1993). Clinicopathologic study of dextran sulfate sodium experimental murine colitis. *Lab Invest, 69*(2), 238-249.

Corpet, D. E., & Pierre, F. (2005). How good are rodent models of carcinogenesis in predicting efficacy in humans? A systematic review and meta-analysis of colon chemoprevention in rats, mice and men. *Eur J Cancer, 41*(13), 1911-1922. doi: 10.1016/j.ejca.2005.06.006

Crawford, H. C., Fingleton, B. M., Rudolph-Owen, L. A., Goss, K. J., Rubinfeld, B., Polakis, P., & Matrisian, L. M. (1999). The metalloproteinase matrilysin is a target of beta-catenin transactivation in intestinal tumors. *Oncogene, 18*(18), 2883-2891. doi: 10.1038/sj.onc.1202627

Dai, Y., Wilson, G., Huang, B., Peng, M., Teng, G., Zhang, D., . . . Qiao, L. (2014). Silencing of Jagged1 inhibits cell growth and invasion in colorectal cancer. *Cell Death Dis, 5*, e1170. doi: 10.1038/cddis.2014.137

Dalerba, P., Dylla, S. J., Park, I. K., Liu, R., Wang, X., Cho, R. W., . . . Clarke, M. F. (2007). Phenotypic characterization of human colorectal cancer stem cells. *Proc Natl Acad Sci U S A, 104*(24), 10158-10163. doi: 10.1073/pnas.0703478104

Danese, S., Malesci, A., & Vetrano, S. (2011). Colitis-associated cancer: the dark side of inflammatory bowel disease. *Gut, 60*(12), 1609-1610. doi: 10.1136/gutjnl-2011-300953

Dass, C. R. (2004). Tumour angiogenesis, vascular biology and enhanced drug delivery. *J Drug Target, 12*(5), 245-255. doi: 10.1080/10611860410001713163

de Gramont, A., Van Cutsem, E., Schmoll, H. J., Tabernero, J., Clarke, S., Moore, M. J., . . . Hoff, P. M. (2012). Bevacizumab plus oxaliplatin-based chemotherapy as adjuvant treatment for colon cancer (AVANT): a phase 3 randomised controlled trial. *Lancet Oncol, 13*(12), 1225-1233. doi: 10.1016/S1470-2045(12)70509-0

de Lau, W., Barker, N., & Clevers, H. (2007). WNT signaling in the normal intestine and colorectal cancer. *Front Biosci, 12*, 471-491.

De Robertis, M., Massi, E., Poeta, M. L., Carotti, S., Morini, S., Cecchetelli, L., . . . Fazio, V. M. (2011). The AOM/DSS murine model for the study of colon carcinogenesis: From pathways to diagnosis and therapy studies. *J Carcinog, 10*, 9. doi: 10.4103/1477-3163.78279

de Vries, C., Escobedo, J. A., Ueno, H., Houck, K., Ferrara, N., & Williams, L. T. (1992). The fms-like tyrosine kinase, a receptor for vascular endothelial growth factor. *Science, 255*(5047), 989-991.

Deacu, E., Mori, Y., Sato, F., Yin, J., Olaru, A., Sterian, A., . . . Meltzer, S. J. (2004). Activin type II receptor restoration in ACVR2-deficient colon cancer cells induces transforming growth factor-beta response pathway genes. *Cancer Res, 64*(21), 7690-7696. doi: 10.1158/0008-5472.CAN-04-2082

Deschenes, C., Vezina, A., Beaulieu, J. F., & Rivard, N. (2001). Role of p27(Kip1) in human intestinal cell differentiation. *Gastroenterology, 120*(2), 423-438.

Djokovic, D., Trindade, A., Gigante, J., Badenes, M., Silva, L., Liu, R., . . . Duarte, A. (2010). Combination of Dll4/Notch and Ephrin-B2/EphB4 targeted therapy is highly effective in disrupting tumor angiogenesis. *BMC Cancer, 10*, 641. doi: 10.1186/1471-2407-10-641

Dong, Y., Li, A., Wang, J., Weber, J. D., & Michel, L. S. (2010). Synthetic lethality through combined Notch-epidermal growth factor receptor pathway inhibition in basal-like breast cancer. *Cancer Res, 70*(13), 5465-5474. doi: 10.1158/0008-5472.CAN-10-0173

Duarte, A. (2004). Dosage-sensitive requirement for mouse Dll4 in artery development. *Genes Dev, 18*(20), 2474-2478. doi: 10.1101/gad.1239004

Dufraine, J., Funahashi, Y., & Kitajewski, J. (2008). Notch signaling regulates tumor angiogenesis by diverse mechanisms. *Oncogene, 27*(38), 5132-5137. doi: 10.1038/onc.2008.227

Dvorak, H. F., Brown, L. F., Detmar, M., & Dvorak, A. M. (1995). Vascular permeability factor/vascular endothelial growth factor, microvascular hyperpermeability, and angiogenesis. *Am J Pathol, 146*(5), 1029-1039.

Efstratiadis, A., Szabolcs, M., & Klinakis, A. (2007). Notch, Myc and breast cancer. *Cell Cycle, 6*(4), 418-429.

Ekbom, A., Helmick, C., Zack, M., & Adami, H. O. (1990). Increased risk of large-bowel cancer in Crohn's disease with colonic involvement. *Lancet, 336*(8711), 357-359. doi: 0140-6736(90)91889-I [pii]

El Kaffas, A., Nofiele, J., Giles, A., Cho, S., Liu, S. K., & Czarnota, G. J. (2014). Dll4-notch signalling blockade synergizes combined ultrasound-stimulated microbubble and radiation therapy in human colon cancer xenografts. *PLoS One, 9*(4), e93888. doi: 10.1371/journal.pone.0093888

Ellis, L. M. (2003). A targeted approach for antiangiogenic therapy of metastatic human colon cancer. *Am Surg, 69*(1), 3-10.

Ellis, L. M. (2004). Angiogenesis and its role in colorectal tumor and metastasis formation. *Semin Oncol, 31*(6 Suppl 17), 3-9. doi: 10.1053/j.seminoncol.2004.11.028

Ellis, L. M., Takahashi, Y., Liu, W., & Shaheen, R. M. (2000). Vascular endothelial growth factor in human colon cancer: biology and therapeutic implications. *Oncologist, 5 Suppl 1*, 11-15.

Elyaman, W., Bradshaw, E. M., Wang, Y., Oukka, M., Kivisakk, P., Chiba, S., . . . Khoury, S. J. (2007). JAGGED1 and delta1 differentially regulate the outcome of experimental autoimmune encephalomyelitis. *J Immunol, 179*(9), 5990-5998.

Eng, C. (2009). Toxic effects and their management: daily clinical challenges in the treatment of colorectal cancer. *Nat Rev Clin Oncol, 6*(4), 207-218. doi: 10.1038/nrclinonc.2009.16

Eppert, K., Scherer, S. W., Ozcelik, H., Pirone, R., Hoodless, P., Kim, H., . . . Attisano, L. (1996). MADR2 maps to 18q21 and encodes a TGFbeta-regulated MAD-related protein that is functionally mutated in colorectal carcinoma. *Cell, 86*(4), 543-552.

Erdman, S. E., Sohn, J. J., Rao, V. P., Nambiar, P. R., Ge, Z., Fox, J. G., & Schauer, D. B. (2005). CD4+CD25+ regulatory lymphocytes induce regression of intestinal tumors in ApcMin/+ mice. *Cancer Res, 65*(10), 3998-4004. doi: 10.1158/0008-5472.CAN-04-3104

Espersen, M. L., Olsen, J., Linnemann, D., Hogdall, E., & Troelsen, J. T. (2015). Clinical Implications of Intestinal Stem Cell Markers in Colorectal Cancer. *Clin Colorectal Cancer, 14*(2), 63-71. doi: 10.1016/j.clcc.2014.12.004

Espinosa, L., Ingles-Esteve, J., Aguilera, C., & Bigas, A. (2003). Phosphorylation by glycogen synthase kinase-3 beta down-regulates Notch activity, a link for Notch and Wnt pathways. *J Biol Chem, 278*(34), 32227-32235. doi: 10.1074/jbc.M304001200

Fang, T. C., Yashiro-Ohtani, Y., Del Bianco, C., Knoblock, D. M., Blacklow, S. C., & Pear, W. S. (2007). Notch directly regulates Gata3 expression during T helper 2 cell differentiation. *Immunity, 27*(1), 100-110. doi: 10.1016/j.immuni.2007.04.018

Farrington, S. M., Tenesa, A., Barnetson, R., Wiltshire, A., Prendergast, J., Porteous, M., . . . Dunlop, M. G. (2005). Germline susceptibility to colorectal cancer due to base-excision repair gene defects. *Am J Hum Genet, 77*(1), 112-119. doi: 10.1086/431213

Fearnhead, N. S., Britton, M. P., & Bodmer, W. F. (2001). The ABC of APC. *Hum Mol Genet, 10*(7), 721-733.

Fearon, E. R., & Vogelstein, B. (1990). A genetic model for colorectal tumorigenesis. *Cell, 61*(5), 759-767.

Ferguson, L. R. (2010). Chronic inflammation and mutagenesis. *Mutat Res, 690*(1-2), 3-11. doi: 10.1016/j.mrfmmm.2010.03.007

Fernandes, S. M., Pires, A. R., Ferreira, C., Foxall, R. B., Rino, J., Santos, C., . . . Sousa, A. E. (2014). Enteric mucosa integrity in the presence of a preserved innate interleukin 22 compartment in HIV type 1-treated individuals. *J Infect Dis, 210*(4), 630-640. doi: 10.1093/infdis/jiu126

Fernandez-Majada, V., Aguilera, C., Villanueva, A., Vilardell, F., Robert-Moreno, A., Aytes, A., . . . Bigas, A. (2007). Nuclear IKK activity leads to dysregulated notch-dependent gene expression in colorectal cancer. *Proc Natl Acad Sci U S A, 104*(1), 276-281. doi: 10.1073/pnas.0606476104

Ferrara, N., Gerber, H. P., & LeCouter, J. (2003). The biology of VEGF and its receptors. *Nat Med, 9*(6), 669-676. doi: 10.1038/nm0603-669

Ferrara, N., Houck, K., Jakeman, L., & Leung, D. W. (1992). Molecular and biological properties of the vascular endothelial growth factor family of proteins. *Endocr Rev, 13*(1), 18-32. doi: 10.1210/edrv-13-1-18

Ferrarotto, R., & Hoff, P. M. (2013). Antiangiogenic drugs for colorectal cancer: exploring new possibilities. *Clin Colorectal Cancer, 12*(1), 1-7. doi: 10.1016/j.clcc.2012.06.002

Fischer, A., & Gessler, M. (2007). Delta-Notch--and then? Protein interactions and proposed modes of repression by Hes and Hey bHLH factors. *Nucleic Acids Res, 35*(14), 4583-4596. doi: 10.1093/nar/gkm477

Fischer, M., Yen, W. C., Kapoun, A. M., Wang, M., O'Young, G., Lewicki, J., . . . Hoey, T. (2010). Anti-DLL4 Inhibits Growth and Reduces Tumor-Initiating Cell Frequency in Colorectal Tumors with Oncogenic KRAS Mutations. *Cancer Res, 71*(5), 1520-1525. doi: 10.1158/0008-5472.can-10-2817

Flavell, R. A., Sanjabi, S., Wrzesinski, S. H., & Licona-Limon, P. (2010). The polarization of immune cells in the tumour environment by TGFbeta. *Nat Rev Immunol, 10*(8), 554-567. doi: 10.1038/nri2808

Foersch, S., & Neurath, M. F. (2014). Colitis-associated neoplasia: molecular basis and clinical translation. *Cell Mol Life Sci, 71*(18), 3523-3535. doi: 10.1007/s00018-014-1636-x

Folkman, J. (1971). Tumor angiogenesis: therapeutic implications. *N Engl J Med, 285*(21), 1182-1186. doi: 10.1056/NEJM197111182852108

Folkman, J. (1990). What is the evidence that tumors are angiogenesis dependent? *J Natl Cancer Inst, 82*(1), 4-6.

Folkman, J. (1992). The role of angiogenesis in tumor growth. *Semin Cancer Biol, 3*(2), 65-71.

Folkman, J., & Hanahan, D. (1991). Switch to the angiogenic phenotype during tumorigenesis. *Princess Takamatsu Symp, 22*, 339-347.

Fouser, L. A., Wright, J. F., Dunussi-Joannopoulos, K., & Collins, M. (2008). Th17 cytokines and their emerging roles in inflammation and autoimmunity. *Immunol Rev, 226*, 87-102. doi: 10.1111/j.1600-065X.2008.00712.x

Fre, S., Huyghe, M., Mourikis, P., Robine, S., Louvard, D., & Artavanis-Tsakonas, S. (2005). Notch signals control the fate of immature progenitor cells in the intestine. *Nature, 435*(7044), 964-968. doi: 10.1038/nature03589

Fre, S., Pallavi, S. K., Huyghe, M., Lae, M., Janssen, K. P., Robine, S., . . . Louvard, D. (2009). Notch and Wnt signals cooperatively control cell proliferation and tumorigenesis in the intestine. *Proc Natl Acad Sci U S A, 106*(15), 6309-6314. doi: 10.1073/pnas.0900427106

Fukuda, D., Aikawa, E., Swirski, F. K., Novobrantseva, T. I., Kotelianski, V., Gorgun, C. Z., . . . Aikawa, M. (2012). Notch ligand delta-like 4 blockade attenuates atherosclerosis and metabolic disorders. *Proc Natl Acad Sci U S A, 109*(27), E1868-1877. doi: 10.1073/pnas.1116889109

Fukushima, A., Sumi, T., Ishida, W., Ojima, A., Kajisako, M., Koyanagi, A., . . . Yagita, H. (2008). Notch ligand Delta-like4 inhibits the development of murine experimental allergic conjunctivitis. *Immunol Lett, 121*(2), 140-147. doi: 10.1016/j.imlet.2008.10.006

Fulton, D., Gratton, J. P., McCabe, T. J., Fontana, J., Fujio, Y., Walsh, K., . . . Sessa, W. C. (1999). Regulation of endothelium-derived nitric oxide production by the protein kinase Akt. *Nature, 399*(6736), 597-601. doi: 10.1038/21218

Funahashi, Y., Shawber, C. J., Sharma, A., Kanamaru, E., Choi, Y. K., & Kitajewski, J. (2011). Notch modulates VEGF action in endothelial cells by inducing Matrix Metalloprotease activity. *Vasc Cell, 3*(1), 2. doi: 10.1186/2045-824X-3-2

Fung, E., Tang, S. M., Canner, J. P., Morishige, K., Arboleda-Velasquez, J. F., Cardoso, A. A., . . . Aikawa, M. (2007). Delta-like 4 induces notch signaling in macrophages: implications for inflammation. *Circulation, 115*(23), 2948-2956. doi: 10.1161/CIRCULATIONAHA.106.675462

Galceran, J., Sustmann, C., Hsu, S. C., Folberth, S., & Grosschedl, R. (2004). LEF1-mediated regulation of Delta-like1 links Wnt and Notch signaling in somitogenesis. *Genes Dev, 18*(22), 2718-2723. doi: 10.1101/gad.1249504

Gale, N. W. (2004). Haploinsufficiency of delta-like 4 ligand results in embryonic lethality due to major defects in arterial and vascular development. *Proceedings of the National Academy of Sciences, 101*(45), 15949-15954. doi: 10.1073/pnas.0407290101

Garabedian, E. M., Roberts, L. J., McNevin, M. S., & Gordon, J. I. (1997). Examining the role of Paneth cells in the small intestine by lineage ablation in transgenic mice. *J Biol Chem, 272*(38), 23729-23740.

Gerbe, F., van Es, J. H., Makrini, L., Brulin, B., Mellitzer, G., Robine, S., . . . Jay, P. (2011). Distinct ATOH1 and Neurog3 requirements define tuft cells as a new secretory cell type in the intestinal epithelium. *J Cell Biol, 192*(5), 767-780. doi: 10.1083/jcb.201010127

Gersemann, M., Becker, S., Kubler, I., Koslowski, M., Wang, G., Herrlinger, K. R., . . . Stange, E. F. (2009). Differences in goblet cell differentiation between Crohn's disease and ulcerative colitis. *Differentiation, 77*(1), 84-94. doi: 10.1016/j.diff.2008.09.008

Ghaleb, A. M., Aggarwal, G., Bialkowska, A. B., Nandan, M. O., & Yang, V. W. (2008). Notch inhibits expression of the Kruppel-like factor 4 tumor suppressor in the intestinal epithelium. *Mol Cancer Res, 6*(12), 1920-1927. doi: 10.1158/1541-7786.MCR-08-0224

Ghaleb, A. M., McConnell, B. B., Nandan, M. O., Katz, J. P., Kaestner, K. H., & Yang, V. W. (2007). Haploinsufficiency of Kruppel-like factor 4 promotes adenomatous polyposis coli dependent intestinal tumorigenesis. *Cancer Res, 67*(15), 7147-7154. doi: 10.1158/0008-5472.CAN-07-1302

Giles, R. H., van Es, J. H., & Clevers, H. (2003). Caught up in a Wnt storm: Wnt signaling in cancer. *Biochim Biophys Acta, 1653*(1), 1-24.

Goel, H. L., & Mercurio, A. M. (2013). VEGF targets the tumour cell. *Nat Rev Cancer, 13*(12), 871-882. doi: 10.1038/nrc3627

Goldstein, N. S., & Armin, M. (2001). Epidermal growth factor receptor immunohistochemical reactivity in patients with American Joint Committee on Cancer Stage IV colon adenocarcinoma: implications for a standardized scoring system. *Cancer, 92*(5), 1331-1346.

Gonzalez, C. A., & Riboli, E. (2010). Diet and cancer prevention: Contributions from the European Prospective Investigation into Cancer and Nutrition (EPIC) study. *Eur J Cancer, 46*(14), 2555-2562. doi: 10.1016/j.ejca.2010.07.025

Gopalakrishnan, N., Saravanakumar, M., Madankumar, P., Thiyagu, M., & Devaraj, H. (2014). Colocalization of beta-catenin with Notch intracellular domain in colon cancer: a possible role of Notch1 signaling in activation of CyclinD1-mediated cell proliferation. *Mol Cell Biochem, 396*(1-2), 281-293. doi: 10.1007/s11010-014-2163-7

Gopalappa, C., Aydogan-Cremaschi, S., Das, T. K., & Orcun, S. (2011). Probability model for estimating colorectal polyp progression rates. *Health Care Manag Sci, 14*(1), 1-21. doi: 10.1007/s10729-010-9138-3

Grady, W. M., & Carethers, J. M. (2008). Genomic and epigenetic instability in colorectal cancer pathogenesis. *Gastroenterology, 135*(4), 1079-1099. doi: 10.1053/j.gastro.2008.07.076

Grady, W. M., Myeroff, L. L., Swinler, S. E., Rajput, A., Thiagalingam, S., Lutterbaugh, J. D., . . . Markowitz, S. (1999). Mutational inactivation of transforming growth factor beta receptor type II in microsatellite stable colon cancers. *Cancer Res, 59*(2), 320-324.

Grant, S., Qiao, L., & Dent, P. (2002). Roles of ERBB family receptor tyrosine kinases, and downstream signaling pathways, in the control of cell growth and survival. *Front Biosci, 7*, d376-389.

Greten, F. R., Eckmann, L., Greten, T. F., Park, J. M., Li, Z. W., Egan, L. J., . . . Karin, M. (2004). IKKbeta links inflammation and tumorigenesis in a mouse model of colitis-associated cancer. *Cell, 118*(3), 285-296. doi: 10.1016/j.cell.2004.07.013

Gridley, T. (1997). Notch signaling in vertebrate development and disease. *Mol Cell Neurosci, 9*(2), 103-108. doi: 10.1006/mcne.1997.0610

Grivennikov, S., Karin, E., Terzic, J., Mucida, D., Yu, G. Y., Vallabhapurapu, S., . . . Karin, M. (2009). IL-6 and Stat3 are required for survival of intestinal epithelial cells and development of colitis-associated cancer. *Cancer Cell, 15*(2), 103-113. doi: 10.1016/j.ccr.2009.01.001

Guilmeau, S., Flandez, M., Mariadason, J. M., & Augenlicht, L. H. (2010). Heterogeneity of Jagged1 expression in human and mouse intestinal tumors: implications for targeting Notch signaling. *Oncogene, 29*(7), 992-1002. doi: 10.1038/onc.2009.393

Hacker, H., & Karin, M. (2006). Regulation and function of IKK and IKK-related kinases. *Sci STKE, 2006*(357), re13. doi: 10.1126/stke.3572006re13

Haggitt, R. C., & Reid, B. J. (1986). Hereditary gastrointestinal polyposis syndromes. *Am J Surg Pathol, 10*(12), 871-887.

Half, E., Bercovich, D., & Rozen, P. (2009). Familial adenomatous polyposis. *Orphanet J Rare Dis, 4*, 22. doi: 10.1186/1750-1172-4-22

Hanahan, D., & Weinberg, R. A. (2000). The hallmarks of cancer. *Cell, 100*(1), 57-70. doi: S0092-8674(00)81683-9 [pii]

Harrington, L. S., Sainson, R. C., Williams, C. K., Taylor, J. M., Shi, W., Li, J. L., & Harris, A. L. (2008). Regulation of multiple angiogenic pathways by Dll4 and Notch in human umbilical vein endothelial cells. *Microvasc Res, 75*(2), 144-154. doi: 10.1016/j.mvr.2007.06.006

Hayden, E. C. (2009). Cutting off cancer's supply lines. *Nature, 458*(7239), 686-687. doi: 10.1038/458686b

He, T. C., Sparks, A. B., Rago, C., Hermeking, H., Zawel, L., da Costa, L. T., . . . Kinzler, K. W. (1998). Identification of c-MYC as a target of the APC pathway. *Science, 281*(5382), 1509-1512.

Hellström, M., Phng, L.-K., Hofmann, J. J., Wallgard, E., Coultas, L., Lindblom, P., . . . Betsholtz, C. (2007). Dll4 signalling through Notch1 regulates formation of tip cells during angiogenesis. *Nature, 445*(7129), 776-780. doi: 10.1038/nature05571

Hermiston, M. L., Wong, M. H., & Gordon, J. I. (1996). Forced expression of E-cadherin in the mouse intestinal epithelium slows cell migration and provides evidence for nonautonomous regulation of cell fate in a self-renewing system. *Genes Dev, 10*(8), 985-996.

Hiratsuka, S., Minowa, O., Kuno, J., Noda, T., & Shibuya, M. (1998). Flt-1 lacking the tyrosine kinase domain is sufficient for normal development and angiogenesis in mice. *Proc Natl Acad Sci U S A, 95*(16), 9349-9354.

Hoentjen, F., Sartor, R. B., Ozaki, M., & Jobin, C. (2005). STAT3 regulates NF-kappaB recruitment to the IL-12p40 promoter in dendritic cells. *Blood, 105*(2), 689-696. doi: 10.1182/blood-2004-04-1309

Hoey, T., Yen, W. C., Axelrod, F., Basi, J., Donigian, L., Dylla, S., . . . Gurney, A. (2009). DLL4 blockade inhibits tumor growth and reduces tumor-initiating cell frequency. *Cell Stem Cell, 5*(2), 168-177. doi: 10.1016/j.stem.2009.05.019

Hofmann, M., Schuster-Gossler, K., Watabe-Rudolph, M., Aulehla, A., Herrmann, B. G., & Gossler, A. (2004). WNT signaling, in synergy with T/TBX6, controls Notch signaling by regulating Dll1 expression in the presomitic mesoderm of mouse embryos. *Genes Dev, 18*(22), 2712-2717. doi: 10.1101/gad.1248604

Hofseth, L. J., Saito, S., Hussain, S. P., Espey, M. G., Miranda, K. M., Araki, Y., . . . Harris, C. C. (2003). Nitric oxide-induced cellular stress and p53 activation in chronic inflammation. *Proc Natl Acad Sci U S A, 100*(1), 143-148. doi: 10.1073/pnas.0237083100

Hsieh, J. J., Zhou, S., Chen, L., Young, D. B., & Hayward, S. D. (1999). CIR, a corepressor linking the DNA binding factor CBF1 to the histone deacetylase complex. *Proc Natl Acad Sci U S A, 96*(1), 23-28.

Huang, S., Xie, K., Bucana, C. D., Ullrich, S. E., & Bar-Eli, M. (1996). Interleukin 10 suppresses tumor growth and metastasis of human melanoma cells: potential inhibition of angiogenesis. *Clin Cancer Res, 2*(12), 1969-1979.

Huelsken, J., & Birchmeier, W. (2001). New aspects of Wnt signaling pathways in higher vertebrates. *Curr Opin Genet Dev, 11*(5), 547-553.

Hulit, J., Wang, C., Li, Z., Albanese, C., Rao, M., Di Vizio, D., . . . Pestell, R. G. (2004). Cyclin D1 genetic heterozygosity regulates colonic epithelial cell differentiation and tumor number in ApcMin mice. *Mol Cell Biol, 24*(17), 7598-7611. doi: 10.1128/MCB.24.17.7598-7611.2004

Hussain, S. P., Hofseth, L. J., & Harris, C. C. (2003). Radical causes of cancer. *Nat Rev Cancer, 3*(4), 276-285. doi: 10.1038/nrc1046

Hynes, N. E., & Lane, H. A. (2005). ERBB receptors and cancer: the complexity of targeted inhibitors. *Nat Rev Cancer, 5*(5), 341-354. doi: 10.1038/nrc1609

Hyun, Y. S., Han, D. S., Lee, A. R., Eun, C. S., Youn, J., & Kim, H. Y. (2012). Role of IL-17A in the development of colitis-associated cancer. *Carcinogenesis, 33*(4), 931-936. doi: 10.1093/carcin/bgs106

Ignatenko, N. A., Holubec, H., Besselsen, D. G., Blohm-Mangone, K. A., Padilla-Torres, J. L., Nagle, R. B., . . . Gerner, E. W. (2006). Role of c-Myc in intestinal tumorigenesis of the ApcMin/+ mouse. *Cancer Biol Ther, 5*(12), 1658-1664.

Iliev, I. D., Funari, V. A., Taylor, K. D., Nguyen, Q., Reyes, C. N., Strom, S. P., . . . Underhill, D. M. (2012). Interactions between commensal fungi and the C-type lectin receptor Dectin-1 influence colitis. *Science, 336*(6086), 1314-1317. doi: 10.1126/science.1221789

Ishibashi, Y., Tanaka, S., Tajima, K., Yoshida, T., & Kuwano, H. (2006). Expression of Foxp3 in non-small cell lung cancer patients is significantly higher in tumor tissues than in normal tissues, especially in tumors smaller than 30 mm. *Oncol Rep, 15*(5), 1315-1319.

Iso, T., Sartorelli, V., Chung, G., Shichinohe, T., Kedes, L., & Hamamori, Y. (2001). HERP, a new primary target of Notch regulated by ligand binding. *Mol Cell Biol, 21*(17), 6071-6079.

Ito, T., Schaller, M., Hogaboam, C. M., Standiford, T. J., Sandor, M., Lukacs, N. W., . . . Kunkel, S. L. (2009). TLR9 regulates the mycobacteria-elicited pulmonary granulomatous immune response in mice through DC-derived Notch ligand delta-like 4. *J Clin Invest, 119*(1), 33-46. doi: 10.1172/JCI35647

Itzkowitz, S. H., & Harpaz, N. (2004). Diagnosis and management of dysplasia in patients with inflammatory bowel diseases. *Gastroenterology, 126*(6), 1634-1648. doi: S0016508504004603 [pii]

Jain, R. K. (2005). Normalization of tumor vasculature: an emerging concept in antiangiogenic therapy. *Science, 307*(5706), 58-62. doi: 10.1126/science.1104819

Jang, S., Schaller, M., Berlin, A. A., & Lukacs, N. W. (2010). Notch ligand delta-like 4 regulates development and pathogenesis of allergic airway responses by modulating IL-2 production and Th2 immunity. *J Immunol, 185*(10), 5835-5844. doi: 10.4049/jimmunol.1000175

Jass, J. R. (1998). Diagnosis of hereditary non-polyposis colorectal cancer. *Histopathology, 32*(6), 491-497.

Jeffries, S., Robbins, D. J., & Capobianco, A. J. (2002). Characterization of a high-molecular-weight Notch complex in the nucleus of Notch(ic)-transformed RKE cells and in a human T-cell leukemia cell line. *Mol Cell Biol, 22*(11), 3927-3941.

Jemal, A., Bray, F., Center, M. M., Ferlay, J., Ward, E., & Forman, D. (2011). Global cancer statistics. *CA Cancer J Clin, 61*(2), 69-90. doi: 10.3322/caac.20107

Jemal, A., Thomas, A., Murray, T., & Thun, M. (2002). Cancer statistics, 2002. *CA Cancer J Clin, 52*(1), 23-47.

Jenkins, B. J., Grail, D., Nheu, T., Najdovska, M., Wang, B., Waring, P., . . . Ernst, M. (2005). Hyperactivation of Stat3 in gp130 mutant mice promotes gastric hyperproliferation and desensitizes TGF-beta signaling. *Nat Med, 11*(8), 845-852. doi: 10.1038/nm1282

Jenny, M., Uhl, C., Roche, C., Duluc, I., Guillermin, V., Guillemot, F., . . . Gradwohl, G. (2002). Neurogenin3 is differentially required for endocrine cell fate specification in the intestinal and gastric epithelium. *EMBO J, 21*(23), 6338-6347.

Jiao, Z., Wang, W., Hua, S., Liu, M., Wang, H., Wang, X., . . . Lu, L. (2014). Blockade of Notch signaling ameliorates murine collagen-induced arthritis via suppressing Th1 and Th17 cell responses. *Am J Pathol, 184*(4), 1085-1093. doi: 10.1016/j.ajpath.2013.12.010

Jubb, A. M., Turley, H., Moeller, H. C., Steers, G., Han, C., Li, J. L., . . . Harris, A. L. (2009). Expression of delta-like ligand 4 (Dll4) and markers of hypoxia in colon cancer. *Br J Cancer, 101*(10), 1749-1757. doi: 10.1038/sj.bjc.6605368

Junqueira de Azevedo, I. L., Farsky, S. H., Oliveira, M. L., & Ho, P. L. (2001). Molecular cloning and expression of a functional snake venom vascular endothelium growth factor (VEGF) from the Bothrops insularis pit viper. A new member of the VEGF family of proteins. *J Biol Chem, 276*(43), 39836-39842. doi: 10.1074/jbc.M106531200

Jurynczyk, M., Jurewicz, A., Raine, C. S., & Selmaj, K. (2008). Notch3 inhibition in myelin-reactive T cells down-regulates protein kinase C theta and attenuates experimental autoimmune encephalomyelitis. *J Immunol, 180*(4), 2634-2640.

Kared, H., Adle-Biassette, H., Fois, E., Masson, A., Bach, J. F., Chatenoud, L., . . . Zavala, F. (2006). Jagged2-expressing hematopoietic progenitors promote regulatory T cell expansion in the periphery through notch signaling. *Immunity, 25*(5), 823-834. doi: 10.1016/j.immuni.2006.09.008

Karin, M. (2009). NF-kappaB as a critical link between inflammation and cancer. *Cold Spring Harb Perspect Biol, 1*(5), a000141. doi: 10.1101/cshperspect.a000141

Karsa, L. V., Lignini, T. A., Patnick, J., Lambert, R., & Sauvaget, C. (2010). The dimensions of the CRC problem. *Best Pract Res Clin Gastroenterol, 24*(4), 381-396. doi: 10.1016/j.bpg.2010.06.004

Katz, J. P., Perreault, N., Goldstein, B. G., Lee, C. S., Labosky, P. A., Yang, V. W., & Kaestner, K. H. (2002). The zinc-finger transcription factor Klf4 is required for terminal differentiation of goblet cells in the colon. *Development, 129*(11), 2619-2628.

Kayahara, T., Sawada, M., Takaishi, S., Fukui, H., Seno, H., Fukuzawa, H., . . . Chiba, T. (2003). Candidate markers for stem and early progenitor cells, Musashi-1 and Hes1,

are expressed in crypt base columnar cells of mouse small intestine. *FEBS Lett, 535*(1-3), 131-135.
Kerbel, R. S. (2008). Tumor angiogenesis. *N Engl J Med, 358*(19), 2039-2049. doi: 10.1056/NEJMra0706596
Kern, S. E., Redston, M., Seymour, A. B., Caldas, C., Powell, S. M., Kornacki, S., & Kinzler, K. W. (1994). Molecular genetic profiles of colitis-associated neoplasms. *Gastroenterology, 107*(2), 420-428.
Khosravi Shahi, P., & Fernandez Pineda, I. (2008). Tumoral angiogenesis: review of the literature. *Cancer Invest, 26*(1), 104-108. doi: 10.1080/07357900701662509
Kim, T. H., & Shivdasani, R. A. (2011). Genetic evidence that intestinal Notch functions vary regionally and operate through a common mechanism of Math1 repression. *J Biol Chem, 286*(13), 11427-11433. doi: 10.1074/jbc.M110.188797
King, D. (2002). PathologyOutlines.com. Retrieved Sept. 7, 2014, from http://www.pathologyoutlines.com/topic/smallbowelsuperpagenontumor.html
Kinzler, K. W., Nilbert, M. C., Su, L. K., Vogelstein, B., Bryan, T. M., Levy, D. B., . . . et al. (1991). Identification of FAP locus genes from chromosome 5q21. *Science, 253*(5020), 661-665.
Kinzler, K. W., & Vogelstein, B. (1996). Lessons from hereditary colorectal cancer. *Cell, 87*(2), 159-170.
Kishimoto, T. (2005). Interleukin-6: from basic science to medicine--40 years in immunology. *Annu Rev Immunol, 23*, 1-21. doi: 10.1146/annurev.immunol.23.021704.115806
Kistner, A., Gossen, M., Zimmermann, F., Jerecic, J., Ullmer, C., Lubbert, H., & Bujard, H. (1996). Doxycycline-mediated quantitative and tissue-specific control of gene expression in transgenic mice. *Proc Natl Acad Sci U S A, 93*(20), 10933-10938.
Kitajima, S., Takuma, S., & Morimoto, M. (1999). Changes in colonic mucosal permeability in mouse colitis induced with dextran sulfate sodium. *Exp Anim, 48*(3), 137-143.
Klagsbrun, M. (1991). Regulators of angiogenesis: stimulators, inhibitors, and extracellular matrix. *J Cell Biochem, 47*(3), 199-200. doi: 10.1002/jcb.240470302
Koch, U., Fiorini, E., Benedito, R., Besseyrias, V., Schuster-Gossler, K., Pierres, M., . . . Radtke, F. (2008). Delta-like 4 is the essential, nonredundant ligand for Notch1 during thymic T cell lineage commitment. *J Exp Med, 205*(11), 2515-2523. doi: 10.1084/jem.20080829
Koo, B. K., Lim, H. S., Chang, H. J., Yoon, M. J., Choi, Y., Kong, M. P., . . . Kong, Y. Y. (2009). Notch signaling promotes the generation of EphrinB1-positive intestinal epithelial cells. *Gastroenterology, 137*(1), 145-155, 155 e141-143. doi: 10.1053/j.gastro.2009.03.046
Korn, T., Bettelli, E., Oukka, M., & Kuchroo, V. K. (2009). IL-17 and Th17 Cells. *Annu Rev Immunol, 27*, 485-517. doi: 10.1146/annurev.immunol.021908.132710
Korsisaari, N., Kasman, I. M., Forrest, W. F., Pal, N., Bai, W., Fuh, G., . . . Ferrara, N. (2007). Inhibition of VEGF-A prevents the angiogenic switch and results in increased survival of Apc+/min mice. *Proc Natl Acad Sci U S A, 104*(25), 10625-10630. doi: 10.1073/pnas.0704213104
Krasinskas, A. M. (2011). EGFR Signaling in Colorectal Carcinoma. *Patholog Res Int, 2011*, 932932. doi: 10.4061/2011/932932
Kraus, S., & Arber, N. (2009). Inflammation and colorectal cancer. *Current Opinion in Pharmacology, 9*(4), 405-410. doi: 10.1016/j.coph.2009.06.006
Krawczyk, C. M., Sun, J., & Pearce, E. J. (2008). Th2 differentiation is unaffected by Jagged2 expression on dendritic cells. *J Immunol, 180*(12), 7931-7937.
Krebs, L. T., Shutter, J. R., Tanigaki, K., Honjo, T., Stark, K. L., & Gridley, T. (2004). Haploinsufficient lethality and formation of arteriovenous malformations in Notch pathway mutants. *Genes Dev, 18*(20), 2469-2473. doi: 10.1101/gad.1239204
Kubota, Y. (2012). Tumor angiogenesis and anti-angiogenic therapy. *Keio J Med, 61*(2), 47-56.
Kuhn, R., Lohler, J., Rennick, D., Rajewsky, K., & Muller, W. (1993). Interleukin-10-deficient mice develop chronic enterocolitis. *Cell, 75*(2), 263-274.
Lakatos, P. L., & Lakatos, L. (2008). Risk for colorectal cancer in ulcerative colitis: changes, causes and management strategies. *World J Gastroenterol, 14*(25), 3937-3947.

Lashner, B. A., Shapiro, B. D., Husain, A., & Goldblum, J. R. (1999). Evaluation of the usefulness of testing for p53 mutations in colorectal cancer surveillance for ulcerative colitis. *Am J Gastroenterol, 94*(2), 456-462. doi: 10.1111/j.1572-0241.1999.877_f.x

Lee, J. J., & Chu, E. (2014). Sequencing of antiangiogenic agents in the treatment of metastatic colorectal cancer. *Clin Colorectal Cancer, 13*(3), 135-144. doi: 10.1016/j.clcc.2014.02.001

Lee, J. W., Soung, Y. H., Kim, S. Y., Park, W. S., Nam, S. W., Lee, J. Y., . . . Lee, S. H. (2005). Absence of EGFR mutation in the kinase domain in common human cancers besides non-small cell lung cancer. *Int J Cancer, 113*(3), 510-511. doi: 10.1002/ijc.20591

Leedham, S. J., Graham, T. A., Oukrif, D., McDonald, S. A., Rodriguez-Justo, M., Harrison, R. F., . . . Wright, N. A. (2009). Clonality, founder mutations, and field cancerization in human ulcerative colitis-associated neoplasia. *Gastroenterology, 136*(2), 542-550 e546. doi: 10.1053/j.gastro.2008.10.086

Li, J. L., Jubb, A. M., & Harris, A. L. (2010). Targeting DLL4 in tumors shows preclinical activity but potentially significant toxicity. *Future Oncol, 6*(7), 1099-1103. doi: 10.2217/fon.10.62

Li, J. L., Sainson, R. C., Shi, W., Leek, R., Harrington, L. S., Preusser, M., . . . Harris, A. L. (2007). Delta-like 4 Notch ligand regulates tumor angiogenesis, improves tumor vascular function, and promotes tumor growth in vivo. *Cancer Res, 67*(23), 11244-11253. doi: 10.1158/0008-5472.CAN-07-0969

Li, J. L., Sainson, R. C. A., Oon, C. E., Turley, H., Leek, R., Sheldon, H., . . . Harris, A. L. (2011). DLL4-Notch Signaling Mediates Tumor Resistance to Anti-VEGF Therapy In Vivo. *Cancer Res, 71*(18), 6073-6083. doi: 10.1158/0008-5472.can-11-1704

Li, L., & Clevers, H. (2010). Coexistence of quiescent and active adult stem cells in mammals. *Science, 327*(5965), 542-545. doi: 10.1126/science.1180794

Li, M. O., Wan, Y. Y., Sanjabi, S., Robertson, A. K., & Flavell, R. A. (2006). Transforming growth factor-beta regulation of immune responses. *Annu Rev Immunol, 24*, 99-146. doi: 10.1146/annurev.immunol.24.021605.090737

Liekens, S., De Clercq, E., & Neyts, J. (2001). Angiogenesis: regulators and clinical applications. *Biochem Pharmacol, 61*(3), 253-270.

Liu, J., Stevens, J., Rote, C. A., Yost, H. J., Hu, Y., Neufeld, K. L., . . . Matsunami, N. (2001). Siah-1 mediates a novel beta-catenin degradation pathway linking p53 to the adenomatous polyposis coli protein. *Mol Cell, 7*(5), 927-936.

Liu, S. K., Bham, S. A. S., Fokas, E., Beech, J., Im, J., Cho, S., . . . Muschel, R. J. (2011). Delta-Like Ligand 4-Notch Blockade and Tumor Radiation Response. *JNCI Journal of the National Cancer Institute, 103*(23), 1778-1798. doi: 10.1093/jnci/djr419

Liu, Y., Cox, S. R., Morita, T., & Kourembanas, S. (1995). Hypoxia regulates vascular endothelial growth factor gene expression in endothelial cells. Identification of a 5' enhancer. *Circ Res, 77*(3), 638-643.

Liu, Y. C., Zou, X. B., Chai, Y. F., & Yao, Y. M. (2014). Macrophage polarization in inflammatory diseases. *Int J Biol Sci, 10*(5), 520-529. doi: 10.7150/ijbs.8879

Lobov, I. B., Renard, R. A., Papadopoulos, N., Gale, N. W., Thurston, G., Yancopoulos, G. D., & Wiegand, S. J. (2007). Delta-like ligand 4 (Dll4) is induced by VEGF as a negative regulator of angiogenic sprouting. *Proceedings of the National Academy of Sciences, 104*(9), 3219-3224. doi: 10.1073/pnas.0611206104

Lu, J., Ye, X., Fan, F., Xia, L., Bhattacharya, R., Bellister, S., . . . Ellis, L. M. (2013). Endothelial cells promote the colorectal cancer stem cell phenotype through a soluble form of Jagged-1. *Cancer Cell, 23*(2), 171-185. doi: 10.1016/j.ccr.2012.12.021

Luongo, C., Moser, A. R., Gledhill, S., & Dove, W. F. (1994). Loss of Apc+ in intestinal adenomas from Min mice. *Cancer Res, 54*(22), 5947-5952.

Lyttle, D. J., Fraser, K. M., Fleming, S. B., Mercer, A. A., & Robinson, A. J. (1994). Homologs of vascular endothelial growth factor are encoded by the poxvirus orf virus. *J Virol, 68*(1), 84-92.

Maekawa, Y., Tsukumo, S., Chiba, S., Hirai, H., Hayashi, Y., Okada, H., . . . Yasutomo, K. (2003). Delta1-Notch3 interactions bias the functional differentiation of activated CD4+ T cells. *Immunity, 19*(4), 549-559.

Maggio-Price, L., Treuting, P., Zeng, W., Tsang, M., Bielefeldt-Ohmann, H., & Iritani, B. M. (2006). Helicobacter infection is required for inflammation and colon cancer in SMAD3-deficient mice. *Cancer Res, 66*(2), 828-838. doi: 10.1158/0008-5472.CAN-05-2448

Mailhos, C., Modlich, U., Lewis, J., Harris, A., Bicknell, R., & Ish-Horowicz, D. (2001). Delta4, an endothelial specific notch ligand expressed at sites of physiological and tumor angiogenesis. *Differentiation, 69*(2-3), 135-144. doi: 10.1046/j.1432-0436.2001.690207.x

Maillard, I., Fang, T., & Pear, W. S. (2005). Regulation of lymphoid development, differentiation, and function by the Notch pathway. *Annu Rev Immunol, 23*, 945-974. doi: 10.1146/annurev.immunol.23.021704.115747

Mancuso, M. R., Davis, R., Norberg, S. M., O'Brien, S., Sennino, B., Nakahara, T., . . . McDonald, D. M. (2006). Rapid vascular regrowth in tumors after reversal of VEGF inhibition. *J Clin Invest, 116*(10), 2610-2621. doi: 10.1172/JCI24612

Mantovani, A., Sozzani, S., Locati, M., Allavena, P., & Sica, A. (2002). Macrophage polarization: tumor-associated macrophages as a paradigm for polarized M2 mononuclear phagocytes. *Trends Immunol, 23*(11), 549-555. doi: S1471490602023025 [pii]

Marshman, E., Booth, C., & Potten, C. S. (2002). The intestinal epithelial stem cell. *Bioessays, 24*(1), 91-98. doi: 10.1002/bies.10028

Massague, J. (2008). TGFbeta in Cancer. *Cell, 134*(2), 215-230. doi: 10.1016/j.cell.2008.07.001

Mathern, D. R., Laitman, L. E., Hovhannisyan, Z., Dunkin, D., Farsio, S., Malik, T. J., . . . Dahan, S. (2014). Mouse and human Notch-1 regulate mucosal immune responses. *Mucosal Immunol, 7*(4), 995-1005. doi: 10.1038/mi.2013.118

Mattar, M. C., Lough, D., Pishvaian, M. J., & Charabaty, A. (2011). Current management of inflammatory bowel disease and colorectal cancer. *Gastrointest Cancer Res, 4*(2), 53-61.

Mayer, L. (2010). Evolving paradigms in the pathogenesis of IBD. *J Gastroenterol, 45*(1), 9-16. doi: 10.1007/s00535-009-0138-3

Maynard, M. A., Ferretti, R., Hilgendorf, K. I., Perret, C., Whyte, P., & Lees, J. A. (2014). Bmi1 is required for tumorigenesis in a mouse model of intestinal cancer. *Oncogene, 33*(28), 3742-3747. doi: 10.1038/onc.2013.333

McCart, A. E., Vickaryous, N. K., & Silver, A. (2008). Apc mice: models, modifiers and mutants. *Pathol Res Pract, 204*(7), 479-490. doi: 10.1016/j.prp.2008.03.004

McKay, J. A., Murray, L. J., Curran, S., Ross, V. G., Clark, C., Murray, G. I., . . . McLeod, H. L. (2002). Evaluation of the epidermal growth factor receptor (EGFR) in colorectal tumours and lymph node metastases. *Eur J Cancer, 38*(17), 2258-2264.

Meng, R. D., Shelton, C. C., Li, Y. M., Qin, L. X., Notterman, D., Paty, P. B., & Schwartz, G. K. (2009). gamma-Secretase inhibitors abrogate oxaliplatin-induced activation of the Notch-1 signaling pathway in colon cancer cells resulting in enhanced chemosensitivity. *Cancer Res, 69*(2), 573-582. doi: 10.1158/0008-5472.CAN-08-2088

Merla, A., & Goel, S. (2012). Novel drugs targeting the epidermal growth factor receptor and its downstream pathways in the treatment of colorectal cancer: a systematic review. *Chemother Res Pract, 2012*, 387172. doi: 10.1155/2012/387172

Mihalache, A., & Rogoveanu, I. (2014). Angiogenesis factors involved in the pathogenesis of colorectal cancer. *Curr Health Sci J, 40*(1), 5-11. doi: 10.12865/CHSJ.40.01.01

Milano, J., McKay, J., Dagenais, C., Foster-Brown, L., Pognan, F., Gadient, R., . . . Ciaccio, P. J. (2004). Modulation of notch processing by gamma-secretase inhibitors causes intestinal goblet cell metaplasia and induction of genes known to specify gut secretory lineage differentiation. *Toxicol Sci, 82*(1), 341-358. doi: 10.1093/toxsci/kfh254

Minter, L. M., Turley, D. M., Das, P., Shin, H. M., Joshi, I., Lawlor, R. G., . . . Osborne, B. A. (2005). Inhibitors of gamma-secretase block in vivo and in vitro T helper type 1 polarization by preventing Notch upregulation of Tbx21. *Nat Immunol, 6*(7), 680-688.

Monteleone, G., Boirivant, M., Pallone, F., & MacDonald, T. T. (2008). TGF-beta1 and Smad7 in the regulation of IBD. *Mucosal Immunol, 1 Suppl 1*, S50-53. doi: 10.1038/mi.2008.55

Monvoisin, A., Alva, J. A., Hofmann, J. J., Zovein, A. C., Lane, T. F., & Iruela-Arispe, M. L. (2006). VE-cadherin-CreERT2 transgenic mouse: a model for inducible recombination in the endothelium. *Dev Dyn, 235*(12), 3413-3422. doi: 10.1002/dvdy.20982

Moohr, O. L. (1919). *Genetics*(4), 252.

Moore, K. W., de Waal Malefyt, R., Coffman, R. L., & O'Garra, A. (2001). Interleukin-10 and the interleukin-10 receptor. *Annu Rev Immunol, 19*, 683-765. doi: 10.1146/annurev.immunol.19.1.683

Moran, A. E., Hunt, D. H., Javid, S. H., Redston, M., Carothers, A. M., & Bertagnolli, M. M. (2004). Apc deficiency is associated with increased Egfr activity in the intestinal enterocytes and adenomas of C57BL/6J-Min/+ mice. *J Biol Chem, 279*(41), 43261-43272. doi: 10.1074/jbc.M404276200

Morgan, T. H. (1917). The theory of the gene. *Am. Nat.*(51), 513-544.

Moser, A. R., Dove, W. F., Roth, K. A., & Gordon, J. I. (1992). The Min (multiple intestinal neoplasia) mutation: its effect on gut epithelial cell differentiation and interaction with a modifier system. *J Cell Biol, 116*(6), 1517-1526.

Moser, A. R., Pitot, H. C., & Dove, W. F. (1990). A dominant mutation that predisposes to multiple intestinal neoplasia in the mouse. *Science, 247*(4940), 322-324.

Mukherjee, S., Schaller, M. A., Neupane, R., Kunkel, S. L., & Lukacs, N. W. (2009). Regulation of T cell activation by Notch ligand, DLL4, promotes IL-17 production and Rorc activation. *J Immunol, 182*(12), 7381-7388. doi: 10.4049/jimmunol.0804322

Munkholm, P. (2003). Review article: the incidence and prevalence of colorectal cancer in inflammatory bowel disease. *Aliment Pharmacol Ther, 18 Suppl 2*, 1-5.

Murta, D., Batista, M., Silva, E., Trindade, A., Henrique, D., Duarte, A., & Lopes-da-Costa, L. (2013). Dynamics of Notch pathway expression during mouse testis post-natal development and along the spermatogenic cycle. *PLoS One, 8*(8), e72767. doi: 10.1371/journal.pone.0072767

Murta, D., Batista, M., Silva, E., Trindade, A., Mateus, L., Duarte, A., & Lopes-da-Costa, L. (2014). Differential expression of Notch component and effector genes during ovarian follicle and corpus luteum development during the oestrous cycle. *Reprod Fertil Dev*. doi: 10.1071/RD13399

Murta, D., Batista, M., Trindade, A., Silva, E., Mateus, L., Duarte, A., & Lopes-da-Costa, L. (2015). Dynamics of Notch signalling in the mouse oviduct and uterus during the oestrous cycle. *Reprod Fertil Dev*. doi: 10.1071/RD15029

Nakamura, Y., Nishisho, I., Kinzler, K. W., Vogelstein, B., Miyoshi, Y., Miki, Y., . . . Horii, A. (1992). Mutations of the APC (adenomatous polyposis coli) gene in FAP (familial polyposis coli) patients and in sporadic colorectal tumors. *Tohoku J Exp Med, 168*(2), 141-147.

Naugler, W. E., & Karin, M. (2008). NF-kappaB and cancer-identifying targets and mechanisms. *Curr Opin Genet Dev, 18*(1), 19-26. doi: 10.1016/j.gde.2008.01.020

Nelson, W. J., & Nusse, R. (2004). Convergence of Wnt, beta-catenin, and cadherin pathways. *Science, 303*(5663), 1483-1487. doi: 10.1126/science.1094291

Neufeld, G., Cohen, T., Gengrinovitch, S., & Poltorak, Z. (1999). Vascular endothelial growth factor (VEGF) and its receptors. *FASEB J, 13*(1), 9-22.

Neufert, C., Becker, C., & Neurath, M. F. (2007). An inducible mouse model of colon carcinogenesis for the analysis of sporadic and inflammation-driven tumor progression. *Nature Protocols, 2*(8), 1998-2004. doi: 10.1038/nprot.2007.279

Noffsinger, A. E. (2009). Serrated polyps and colorectal cancer: new pathway to malignancy. *Annu Rev Pathol, 4*, 343-364. doi: 10.1146/annurev.pathol.4.110807.092317

Noguera-Troise, I., Daly, C., Papadopoulos, N. J., Coetzee, S., Boland, P., Gale, N. W., . . . Thurston, G. (2006). Blockade of Dll4 inhibits tumour growth by promoting non-productive angiogenesis. *Nature, 444*(7122), 1032-1037. doi: 10.1038/nature05355

Nucci, M. R., Robinson, C. R., Longo, P., Campbell, P., & Hamilton, S. R. (1997). Phenotypic and genotypic characteristics of aberrant crypt foci in human colorectal mucosa. *Hum Pathol, 28*(12), 1396-1407.

O'Brien, C. A., Pollett, A., Gallinger, S., & Dick, J. E. (2007). A human colon cancer cell capable of initiating tumour growth in immunodeficient mice. *Nature, 445*(7123), 106-110. doi: 10.1038/nature05372

Obata, Y., Takahashi, D., Ebisawa, M., Kakiguchi, K., Yonemura, S., Jinnohara, T., . . . Ohno, H. (2012). Epithelial cell-intrinsic Notch signaling plays an essential role in the maintenance of gut immune homeostasis. *J Immunol, 188*(5), 2427-2436. doi: 10.4049/jimmunol.1101128

Ohtsuka, T., Ishibashi, M., Gradwohl, G., Nakanishi, S., Guillemot, F., & Kageyama, R. (1999). Hes1 and Hes5 as notch effectors in mammalian neuronal differentiation. *EMBO J, 18*(8), 2196-2207. doi: 10.1093/emboj/18.8.2196

Okamoto, R., Tsuchiya, K., Nemoto, Y., Akiyama, J., Nakamura, T., Kanai, T., & Watanabe, M. (2009). Requirement of Notch activation during regeneration of the intestinal epithelia. *Am J Physiol Gastrointest Liver Physiol, 296*(1), G23-35. doi: 10.1152/ajpgi.90225.2008

Osawa, E., Nakajima, A., Fujisawa, T., Kawamura, Y. I., Toyama-Sorimachi, N., Nakagama, H., & Dohi, T. (2006). Predominant T helper type 2-inflammatory responses promote murine colon cancers. *Int J Cancer, 118*(9), 2232-2236. doi: 10.1002/ijc.21639

Pajusola, K., Aprelikova, O., Korhonen, J., Kaipainen, A., Pertovaara, L., Alitalo, R., & Alitalo, K. (1992). FLT4 receptor tyrosine kinase contains seven immunoglobulin-like loops and is expressed in multiple human tissues and cell lines. *Cancer Res, 52*(20), 5738-5743.

Papanikolaou, A., Wang, Q. S., Delker, D. A., & Rosenberg, D. W. (1998). Azoxymethane-induced colon tumors and aberrant crypt foci in mice of different genetic susceptibility. *Cancer Lett, 130*(1-2), 29-34.

Pastille, E., Bardini, K., Fleissner, D., Adamczyk, A., Frede, A., Wadwa, M., . . . Westendorf, A. M. (2014). Transient ablation of regulatory T cells improves antitumor immunity in colitis-associated colon cancer. *Cancer Res, 74*(16), 4258-4269. doi: 10.1158/0008-5472.CAN-13-3065

Pastille, E., Pohlmann, S., Wirsdorfer, F., Reib, A., & Flohe, S. B. (2015). A disturbed interaction with accessory cells upon opportunistic infection with Pseudomonas aeruginosa contributes to an impaired IFN-gamma production of NK cells in the lung during sepsis-induced immunosuppression. *Innate Immun, 21*(2), 115-126. doi: 10.1177/1753425913517274

Patel, N. S., Dobbie, M. S., Rochester, M., Steers, G., Poulsom, R., Le Monnier, K., . . . Harris, A. L. (2006). Up-regulation of endothelial delta-like 4 expression correlates with vessel maturation in bladder cancer. *Clin Cancer Res, 12*(16), 4836-4844. doi: 10.1158/1078-0432.CCR-06-0285

Patel, N. S., Li, J. L., Generali, D., Poulsom, R., Cranston, D. W., & Harris, A. L. (2005). Up-regulation of delta-like 4 ligand in human tumor vasculature and the role of basal expression in endothelial cell function. *Cancer Res, 65*(19), 8690-8697. doi: 10.1158/0008-5472.CAN-05-1208

Payne, J. E. (1990). Colorectal carcinogenesis. *Aust N Z J Surg, 60*(1), 11-18.

Peignon, G., Durand, A., Cacheux, W., Ayrault, O., Terris, B., Laurent-Puig, P., . . . Romagnolo, B. (2011). Complex interplay between beta-catenin signalling and Notch effectors in intestinal tumorigenesis. *Gut, 60*(2), 166-176. doi: 10.1136/gut.2009.204719

Pellegrinet, L., Rodilla, V., Liu, Z., Chen, S., Koch, U., Espinosa, L., . . . Radtke, F. (2011). Dll1- and Dll4-Mediated Notch Signaling Are Required for Homeostasis of Intestinal Stem Cells. *Gastroenterology, 140*(4), 1230-1240.e1237. doi: 10.1053/j.gastro.2011.01.005

Peng, X. H., Karna, P., Cao, Z., Jiang, B. H., Zhou, M., & Yang, L. (2006). Cross-talk between epidermal growth factor receptor and hypoxia-inducible factor-1alpha signal pathways increases resistance to apoptosis by up-regulating survivin gene expression. *J Biol Chem, 281*(36), 25903-25914. doi: 10.1074/jbc.M603414200

Perse, M., & Cerar, A. (2012). Dextran sodium sulphate colitis mouse model: traps and tricks. *J Biomed Biotechnol, 2012*, 718617. doi: 10.1155/2012/718617

Philip, M., Rowley, D. A., & Schreiber, H. (2004). Inflammation as a tumor promoter in cancer induction. *Semin Cancer Biol, 14*(6), 433-439. doi: 10.1016/j.semcancer.2004.06.006

Pinol, V., Castells, A., Andreu, M., Castellvi-Bel, S., Alenda, C., Llor, X., . . . Gastrointestinal Oncology Group of the Spanish Gastroenterological, A. (2005). Accuracy of revised Bethesda guidelines, microsatellite instability, and immunohistochemistry for the identification of patients with hereditary nonpolyposis colorectal cancer. *JAMA, 293*(16), 1986-1994. doi: 10.1001/jama.293.16.1986

Pinto, D., Gregorieff, A., Begthel, H., & Clevers, H. (2003). Canonical Wnt signals are essential for homeostasis of the intestinal epithelium. *Genes Dev, 17*(14), 1709-1713. doi: 10.1101/gad.267103

Plouet, J., Schilling, J., & Gospodarowicz, D. (1989). Isolation and characterization of a newly identified endothelial cell mitogen produced by AtT-20 cells. *EMBO J, 8*(12), 3801-3806.

Polakis, P. (2000). Wnt signaling and cancer. *Genes Dev, 14*(15), 1837-1851.

Popivanova, B. K., Kitamura, K., Wu, Y., Kondo, T., Kagaya, T., Kaneko, S., . . . Mukaida, N. (2008). Blocking TNF-alpha in mice reduces colorectal carcinogenesis associated with chronic colitis. *J Clin Invest, 118*(2), 560-570. doi: 10.1172/JCI32453

Porter, E. M., Bevins, C. L., Ghosh, D., & Ganz, T. (2002). The multifaceted Paneth cell. *Cell Mol Life Sci, 59*(1), 156-170.

Potten, C. S. (1998). Stem cells in gastrointestinal epithelium: numbers, characteristics and death. *Philos Trans R Soc Lond B Biol Sci, 353*(1370), 821-830. doi: 10.1098/rstb.1998.0246

Potten, C. S., Owen, G., & Booth, D. (2002). Intestinal stem cells protect their genome by selective segregation of template DNA strands. *J Cell Sci, 115*(Pt 11), 2381-2388.

Powell, S. M., Petersen, G. M., Krush, A. J., Booker, S., Jen, J., Giardiello, F. M., . . . Kinzler, K. W. (1993). Molecular diagnosis of familial adenomatous polyposis. *N Engl J Med, 329*(27), 1982-1987. doi: 10.1056/NEJM199312303292702

Preston, S. L., Wong, W. M., Chan, A. O., Poulsom, R., Jeffery, R., Goodlad, R. A., . . . Wright, N. A. (2003). Bottom-up histogenesis of colorectal adenomas: origin in the monocryptal adenoma and initial expansion by crypt fission. *Cancer Res, 63*(13), 3819-3825.

Previs, R. A., Coleman, R. L., Harris, A. L., & Sood, A. K. (2015). Molecular pathways: translational and therapeutic implications of the notch signaling pathway in cancer. *Clin Cancer Res, 21*(5), 955-961. doi: 10.1158/1078-0432.CCR-14-0809

Pritchard, C. C., & Grady, W. M. (2011). Colorectal cancer molecular biology moves into clinical practice. *Gut, 60*(1), 116-129. doi: 10.1136/gut.2009.206250

Qiao, L., & Wong, B. C. Y. (2009). Role of Notch signaling in colorectal cancer. *Carcinogenesis, 30*(12), 1979-1986. doi: 10.1093/carcin/bgp236

Radtke, F., Clevers, H., & Riccio, O. (2006). From gut homeostasis to cancer. *Curr Mol Med, 6*(3), 275-289.

Radtke, F., Fasnacht, N., & Macdonald, H. R. (2010). Notch signaling in the immune system. *Immunity, 32*(1), 14-27. doi: 10.1016/j.immuni.2010.01.004

Ranieri, G., Patruno, R., Ruggieri, E., Montemurro, S., Valerio, P., & Ribatti, D. (2006). Vascular endothelial growth factor (VEGF) as a target of bevacizumab in cancer: from the biology to the clinic. *Curr Med Chem, 13*(16), 1845-1857.

Real, C., Remedio, L., Caiado, F., Igreja, C., Borges, C., Trindade, A., . . . Dias, S. (2011). Bone marrow-derived endothelial progenitors expressing Delta-like 4 (Dll4) regulate tumor angiogenesis. *PLoS One, 6*(4), e18323. doi: 10.1371/journal.pone.0018323

Reed, K. K., & Wickham, R. (2009). Review of the gastrointestinal tract: from macro to micro. *Semin Oncol Nurs, 25*(1), 3-14. doi: 10.1016/j.soncn.2008.10.002

Reedijk, M., Odorcic, S., Zhang, H., Chetty, R., Tennert, C., Dickson, B. C., . . . Egan, S. E. (2008). Activation of Notch signaling in human colon adenocarcinoma. *Int J Oncol, 33*(6), 1223-1229.

Resnick, M. B., Routhier, J., Konkin, T., Sabo, E., & Pricolo, V. E. (2004). Epidermal growth factor receptor, c-MET, beta-catenin, and p53 expression as prognostic indicators in stage II colon cancer: a tissue microarray study. *Clin Cancer Res, 10*(9), 3069-3075.

Ricci-Vitiani, L., Lombardi, D. G., Pilozzi, E., Biffoni, M., Todaro, M., Peschle, C., & De Maria, R. (2007). Identification and expansion of human colon-cancer-initiating cells. *Nature, 445*(7123), 111-115. doi: 10.1038/nature05384

Riccio, O., van Gijn, M. E., Bezdek, A. C., Pellegrinet, L., van Es, J. H., Zimber-Strobl, U., . . . Radtke, F. (2008). Loss of intestinal crypt progenitor cells owing to inactivation of both Notch1 and Notch2 is accompanied by derepression of CDK inhibitors p27Kip1 and p57Kip2. *EMBO Rep, 9*(4), 377-383. doi: 10.1038/embor.2008.7

Ridgway, J., Zhang, G., Wu, Y., Stawicki, S., Liang, W. C., Chanthery, Y., . . . Yan, M. (2006). Inhibition of Dll4 signalling inhibits tumour growth by deregulating angiogenesis. *Nature, 444*(7122), 1083-1087. doi: 10.1038/nature05313

Rizzo, A., Pallone, F., Monteleone, G., & Fantini, M. C. (2011). Intestinal inflammation and colorectal cancer: a double-edged sword? *World J Gastroenterol, 17*(26), 3092-3100. doi: 10.3748/wjg.v17.i26.3092

Roberts, R. B., Min, L., Washington, M. K., Olsen, S. J., Settle, S. H., Coffey, R. J., & Threadgill, D. W. (2002). Importance of epidermal growth factor receptor signaling in establishment of adenomas and maintenance of carcinomas during intestinal tumorigenesis. *Proc Natl Acad Sci U S A, 99*(3), 1521-1526. doi: 10.1073/pnas.032678499

Roda, G., Marocchi, M., Sartini, A., & Roda, E. (2011). Cytokine Networks in Ulcerative Colitis. *Ulcers, 2011*, 1-5.

Rodilla, V., Villanueva, A., Obrador-Hevia, A., Robert-Moreno, A., Fernandez-Majada, V., Grilli, A., . . . Espinosa, L. (2009). Jagged1 is the pathological link between Wnt and Notch pathways in colorectal cancer. *Proc Natl Acad Sci U S A, 106*(15), 6315-6320. doi: 10.1073/pnas.0813221106

Rolfo, C., Bronte, G., Sortino, G., Papadimitriou, K., Passiglia, F., Fiorentino, E., . . . Peeters, M. (2014). The role of targeted therapy for gastrointestinal tumors. *Expert Rev Gastroenterol Hepatol, 8*(8), 875-885. doi: 10.1586/17474124.2014.922870

Rosen, J. M., & Jordan, C. T. (2009). The increasing complexity of the cancer stem cell paradigm. *Science, 324*(5935), 1670-1673. doi: 10.1126/science.1171837

Rustgi, A. K. (1994). Hereditary gastrointestinal polyposis and nonpolyposis syndromes. *N Engl J Med, 331*(25), 1694-1702. doi: 10.1056/NEJM199412223312507

Rutz, S., Janke, M., Kassner, N., Hohnstein, T., Krueger, M., & Scheffold, A. (2008). Notch regulates IL-10 production by T helper 1 cells. *Proc Natl Acad Sci U S A, 105*(9), 3497-3502. doi: 10.1073/pnas.0712102105

Ryan, H. E., Poloni, M., McNulty, W., Elson, D., Gassmann, M., Arbeit, J. M., & Johnson, R. S. (2000). Hypoxia-inducible factor-1alpha is a positive factor in solid tumor growth. *Cancer Res, 60*(15), 4010-4015.

Sakaguchi, S., Wing, K., Onishi, Y., Prieto-Martin, P., & Yamaguchi, T. (2009). Regulatory T cells: how do they suppress immune responses? *Int Immunol, 21*(10), 1105-1111. doi: 10.1093/intimm/dxp095

Sakai, K., & Miyazaki, J. (1997). A transgenic mouse line that retains Cre recombinase activity in mature oocytes irrespective of the cre transgene transmission. *Biochem Biophys Res Commun, 237*(2), 318-324.

Samon, J. B., Champhekar, A., Minter, L. M., Telfer, J. C., Miele, L., Fauq, A., . . . Osborne, B. A. (2008). Notch1 and TGFbeta1 cooperatively regulate Foxp3 expression and the maintenance of peripheral regulatory T cells. *Blood, 112*(5), 1813-1821. doi: 10.1182/blood-2008-03-144980

Sander, G. R., & Powell, B. C. (2004). Expression of notch receptors and ligands in the adult gut. *J Histochem Cytochem, 52*(4), 509-516.

Sangiorgi, E., & Capecchi, M. R. (2008). Bmi1 is expressed in vivo in intestinal stem cells. *Nat Genet, 40*(7), 915-920. doi: 10.1038/ng.165

Sansom, O. J. (2004). Loss of Apc in vivo immediately perturbs Wnt signaling, differentiation, and migration. *Genes Dev, 18*(12), 1385-1390. doi: 10.1101/gad.287404

Sato, T., van Es, J. H., Snippert, H. J., Stange, D. E., Vries, R. G., van den Born, M., . . . Clevers, H. (2011). Paneth cells constitute the niche for Lgr5 stem cells in intestinal crypts. *Nature, 469*(7330), 415-418. doi: 10.1038/nature09637

Satoh, Y., Matsumura, I., Tanaka, H., Ezoe, S., Sugahara, H., Mizuki, M., . . . Kanakura, Y. (2004). Roles for c-Myc in self-renewal of hematopoietic stem cells. *J Biol Chem, 279*(24), 24986-24993. doi: 10.1074/jbc.M400407200

Scehnet, J. S., Jiang, W., Kumar, S. R., Krasnoperov, V., Trindade, A., Benedito, R., . . . Gill, P. S. (2007). Inhibition of Dll4-mediated signaling induces proliferation of immature vessels and results in poor tissue perfusion. *Blood, 109*(11), 4753-4760. doi: 10.1182/blood-2006-12-063933

Schepers, A. G., Snippert, H. J., Stange, D. E., van den Born, M., van Es, J. H., van de Wetering, M., & Clevers, H. (2012). Lineage tracing reveals Lgr5+ stem cell activity in mouse intestinal adenomas. *Science, 337*(6095), 730-735. doi: 10.1126/science.1224676

Schottelius, A. J., Mayo, M. W., Sartor, R. B., & Baldwin, A. S., Jr. (1999). Interleukin-10 signaling blocks inhibitor of kappaB kinase activity and nuclear factor kappaB DNA binding. *J Biol Chem, 274*(45), 31868-31874.

Schroder, N., & Gossler, A. (2002). Expression of Notch pathway components in fetal and adult mouse small intestine. *Gene Expr Patterns, 2*(3-4), 247-250. doi: S1567133X02000601

Segarra, M., Williams, C. K., Sierra Mde, L., Bernardo, M., McCormick, P. J., Maric, D., . . . Tosato, G. (2008). Dll4 activation of Notch signaling reduces tumor vascularity and inhibits tumor growth. *Blood, 112*(5), 1904-1911. doi: 10.1182/blood-2007-11-126045

Senik, A., Stefanos, S., Kolb, J. P., Lucero, M., & Falcoff, E. (1980). Enhancement of mouse natural killer cell activity by type II interferon. *Ann Immunol (Paris), 131C*(3), 349-361.

Sharma, S., Sharma, M. C., & Sarkar, C. (2005). Morphology of angiogenesis in human cancer: a conceptual overview, histoprognostic perspective and significance of neoangiogenesis. *Histopathology, 46*(5), 481-489. doi: 10.1111/j.1365-2559.2005.02142.x

Sheldon, H., Heikamp, E., Turley, H., Dragovic, R., Thomas, P., Oon, C. E., . . . Harris, A. L. (2010). New mechanism for Notch signaling to endothelium at a distance by Delta-like 4 incorporation into exosomes. *Blood, 116*(13), 2385-2394. doi: 10.1182/blood-2009-08-239228

Shi, Y., & Massague, J. (2003). Mechanisms of TGF-beta signaling from cell membrane to the nucleus. *Cell, 113*(6), 685-700.

Shia, J., Klimstra, D. S., Li, A. R., Qin, J., Saltz, L., Teruya-Feldstein, J., . . . Chen, B. (2005). Epidermal growth factor receptor expression and gene amplification in colorectal carcinoma: an immunohistochemical and chromogenic in situ hybridization study. *Mod Pathol, 18*(10), 1350-1356. doi: 10.1038/modpathol.3800417

Shibuya, M. (2006). Differential roles of vascular endothelial growth factor receptor-1 and receptor-2 in angiogenesis. *J Biochem Mol Biol, 39*(5), 469-478.

Shih, I. M., Wang, T. L., Traverso, G., Romans, K., Hamilton, S. R., Ben-Sasson, S., . . . Vogelstein, B. (2001). Top-down morphogenesis of colorectal tumors. *Proc Natl Acad Sci U S A, 98*(5), 2640-2645. doi: 10.1073/pnas.051629398

Shimizu, H., Okamoto, R., Ito, G., Fujii, S., Nakata, T., Suzuki, K., . . . Watanabe, M. (2014). Distinct expression patterns of Notch ligands, Dll1 and Dll4, in normal and inflamed mice intestine. *PeerJ, 2*, e370. doi: 10.7717/peerj.370

Shin, H. M., Minter, L. M., Cho, O. H., Gottipati, S., Fauq, A. H., Golde, T. E., . . . Osborne, B. A. (2006). Notch1 augments NF-kappaB activity by facilitating its nuclear retention. *EMBO J, 25*(1), 129-138. doi: 10.1038/sj.emboj.7600902

Shinoda, M., Shin-Ya, M., Naito, Y., Kishida, T., Ito, R., Suzuki, N., . . . Yoshikawa, T. (2010). Early-stage blocking of Notch signaling inhibits the depletion of goblet cells in dextran sodium sulfate-induced colitis in mice. *J Gastroenterol, 45*(6), 608-617. doi: 10.1007/s00535-010-0210-z

Shussman, N., & Wexner, S. D. (2014). Colorectal polyps and polyposis syndromes. *Gastroenterol Rep (Oxf), 2*(1), 1-15. doi: 10.1093/gastro/got041

Siegel, R., Desantis, C., & Jemal, A. (2014). Colorectal cancer statistics, 2014. *CA Cancer J Clin, 64*(2), 104-117. doi: 10.3322/caac.21220

Sikandar, S. S., Pate, K. T., Anderson, S., Dizon, D., Edwards, R. A., Waterman, M. L., & Lipkin, S. M. (2010). NOTCH signaling is required for formation and self-renewal of

tumor-initiating cells and for repression of secretory cell differentiation in colon cancer. *Cancer Res, 70*(4), 1469-1478. doi: 10.1158/0008-5472.CAN-09-2557

Skokos, D., & Nussenzweig, M. C. (2007). CD8- DCs induce IL-12-independent Th1 differentiation through Delta 4 Notch-like ligand in response to bacterial LPS. *J Exp Med, 204*(7), 1525-1531. doi: 10.1084/jem.20062305

Snippert, H. J., van der Flier, L. G., Sato, T., van Es, J. H., van den Born, M., Kroon-Veenboer, C., . . . Clevers, H. (2010). Intestinal crypt homeostasis results from neutral competition between symmetrically dividing Lgr5 stem cells. *Cell, 143*(1), 134-144. doi: 10.1016/j.cell.2010.09.016

Soker, S., Takashima, S., Miao, H. Q., Neufeld, G., & Klagsbrun, M. (1998). Neuropilin-1 is expressed by endothelial and tumor cells as an isoform-specific receptor for vascular endothelial growth factor. *Cell, 92*(6), 735-745.

Solomon, E., Voss, R., Hall, V., Bodmer, W. F., Jass, J. R., Jeffreys, A. J., . . . Rider, S. H. (1987). Chromosome 5 allele loss in human colorectal carcinomas. *Nature, 328*(6131), 616-619. doi: 10.1038/328616a0

Sonoshita, M., Aoki, M., Fuwa, H., Aoki, K., Hosogi, H., Sakai, Y., . . . Taketo, M. M. (2011). Suppression of colon cancer metastasis by Aes through inhibition of Notch signaling. *Cancer Cell, 19*(1), 125-137. doi: 10.1016/j.ccr.2010.11.008

Spano, J. P., Fagard, R., Soria, J. C., Rixe, O., Khayat, D., & Milano, G. (2005). Epidermal growth factor receptor signaling in colorectal cancer: preclinical data and therapeutic perspectives. *Ann Oncol, 16*(2), 189-194. doi: 10.1093/annonc/mdi057

Spindler, K. L., Lindebjerg, J., Nielsen, J. N., Olsen, D. A., Bisgard, C., Brandslund, I., & Jakobsen, A. (2006). Epidermal growth factor receptor analyses in colorectal cancer: a comparison of methods. *Int J Oncol, 29*(5), 1159-1165.

Sprent, J. (2005). Direct stimulation of naive T cells by antigen-presenting cell vesicles. *Blood Cells Mol Dis, 35*(1), 17-20. doi: 10.1016/j.bcmd.2005.04.004

Stanger, B. Z., Datar, R., Murtaugh, L. C., & Melton, D. A. (2005). Direct regulation of intestinal fate by Notch. *Proc Natl Acad Sci U S A, 102*(35), 12443-12448. doi: 10.1073/pnas.0505690102

Stappenbeck, T. S., Mills, J. C., & Gordon, J. I. (2003). Molecular features of adult mouse small intestinal epithelial progenitors. *Proc Natl Acad Sci U S A, 100*(3), 1004-1009. doi: 10.1073/pnas.242735899

Starling, N., Neoptolemos, J., & Cunningham, D. (2006). Role of erlotinib in the management of pancreatic cancer. *Ther Clin Risk Manag, 2*(4), 435-445.

Street, S. E., Trapani, J. A., MacGregor, D., & Smyth, M. J. (2002). Suppression of lymphoma and epithelial malignancies effected by interferon gamma. *J Exp Med, 196*(1), 129-134.

Su, L. K., Kinzler, K. W., Vogelstein, B., Preisinger, A. C., Moser, A. R., Luongo, C., . . . Dove, W. F. (1992). Multiple intestinal neoplasia caused by a mutation in the murine homolog of the APC gene. *Science, 256*(5057), 668-670.

Sun, J., Krawczyk, C. J., & Pearce, E. J. (2008). Suppression of Th2 cell development by Notch ligands Delta1 and Delta4. *J Immunol, 180*(3), 1655-1661.

Svartz, N., & Ernberg, T. (1949). Cancer coli in cases of colitis ulcerosa. *Acta Med Scand*(135), 444-447.

Szlosarek, P., Charles, K. A., & Balkwill, F. R. (2006). Tumour necrosis factor-alpha as a tumour promoter. *Eur J Cancer, 42*(6), 745-750. doi: 10.1016/j.ejca.2006.01.012

Tacchini-Cottier, F., Allenbach, C., Otten, L. A., & Radtke, F. (2004). Notch1 expression on T cells is not required for CD4+ T helper differentiation. *Eur J Immunol, 34*(6), 1588-1596. doi: 10.1002/eji.200324337

Takahashi, Y., Ellis, L. M., & Mai, M. (2003). The angiogenic switch of human colon cancer occurs simultaneous to initiation of invasion. *Oncol Rep, 10*(1), 9-13.

Takeda, A., Shimada, H., Imaseki, H., Okazumi, S., Natsume, T., Suzuki, T., & Ochiai, T. (2000). Clinical significance of serum vascular endothelial growth factor in colorectal cancer patients: correlation with clinicopathological factors and tumor markers. *Oncol Rep, 7*(2), 333-338.

Takeichi, N., Yanagisawa, S., Kaneyama, T., Yagita, H., Jin, Y. H., Kim, B. S., & Koh, C. S. (2010). Ameliorating effects of anti-Dll4 mAb on Theiler's murine encephalomyelitis

virus-induced demyelinating disease. *Int Immunol, 22*(9), 729-738. doi: 10.1093/intimm/dxq059

Tan, B. T., Park, C. Y., Ailles, L. E., & Weissman, I. L. (2006). The cancer stem cell hypothesis: a work in progress. *Lab Invest, 86*(12), 1203-1207. doi: 10.1038/labinvest.3700488

Tanaka, S., Tsukada, J., Suzuki, W., Hayashi, K., Tanigaki, K., Tsuji, M., . . . Kubo, M. (2006). The interleukin-4 enhancer CNS-2 is regulated by Notch signals and controls initial expression in NKT cells and memory-type CD4 T cells. *Immunity, 24*(6), 689-701. doi: 10.1016/j.immuni.2006.04.009

Tanaka, T., Kohno, H., Suzuki, R., Yamada, Y., Sugie, S., & Mori, H. (2003). A novel inflammation-related mouse colon carcinogenesis model induced by azoxymethane and dextran sodium sulfate. *Cancer Sci, 94*(11), 965-973.

Tarmin, L., Yin, J., Harpaz, N., Kozam, M., Noordzij, J., Antonio, L. B., . . . Meltzer, S. J. (1995). Adenomatous polyposis coli gene mutations in ulcerative colitis-associated dysplasias and cancers versus sporadic colon neoplasms. *Cancer Res, 55*(10), 2035-2038.

Tavazoie, S. F., Alarcon, C., Oskarsson, T., Padua, D., Wang, Q., Bos, P. D., . . . Massague, J. (2008). Endogenous human microRNAs that suppress breast cancer metastasis. *Nature, 451*(7175), 147-152. doi: 10.1038/nature06487

Tetsu, O., & McCormick, F. (1999). Beta-catenin regulates expression of cyclin D1 in colon carcinoma cells. *Nature, 398*(6726), 422-426. doi: 10.1038/18884

Theodoratou, E., Campbell, H., Tenesa, A., Houlston, R., Webb, E., Lubbe, S., . . . Farrington, S. M. (2010). A large-scale meta-analysis to refine colorectal cancer risk estimates associated with MUTYH variants. *Br J Cancer, 103*(12), 1875-1884. doi: 10.1038/sj.bjc.6605966

Tian, H., Biehs, B., Warming, S., Leong, K. G., Rangell, L., Klein, O. D., & de Sauvage, F. J. (2011). A reserve stem cell population in small intestine renders Lgr5-positive cells dispensable. *Nature, 478*(7368), 255-259. doi: 10.1038/nature10408

Totafurno, J., Bjerknes, M., & Cheng, H. (1987). The crypt cycle. Crypt and villus production in the adult intestinal epithelium. *Biophys J, 52*(2), 279-294. doi: 10.1016/S0006-3495(87)83215-0

Tran, I. T., Sandy, A. R., Carulli, A. J., Ebens, C., Chung, J., Shan, G. T., . . . Maillard, I. (2013). Blockade of individual Notch ligands and receptors controls graft-versus-host disease. *J Clin Invest, 123*(4), 1590-1604. doi: 10.1172/JCI65477

Trindade, A., Djokovic, D., Gigante, J., Badenes, M., Pedrosa, A.-R., Fernandes, A.-C., . . . Duarte, A. (2012). Low-Dosage Inhibition of Dll4 Signaling Promotes Wound Healing by Inducing Functional Neo-Angiogenesis. *PLoS One, 7*(1), e29863. doi: 10.1371/journal.pone.0029863

Trindade, A., Kumar, S. R., Scehnet, J. S., Lopes-da-Costa, L., Becker, J., Jiang, W., . . . Duarte, A. (2008). Overexpression of delta-like 4 induces arterialization and attenuates vessel formation in developing mouse embryos. *Blood, 112*(5), 1720-1729. doi: 10.1182/blood-2007-09-112748

Tsanou, E., Peschos, D., Batistatou, A., Charalabopoulos, A., & Charalabopoulos, K. (2008). The E-cadherin adhesion molecule and colorectal cancer. A global literature approach. *Anticancer Res, 28*(6A), 3815-3826.

Vaiopoulos, A. G., Kostakis, I. D., Koutsilieris, M., & Papavassiliou, A. G. (2012). Colorectal cancer stem cells. *Stem Cells, 30*(3), 363-371. doi: 10.1002/stem.1031

van de Wetering, M., Sancho, E., Verweij, C., de Lau, W., Oving, I., Hurlstone, A., . . . Clevers, H. (2002). The beta-catenin/TCF-4 complex imposes a crypt progenitor phenotype on colorectal cancer cells. *Cell, 111*(2), 241-250.

van Es, J. H., & Clevers, H. (2005). Notch and Wnt inhibitors as potential new drugs for intestinal neoplastic disease. *Trends Mol Med, 11*(11), 496-502. doi: 10.1016/j.molmed.2005.09.008

van Es, J. H., de Geest, N., van de Born, M., Clevers, H., & Hassan, B. A. (2010). Intestinal stem cells lacking the Math1 tumour suppressor are refractory to Notch inhibitors. *Nat Commun, 1*, 18. doi: 10.1038/ncomms1017

van Es, J. H., Jay, P., Gregorieff, A., van Gijn, M. E., Jonkheer, S., Hatzis, P., . . . Clevers, H. (2005). Wnt signalling induces maturation of Paneth cells in intestinal crypts. *Nat Cell Biol, 7*(4), 381-386. doi: 10.1038/ncb1240

van Es, J. H., van Gijn, M. E., Riccio, O., van den Born, M., Vooijs, M., Begthel, H., . . . Clevers, H. (2005). Notch/gamma-secretase inhibition turns proliferative cells in intestinal crypts and adenomas into goblet cells. *Nature, 435*(7044), 959-963. doi: 10.1038/nature03659

VanDussen, K. L., Carulli, A. J., Keeley, T. M., Patel, S. R., Puthoff, B. J., Magness, S. T., . . . Samuelson, L. C. (2012). Notch signaling modulates proliferation and differentiation of intestinal crypt base columnar stem cells. *Development, 139*(3), 488-497. doi: 10.1242/dev.070763

Vasudev, N. S., & Reynolds, A. R. (2014). Anti-angiogenic therapy for cancer: current progress, unresolved questions and future directions. *Angiogenesis, 17*(3), 471-494. doi: 10.1007/s10456-014-9420-y

Veenendaal, L. M., Kranenburg, O., Smakman, N., Klomp, A., Borel Rinkes, I. H., & van Diest, P. J. (2008). Differential Notch and TGFbeta signaling in primary colorectal tumors and their corresponding metastases. *Cell Oncol, 30*(1), 1-11.

Vignali, D. A., Collison, L. W., & Workman, C. J. (2008). How regulatory T cells work. *Nat Rev Immunol, 8*(7), 523-532. doi: 10.1038/nri2343

Vigouroux, S., Yvon, E., Wagner, H. J., Biagi, E., Dotti, G., Sili, U., . . . Brenner, M. K. (2003). Induction of antigen-specific regulatory T cells following overexpression of a Notch ligand by human B lymphocytes. *J Virol, 77*(20), 10872-10880.

Vogelstein, B., & Kinzler, K. W. (2004). Cancer genes and the pathways they control. *Nat Med, 10*(8), 789-799. doi: 10.1038/nm1087

Vokes, E. E., & Chu, E. (2006). Anti-EGFR therapies: clinical experience in colorectal, lung, and head and neck cancers. *Oncology (Williston Park), 20*(5 Suppl 2), 15-25.

Vooijs, M., Liu, Z., & Kopan, R. (2011). Notch: architect, landscaper, and guardian of the intestine. *Gastroenterology, 141*(2), 448-459. doi: 10.1053/j.gastro.2011.06.003

Vooijs, M., Ong, C. T., Hadland, B., Huppert, S., Liu, Z., Korving, J., . . . Kopan, R. (2007). Mapping the consequence of Notch1 proteolysis in vivo with NIP-CRE. *Development, 134*(3), 535-544. doi: 10.1242/dev.02733

Wada, R., Miwa, H., Abe, H., Santo, R. M., Kitamura, S., Kuwabara, N., . . . et al. (1992). Incidence of Paneth cells in minute tubular adenomas and adenocarcinomas of the large bowel. *Acta Pathol Jpn, 42*(8), 579-584.

Waldner, M. J., & Neurath, M. F. (2009). Colitis-associated cancer: the role of T cells in tumor development. *Semin Immunopathol, 31*(2), 249-256. doi: 10.1007/s00281-009-0161-8

Waldner, M. J. N., M. F. (2015). Mechanisms of Immune Signaling in Colitis-Associated Cancer. *Cellular and Molecular Gastroenterology and Hepatology, 1*(1), 6-16.

Wang, W., Li, X., Zheng, D., Zhang, D., Peng, X., Zhang, X., . . . Shen, S. (2015). Dynamic changes and functions of macrophages and M1/M2 subpopulations during ulcerative colitis-associated carcinogenesis in an AOM/DSS mouse model. *Mol Med Rep, 11*(4), 2397-2406. doi: 10.3892/mmr.2014.3018

Wen, Z., & Fiocchi, C. (2004). Inflammatory bowel disease: autoimmune or immune-mediated pathogenesis? *Clin Dev Immunol, 11*(3-4), 195-204.

Westbrook, A. M., Wei, B., Braun, J., & Schiestl, R. H. (2009). Intestinal mucosal inflammation leads to systemic genotoxicity in mice. *Cancer Res, 69*(11), 4827-4834. doi: 10.1158/0008-5472.CAN-08-4416

Williams, C. K., Li, J. L., Murga, M., Harris, A. L., & Tosato, G. (2006). Up-regulation of the Notch ligand Delta-like 4 inhibits VEGF-induced endothelial cell function. *Blood, 107*(3), 931-939. doi: 10.1182/blood-2005-03-1000

Winawer, S. J., Fletcher, R. H., Miller, L., Godlee, F., Stolar, M. H., Mulrow, C. D., . . . Mayer, R. J. (1997). Colorectal cancer screening: clinical guidelines and rationale. *Gastroenterology, 112*(2), 594-642.

Wolf, D., Wolf, A. M., Rumpold, H., Fiegl, H., Zeimet, A. G., Muller-Holzner, E., . . . Marth, C. (2005). The expression of the regulatory T cell-specific forkhead box transcription

factor FoxP3 is associated with poor prognosis in ovarian cancer. *Clin Cancer Res, 11*(23), 8326-8331. doi: 10.1158/1078-0432.CCR-05-1244

Wong, G. T., Manfra, D., Poulet, F. M., Zhang, Q., Josien, H., Bara, T., . . . Parker, E. M. (2004). Chronic treatment with the gamma-secretase inhibitor LY-411,575 inhibits beta-amyloid peptide production and alters lymphopoiesis and intestinal cell differentiation. *J Biol Chem, 279*(13), 12876-12882. doi: 10.1074/jbc.M311652200

Wong, W. M., & Wright, N. A. (1999). Cell proliferation in gastrointestinal mucosa. *J Clin Pathol, 52*(5), 321-333.

Wu, L., Aster, J. C., Blacklow, S. C., Lake, R., Artavanis-Tsakonas, S., & Griffin, J. D. (2000). MAML1, a human homologue of Drosophila mastermind, is a transcriptional co-activator for NOTCH receptors. *Nat Genet, 26*(4), 484-489. doi: 10.1038/82644

Wu, S., Rhee, K. J., Albesiano, E., Rabizadeh, S., Wu, X., Yen, H. R., . . . Sears, C. L. (2009). A human colonic commensal promotes colon tumorigenesis via activation of T helper type 17 T cell responses. *Nat Med, 15*(9), 1016-1022. doi: 10.1038/nm.2015

Yamada, Y., & Mori, H. (2007). Multistep carcinogenesis of the colon in ApcMin/+mouse. *Cancer Sci, 98*(1), 6-10. doi: 10.1111/j.1349-7006.2006.00348.x

Yamada, Y., Yoshimi, N., Hirose, Y., Kawabata, K., Matsunaga, K., Shimizu, M., . . . Mori, H. (2000). Frequent beta-catenin gene mutations and accumulations of the protein in the putative preneoplastic lesions lacking macroscopic aberrant crypt foci appearance, in rat colon carcinogenesis. *Cancer Res, 60*(13), 3323-3327.

Yamaguchi, E., Chiba, S., Kumano, K., Kunisato, A., Takahashi, T., Takahashi, T., & Hirai, H. (2002). Expression of Notch ligands, Jagged1, 2 and Delta1 in antigen presenting cells in mice. *Immunol Lett, 81*(1), 59-64.

Yamaguchi, H., Chang, S. S., Hsu, J. L., & Hung, M. C. (2014). Signaling cross-talk in the resistance to HER family receptor targeted therapy. *Oncogene, 33*(9), 1073-1081. doi: 10.1038/onc.2013.74

Yan, M., Callahan, C. A., Beyer, J. C., Allamneni, K. P., Zhang, G., Ridgway, J. B., . . . Plowman, G. D. (2010). Chronic DLL4 blockade induces vascular neoplasms. *Nature, 463*(7282), E6-E7. doi: 10.1038/nature08751

Yan, M., & Plowman, G. D. (2007). Delta-like 4/Notch signaling and its therapeutic implications. *Clin Cancer Res, 13*(24), 7243-7246. doi: 10.1158/1078-0432.CCR-07-1393

Yang, Q., Bermingham, N. A., Finegold, M. J., & Zoghbi, H. Y. (2001). Requirement of Math1 for secretory cell lineage commitment in the mouse intestine. *Science, 294*(5549), 2155-2158. doi: 10.1126/science.1065718

Yap, T. A. (2015). Challenges in combining novel molecularly targeted agents in cancer medicine. *Ann Oncol, 26*(1), 9-11. doi: 10.1093/annonc/mdu483

Yuan, Y., Huang, J., & Zheng, S. (1999). [Mutation of human mismatch repair genes in hereditary nonpolyposis colorectal cancer (HNPCC) families]. *Zhonghua Zhong Liu Za Zhi, 21*(2), 105-107.

Zecchini, V., Domaschenz, R., Winton, D., & Jones, P. (2005). Notch signaling regulates the differentiation of post-mitotic intestinal epithelial cells. *Genes Dev, 19*(14), 1686-1691. doi: 10.1101/gad.341705

Zetter, B. R. (1998). Angiogenesis and tumor metastasis. *Annu Rev Med, 49*, 407-424. doi: 10.1146/annurev.med.49.1.407

Zhang, Y., Li, B., Ji, Z. Z., & Zheng, P. S. (2010). Notch1 regulates the growth of human colon cancers. *Cancer, 116*(22), 5207-5218. doi: 10.1002/cncr.25449

Zhao, Y., Bao, Q., Renner, A., Camaj, P., Eichhorn, M., Ischenko, I., . . . Bruns, C. (2011). Cancer stem cells and angiogenesis. *Int J Dev Biol, 55*(4-5), 477-482. doi: 10.1387/ijdb.103225yz

Zheng, H., Pritchard, D. M., Yang, X., Bennett, E., Liu, G., Liu, C., & Ai, W. (2009). KLF4 gene expression is inhibited by the notch signaling pathway that controls goblet cell differentiation in mouse gastrointestinal tract. *Am J Physiol Gastrointest Liver Physiol, 296*(3), G490-498. doi: 10.1152/ajpgi.90393.2008

Zhou, S., Fujimuro, M., Hsieh, J. J., Chen, L., Miyamoto, A., Weinmaster, G., & Hayward, S. D. (2000). SKIP, a CBF1-associated protein, interacts with the ankyrin repeat domain of NotchIC To facilitate NotchIC function. *Mol Cell Biol, 20*(7), 2400-2410.

7 ANNEX I – Dll4 transgenic mouse strains

Dll4$^{+/LacZ}$ mouse strain

This mouse strain was generated in a CD1 background. The *Dll4* gene was inactivated by targeted disruption in embryonic stem cells. The targeting vector was designed to replace the initiation codon and the first three coding exons with the β-galactosidase (*lacZ*) reporter gene (Duarte, 2004).

Dll4$^{lox/lox}$ *VE-Cadherin-CreER*$_{T2}$ and *Dll4*$^{lox/lox}$ *Cag-CreER*$_{T2}$ mouse strains

These mouse strains carry loxP sites flanking the first three coding exons of the *Dll4* gene (*Dll4*$^{lox/lox}$) (Koch et al., 2008), which enables binding by the recombinase Cre (that recognizes the loxP sites) and excision of this sequence therefore inactivating *Dll4*. The expression of the recombinase Cre, which is activated by the administration of tamoxifen, occurs in the endothelium under the VE-Cadherin promoter in the case of the *VE-Cadherin-CreER*$_{T2}$ mice (Monvoisin et al., 2006) and ubiquitously under the CAG promoter in the *Cag-CreER*$_{T2}$ mice (Sakai & Miyazaki, 1997).

Tie2-rtTA-TetO$_7$*-Dll4* mouse strain

The *TetO*$_7$*-Dll4* transgenic construct was produced by cloning the mouse *Dll4* cDNA into p(tetO$_7$)-CMV-bGH and was used in pronuclear microinjection to generate Dll4 conditional overexpression transgenics (A. Trindade et al., 2008). *rtTA* is a fusion protein comprised of the Tet repressor DNA binding protein (TetR) and the VP16 transactivation domain. A four amino acid change in the tetR DNA binding moiety alters *rtTA's* binding characteristics such that it can only recognize the tetO sequences in the tetracycline-responsive promoter element (TRE) of the target transgene in the presence of the doxycicline effector (Kistner et al., 1996).

8 ANNEX II – Primer pair sequences list

1. Primer pair sequences list used in RT-PCR reactions:

β-actin_F: 5’ TGTTACCAACTGGGACGACA 3’

β-actin_R: 5’ GGGGTGTTGAAGGTCTCAAA 3’

Notch1_F: 5’ ACAGTAACCCCTGCATCCAC 3’

Notch1_R: 5’ GGTTGGACTCACACTCGTTG 3’

Notch2_F: 5’ GACTGCACAGAAGACGTGGA 3’

Notch2_R: 5’ GCGTAGCCCTTCAGACACTC 3’

Notch3_F: 5’ GTGTCAATGGTGGTGTCTGC 3’

Notch3_R: 5’ GCACACTCATCCACATCCAG 3’

Notch4_F: 5’ GAGGGACACTCCACCTTTCA 3’

Notch4_R: 5’ CTGGTGCCTGACACAGTCAT 3’

Dll1_F: 5’ GTTGTCTCCATGGCACCTG 3’

Dll1_R: 5’ TGCACGGCTTATGGTGAGTA 3’

Dll4_F: 5’ GGAACCTTCTCACTCAAATCT 3’

Dll4_R: 5’ CTCGTCTGTTCGCCAAATCT 3’

Jag1_F: 5’ CCAGCCAGTGAAGACCAAGT 3’

Jag1_R: 5’ CAATTCGCTGCAAATGTGTT 3’

Hes1_F: 5’ GCGAAGGGCAAGAATAAATG 3’

Hes1_R: 5’ TGTCTGCCTTCTCTAGCTTGG 3’

Hes5_F: 5’ GCACCAGCCCAACTCCAA 3’

Hes5_R: 5’ GGCGAAGGCTTTGCTGTGT 3’

Hey2_F: 5’ TGCCAAGTTAGAAAAGGCTGA 3’

Hey2_R: 5’ CACTCTCGGAATCCAATGCT 3’

VEGFR1_F: 5’ GACCCTCTTTTGGCTCCTTC 3’

VEGFR1_R: 5’ CAGTCTCTCCCGTGCAAACT 3’

VEGFR2_F: 5’ GGCGGTGGTGACAGTATCTT 3’

VEGFR2_R: 5’ GAGGCGATGAATGGTGATCT 3’

VEGFR3_F: 5’ CGAAGCAGACGCTGATGATA 3’

VEGFR3_R: 5’ CCCAGGAAAGGACACACAGT 3’

VEGFA_F: 5’ GGAGAGCAGAAGTCCCATGA 3’

VEGFA_R: 5’ ACACAGGACGGCTTGAAGAT 3’

VEGFC_F: 5’ CCTGAATCCTGGGAAATGTG 3’

VEGFC_R: 5’ TCGCACACGGTCTTCTGTAA 3’

PECAM-1_F: 5’ CAAGCAAAGCAGTGAAGCTG 3’

PECAM-1_R: 5’ TCTAACTTCGGCTTGGGAAA 3’

Atoh1_F: 5’ CAACGACAAGAAGCTGTCCA 3’

Atoh1_R: 5’ CTCTCCGACATTGGGAGTCT 3’
KLF4_F: 5’ GCAGTCACAAGTCCCCTCTC 3’
KLF4_R: 5’ GACCTTCTTCCCCTCTTTGG 3’
Muc2_F: 5’ CACATCACCACCTTTGATGG 3’
Muc2_R: 5’ GGAGGGCATAGGAGTCATTG 3’
Neurog3_F: 5’ AAGAGCGAGTTGGCACTCAG 3’
Neurog3_R: 5’ CCGAGTTGAGGTTGTGCAT 3’
Akp3_F: 5’ GCTGTCTGGGACCTGTCTGT 3’
Akp3_R: 5’ CAGTTGGAAGGCCATCTAGG 3’
Lyz1_F: 5’ ATGGAATGGATGGCTACCGT 3’
Lyz1_R: 5’ ATAGTCGGTGCTTCGGTCTC 3’
Cdkn1b_F: 5’ TCTGTTGGCCCTTTTGTTTT 3’
Cdkn1b_R: 5’ GTGGACCAAATGCCTGACTC 3’
Cdkn1c_F: 5’ GTTCTCCTGCGCAGTTCTCT 3’
*Cdkn1c*_R: 5’ CTGAAGGACCAGCCTCTCTC 3’
Myc_F: 5’ GCCCAGTGAGGATATCTGGA 3’
Myc_R: 5’ GACCGCAACATAGGATGGAG 3’
Ccnd2_F: 5’ CAGTCACCCCTCACGACTTC 3’
Ccnd2_R: 5’ ACAGAGCGATGAAGGTCTGC 3’
Lgr5_F: 5’ CCCATCCAATTTGTTGGAGTA 3’
Lgr5_R: 5’ GTGGCAGTTCCTGTCAAGTG 3’
Bmi1_F: 5’ AGAGATTTTTATGCAGCTCACC 3’
Bmi1_R: 5’ AATCCTCTTCTCCTCATCTGC 3’
STAT3_F: 5’ GAGCTGGCTGACTGGAAGAG 3’
STAT3_R: 5’ GCGGGTCTGAAGTTGAGATT 3’
INF-γ_F: 5’ CACGGCACAGTCATTGAAAG 3’
INF-γ_R: 5’ CTTTTGCCAGTTCCTCCAGA 3’
IL2_F: 5’ ACCTGGAGCAGCTGTTGATG 3’
IL2_R: 5’ GGGCAAGTAAAATTTGAAGGTG 3’
IL4_F: 5’ TGTTCTCATGGAGCTGCAGA 3’
IL4_R: 5’ GTGATGTGGACTTGGACTCA 3’
IL10_F: 5’ CCTTCAGCCAGGTGAAGACT 3’
IL10_R: 5’ GGCAACCCAAGTAACCCTTA 3’
IL13_F: 5’ GCAATGCCATCTACAGGACC 3’
IL13_R: 5’ GATTTTGGTATCGGGGAGGC 3’
IL6_F: 5’ TGTTCTCATGGAGCTGCAGA 3’
IL6_R: 5’ GTGATGTGGACTTGGACTCA 3’
IL1β_F: 5’ TGAGGACATGAGCACCTTCT 3’

IL1β _R: 5’ GAACGTCACACACCAGCAG 3’

TNF-α_F: 5’ TCAGTTCTATGGCCCAGACC 3’

TNF-α_R: 5’ CACTTGGTGGTTTGCTACGA 3’

TGF-β_F: 5’ TGGAGCAACATGTGGAACTC 3’

TGF-β_R: 5’ CGTCAAAAGACAGCCACTCA 3’

IL17_F: 5’ AAACCTGCTGCTCACCTTGT 3’

IL17_R: 5’ GGAGGGAGTTGTTGCTCAAA 3’

NFKB2_F: 5’ GCTGTGCCCCAAATATTGCA 3’

NFKB2_R: 5’ CACTTCAGCTCCACAGTCAAC 3’

COX2_F: 5’ TGAGTGGGGTGATGAGCAAC 3’

COX2_R: 5’ TGAGTTTGAAGTGGTAACCGC 3’

iNOS_F: 5’ AGATGGTCCGCAAGAGAGTG 3’

iNOS_R: 5’ TGCAGGATGTCCTGAACGTA 3’

2. Primer pair sequences list used in PCR reactions:

Genotyping of *Apc*$^{Min/+}$ mouse:

oIMR0033: 5’ GCCATCCCTTCACGTTAG 3’

oIMR0034: 5’ TTCCACTTTGGCATAAGGC 3’

oIMR0758: 5’ TTCTGAGAAAGACAGAAGTTA 3’

Size of the mutant band: 340pb

Program:

1cycle: 94ºC: 3min

35 cycles: 94ºC 30s, 55ºC 30s, 72ºC: 1min

1 cycle: 72ºC 2min

1 cycle: 4ºC: ∞

Genotyping of *Dll4*$^{lox/lox}$:

Dll4^{lox} *5’*: 5’ GTG CTG GGA CTG TAG CCA CT 3’

Dll4^{lox} *3’*: 5’ TGT TAG GGA TGT CGC TCT CC 3’

Size of the mutant band: 455pb

Program:

1cycle: 94ºC: 2min

34 cycles: 94ºC 45s, 60ºC 30s, 72ºC: 30s

1 cycle: 72ºC 10min

1 cycle: 4ºC: ∞

Genotyping of *Cre*:

Cre 313U: 5' CCAGCTAAACATGCTTCATC 3'

Cre 6831: 5' CGCTCGACCAGTTTAGTTAC 3'

Size of the band: 350pb

Program:

1cycle: 95ºC: 3min

35 cycles: 95ºC 30s, 60ºC 30s, 72ºC: 35s

1 cycle: 72ºC 3min

1 cycle: 4ºC: ∞

Genotyping of *Tie2-rtTA*:

HH FW1: 5' CACTGGCGTGGTCTGGACACCA 3'

M2 REV2: 5' CCACCTGGTCCTGTCCAGGTAC 3'

Size of the band: 200pb

Program:

1cycle: 95ºC: 4min

35 cycles: 95ºC 30s, 60ºC 45s, 72ºC: 45s

1 cycle: 72ºC 5min

1 cycle: 4ºC: ∞

Genotyping of *TetO7-Dll4*:

Tet_Dll4_L: 5' ATCCACGCTGTTTTGACCTC 3'

Tet_Dll4_R: 5' GTGGAGACATTGCCAAAGGT 3'

Size of the band: 500pb

Program:

1cycle: 95ºC: 3min

40 cycles: 95ºC 30s, 60ºC 30s, 72ºC: 35s

1 cycle: 72ºC 3min

1 cycle: 4ºC: ∞

Genotyping of *Dll4+/LacZ*:

Dll4-S3: 5' GGGGAATCAGCTTTTCAGGAA 3'

Dll4-A1: 5' CGAACTCCTGCAGCCGCAGCT 3'

Dll4-lacZ2: 5' GGGTTTTCCCAGTCACGACGTT 3'

Size of the mutant band: 140pb

Program:

1cycle: 94ºC: 5min

35 cycles: 94ºC 45s, 65ºC 1min, 72ºC: 45s

1 cycle: 72ºC 10min

1 cycle: 4ºC: ∞

9 ANNEX III – Collaborations

Basto A., Badenes M, Almeida S, Martins C, Duarte A, Santos D, Leitão A. «Immune response profile elicited by the model antigen ovalbumin expressed in fusion with the bacterial OprI lipoprotein.», Molecular Immunology 2014;10:020.